LIBRARY
Michigan State
University

This is to certify that the

dissertation entitled

The Use of Thermionic Emission Materials in Mass Spectrometry and Gas Chromatography

presented by

Daniel Bombick

has been accepted towards fulfillment
of the requirements for

Ph.D. degree in Chemistry

John Allison
Major professor

Date 27 March 1987

MSU is an Affirmative Action/Equal Opportunity Institution

O-12771



RETURNING MATERIALS:
Place in book drop to remove this checkout from your record. FINES will be charged if book is returned after the date stamped below.

THE USE OF THERMIONIC EMISSION MATERIALS IN MASS SPECTROMETRY AND GAS CHROMATOGRAPHY

By

Daniel Bombick

A DISSERTATION

Submitted to
Michigan State University
in partial fulfillment of the requirements
for the degree of

DOCTOR OF PHILOSOPHY

Department of Chemistry

1986

This is dedicated to my family, especially my brother, Dave, for the understanding and cooperation they showed me while this work was being completed.

ACKNOWLEDGEMENTS

I would like to thank John Allison for his guidance, encouragement, and friendship. No one could ask for a better research advisor and friend. I would like to thank Matthew Zabik and J.T. Watson for their help in the writing of this thesis.

The friendship and help of my fellow students will be remembered always. Tony, Barb, Pinky and Mac continue to be very special people to me. Mac made the late nights at the Chem building interesting. Tony "opened my eyes" to Greek food. Pinky deserves a round of applause for his organization of our group "picnics". When I thought that I was being swamped with work, I would take a look at Barb and the kids and quickly decide otherwise. D.K., Rich, Paul, and Mark (my "second research group") were excellent companions. (Rich causes me to believe I should have taken debate in high school). Karen, Kris, and Ellen (the Flamingo crew) caused my leaving to be a very difficult one. I wish everyone continued success.

I would like to thank the faculty and staff of the MSU chemistry department for all the excellent help during my stay.

I wish to thank the MSU/NIH Mass Spectrometry Facility for all their help. The staff at the facility were #1.

ABSTRACT

THE USE OF THERMIONIC EMISSION MATERIALS IN MASS SPECTROMETRY AND GAS CHROMATOGRAPHY

By

Daniel Bombick

Certain solids when heated and positively biased emit ions. Here, an aluminosilicate matrix containing K_2O is used as a source of gaseous potassium ions. A simple method is presented for introducing these emitters into the chemical ionization (CI) source of a mass spectrometer. K^+ adds to most compounds containing π- or n-donor sites to produce an $(M+K)^+$ ion. This method provides a novel means for performing K^+ CI. Some compounds, notably amines, react on the hot surface to produce ions. The behavior parallels the response of thermionic ionization gas chromatography detectors. When nonvolatile compounds are deposited on the emitter, ions representative of the compound are formed. This method is referred to as K^+IDS (potassium ionization of desorbed species). The use of the thermionic emission probe in K^+CI is presented first. The analysis of nonvolatile compounds including polymers follows. Finally, the use of the K^+ probe in the elucidation of the mechanism of the gas chromatographic thermionic ionization detector is presented.

TABLE OF CONTENTS

Page

LIST OF TABLES....viii

LIST OF FIGURES....ix

LIST OF SCHEMES....xix

CHAPTER 1 - INTRODUCTION....1

I. Introduction....1

II. Thermionic Emission....4

III. Surface Ionization....19

A. Positive Surface Ionization....19

B. Negative Surface Ionization....34

IV. Final Comments....40

CHAPTER 2 - POTASSIUM ION CHEMICAL IONIZATION AND OTHER USES OF AN ALKALI THERMIONIC EMITTER IN MASS SPECTROMETRY....41

I. Introduction....41

II. Experimental....45

III. Results and Discussion....48

A. Other Uses of the K^+ Thermionic Emitter Probe in Mass Spectrometry....63

Page

CHAPTER 3 - A NEW DESORPTION/IONIZATION MASS SPECTROMETRIC TECHNIQUE FOR THE ANALYSIS OF THERMALLY LABILE COMPOUNDS BASED ON THERMIONIC EMISSION MATERIALS....78

I. Introduction....78

II. Experimental....83

III. Results and Discussion....86

A. Applications Using K^+IDS....90

1. Saccharides....90

2. Pharmaceuticals....95

3. Peptides....98

4. Steroids....103

5. Mixture Analysis....106

B. Sensitivity....114

C. Surface Ionization of Thermally Labile Compounds....116

IV. Final Comments on Chapter 3....121

CHAPTER 4 - MASS SPECTROMETRIC ANALYSIS OF POLYMERS USING K^+IDS....124

I. Introduction....124

II. Experimental....127

III. Results and Discussion....128

Page

A. General Considerations of Using K^+IDS For Polymer Analysis....128

B. Short-Lived Polymers....134

1. General Considerations....134

2. Cyanoethylmethyl Silicone (XF-1150)....139

3. Polyvinylpyrrolidone....146

4. Polyesters....149

5. Polyamides....153

C. Long-Lived Polymers....155

IV. Final Comments on Chapter 4....171

CHAPTER 5 - MASS SPECTRAL AND GAS CHROMATOGRAPHIC INVESTIGATION INTO THE RESPONSE MECHANISM OF THE THERMIONIC IONIZATION DETECTOR FOR GAS CHROMATOGRAPHY....172

I. Introduction....172

II. Experimental....181

III. Results and Discussion....183

A. What Happens to an Analyte in the TID in the Absence of Any Other Gases?....183

1. Negative Ion Formation....184

2. Positive Ion Formation....192

Page

3. The GC-TID in the Absence of Gases.....197

B. What Role Do Gases Have Between an Analyte and the Hot Surface?.....198

1. The Effects of Gases in the MS-TID.....198

2. The Effects of Gases in the GC-TID.....204

a. Temperature of the Bead.....204

b. Air in the GC-TID.....209

c. The H_2/Air System in the GC-TID.....218

d. Nitrogen in the GC-TID.....228

C. What are the Similarities Between the MS-TID and the GC-TID.....232

APPENDIX A - REPRESENTATIVE K^+IDS SPECTRA.....236

LIST OF REFERENCES.....286

LIST OF TABLES

Table		Page
1	List of Compounds Studied Using the K^+ Emitter Probe in the K^+Cl Mode	53
2	Formulas of the Polymers Used in the K^+IDS Analyses	140
3	Potassium Ion Adduct Series for Cyanoethylmethyl Silicone (XF-1150)	142
4	Potassium Ion Adduct Series For Poly(Ethylene-adipate)	152
5	Apparent Average Molecular Weights Using the First Ten K^+IDS Spectra For the PPG and PEG Polymers	169
6	Comparison of Positive Surface Ionization of Some Amines on Heated Alkali Aluminosilicate and Oxidized Tungsten Surfaces	196

LIST OF FIGURES

Figure		Page
1	The Thermionic Emission Experiment	3
2	A Free Electron in a Potential Well	8
3	The Energetics Involved in the Emission of Gas Phase Metal Ions From the Solid Metal	13
4	The Energetics Involved in the Emission of Gas Phase Metal Ions From an Aluminosilicate Surface	16
5	Schematic Diagram of Thermionic Emission Probe in the Mass Spectrometer's Ion Source	46
6	K^+Cl Spectrum of 2-Butanone	49
7	K^+Cl Spectrum of Diethyl Ether	50
8	K^+Cl Spectrum of Acetonitrile	51
9	K^+Cl Spectrum of Ethyl Acetate	52
10	A Log-log Plot of $I(M+K)^+/[I(M+K)^+ + I(K^+)]$ vs. Pressure of Acetone (I Refers to Intensity)	55
11	K^+Cl (Surface Ionization) Mass Spectrum of Triethylamine. Bead Bias is Above K^+ Addition Bias Window	56
12	Plot of I (Product Ion i)/[I(m/z 112) + I(m/z 72) + I(m/z 58)] vs Bead Bias For Diethylamine. Pressure and Heating Current Were Constant at 650 mTorr and 2.0 A, Respectively	59
13	K^+Cl Spectrum of 2-Propanol With Bead Biased Within K^+ Addition Bias Window	61

Figure Page

14 Plot of I (Product Ion)/[I(m/z 98) + I(m/z 99) + I(m/z 137)] vs. Bead Bias.... 62

15 K^+Cl Spectrum of 12-Crown-4. Bead Bias is Within Addition Bias Window.... 64

16 K^+Cl Spectrum of Triethylene Glycol Dimethyl Ether. Bead Bias is Within Addition Bias Window.... 65

17 K^+Cl Spectrum of 15-Crown-5. Bead Bias Within the Addition Window.... 67

18 EI Spectrum of 15-Crown-5. Bead Bias Was -23 V With Respect to the CI Volume in This Case.... 68

19 The Mass Chromatograms and Total Ion Intensity Obtained From GC/ K^+Cl/MS Run in the Analysis of 1µl of a Neat 1:1 Mixture of a Ketone and an Amine. Mass Spectra Were Collected From m/z 42 to 150. The Bead Bias is Within the K^+ Addition Window.... 70

20 The Mass Chromatograms and Total Ion Intensity Obtained From GC/ K^+Cl/MS Run in the Analysis of 1µl of a 1:1 Neat Mixture of a Ketone and Amine. Conditions the Same as in Figure 19 Except Bead Bias Above K^+ Addition Bias Window.... 71

21 K^+Cl/Surface Ionization of Glycylglycine. Heating Current Was 2.0 A.... 73

22 K^+Cl/Surface Ionization of Glycyl Prolyl Alanine. Heating Current Was 2.0 A.... 74

23 K^+Cl/Surface Ionization of Leucyl Glycyl Phenylalanine. Heating Current Was 2.0 A.... 75

24 Schematic Diagram of Thermionic Emission Probe in

Figure Page

the Mass Spectrometer's Source. The Structure of the Probe Tip is Shown Enlarged.... 82

25 K^+IDS Spectrum of Glucose.... 92

26 K^+IDS Spectrum of Sucrose.... 94

27 K^+IDS Spectrum of Ampicillin.... 96

28 K^+IDS Spectrum of Hexaglycine. A Heating Current of 2 A Was Used. The Insert Shows the Molecular Ion Region For Which the Heating Current Was 2.5 A. The Relative Intensity in the Latter Case Was Approximately 2.5 Times That of the Previous (2 A) Spectrum.... 100

29 K^+IDS Spectrum of 20 Year Old Cholesterol.... 104

30 K^+IDS Spectrum of "Fresh" Cholesterol. Conditions the Same as in Figure 29.... 105

31 K^+IDS Spectrum of Poly(Ethylene Glycol) 1000 at a Heating Current of 2.5 A.... 108

32 K^+IDS Spectrum of Poly(Ethylene Glycol) 1000 at a Heating Current of 2.0 A.... 109

33 Total Ion Intensity vs. Scan Number of Poly(Propylene Glycol) 725. The Scan Rate Was 1.0 Scan/s.... 111

34 Total Ion Intensity vs. Scan Number of Ampicillin. The Scan Rate Was 0.6 Scan/s.... 112

35 K^+IDS Spectrum of Poly(Propylene Glycol) 725. A Heating Current of 2 A Was Used.... 113

36 Total Ion Intensity at Peak Maximum of Polyphenyl Ether Plotted vs. Amount Deposited on the Thermionic

Figure Page

Emission Material. A Heating Current of 2 A Was Used....115

37 K^+IDS/Surface Ionization Spectrum of Xanthine. A Heating Current of 2.5 A Was Used....118

38 K^+IDS/Surface Ionization Spectrum of Theophylline. A Heating Current of 2.5 A Was Used....119

39 Negative Surface Ionization Spectrum of L-Methionyl Glycine Deposited on the Thermionic Emission Material. The Bias on the Bead Relative to the Source Was -1.0 V. A Heating Current of 2.5 A Was Used....122

40 Total Ion Intensity For K^+IDS Analysis of Nylon 6. Arrow Indicates When Current Was Applied....129

41 Total Ion Intensity for K^+IDS Analysis of Poly(Ethylene Glycol) 600. The Total Run Time Shown Here is Approximately 7 Minutes. Current Was Applied at Scan 7....130

42 Intensity as a Function of Time for the Desorption of Species Due to Rapid Heating and the Emission of K^+. The Overlap Region Shows Where K^+ Spectra are Produced....132

43 Averaged Spectrum of Nylon 6 From Scans 11-20 (See Figure 40)....136

44 Averaged Spectrum of Nylon 6 From Scans 20-40 (See Figure 40)....137

45 Averaged Spectrum of Nylon 6 From Scans 11-40 (See Figure 40)....138

46 Averaged K^+IDS Spectrum of XF-1150....141

Figure Page

47 Averaged K^+IDS Spectrum of Polyvinylpyrrolidone.....147

48 Averaged K^+IDS Spectrum of Poly(Ethyleneadipate).....151

49 Averaged K^+IDS Spectrum of Poly(Propylene Glycol) 725 Using Spectra Late in the K^+IDS Analysis.....156

50 Averaged K^+IDS Spectrum of Poly(Propylene Glycol) 725 Using Spectra Early in the K^+IDS Analysis.....157

51 Schematic Diagram of Potassium Thermionic Emission Probe in the Mass Spectrometer's Source Showing Various Thermal Regions.....159

52 The Apparent Average Molecular Weight of Poly (Ethylene Gylcol) 400 as a Function of Scan Number.....161

53 The Relative Intensities of the Oligomer-Potassium Ion Adducts of Poly(Ethylene Glycol) 400 Plottes as a Function of Scan Number.....162

54 Intensity as a Function of Time for the Desorption of Species Due to Rapid Heating; the Distillation of Species From "Cold" Regions; and the Emission of K^+ Ions. The Overlap Regions Shows Where K^+IDS Spectra are Produced.....164

55 The Percent of the Total Ion Intensity as a Function of Scan Number for the Potassium Ion Adducts of Decomposition Species of Poly(Ethylene Glycol) 600. The Heating Currents Used are 2.5 Amps for Curve B and 3.5 Amps for Curve A.....166

56 The Two Modes of Operation in the Kolb-Bischoff TID.....175

57 Negative SI Spectrum of Acetonitrile Obtained Using the Alkali Aluminosilicate Bead.....185

Figure Page

58 Negative SI Spectrum of Nitromethane Obtained Using the Alkali Aluminosilicate Bead....187

59 Negative SI Spectrum of n-Butyl Nitrite Obtained Using the Alkali Aluminosilicate Bead....188

60 Negative SI Spectrum of Tri-n-Butyl Phosphate Obtained Using the Alkali Aluminosilicate Bead....190

61 Negative SI Spectrum of Hexane Obtained Using the Alkali Aluminosilicate Bead....191

62 Positive SI Spectrum of Triethylamine Obtained Using the Alkali Aluminosilicate Bead....194

63 Negative SI Spectrum of Tri-n-Butyl Phosphate Obtained Using the Alkali Aluminosilicate Bead. This Spectrum Was Obtained With a Source Pressure of 100 mTorr of Air....202

64 Bead Temperature as a Function of Detector Gas Flow Rate....205

65 A Typical Configuration of a TID....207

66 Plot of Log Response as a Function of Bead Current For Several Compounds at a Constant Air Flow Rate of 160 ml/min....211

67 Response as a Function of the Number of Injections For Trimethyl Phosphate....213

68 Response as a Function of Air Flow Rate For Several Test Compounds....216

69 Response as a Function of H_2 Flow rate For Some Test Compounds at Constant Current and Air Flow Rate....219

Figure Page

70 Chromatograms of Test Mixture at Two Different H_2 Flow Rates....221

71 Response as a Function of Air Flow Rate For Some Test Compounds at Constant Current and H_2 Flow rate....223

72 Log Response as a Function of Bead Current For Several Test Compounds....224

73 Response as a Function of Bead Current For Several Test Compounds With a Constant 160 ml/min N_2 Flow Rate....230

74 K^+IDS Spectrum of PhenolPhthalein....237

75 K^+IDS Spectrum of Methyl Red....238

76 K^+IDS Spectrum of Methylene Blue....239

77 K^+IDS Spectrum of Methyl Violet....240

78 K^+IDS Spectrum of Martius Yellow....241

79 K^+IDS Spectrum of Murexide....242

80 K^+IDS Spectrum of Nile Blue A....243

81 K^+IDS Spectrum of Magdala Red....244

82 K^+IDS Spectrum of Bromocresol Green (Na Salt)....245

83 K^+IDS Spectrum of Chlorophenol Red....246

84 K^+IDS Spectrum of of Phenosafranine....247

85 K^+IDS Spectrum of Quinine....248

Figure Page

86 K^+IDS Spectrum of Caffeine....249

87 K^+IDS Spectrum of Riboflavin....250

88 K^+IDS Spectrum of Hypoxanthine....251

89 K^+IDS Spectrum of F-50 (Methyl Silicone)....252

90 K^+IDS Spectrum of EPON 1001....253

91 K^+IDS Spectrum of Maltose....254

92 K^+IDS Spectrum of Fructose....255

93 K^+IDS Spectrum of Lactose....256

94 K^+IDS Spectrum of Gum Arabic....257

95 K^+IDS Spectrum of Gum Ghatti....258

96 K^+IDS Spectrum of Phenobarbital....259

97 K^+IDS Spectrum of Penicillin G....260

98 K^+IDS Spectrum of Rhamnose....261

99 K^+IDS Spectrum of Sorbose....262

100 K^+IDS Spectrum of Ribose....263

101 K^+IDS Spectrum of Dextran....264

102 K^+IDS Spectrum of Glycogen....265

103 K^+IDS Spectrum of Ascorbic Acid....266

Figure Page

104 K^+IDS Spectrum of Melezitose....267

105 K^+IDS Spectrum of Raffinose....268

106 K^+IDS Spectrum of Inulin....269

107 K^+IDS Spectrum of Amylose....270

108 K^+IDS Spectrum of Amylopectin....271

109 K^+IDS Spectrum of Locust Bean Gum....272

110 K^+IDS Spectrum of Allantoin....273

111 K^+IDS Spectrum of Porphyrin (MW=604)....274

112 K^+IDS Spectrum of Triton X100....275

113 K^+IDS Spectrum of Tween 80....276

114 K^+IDS Spectrum of SE-54 (Methyl Silicone)....277

115 K^+IDS Spectrum of Polybutadiene....278

116 K^+IDS Spectrum of Polyoxyethylene Lauryl Ether....279

117 K^+IDS Spectrum of Brij 30....280

118 K^+IDS Spectrum of Quadrol....281

119 K^+IDS Spectrum of Poly(Cylcohexanedimethanol Succinate)....282

120 K^+IDS Spectrum of W-98....283

121 K^+IDS Spectrum of Cupric Acetate....284

Figure Page

122 K^+IDS Spectrum of Juicy Fruit Gum.....285

LIST OF SCHEMES

Scheme Page

1 Scheme 1.....97

2 Scheme 2.....101

3 Scheme 3.....120

4 Scheme 4.....144

5 Scheme 5.....148

LIST OF SCHEMES

Scheme		Page
1	Scheme 1	97
2	Scheme 2	101
3	Scheme 3	120
4	Scheme 4	144
5	Scheme 5	148

CHAPTER I

I. INTRODUCTION

This work discusses the uses of thermionic emission (TE) materials in the areas of mass spectrometry (MS) and gas chromatography (GC). Thermionic emission materials, as will be shown, are potentially useful in both of these areas. Three projects will be described and discussed which use various types of thermionic emission substances. The first project is an investigation of thermionic emission materials for producing gaseous metal ions as chemical ionization (CI) reagent ions for mass spectrometry. Secondly, these thermionic emitters can be used, in a particular manner that will be described, for the mass spectrometric analysis of nonvolatile and thermally labile compounds. The final project discusses the N,P-GC detector which contains a thermionic emission material. The latter investigation pertains to the response mechanism of these detectors. While these topics may seem unrelated the underlying "theme" is the thermionic emitter. In addition, the manufacture of a thermionic emission probe for a mass spectrometer facilitated the study of all three experiments. It was found that during the course of these investigations information obtained from one study was useful for another. An introduction of each project will not be made here but will precede its respective section in the manuscript. This introduction will curtail a discussion of thermionic emission and surface ionization. These

principles will serve as a foundation for all three projects since they are necessary ingredients underlying the behavior of thermionic emitters.

Consider the experiment, shown in Figure 1 which is maintained at a low pressure. An appropriate solid, when heated and positively biased, emits positively charged species which can be collected. This process can occur for some solids that are negatively biased and results in the emission of negative charge carriers. This process, involving the emission of charged particles (positive and negative) from a surface is called thermionic emission.

The surface ionization (SI) experiment is designed in a similar fashion as that shown in Figure 1. Emission of negatively or positively charged species occurs when a gas phase molecule is allowed to strike and adsorb onto the surface. This is in contrast to thermionic emission where the species to be ionized must first "unfasten" itself from the solid matrix and diffuse towards the surface. In both SI and TE, ionization occurs when a particular species is adsorbed onto the surface, however, the route the species took before adsorption on the surface is the fundamental difference between the two processes. It is my opinion that this difference calls for a distinction to be made between these two processes.

In this manuscript, thermionic emission will only be referred to as that process which produces emission of species which were originally a part of the solid matrix. The surface ionization process will include only those processes in which an external

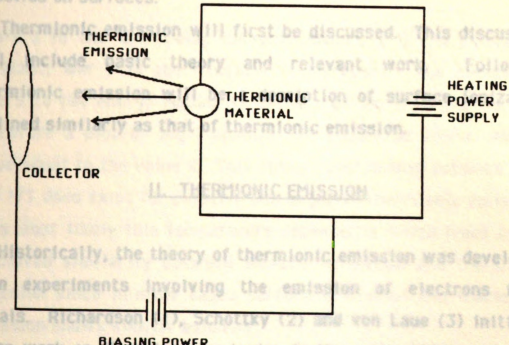


Figure 1. The Thermionic Emission Experiment.

source (not originally part of the solid matrix) of molecules directs them to a surface. This deposition can take place via the gas phase or by direct deposition of a solid onto the surface. These two different deposition modes alter those expressions characterizing surface ionization efficiency. Here, only the gas phase case will be considered since it has been more widely studied. Much work remains to be done on the surface ionization of solids on surfaces.

Thermionic emission will first be discussed. This discussion will include basic theory and relevant work. Following thermionic emission will be a desription of surface ionization outlined similarly as that of thermionic emission.

II. THERMIONIC EMISSION

Historically, the theory of thermionic emission was developed from experiments involving the emission of electrons from metals. Richardson (1), Schottky (2) and von Laue (3) initially began work on thermionic emission in the early 1900's. Fowler and Nordheim (4) developed the theory, based on the supposition that electrons within a metal behave as free particles. This theory is believed to be the cornerstone describing the emission of electrons from surfaces. A number of books and review articles concerning thermionic emission can be found (5-9). These references can be used for complete derivations of the formulae which will be presented. What is covered here is a brief introduction of several fundamental equations governing

thermionic emission with respect to temperature, surface composition, and applied fields. The thermionic emission of both positively (cations) and negatively charged (electrons, anions) species display a temperature dependence which can be described empirically as

$$i = f * \exp(-X/kt) \qquad (1)$$

where i is the thermionic current (Amps), k is the Boltzmann constant, and T is the absolute temperature. The constant X refers to the energy needed to extract an ion from the surface. Therefore a plot of log i against 1/T should be linear and the slope equal to the value X. This linear relationship between log i and 1/T does exist for positive and negative thermionic emission. It is most likely this temperature dependence which leads to the perceived similarity between surface ionization and thermionic emission since in many cases surface ionization and thermionic emission shows similar behavior.

The actual energy required for separating an electron from a surface is somewhat less than X and is called the work function (Φ); sometimes referred to as the thermionic work function. In addition, from emission data, equation 1 was modified to include a pre-exponential term which is moderately dependent upon temperature. This led to the expression

$$i = AT^2\exp(\Phi/kt) \qquad (2)$$

where A is a constant. At first it may be difficult to believe that equations 1 and 2 can be used to explain the same phenomenon. This is the case since the temperature dependence on emission is dominated by the exponential term. In fact, thermionic emission can be expressed by an equation which has the form

$$i = \text{constant} \times f(T) \times \exp(-E/kT) \qquad (3)$$

where f(T) is only moderately temperature dependent and E represents the energy involved in the emission of the charged species.

Several modifications of equation 3 led to the well-known Richardson-Schottky formula which is in terms of the emitted current density. Incorporated in this expression is the effect of electric field and the transmission coefficient, D. This expression is given in equation 4.

$$J\,(A/cm^2) = ADT^2\exp(-\Phi-(e^3F)^{1/2}/kT) \qquad (4)$$

Here A is a universal constant which is equal to 120 $Acm^{-2}K^{-2}$ and referred to as the Richardson constant. F and e refer to the electric field strength and electronic charge, respectively. D, the transmission coefficient, is a function of the reflection coefficient (r) such that D=(1-r). The reflection coefficient refers to that fraction of species which do not have sufficient thermal energies to surpass the potential barrier at the surface of the emitter. Generally, r is approximately zero when the

temperature exceeds 1000K so that D is unity. The importance of reflection coefficients has been discussed previously (8, 10-11). For simplicity, in any discussion using equation 4, D will be assumed to be unity.

The field strength term, $(e^3F)^{1/2}$, can have a small contribution to the energy term in equation 4 considering typical field strengths used for thermionic emission. In the field emission of electrons (high field strengths, lower temperatures) this term becomes more important. Consider the typical electric field ($6.5 \times 10^{-5} < F < 6.5 \times 10^{-3}$ V/Å) used in thermionic emission. This results in an energy between 0.03 eV and 0.3 eV. The contribution from this term would be more substantial for low work function materials which may be as high as ~20% of the work function. We can express pictorially the considerations important to the emission of an electron from a material (here a metal). Consider a free electron in a potential well as shown in Figure 2. The electron can occupy a variety of energy levels within the metal up to the Fermi level, the highest energy state in the metal an electron can have. The Fermi energy (E_F) is the energy of this particular state. The work function, Φ, is that energy difference between the Fermi level and some finite value, V, of the potential well of the metal. From this simple representation the effect of Φ, T, and field strength is evident. The work function is a property of the metal. Low work function metals can more easily emit electrons under similar conditions than a high work function metal. The Fermi level is temperature

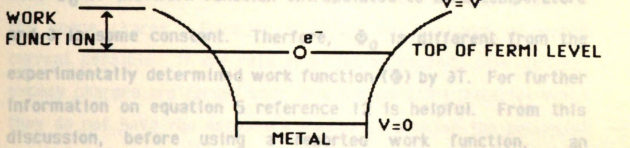


Figure 2. A Free Electron in a Potential Well.

dependent. Increasing the temperature lowers $V-E_F$ and at first may cause some confusion since it has been claimed that work functions are temperature dependent. The actual work function in equation 4 is actually slightly temperatue dependent as can be seen from equation 5

$$\Phi = \Phi_0 + \partial T \qquad (5)$$

Here Φ_0 is the work function extrapolated to zero temperature and ∂ is some constant. Therfore, Φ_0 is different from the experimentally determined work function (Φ) by ∂T. For further information on equation 5 reference 12 is helpful. From this discussion, before using a reported work function, an investigator should be aware of how the value was obtained and in what temperature range. Finally, the field strength affects electron emission by lowering the potential well in the metal. From Figure 2 and equation 4 it is easy to ascertain the variables which are important in the thermionic emission of electrons.

The thermionic emission of electrons has been shown to have an exponential dependence on temperature. It has been shown that thermionic emission does not follow Ohm's law, i.e., i varies with potential (V) to some power other than one. In the early 1900's Child (13) and Langmuir (14) independently investigated the dependence of the potential on emission which led to the well-known Langmuir-Child law or sometimes referred to as the three-halves power law. The equation, derived for two electrodes

consisting of parallel plates, is given as

$$i_a = 2.33 \times 10^{-6} V^{3/2}/x^2 \quad (A\ m^{-2}) \qquad (6)$$

where V is the potential difference between the plates in volts and x is the distance between plates in meters. Here i_a is the maximum current density. Equation 6 simply states that the actual current of the emitter (i.e., charged species which are collected) does not necessarily increase with emission due to the space charge. Equation 6 gives the maximum allowable current possible. If the rate of emission exceeds this current, excess charges are forced back into the emitting material since they do not have the necessary energy to surpass the potential barrier at the surface created by the space charge.

So far only thermionic emission of electrons has been considered; equation 4 applies to this case. Are there other factors which need to be taken into account in the thermionic emission of other negatively charged species and positive ions? The following is a discussion of these points.

Thermionic emission of positive ions has been studied from impregnated metals (15) and from aluminosilicates (16-17). Recently, the thermionic emission of negatively charged species other than electrons have been reported (18). A compilation of some thermionic properties of a variety of substances has also been made (9). Initial work on positive thermionic emission showed that thermionic current had a similar exponential

temperature dependence as in the emission of electrons. For this discussion equation 7 will be useful,

$$i = a\exp(-C/kT) \qquad (7)$$

where a is some constant and C is an energy term needed to describe the formation of the charged species. Early in the history of thermionic emission a number of investigators were perplexed by the behavior of heated metallic salts. These salts showed maxima and minima in log i versus temperature plots. Richardson, as well as others, believed this was due to chemical changes taking place in the solid and, in addition to this, the emission of more than one type of positive species (5). It was soon realized that these positive species were metal ions. This led to a new work function, Φ_p, called the positive-ion work function which refers to the work function involved in the extraction of a positive ion from a particular substance. Moon and Oliphant (19) are credited for initially calculating Φ_p for potassium on a clean tungsten surface.

Smith (20-21) applied a thermodynamic analysis to the positive emission from metals (e.g., tungsten). He considered the overall process as a combination of the heat of vaporization of a molecule, the ionization energy of the metal, and the work function of the metal. Therefore

$$C = I + X_A - \Phi \qquad (8)$$

where I is the ionization energy and X_A is the energy needed to transfer a neutral atom from the solid state to a gaseous state. If $C = \Phi_p = I + X_A - \Phi$ then experimentally determined values of Φ_p (from log i versus 1/T curves) can be compared to calculated values. In general, a relatively good agreement can be made between calculated and experimental values. This behavior has been recently reviewed by Scheer for the thermionic behavior of some transition metals for emission of both positive and negative metal ions (22). From Scheer's work a simple diagram showing which energies are involved in the emission of metal ions from the solid is shown in Figure 3. Here A refers to the electron affinity of species M and $I_\pm$ is, according to Scheer, the energy of positive or negative ion "sublimation". The value of $I_\pm$ would correspond to that of C in equation 7. From the thermodynamic cycle in Figure 3 we have

$$C = X_A + I - \Phi \qquad (9)$$

for positive thermionic emission and

$$C = X_A - A + \Phi \qquad (10)$$

for negative thermionic emission.

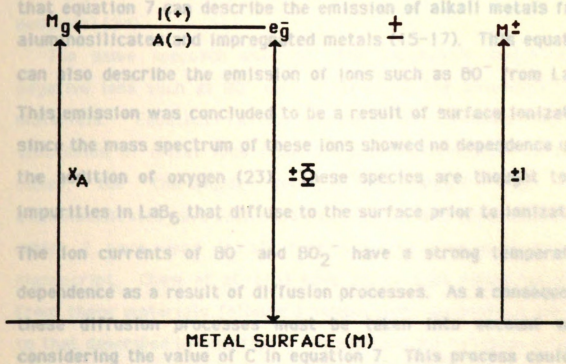


Figure 3. The Energetics Involved in the Emission of Gas Phase Metal Ions From the Solid Metal.

To this point only thermionic emission of electrons and positive/negative metal ions from pure metals have been described. What is the thermionic behavior when the emission of a charged species originates from a mixture? It has been shown that equation 7 can describe the emission of alkali metals from aluminosilicates and impregnated metals (15-17). This equation can also describe the emission of ions such as BO^- from LaB_6. This emission was concluded to be a result of surface ionization since the mass spectrum of these ions showed no dependence upon the addition of oxygen (23). These species are thought to be impurities in LaB_6 that diffuse to the surface prior to ionization. The ion currents of BO^- and BO_2^- have a strong temperature dependence as a result of diffusion processes. As a consequence these diffusion processes must be taken into account when considering the value of C in equation 7. This process could be described by E_D, the diffusion activation energy. In addition to E_D, the adsorption energy, E_A, of the species would also contribute to the energy term C from equation 7. Therefore this process could be described as follows

$$C = \Phi - A + E_D + E_A \qquad (11)$$

for negative ion emission and

$$C = I + E_D + E_A + \Phi \qquad (12)$$

for positive ion emission. Both of these processes can be shown graphically in Figure 4. The value of E_A can be between 0.2 eV (for physically adsorbed species) and 3 eV (for chemisorbed neutrals) (24).

The same approach used for the thermionic emission of negative ions such as BO^- can be taken for the aluminosilicate materials. Equation 12 and Figure 4 are suitable for the discussion of metal ions from the aluminosilicates. In most cases, the thermionic emission of alkali ions from aluminosilicates have been studied (15-17). It is these materials which I have used in all four projects discussed in this manuscript. Chow et al. (15) have shown that alkali emission from these materials follows a temperature dependence similar to that described by equation 7. In addition the emission follows the Child-Langmuir law (equation 6) similar to the emission of electrons from metals.

The emission characteristics of these emitters depend upon the composition, the type of aluminosilicate, and alkali metal used. The percentage of an alkali metal in the matrix has been shown to affect markedly the slope of log i versus 1/T curves. Blewett and Jones (17) have shown that the slope of these curves for a particular emitter decreased slowly with time, i.e., the emission was dependent upon the percentage of alkali metal present. They attributed this behavior to a change in work

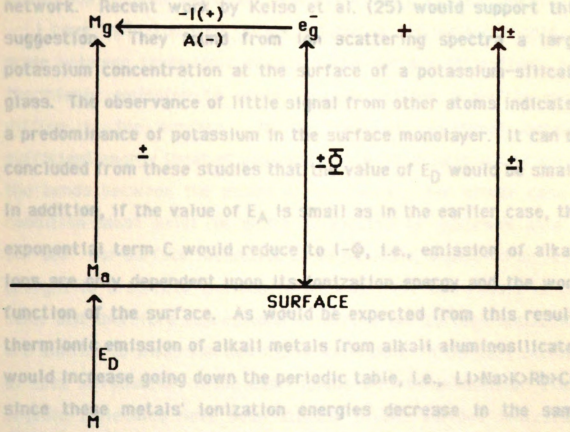


Figure 4. The Energetics Involved in the Emission of Gas Phase Metal Ions From an Aluminosilicate Surface.

function without considering other possible alternatives. Consider the possibilities from equation 12. What is known about the diffusion of alkali metals in these matrices (E_D)? Blewett and Jones suggested that the alkali metal is free to migrate to the surface due to the structure of the aluminum-oxygen-silicon network. Recent work by Kelso et al. (25) would support this suggestion. They found from ion scattering spectra a large potassium concentration at the surface of a potassium-silicate glass. The observance of little signal from other atoms indicated a predominance of potassium in the surface monolayer. It can be concluded from these studies that the value of E_D would be small. In addition, if the value of E_A is small as in the earlier case, the exponential term C would reduce to $1-\Phi$, i.e., emission of alkali ions are only dependent upon its ionization energy and the work function of the surface. As would be expected from this result, thermionic emission of alkali metals from alkali aluminosilicates would increase going down the periodic table, i.e., Li>Na>K>Rb>Cs, since these metals' ionization energies decrease in the same direction. Experimentally, the emission of alkali metals follow the trend in ionization energies.

I have discussed the thermionic emission of electrons from metals and introduced several fundamental equations describing this behavior. The emission of other species, both positive and negative, was similar to this behavior but required some modification to the electron emission formulae. Figures 3 and 4 can be used constructively to envision the important processes

involved in thermionic emission. The projects that will be described in this work rely on these thermionic emitters, however, do not involve research entailing the development of new emitters or a theoretical investigation of thermionic emission. These pursuits would be worthwhile in light of the many uses of these materials, some of which are discussed here.

I have indicated why, in my opinion, a distinction should be made between thermionic emission and surface ionization. For thermionic emission to occur, species within a matrix must diffuse to the surface. In the case of condensed metals, sufficient energy (heat of sublimation) must be supplied to break the bonds between the atoms of the metal. For either case a condition must exist in which a species is adsorbed onto a surface. For surface ionization to be possible, a species must be brought to a surface and adsorb onto it. The end result is the same and therefore expressions developed for surface ionization are similar to those for thermionic emission. In the last section of this introduction these expressions will be presented. Many organic molecules have been studied in the surface ionization experiment. It is these molecular species which are of importance in this manuscript and, therefore, this description of surface ionization will primarily focus upon these.

III. SURFACE IONIZATION

A. POSITIVE SURFACE IONIZATION

A number of excellent review articles can be found for positive and negative surface ionization involving theory (7, 26-28) and experimental results (7, 29-31). This description will be divided into two sections; positive and negative surface ionization. The theory of positive surface ionization (PSI) will first be described using simple models. These models usually involve beams of atoms hitting a hot metal surface. A more complex system, as will be described, exists for molecular systems.

The phenomenon of surface ionization can be divided into three distinct stages: the arrival of a species to the surface; adsorption; and evaporation (desorption). Here adsorption refers to a condition in which the adsorbed species is in charge and thermal equilibria with the surface. The evaporation of the species determines its charge. Simply, an electron competes between the surface and the desorbing atom or molecule. For atomic neutrals a simple relationship has been derived which discribes the efficiency of surface ionization. This equation is the well-known Saha-Langmuir relationship given in equation 13 (32-33). A simple and clear derivation of this expression can be found elsewhere (34).

$$N^+/N = [(1-r_+)w_1/(1-r_0)w_0]\exp(\Phi-I/kT) \qquad (13)$$

In equation 13, r_+ and r_0 are the reflection coefficients of the positive ion and neutral, respectively. The terms w_1 and w_0 refer to the statistical weights of the ion and neutral respectively. When Φ and I are expressed in units of electron volts (eV) equation 13 can be expressed as follows.

$$N_+/N = [(1-r_+)w_1/(1-r_0)w_0]\exp[11600(\Phi-I)/kT] \qquad (14)$$

Using equation 14 we can calculate the efficiency of ionization for several alkali metals. Consider the system of an alkali metal placed on a tungsten filament and heated to a temperature of 1500K. Typical values of I for lithium, potassium, and cesium are 5.38, 4.34, and 3.90 eV, respectively. The work function of tungsten is 4.5 eV (9). The reflection coefficients r_+ and r_0 are zero; the ratio of statistical weight w_1/w_0 is 1/2 for the alkali metals. Using these values in equation 14 the percent of species leaving the surface as positive ions is 0.06%, 63%, and 98% for lithium, potassium, and cesium respectively.

Equation 13 applies only in the absence of an electric field. The thermodynamic equilibrium between an atom and the surface is altered so that equation 13 must be modified. This is similar to the case in which the Richardson-Schottky formula (equation 4) is necessary to describe the thermionic emission of an electron in the presence of an electric field. The electric field (F) reduces the energy difference between the work function and

the ionization energy of the atom, i.e., the field opposes the attraction of an ion to the surface. Equation 13 can then be altered to give the following approximate expression.

$$N^+/N \approx [(1-r_+)w_1/(1-r_0)w_0]\exp[(\Phi-I+(e^3F)^{1/2})/kT] \quad (15)$$

This equation is only an approximation since several terms which are dependent upon the polarizabilities of the atom and ion are neglected. If the electric field is less than 10^6 V/cm this approximation is valid.

Thermodynamically, surface ionization of an atom can be represented as follows:

PROCESS	ENERGY	
$M_S \rightarrow M$	(EA, +3eV)	(16)
$M \rightarrow M^+ + e^-$	(+I)	(17)
$e^- \rightarrow e_S^-$	(Φ, -5eV)	(18)
$M^+ \rightarrow M_S^+$	(EI, -3.6eV)	(19)

Equations 16-19 describe the overall process $M_S \rightarrow M_S^+ + e_S^-$ where the subscript s refers to the surface and the absence of any subscripts denotes a gas phase species. The term E_I is the heat of adsorption for an ion. E_I can be estimated using the following

$$E_I = 3.60/r_I \quad (eV) \qquad (20)$$

where r_I is the ion radius in angstroms. Equation 20 is derived from the fact that an ion is attracted to a metal surface by an image force equal and opposite in sign to the ion. The image force obeys Coulomb's law. Equation 20 is only an approximation since it considers an ion as a sphere of radius r_I. This approximation is better for atomic ions (e.g., K^+) than polyatomic ions since r_I's for the latter are more difficult to obtain. In equation 19 r_I is assumed to be 1 angstrom. From a thermodynamic standpoint the highest ionization energy (I) that the system will allow is 5.6 eV. This value is above all the ionization energies for the alkali metals.

To this point we have only considered the Saha-Langmuir equation for atomic species. This equation determines the "efficiency" of ionization of atoms adsorbed on a surface in which equilibrium has been established. A more useful expression would be an equation for the current generated due to surface ionization. We will call this value i_S. Consider an incident flux of atoms N_0 to the surface. Evaporating from the surface will be positive ions and neutrals characterized by the fluxes N_+ and N, respectively. We will define two new terms, the ionization efficiency α, and β, the ionization coefficient. These terms are defined as

$$\alpha = N_+/N \tag{21}$$

and

$$\beta = N_+/N_0 \tag{22}$$

If the atomic flux N_0 is equal to the evaporating flux (steady state condition) then $N_0 = N + N_+$ and α and β are related to each other by the relation

$$\beta = (1 + 1/\alpha)^{-1}. \tag{23}$$

The current can then be expressed by

$$i_S = eN_0\beta Z \tag{24}$$

where Z is the area of the emitting surface. Using equations 15, 23, and 24 the equation for i_S becomes

$$i_S = eN_0Z/[1 + C\exp(I-\Phi-(e^3F)^{1/2}/kT)] \tag{25}$$

where C equals $(1-r_0)w_0/(1-r_+)w_1$. This equation can be simplified if two cases are considered. If the ionization energy is high in relation to Φ then $[I-\Phi-(e^3F)^{1/2}] >> kT$ and equation 25 becomes

$$i_s \approx eN_0Z(1/C)\exp[(\Phi + (e^3F)^{1/2} - 1)/kT]. \qquad (26)$$

For the second case, where ionization is favored ($\Phi>1$), the term $[\Phi+(e^3F)^{1/2}-1]$ is much greater than kT and equation 25 becomes

$$i_s \approx eN_0Z \qquad (27)$$

and i_s is practically independent of T and F in their possible ranges.

Up to this point only homogeneous surfaces have been considered. This is not usually the case. For most metals the surface is comprised of several different crystal faces. The work functions of each of these faces can be different, e.g., for tungsten there is a 1.8 eV difference in work function between a (110) face and a (116) face (26). Frequently, inappropriate use of equations 13 and 25 lead to erroneous conclusions. Consider an inhomogeneous surface containing a collection of unique regions Z_k each with a work function Φ_k. Equation 25 can be rewritten to account for the inhomogeneity of the surface; then

$$i_s = \Sigma eN_0Z/[1 + C\exp[(1-\Phi-(e^3F)^{1/2})/kT]]. \qquad (28)$$

For the case when $(1-\Phi_{k(max)}-(e^3F)^{1/2})$ is much greater than kT, equation 26 becomes

$$i_s = eC^*\exp[(\Phi^* + (e^3F)^{1/2} - I)/kT] \quad (29)$$

where

$$C^* = (1/C)N_0\Sigma Z_k\exp[(\Phi_k - \Phi^*)/kT]. \quad (30)$$

The work function Φ^* is called the effective work function and lies between $\Phi_{k(min)}$ and $\Phi_{k(max)}$. Its value depends upon the number of regions with a work function Φ_k. The temperature dependence of C* is much weaker than the exponential term $(\Phi^*+(e^3F)^{1/2}-I)/kT$ and a plot of i_s against 1/T will be a straight line. This seems contradictory since C* contains an exponential term, however, the sum contains terms of opposite sign, and, thus is much less temperature dependent. When $(\Phi_{k(min)}+(e^3F)^{1/2}-I)>>kT$ equation 27 still holds and it is independent of temperature, field strength, and work function.

In most cases I will be at a value between $[\Phi_{k(min)}+(e^3F)^{1/2}]$ and $[\Phi_{k(max)}+(e^3F)^{1/2}]$ and, therefore, i_s can show increasing or decreasing behavior against 1/T. For this case C* becomes complex and differs from equation 30 since two summation terms must be included. One summation term includes those areas on the surface where $(I-\Phi k-(e^3F)^{1/2})>>kT$ applies; the other term is for those areas in which this relation does not apply. A graph of is as a function of 1/T may deviate from a straight line, being

either convex or concave. Deviations will depend upon the temperature dependence of C*.

Most surface ionization experiments are carried out on non-homogeneous surfaces. Often this point is neglected and erroneous conclusions are made. The summary of surface ionization results of atomic species on inhomogeneous surfaces can be summarized briefly here. The Saha-Langmuir equation (equation 13) cannot be used to describe surface ionization of atoms on inhomogeneous surfaces. The work function determined for inhomogeneous surfaces is the effective work function Φ^* and can be shown to be dependent on temperature, electric field strength, and ionization potential of the atom (i.e., $\Phi = f(T,F,I)$). Importantly, Φ^* does not have to agree with Φ_e^* where Φ_e^* is the effective electronic work function. Finally, to calculate reflection coefficients, C* and C have been confused (11). As indicated by this description, these two quantities cannot be considered as equal.

Atomic species, once they attain equilibrium with the surface, can either desorb as an ion or as the neutral. Molecular species are more complex. They can form i species on the surface each with some probability of desorbing as an ion. Consider a molecular flux ν arriving on a surface with i effective fluxes ν_i, each producing species of only one kind. The relation between ν and ν_i is then

$$\nu_i = \gamma_i \nu \qquad (31)$$

where γ_i is a coefficient dependent upon the molecule and emitting species. This coefficient describes what ratio of the incoming flux has been made suitable to be considered for the ionization of species i. This term is dependent upon temperature and the electric field strength. We treat the ionization of each ith species separately from any other, i.e., the surface ionization of one species is independent upon the ionization of another species.

Much like before we can define the ionization efficiency as

$$\alpha_i = \nu_i^+/\nu_i^0 \tag{32}$$

and the ionization coefficient as

$$\beta_i = \nu_i^+/\nu_i. \tag{33}$$

The current then can be expressed by

$$i_s = e\nu\gamma_i\beta_i Z. \tag{34}$$

Using equations 15, 31, 32, and 33 the equation for i_s becomes

$$i_s = e\nu\gamma_i Z/[1 + C_i\exp[(I-\Phi-(e^3F)^{1/2})/kT]]. \tag{35}$$

As before, this equation can be simplified if two cases are

considered. If the ionization energy is high in relation to Φ then $[I-\Phi-(e^3F)^{1/2}]>>kT$ and equation 35 becomes

$$i_s \approx e\nu\gamma_i Z(1/C)\exp[(\Phi + (e^3F)^{1/2} - I)/kT]. \qquad (36)$$

The second case, where ionization is favored ($\Phi>1$), the term $[\Phi+(e^3F)^{1/2}-I]$ is much greater than kT and equation 35 becomes

$$i_s \approx e\nu\gamma_i Z. \qquad (37)$$

In equation 37 is is still dependent upon the electric field strength and temperature since γ_i is dependent upon these parameters.

As for atomic species, the surface ionization of molecular species on inhomogeneous surfaces must be expressed differently than in equation 35. The parameters Φ, γ_i, and C are replaced by the effective parameters of Φ^*, γ_i, amd C_i^*. The coefficient γ_i must be considered here since, in most cases, a molecule may "react" differently on various patches on the surface. For the surface ionization of molecules on inhomogeneous surfaces we can simply replace N_0 in equation 28 with $\nu\gamma_i^*$ and follow through with the same reasoning to describe surface ionization of atomic species on inhomogeneous surfaces. As an example, for the case $(I-\Phi-(e^3F)^{1/2})>>kT$ equation 35 becomes

$$i_s \approx eC_i^* \exp[(\Phi^* + (e^3F)^{1/2} - I)/kT] \qquad (38)$$

where

$$C_i^* = (1/C_i)\nu\gamma_i^* \Sigma\{Z_k \exp[(\Phi_k - \Phi^*)/kT]\}. \qquad (39)$$

The terms in equations 38 and 39 have the same meaning as before.

Equation 34 only considers the current for one species. The total surface ionization current, i_s^{tot}, is the summation of all currents from each respective ith species. The total current is then

$$i_s^{tot} = \Sigma e\nu\gamma_i\beta_i Z. \qquad (40)$$

Equation 40 is therefore a complex function since each neutral-ion pair will have a set of γ_i and β_i values whose temperature and electric field strength dependence will be different. Since this is the case, generally each neutral-ion pair is considered separately. Here, mass spectrometry can be a powerful tool since one ion can be selected and monitored independently of the others.

Thermodynamically, the positive surface ionization of organic molecules can be represented by a series of equations similar to those in equations 16-19. The overall surface ionization process

for a molecule AB can be represented by $AB_S \rightarrow A_S^+ + e_S + B_S$. The subscripts used are the same as before (equations 16-19). Equations leading to this result are listed as follows.

PROCESS	ENERGY	
$AB_S \rightarrow AB$	(E_A(AB),+0.2 eV)	(41)
$AB \rightarrow A + B$	(D(A-B), +2 eV)	(42)
$A \rightarrow A^+ + e^-$	(I)	(43)
$e^- \rightarrow e_S^-$	(Φ, -5 eV)	(44)
$B \rightarrow B_S$	(E_A(B), -3 eV)	(45)
$A^+ \rightarrow A_S^+$	(E_I, -3.6 eV)	(46)

Typical values of EA and D(A-B) are used here. A molecule usually is physically adsorbed which leads to the low E_A value in equation 41. Typically, a part of the molecule (here B) is chemisorbed on the surface, thus, the much higher value of E_A in equation 45. Here a value of 3.6 eV is used for E_I assuming a radius of 1 Å (see equation 20). In this example the ionization energy of fragment A must be less than 9.4 eV on this 5 eV work function surface.

The thermodynamic approach just described is a simplification of positive surface ionization. The energy associated with the ionic desorption of A^+ from the surface is only approximated here. In reality, for a large number of species,

this value is unknown. In addition, it has been shown that a correlation does not exist between the dissociation energy (D(A-B)) and surface ionization (35). This would be expected if the products are ionized after establishment of equilibrium. One cannot predict that a compound would yield more current than another compound based on these thermodynamic relationships. Some fraction of molecules striking the surface will be ineffectual, i.e., may produce an ith species but not in charge and thermal equilibrium with the surface. We have already defined a function (equation 31) which describes those species which are effective (i.e., in equilibrium with the surface). This function, ν_i, is determined by the rate of the chemical reaction, the surface temperature, and the electric field strength. The function ν_i must be determined experimentally.

A number of equations and associated principles have been presented. In the preceding paragraph I have presented some points that a simple energetic approach does not consider. This section is not meant to deter anyone from using an approach such as this, but rather to indicate possible areas where it can fail. The following is an attempt to put surface ionization theory into perspective and to indicate the types of applications where surface ionization can be useful.

1.) Simple energetics give a clue as to what might be expected. The relationships between ionization energy and work function, for example, indicates the <u>possibility</u> of forming an ion. For atomic species, ionic desorption energies can be better

approximated and, therefore, easier to describe energetically (equations 16-19). In general, the surface ionization of atomic species, when compared to molecules, is much simpler system since the atom must either desorb as a neutral or an ion. A molecule can desorb, ionize, or react on the surface.

2.) When considering the work function for a particular surface, one needs to know how they were obtained and the condition of the surface. In most cases nonuniform surfaces are studied. These surfaces are best characterized by the effective work function, Φ^*. The effective work function is a weighted average of the work functions of different areas on the surface. How would Φ^* be affected if a change is made to the surface? Would certain areas be unchanged and others altered remarkedly? Questions such as these are not yet fully answered.

3). Perhaps the largest unknown in the surface ionization of molecular species is the minimal amount of knowledge of surface chemical reactions. The fate of a molecule on a hot surface determines the extent of surface ionization and what ionic species are produced. Little is known as to residence times of species on hot surfaces, a parameter needed for a kinetic treatment of polyatomic ion desorption characteristics. Presently, the effective flux ν_i must be determined experimentally. Perhaps with further experimental results this parameter can be calculated <u>a priori</u>. In order for this to be accomplished the chemistry of a molecule on the surface must be totally understood.

4). Even though surface ionization has been known for some

time the many uses of this technique have not yet reached their full potential. The experimental determination of values found in SI expressions are the basis for the physical investigation of many properties of solids, ionizable species, and fundamental characteristics of the interaction between a species and a solid. Surface ionization can be used for the determination of ionization energies, electron affinities, desorption energies of neutral and ionic species, solid phase transitions, and the study of heterogeneous chemical reactions. In addition to applications in physical chemistry, surface ionization is useful in analytical chemistry. Here the theory is sufficient to provide a foundation for the analysis of certain organic molecules and their structural elucidation. Most of the early surface ionization experiments considered only atomic species. More recently organic molecules have been investigated. These investigations include nitrogen-containing compounds (29, 35-48), phosphorus compounds (29, 49), and arsenic compounds (49). Most of these studies have been done on tungsten or oxidized tungsten surfaces. Other solids such as molybdenum, nickel, rhenium, and platinum have been used (50-52).

Experimental and theoretical aspects of surface ionization began with the emission of positive ions. So far this introduction has focussed only on positive SI of atomic and molecular species. Many principles of positive SI can be applied to negative surface ionization (NSI). The following is a brief discussion of NSI which will rely on the previous discussion of positive SI.

B. NEGATIVE SURFACE IONIZATION

If we consider the following equilibrium of an atom A on a hot surface

$$A + e_s^- \rightleftarrows A^- \qquad (47)$$

an analogous equation for NSI can be derived which is comparable to that for positive SI (equation 13).

$$\alpha = N^-/N = [(1-r^-)w^-/(1-r)w]\{\exp(A+(e^3F)^{1/2}-\Phi')/kT\} \qquad (48)$$

where all the terms used here are as before except they relate to the negative ion. The effective work function Φ' does not necessarily correspond to Φ^* for positive SI but is defined as an average work function effective for producing the negative ion. If the Schottky term ($(e^3F)^{1/2}$) can be neglected (as usually is the case for low field strengths) and if $\Phi' = \Phi$, equation 48 becomes the well-known Saha-Langmuir equation for NSI.

$$\alpha^- = (w^-/w)\exp[(A - \Phi)/kT] \qquad (49)$$

In the derivation of equation 48 the reflection coefficients r and r^- are assumed to be zero. This assumption has not been verified either experimentally or theoretically however, for positive

surface ionization r^+ and r are considered zero in the temperature range above 1000 K. By analogy this has been carried over to NSI. The statistical weights of ions and atoms can be calculated using an expression derived by Scheer and Fine (53). As mentioned before w^+/w has an approximate value of 0.5 for the alkali metals. Using the equation in reference 56, w^-/w for halogens has an approximate value of 0.25.

An expression for the current, i_s^-, produced by negative surface ionization can be obtained in a similar fashion as positive SI. The ionization coefficient β^- is defined as

$$\beta^- = [1 + (1/\alpha^-)]-1 \qquad (50)$$

and the current i_s^- can then be expressed by

$$i_s^- = eN_0\beta^-Z. \qquad (51)$$

Using the equations of 48 and 49, equation 51 becomes

$$i_s^- = eN_0Z/[1 + C'\exp[(A + (e^3F)^{1/2} - \Phi')/kT]]; \qquad (52)$$

the NSI analogue of equation 25. Here C' equals $(1-r_0)w_0/(1-r^-)w_1$.

The negative surface ionization of polyatomic species is analogous to positive SI. Since this is the case the ionization

efficiency and ionization coefficient can be written, respectively, as

$$\alpha^- = (N^-/N) = (1/C')\exp[(-\Phi' + (e^3F)^{1/2} + A)/kT] \qquad (53)$$

and

$$\beta^- = (N^-/N) = \nu\gamma_i[\alpha^-/(1 + \alpha^-)] \qquad (54)$$

where ν_i and γ_i have the same meaning as before. The NSI current can be appropriately expressed by the equation

$$i_s^- = eN_0\beta^- Z = eN_0\nu\gamma_i Z[\alpha^-/(1 + \alpha^-)]. \qquad (55)$$

A description of any simplifying approximations will not be considered here as was done for positive SI and for equation 35. Some authors (28) prefer to include a parameter σ into equation 55 which accounts for the "sticking" probability of a molecule to the surface. It is difficult to evaluate σ due to the lack of sufficient thermochemical data and often σ is assumed to be unity. This is the case when the coefficient γ_i is determined. It seems arbritrary to set aside this parameter (σ) since, in reality, γ_i sufficiently encompasses the process of forming a species capable of ionizing on the surface.

At this point in this discussion of NSI it should be clear that

the principles of NSI parallel those of positive surface ionization. It is unnecessary to parallel each positive SI equation with a corresponding NSI partner. I have defined a number of work functions to this point and perhaps it is now necessary to reevaluate this parameter since it is crucial in all expressions for surface ionization and thermionic emission. Below is a list of work functions used thus far in this discussion.

Φ	work function (thermionic emission of electrons from a homogeneous surface)
Φ_i	work function for area i on an inhomogeneous surface
Φ_p	positive ion work function for thermionic emission
Φ_e^*	effective electronic work function (inhomogeneous surface)
Φ^*	effective work function for positive ion formation (inhomogeneous surface)
Φ'	effective work function for negative ion formation (inhomogeneous surface)
Φ_e'	effective electronic work function in presence of a sample on an inhomogeneous surface

The energy required to remove an electron from a surface is given by the work function. Should this energy be equivalent for

all processes of surface ionization and thermionic emission on a particular surface? It has been determined that these work functions listed above are not equal to each other and in some cases are remarkably different. For example, when tungsten (Φ_e^* = 4.48 eV) is exposed to tetracyanoethylene Φ_e' was found to be 2.70 eV (54). Consequently, as is sometimes the case, the approximation that $\Phi_e' \approx \Phi_e^*$ is made for the calculation of the ionization efficiency or the ionization coefficient. Such an assumption can lead to a substantial error in these calculations. Recently, researchers in surface phenomena have begun investigating the role of surface processes in regards to changes in work function (55-56).

It should not be suprising that all the various types of work functions are not equivalent since each is associated with a particular surface process. For NSI an electron is transferred to an adsorbed neutral. In positive surface ionization an adsorbed species "loses" an electron to the surface. For the case of Φ_e' and Φ_e^* can we expect a surface to remain the same in the presence or absence of an adsorbing species? All these processes are different so one would not expect one common work function. In this text I will refer to the work function as that energy involved in the transfer of an electron to or from the surface for any system (e.g., NSI, thermionic emission, etc.). Comment 2 made earlier in this section should be reinforced here. Often, the term "work function" is used loosely. When a "work function" is

calculated, it should be made clear as to the circumstances under which the value was obtained.

An energetic treatment of NSI can be made in a similar fashion as was done for positive SI (see equations 41-46). Here, we will consider the production of a negative ion B- in an overall surface reaction given by

$$e_S^- + AB_S \rightarrow A_S + B_S^-. \qquad (56)$$

The series of equations representing negative surface ionization are

PROCESS	ENERGY	
$AB_S \rightarrow AB$	($E_A(AB)$, +0.2 eV)	(57)
$AB \rightarrow A + B$	(D(A-B), +2 eV)	(58)
$e_S \rightarrow e$	(Φ, +5 eV)	(59)
$e + B \rightarrow B^-$	(A, +0.6 eV)	(60)
$B \rightarrow B_S^-$	(E_I, -3.6 eV)	(61)
$A \rightarrow A_S$	($E_A(A)$, -3.0 eV)	(62)

When typical values are used as before (see equations 41-46), the minimum electron affinity calculated for ionization is 0.6 eV. Here, using the same arguments for positive SI, this simple energetic treatment can be useful in determining if a species is capable of ionization. Recently, large compilations of electron affinities for atomic, radical, and molecular species have become

available (31, 57).

IV. FINAL COMMENTS

This introduction is perhaps over-zealous in regards to the discussion of the following projects. I believe I have accomplished the objective of distinguishing the difference between thermionic emission and surface ionization. In addition, with regard to some of the proposed equations, the complexity of these seemingly simple processes is presented. The work function has been discussed and, perhaps from this introduction, a better understanding of this parameter can be perceived.

This introduction may prove useful for those who "follow in my footsteps" by aiding in the investigation of other solids for surface ionization or as thermionic emitters in the particular applications which will follow.

CHAPTER 2. POTASSIUM ION CHEMICAL IONIZATION AND OTHER USES OF AN ALKALI THERMIONIC EMITTER IN MASS SPECTROMETRY

I. INTRODUCTION

When mass spectrometry (MS) is used for chemical analysis, molecular weight, functional group, and structural information can frequently be obtained. Of these, molecular weight information (i.e., the detection of a molecular ion, $M^{+\cdot}$) is usually the most valuable, because it determines both the elemental composition and the "molecular boundaries into which the structural fragments indicated in the mass spectrum must be fitted" (58). Unfortunately, for a number of reasons, many compounds do not form detectable amounts of the molecular ion following electron impact (EI) ionization (58).

Chemical ionization (CI) is another common technique available to mass spectrometrist (59). Chemical ionization is considered one of the "soft" ionization methods, since it usually induces less fragmentation that does EI, simplifying the mass spectrum. Also, the protonated parent, MH^+, is frequently formed - i.e., molecular weight information is produced. Munson and Field (60) were the first to demonstrate the analytical applications of CI by using CH_4 as a reagnet gas and generated spectra in which the analyte molecules reacted with CH_5^+ and $C_2H_5^+$ (the "reagent ions") in the gas phase. Since this work, many other species have been used as CI reagents. Proton

transfer reagents such as H_3^+ will react with most compounds since the proton affinity (PA) of H_2 is low (approximately 101 kcal/mol). Isobutene has a much higher PA (195 kcal/mol); therefore i-C_4H_{10} CI only protonates molecules with PA's greater than approximately 195 kcal/mol. Thus, the proton affinity of the species used in CI is the "working variable" which can be adjusted to provide a "universal" or selective ionization method.

Charge exchange (CE) chemical ionization is another CI alternative. In CE, ions such as Ar^+, N_2^+, or CO^+ react with analyte molecules by electron transfer. As in proton transfer CI, varying the reagent varies the response-in CE, the variable is not proton affinity, but instead ionization potential.

The popularity of CI is due in part to its compatibility with most MS techniques. Unlike other ionization methods such as field desorption (which usually requires a double focusing magnetic mass spectrometer) CI can be performed with most types of mass spectrometers. Also, CI is compatible with chromatographic inlet systems (i.e., gas chromatography GC/MS, liquid chromatography LC/MS).

In spite of the many advantages of CI, there are a number of disadvantages. An $(M+1)^+$ ion is not always observed in CI (as is often the case with alcohols) and a parent ion is not always observed in CE. Also, it is difficult to catalog CI spectra because they can be strongly pressure dependent. Pressure effects arise in many ways. Frequently, more than one reactive species is

generated in CI sources (e.g., CH_5^+ and $C_2H_5^+$ in methane CI, CO^+ and $(CO)_2^+$ in carbon monoxide CE). THe relative amounts of these reagent ions vary with pressure. Also, product ions can be collisionally stabilized at high pressures. Thus, small pressure changes can dramatically affect the number and relative intensities of ions in a CI mass spectrum.

In part, this section of the dissertation discusses the use of metal ions, here K^+, as CI reagent ions. Studies presented here show that K^+ reacts with most types of molecules (M) to from the "pseudomolecular ion" $(M+K)^+$; i.e., molecular weight information is easily obtained. By the technique described, metal ions can be generated (with a selected kinetic energy) in the absence of corresponding neutrals-providing the basis for a relatively low pressure CI method.

Recently, a large body of literature has appeared concerning the gas phase chemistry of metal ions with organic molecules. Both transition-metal and alkali ions have been studied (61-63).

Transition-metal ions can be generated in the gas phase by EI on organometallic compounds (64) or by laser desorption/ionization from solid surfaces (65). The chemistry of gaseous transition-metal ions with organic molecules is rich, often producing products which provide both molecular weight and structural information.

In contrast, alkali ions generally react by simpler mechanisms (61-63). Ions such as Li^+ form electrostatic complexes with many analytes such as π-donor bases (e.g., benzene) and n-donor

bases (e.g., ethers). Adduct ions (also referred to as "cationized molecular ions") of the type $(M+Na)^+$ have also been reported (61-63). Alkali metal ions appear to be useful CI reagents for obtaining molecular weight information due to the low IE's of these metals. In the case of the $(M+K)^+$ adduct, for example, the charge presumably remains localized on the metal. Thus, the decomposition pathway with the lowest activation energy is simply the loss of K^+, instead of the fragmentation of the attached molecule. The probability of a metal induced reaction relative to attachment appears to decrease as the metal is varied from Li^+ to K^+ (61-63).

As mentioned earlier, Blewett and Jones (17) described a convenient method for producing metal ions in the gas phase. Metal ions are produced by heating and biasing a glass or metal oxide. The glasses are usually metal oxides in an aluminosilicate matrix. Oxides such as In_2O_3 behave similarly. Thermionic emission sources were reported for 17 metal ions. Those for alkali metals are particularly copius emitters.

This part will focus on uses of thermionic sources of K^+ ions. A simple, low cost method is presented for producing variable energy metal ions for use as CI reagents. The method is adaptable to any mass spectometer with a CI source and direct inlet probe. In addition, alternate modes of operation are presented which will provide additional dimensions of mass spectral information.

II. EXPERIMENTAL

All experiments were performed on an unmodified Hewlett-Packard 5985 GC/MS/DS, equipped for manual tuning as described elsewhere (66). Thermionic emitters were mounted on a fabricated probe assembly and inserted into the CI volume of the ion sourve through the direct insertion probe inlet (see Figure 5). The tip of the thermionic emitter was made by inserting 0.007 in. (0.178 mm) rhenium wire through a 0.5 in. (1.30 cm) length of two-holed ceramic rod of 0.047 in. (1.19 cm) diameter. The ceramic rod gives mechanical stability to the probe tip and insulates the rhenium wire from the ion source. A small loop of the rhenium wire extends from one end of the ceramic rod. The two free ends of this wire are spot-welded onto insulated leads housed within the probe assembly.

"Thermionic K^+ glass" has the composition $1K_2O:1Al_2O_3:2SiO_2$. Its preparation has been described elsewhere (17). The wire loop on the probe tip is dipped into a molten mixture of the thermionic glass, withdrawn, and allowed to cool. This procedure produces a bead of glass (approximately 0.030 in. (0.76 mm) in diameter) on the wire loop. This bead is small enough to fit through an existing hole in the CI source volume and was sufficient for at least 40 hours of continuous operation.

A 0-4 A, low-voltage power supply is used to resistively heat the thermionic glass bead on the wire loop. A 0-20 V, low-current power supply biases the bead positively with respect to the CI volume. Biases from 0 to +20 V were used in these

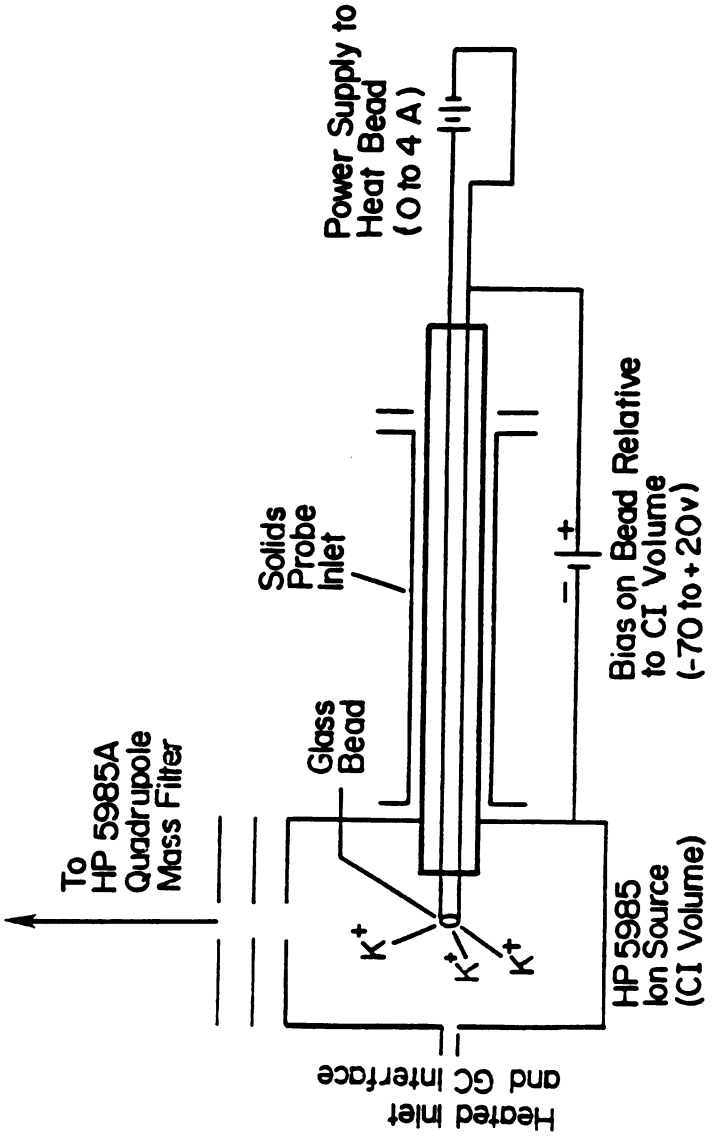


Figure 5. Schematic Diagram of Thermionic Emission Probe in the Mass Spectrometer's Ion Source.

studies. For EI studies using the K^+Cl probe, the emitter was biased from -20 to -70 V with respect to the CI volume. A current of 1.5 to 2.0 A through the wire is sufficient to induce thermionic emission from the glass.

The GC oven was used as a heated gaseous batch inlet. Most samples were introduced through the "capillary direct" port of the GC/MS interface. Typical pressures in the CI volume were between 20 to 700 mtorr as measured by a thermocouple gauge mounted on a stainless steel tube which was brought into contact with the CI volume through the direct insertion probe inlet. The GC studies were performed with a 6 ft. x 1/16 in. glass column packed with 3% OV-101, interfaced to the ion source through the jet separator. Helium was used as a carrier gas at a flow rate of 30 ml/min. Temperature programmed runs (50-100 ^{0}C., 5 ^{0}C/min) were used.

Experiments involving direct introduction of thermally labile samples on the probe were performed by using a saturated solution in methanol, depositing a drop on the glass bead, and drying. In these experiments, it was found that a thin coating of glass on the rhenium wire worked better than a larger glass bead. All (commonly available) chemicals were ACS reagent grade and were used without further purification. All peptides were obtained from Sigma Chemical Co. The crown ethers were obtained from Aldrich Chemical Co. All were used without additional purification except for outgassing liquid samples with several freeze-pump-thaw cycles.

III. RESULTS AND DISCUSSION

Results of K^+Cl experiments are presented here. Also, a number of alternate uses of the K^+ emitter probe will be suggested.

When the probe as described is inserted into the CI volume of the mass spectrometer, heated , and biased, K^+ ions are formed with no apparent rise in pressure. In addition to the dominant K^+ peak in the spectrum, small amounts of sodium, cesium, and rubidium ions are formed.

In most cases, when organic vapors are admitted into the CI volume, only $(M+K)^+$ ions are formed. Most n- and π-donor bases produce especially intense cationized species. The K^+ addition process is kinetic energy dependent. Addition products are observed when the K^+ emitter bead is biased relative to the CI volume only in a "bias window" ranging from 0.5 V to approximately 5 V. The exact value of the upper voltage cutoff depends upon the particular compound. Figures 6-9 show K^+ CI spectra for molecules representative of four organic function groups. Of the more than 30 compounds studied (see Table 1), K^+Cl produced $(M+K)^+$ as the only product, except in a few cases. No products were formed with cyclohexane. Alkylamines and 2-propanol give more complex spectra. On the basis of these observations, K^+Cl may be superior to other CI techniques for obtaining molecular weight information.

The formation of an addition product in the gas phase has been reported to occur in a bimolecular process, if the complex can in

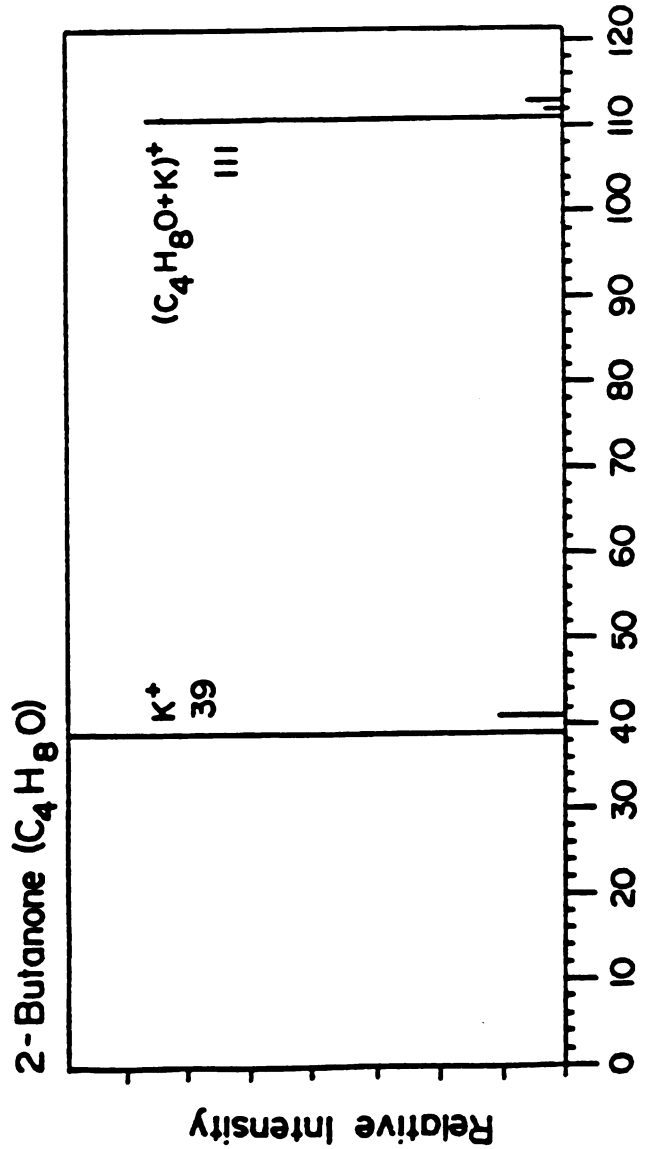


Figure 6. K^+Cl Spectrum of 2-Butanone.

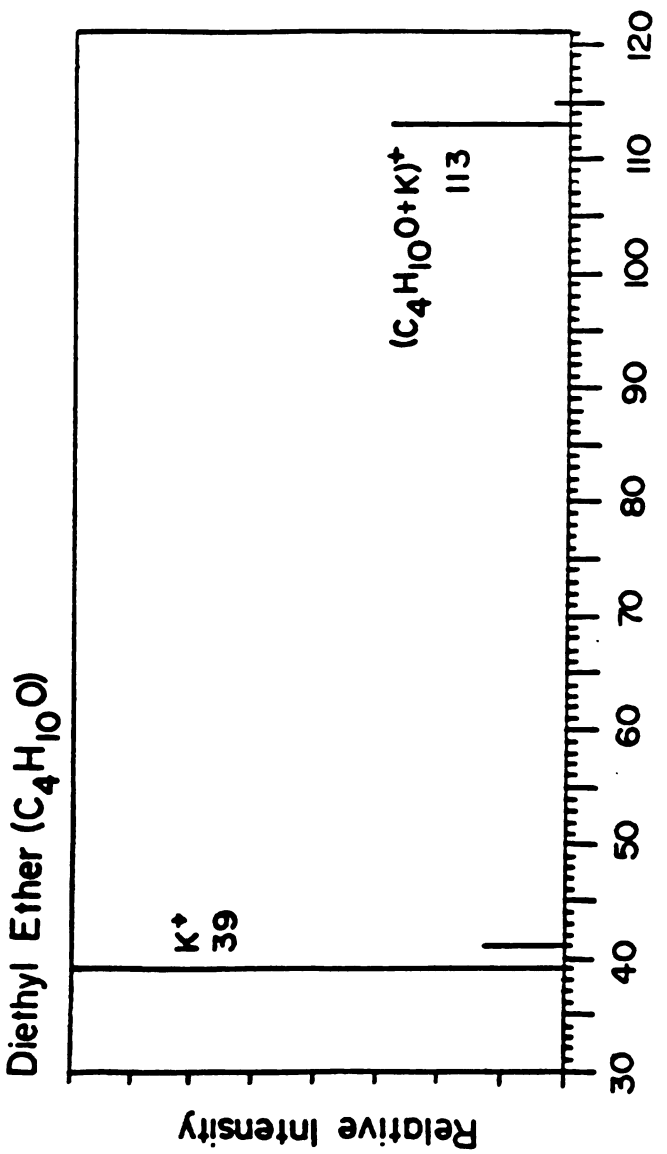


Figure 7. K^+Cl Spectrum of Diethyl Ether.

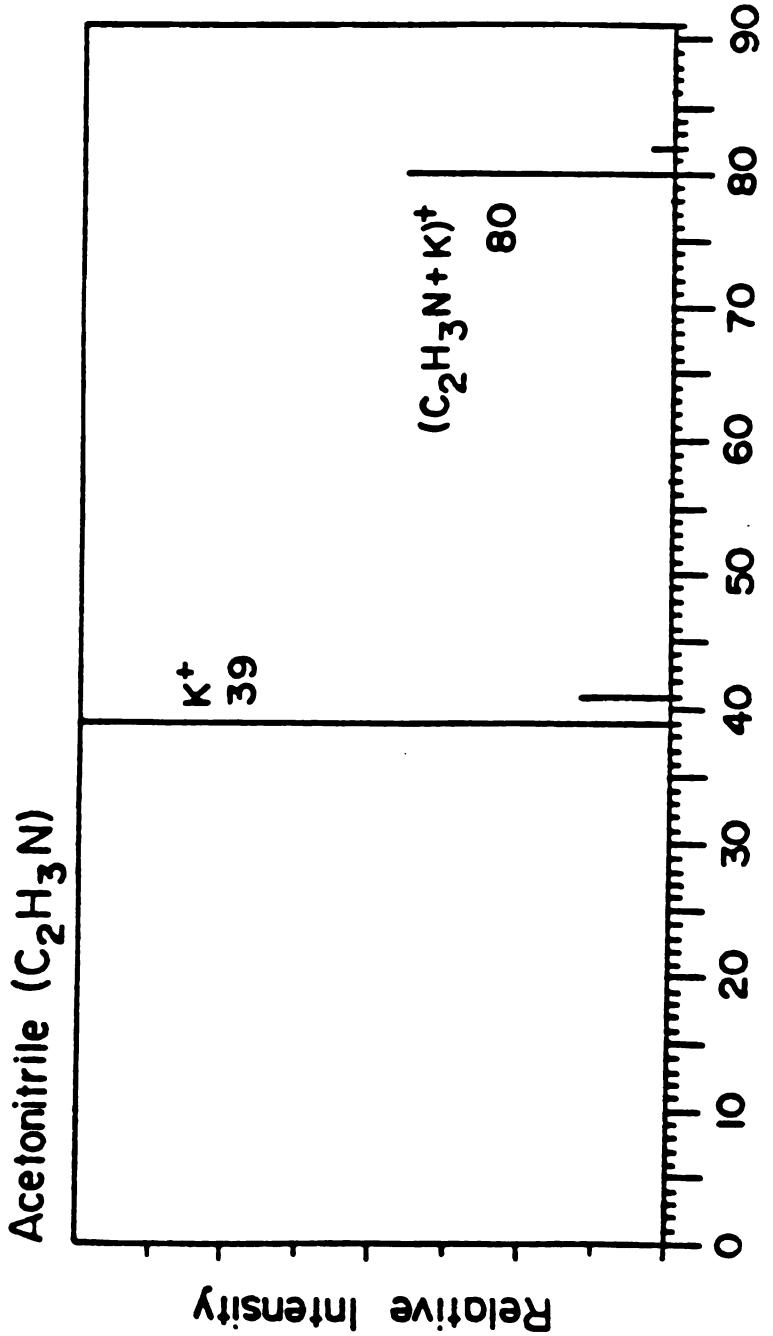


Figure 8. K^+Cl Spectrum of Acetonitrile.

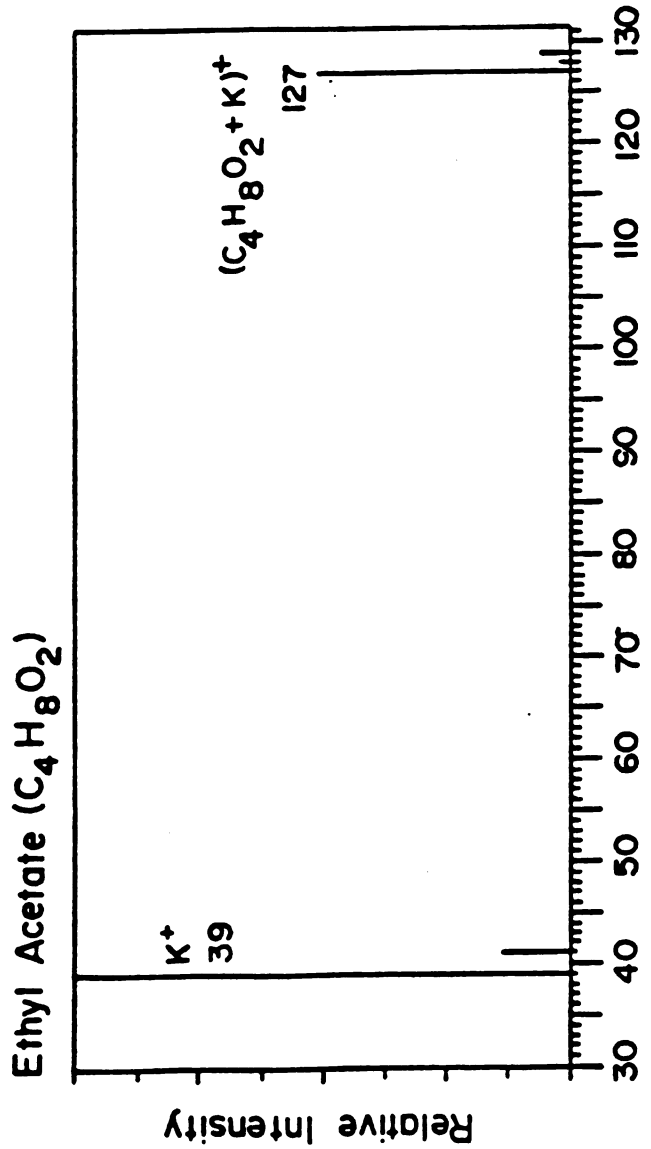


Figure 9. K^+Cl Spectrum of Ethyl Acetate.

Table 1

List of Compounds Studied Using the K^+ Emitter Probe in the K^+Cl Mode.

COMPOUND	$(M+K)^+$	OTHER IONS
Pyridine	yes	no
Isobutyl chloride	yes	no
Benzene	yes	no
cyclohexane	no	no
hexane	no	no
n-propanol	yes	$(M-H+2K)^+$
ethanol	yes	no
acetone	yes	no
butyraldehyde	yes	no
acetaldehyde	yes	no
aniline	yes	no
N,N-dimethylaniline	yes	no
$Fe(CO)_5$	no	no

All of the above data was obtained when the K^+Cl thermionic emitter probe was operated within the addition bias window.

some way lose its excess energy (e.g., emit a photon) (67). Addition is more commonly assumed to be a three-body process, in which a neutral molecule collides with an ion-molecule complex and removes an amount of energy, stabilizing the $(M+K)^+$ complex. Ketones give abundant $(M+K)^+$ ions in their K^+Cl spectra. Figure 10 shows a log-log plot of $I(M+K)^+ / [I(M+K)^+ + I(K^+)]$ versus pressure of acetone (in the CI volume). Apparently, the process leading to the formation of (acetone + $K)^+$ is a reaction which is second order in acetone. At the higher pressures, the K^+ concentration is reduced substantially and the apparent order begins to change. Thus, at least for acetone, the reaction for K^+Cl can be written as

$$K^+ + 2C_3H_6O \rightarrow (C_3H_6O + K)^+ + C_3H_6O.$$

The termolecular nature of the adduct formation which was observed is consistent with the previously reported kinetics of alkali ion adduct formation (68). Based on this, K^+Cl would be very suitable for GC/MS without a splitter, since no response for carrier gas molecules will be seen, and the carrier gas can act as the third body in the analyte addition reactions with K^+.

Amines gave richer K^+Cl spectra than the other compounds studied. Figure 11 is an example of a typical K^+Cl spectrum of triethylamine. In this particular spectrum triethylamine exhibited no $(M+K)^+$ ion. The ions at m/z 102, 100, 86, and 72 can be identified as $(M+H)^+$, $(M-H)^+$, $(M-CH_3)^+$, and $(M-C_2H_5)^+$,

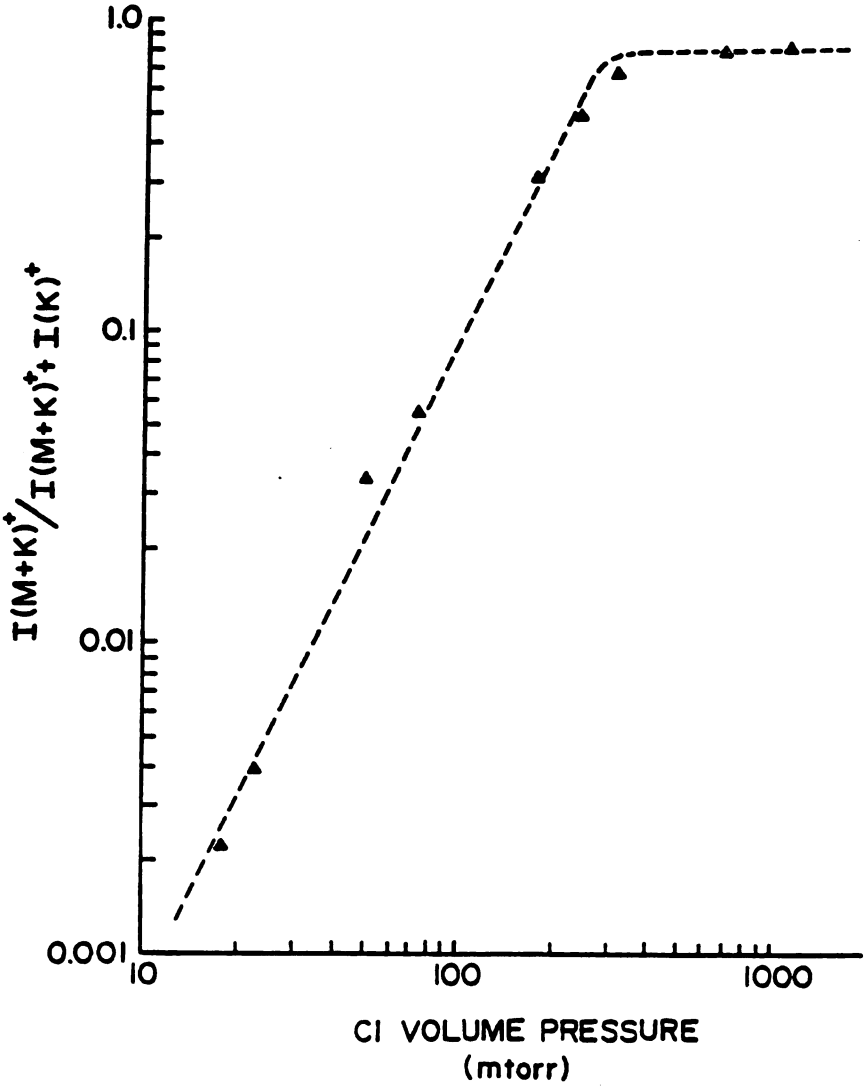


Figure 10. A Log-log Plot of $I(M+K)^+/[I(M+K)^+ + I(K^+)]$ vs. Pressure of Acetone (I Refers to Intensity).

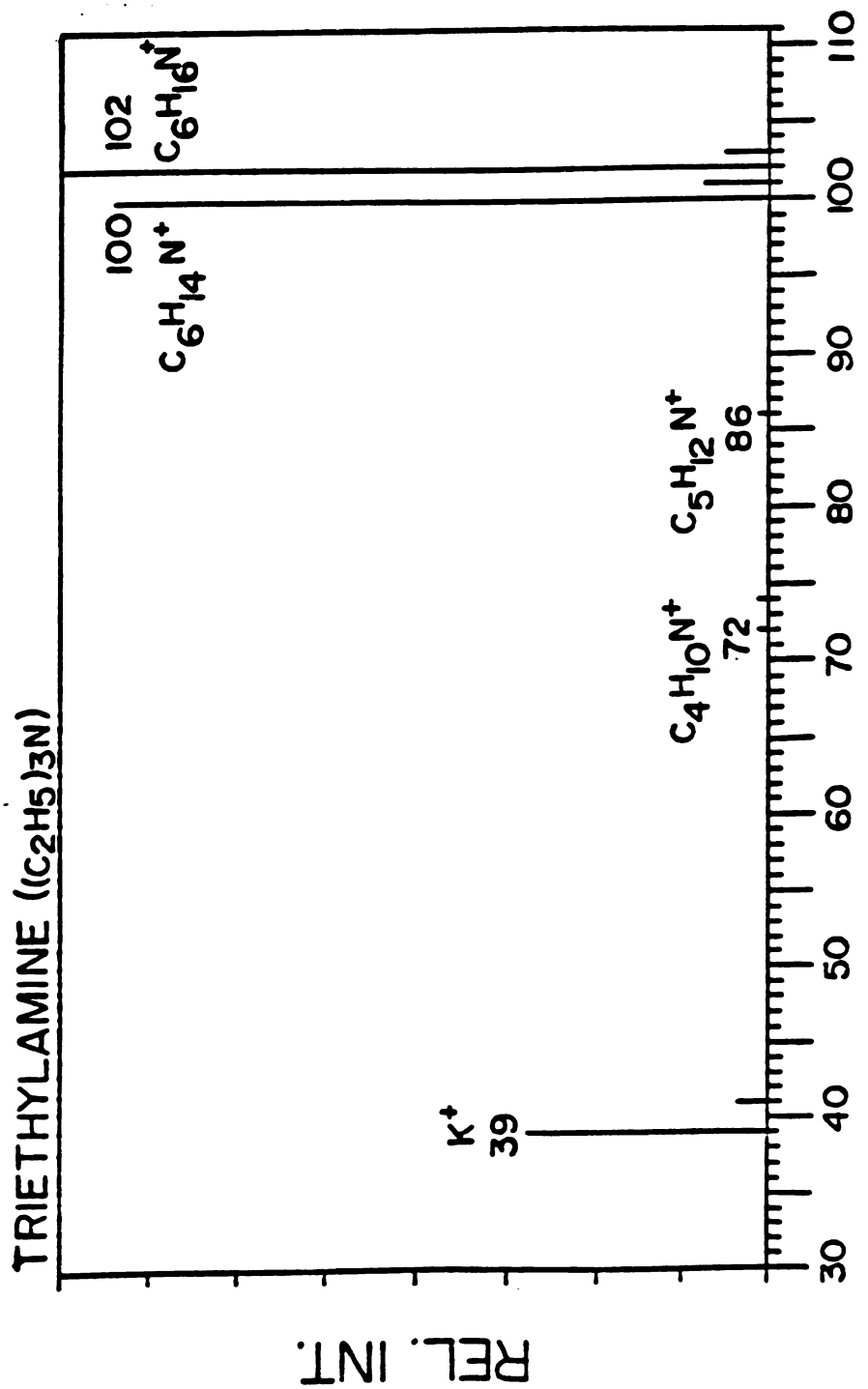


Figure 11. K^+Cl (Surface Ionization) Mass Spectrum of Triethylamine. Bead Bias Is Above K^+ Addition Bias Window.

respectively. The product ions in the K^+Cl spectrum are also the major ions in the EI spectrum of this compound. This fact, along with the fact that, of the compounds studied, amines had the lowest ionization energy, led us to believe that a charge transfer process was occurring (69). That is, the mechanism could be written as follows:

$$K^+ + M \rightarrow \begin{cases} M^{+*} + K\cdot \\ (M-1)^+,\ (M-CH_3)^+,\ (M-C_2H_5)^+,\ \text{etc.} \end{cases}$$

Upon further investigation with a bare heated wire probe tip (no glass bead) the same product ions were produced (in contrast to, e.g., acetone, for which no ions are generated from contact with a bare heated wire). In this case gas-phase potassium ions were absent. Therefore, this suggested that the observed product ions for the amines were a result of surface ionization. Our results found here parallel those found previously (29). The formation of the $(M+1)^+$ ion can be attributed at least in part to a gas-phase ion/molecule reaction (presumably of $(M-1)^+$) since the $(M+1)^+/(M-1)^+$ ratio increases with increasing pressure of the amine.

The products observed for the amines were greatly influenced by the bias voltage applied to the glass bead. The addition product $(M+K)^+$ was seen for all compounds studied at bias voltages between approximately 0.5 and 5 V. However, ions formed due to surface ionization from amines are produced at much higher values of the bead bias. This can be seen graphically

in the case of diethylamine in Figure 12. At low voltages the potassium ion adduct of diethylamine is the major product. With increasing bias voltages only the surface ionization products are observed. This bias-dependent behavior can be an advantage as will be shown later.

Surface ionization studies have predominantly been done on pure and oxidized metal surfaces. In our system, the hot surface consists of the thermionic glass bead (and some exposed rhenium wire). The thermionic glass we use in our probe tip is very similar to the thermionic material contained in thermionic ionization detectors (TID) for gas chromatography. Several surface ionization mechanisms have been proposed for these detectors (70, 71) which account for the observed signal in the presence of nitrogen-containing compounds. Chapter 5 of this thesis will be, in part, a study of surface ionization product ions of N- and P-containing molecules with the hot thermionic material in an attempt to elucidate a mechanism that explains the behavior of TID's. (To date, the link between TID response and the large body of literature on surface ionization mass spectrometry has apparently not been made).

Energy-variable CI reagent ions can be a very useful tool, since it has been demonstrated that ion/molecule reactions can be made to occur (i.e., made exothermic) by the addition of kinetic energy to the reactant ion (72). In the case of K^+, however, this effect is not observed. We do, however, see dramatic changes in the K^+CI spectrum for some molecules as the K^+ emitter bead bias varies. Low biases favor adduct formation, $(M+K)^+$. As the bias is

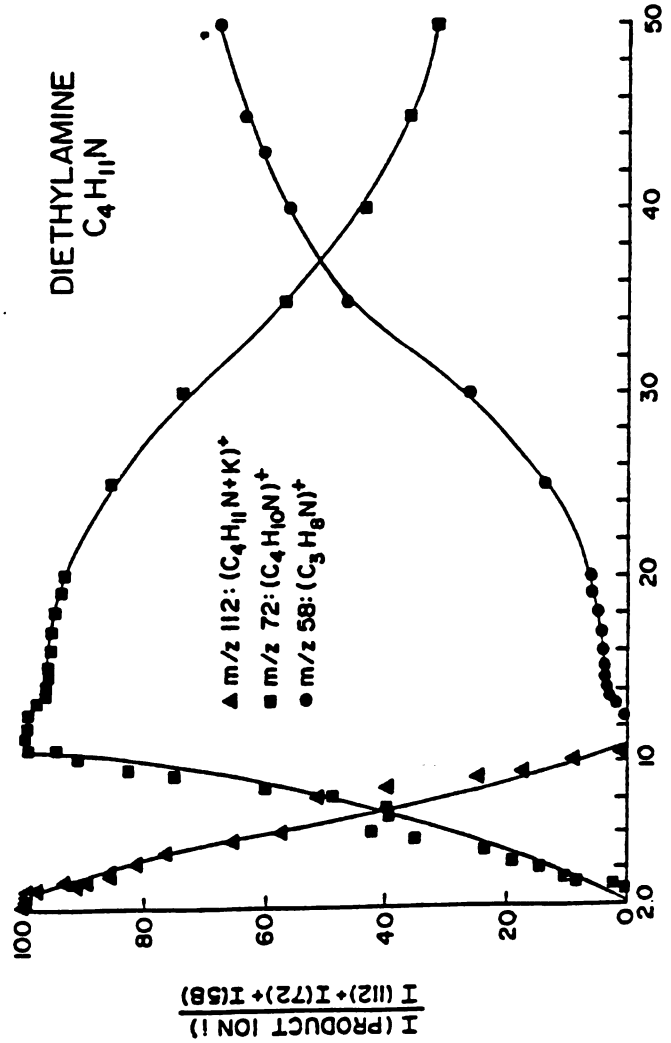


Figure 12. Plot of I (Product Ion I)/(I(m/z 112)+I(m/z 72)+I(m/z 58)) vs. Bead Bias For Diethylamine. Pressure and Heating Current Were Constant at 650 mtorr and 2.0 A, Respectively.

raised, the probability for this process dramatically decreases. For many compounds, "fast" K^+Cl gives no products. As was seen for amines, if surface ionization occurs, higher biases are required to remove these ions from the surface. 2-propanol was found to participate in both gas phase and surface processes. Figure 13 shows a K^+Cl spectrum of 2-propanol (low bias). The predominant ion is the $(M+K)^+$ at m/z 99 and an $(M+K-H_2)^+$ at 97. There is also an ion at higher mass, m/z 137. The m/z 97 and 99 ions decrease as bead bias increases (Figure 14). The intensity of m/z 137 increases as bead bias increases, typical of a surface process.

An ion of m/z 137 cannot be formed by K^+ and 2-propanol in a simple process, since the mass of these two reactants only totals 99u. Initially, we identified this ions as $(C_6H_{10}O+K)^+$. That is, by some surface process, a six-carbon species was being formed from two propanol molecules. Closer inspection of isotope ratios suggested that m/z 137 contained two potassium atoms, i.e., $(C_3H_7O+K_2)^+$. Presumably some surface process such as

$$C_3H_7OH + K \rightarrow C_3H_7OK + H$$

occurs. The C_3H_7OK then complexes with a K^+ ion emitted from the surface. Similar species have been observed in other techniques such as fast atom bombardment (FAB) ionization (73). The "sampling" of species formed on the bead surface by K^+ ions

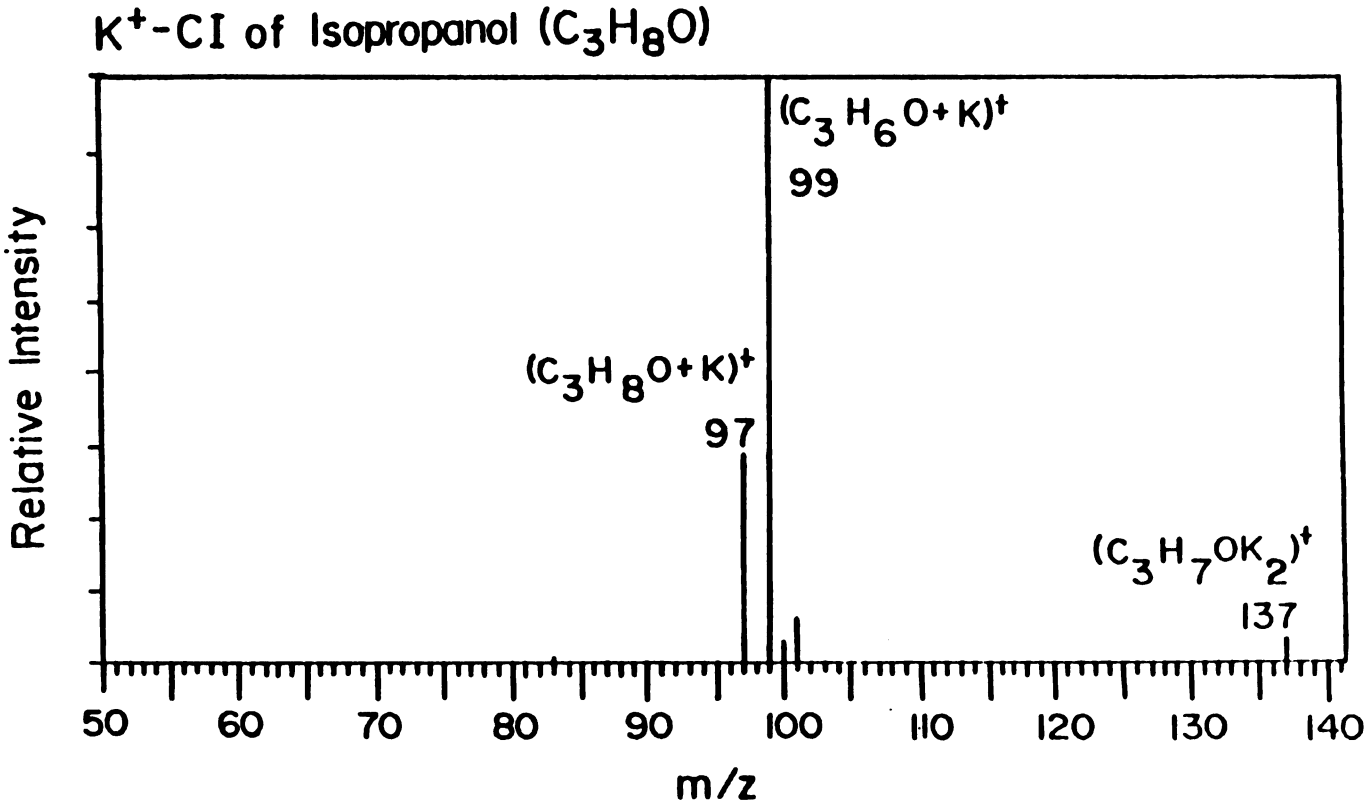


Figure 13. K^+CI Spectrum of 2-Propanol With Bead Biased Within K^+ Addition Bias Window.

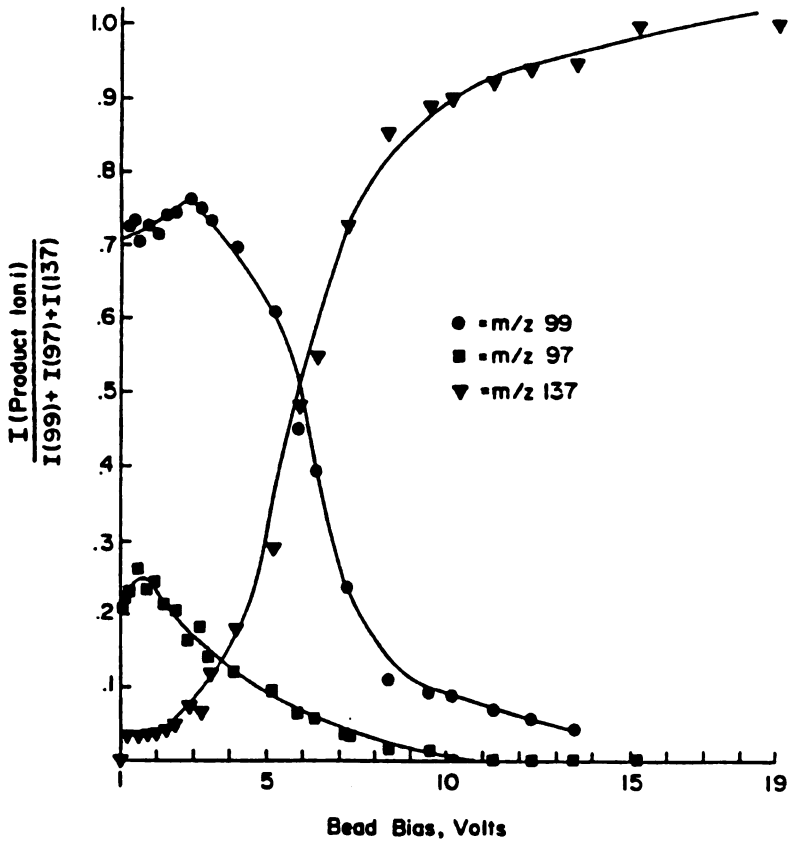


Figure 14. Plot of I (Product Ion)/[I(m/z 98)+I(m/z 99)+I(m/z 137)] vs. Bead Bias.

which are emitted as discussed in more detail in the case of peptide analysis and is the basis of Chapter 3 of this dissertation.

In summary, K^+ appears to be useful in providing molecular weight information, except with certain types of compounds, for which ionization on a hot surface is known to be a facile process.

Other Uses of the K^+ Thermionic Emitter Probe in Mass Spectrometry.

Five other alternate uses of the probe will be described here.

Complexation Studies-Solution Parallels. In solution, crown ethers have proven to be useful species for kinetic and thermodynamic investigations of ion-solvent interactions (74). In the gas phase, such species can be studied in the absence of solvent (75). Crown ethers form strong complexes with alkali ions in solution. With the K^+ emitter, crown-K^+ complexes can also be formed in the gas phase. Figures 15 and 16 show the K^+Cl spectra of 12-crown-4 ($-(C_2H_4O)-$) and its linear analogue, triethylene glycol dimethyl ether $CH_3(OC_2H_4)_3OCH_3$. Studies of competitive ligand exchange of such species may provide thermochemical insights into such metal-ligand complexes.

An Alternating EI/CI Source. In the context of GC/MS, the production of both EI and CI mass spectra from a single sample component is advantageous since both the molecular weight information common in CI and the structural information of EI are

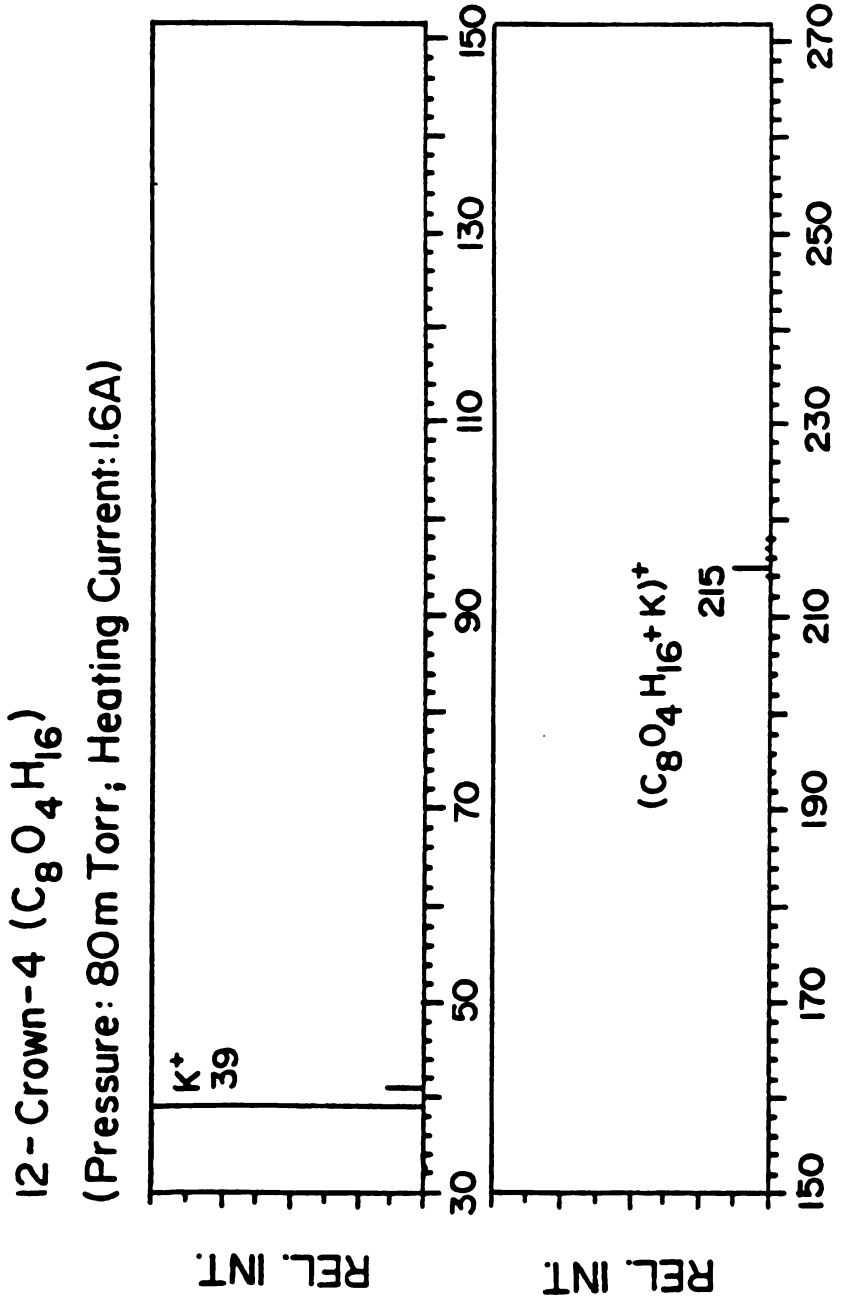


Figure 15. K^+Cl Spectrum of 12-Crown-4. Bead Bias is Within Addition Bias Window.

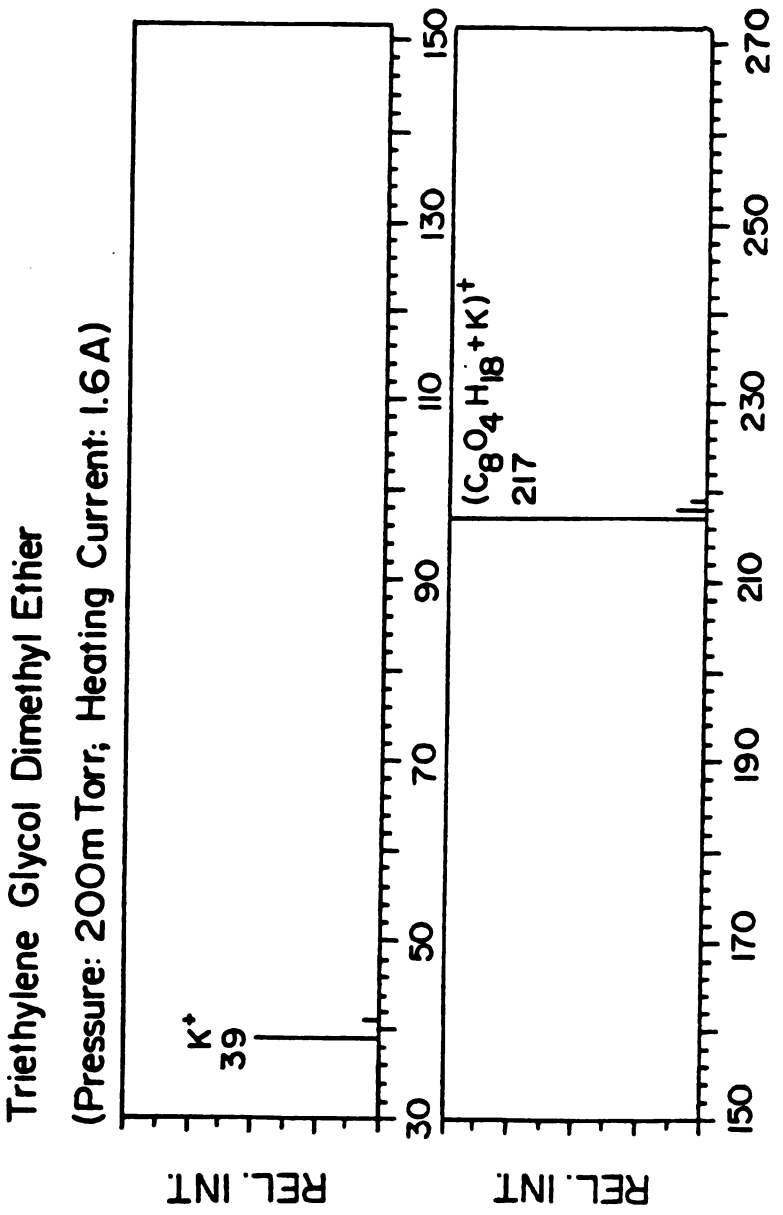


Figure 16. K^+CI Spectrum of Triethylene Glycol Dimethyl Ether.

Bead Bias Is Within Addition Bias Window.

available. A number of approaches have been demonstrated. Instruments utilizing dual sources, dual ion beams, and dual detectors have been used. Also, combination EI/CI sources have been used. In the latter, sequential EI and CI spectra can be produced (alternating for each scan).

The K^+Cl^- probe, when negatively biased, produces electrons. Apparently, electrons are generated from both the thermionic glass and the rhenium wire when heated. Thus, the bias can be sychronized to the scan flag of the mass spectrometer data system such that, for one mass scan, the bead bias is at, e.g., 2 V (K^+Cl^- mode), and the next scan at e.g., -70 V (EI mode). To demonstrate this, 15-crown-5 was chosen, since the EI mass spectra of crown ethers are very similar and characteristic of a crown ether, but with essentially no molecular ion to identify the particular crown ether under study. Figures 17 and 18 show the respective EI and CI spectra obtained by using the K^+ emitter in the CI volume. In an EI mode (here, bias= -23 V) the spectrum agrees well with the expected EI spectrum (76). In the K^+Cl^- mode (bias of +2 V), the $(15\text{-crown-5} + K)^+$ adduct is prominent, providing the necessary molecular weight information.

This simple technique can extend the information available from a mass spectrometer without costly redesigned sources, in fact, with no instrumental alterations at all.

Operation of an MS in a "TCD" Mode. When a gas chromatograph is coupled to a mass spectrometer, the GC detector is removed in most cases. Many detectors, such as the thermal conductivity

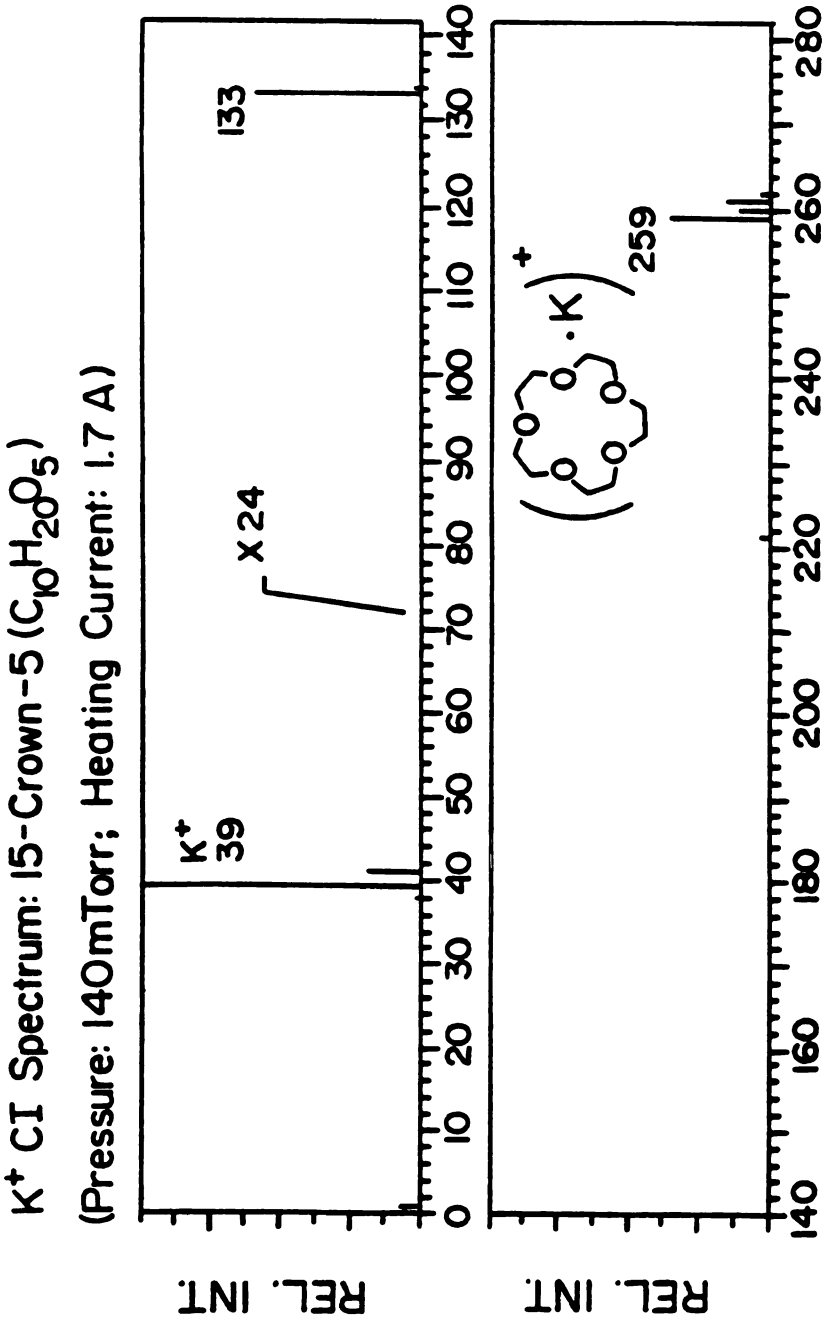


Figure 17. K^+CI Spectrum of 15-Crown-5. Bead Bias Within the Addition Window.

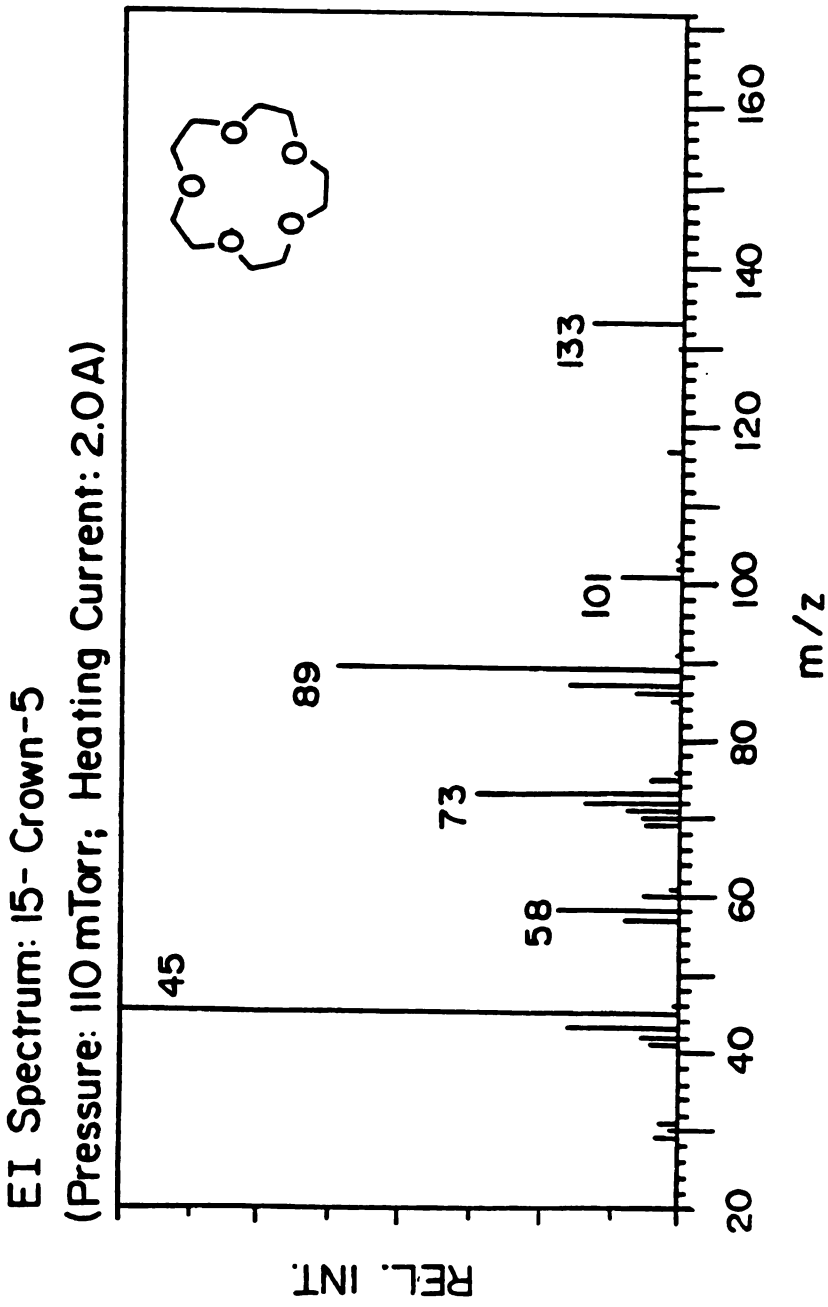


Figure 18. EI Spectrum of 15-Crown-5. Bead Bias Was -23 V With Respect to the CI Volume In This Case.

detector, are very useful. The thermal conductivity detector (TCD) works on the principle that a hot filament will lose heat according to the composition of its gaseous environment. The concentration of a certain gas in this environment determines the amount and type of gas surrounding the filament.

The K^+ emitter can be used to mimic this type of detector response. The intensity of the K^+ ion signal reflects the temperature of the emitting glass bead. If the total ion intensity (TII) is monitored in a GC/MS experiment, a TCD-like response will be observed. The concentration and thermal conductivities of solute eluting into the CI volume determine to what extent the bead is collisionally cooled. Cooling reduces the K^+ ion intensity. The response should parallel the conventional TCD. A mass spectrometer is an expensive TCD; however, this option may be preferable to using a second GC which has a TCD in addition to GC/MS for analysis.

Uses of the K^+ Emitter in GC/MS Experiments. Selective detectors in gas chromatography have proven to be useful in applications such as quantitating compounds which are unresolved by the chromatograph. The bias dependence of the K^+CI response can be used as the basis for a "selective" ionization method. In context of GC/MS, if the K^+ bead is operating at low bias, $(M+K)^+$ ions are observed for most compounds. If the bead is at higher bias, addition will not occur, and only compounds which can react by surface ionization will be detected. This is shown in Figures 19 and 20.

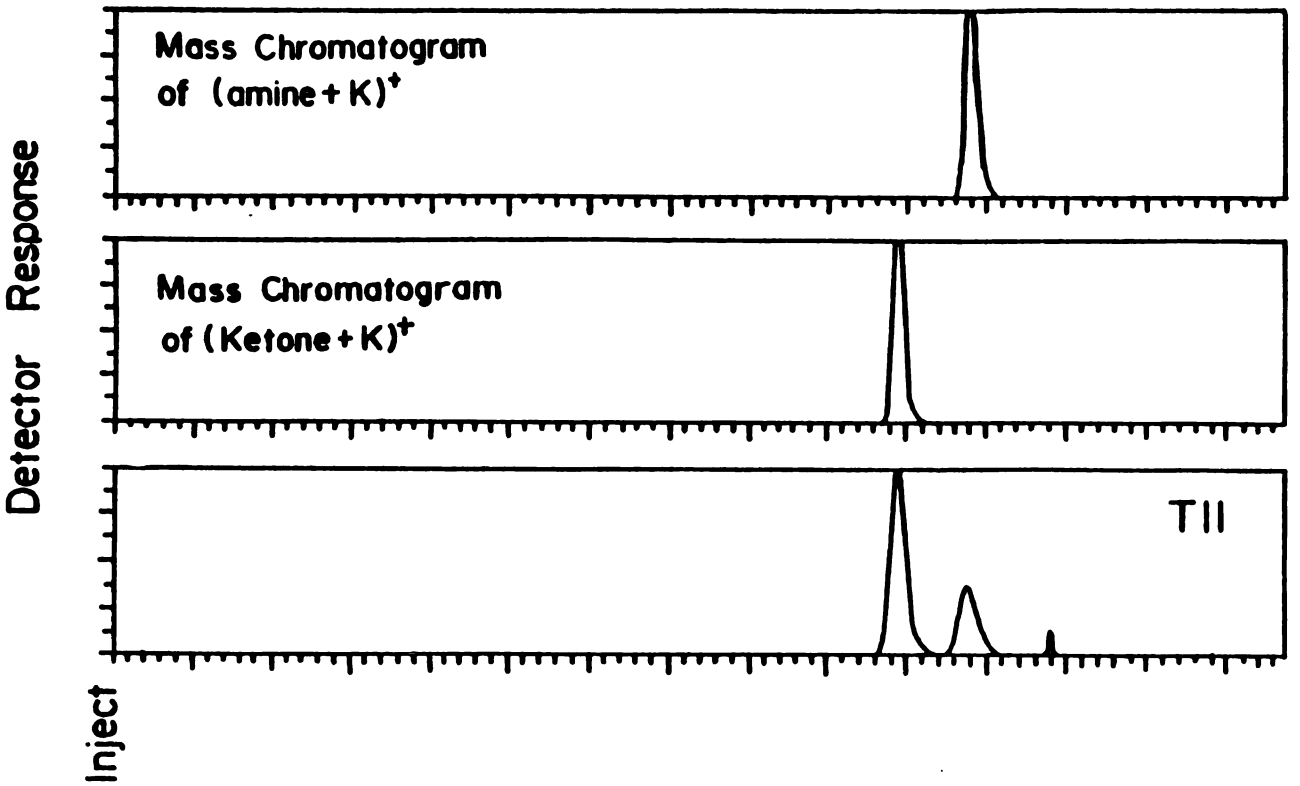


Figure 19. The Mass Chromatograms and Total Ion Intensity Obtained From GC/K^+CI/MS Run in the Analysis of 1 µl of a neat 1:1 Mixture of a Ketone and an Amine. Mass Spectra Were Collected From m/z 42 to 150. The Bead Bias is Within the K^+ Addition Window.

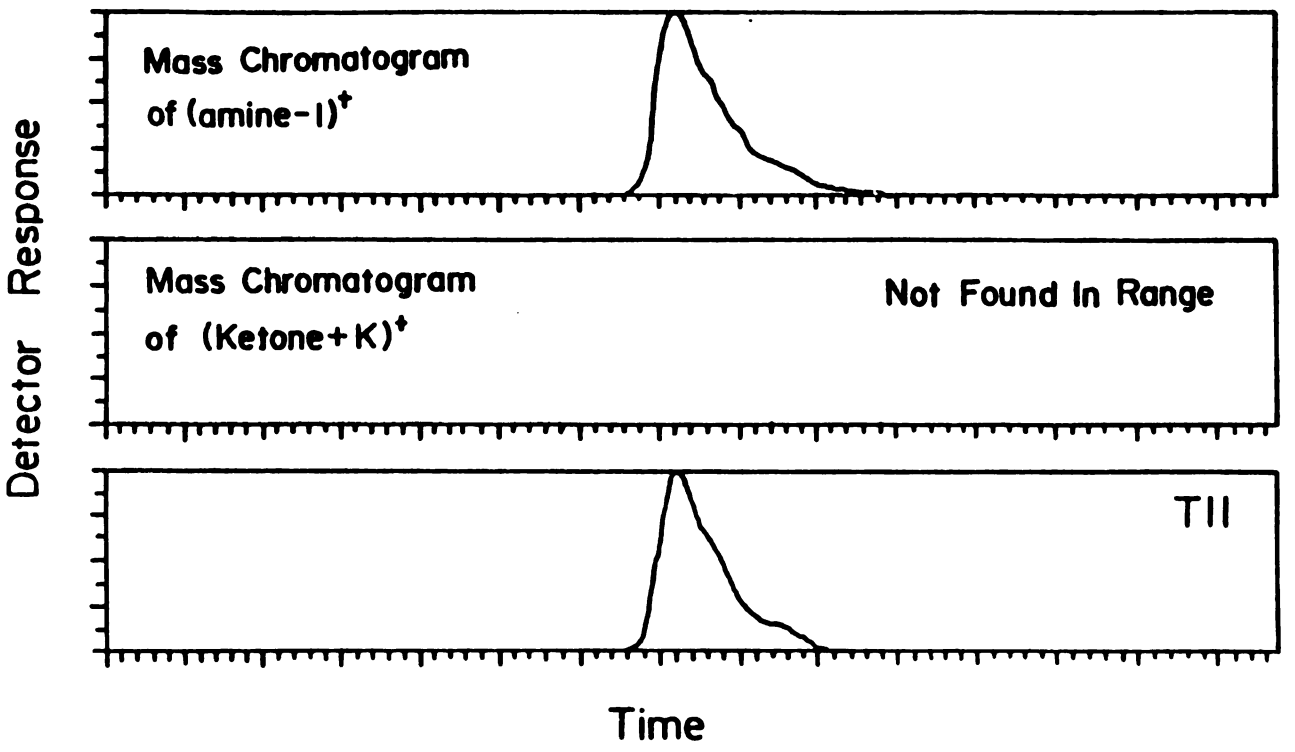
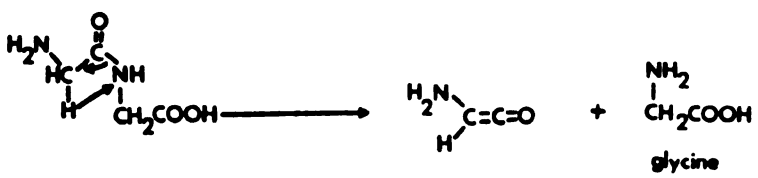


Figure 20. The Mass Chromatograms and Total Ion Intensity Obtained From GC/K^+CI/MS Run in the Analysis of 1µl of a 1:1 Neat Mixture of a Ketone and Amine. Conditions the Same as in Figure 19 Except Bead Bias Above K^+ Addition Bias Window.

Analysis of Nonvolatile and Thermally Labile Compounds. We have observed that, when a solution containing a nonvolatile/thermally labile compound is evaporated onto the K^+ glass bead, ions representative of the compound will be generated when the probe is heated. These ions usually last for 10-15 seconds after the bead is brought up to operating temperature. This technique was investigated by using di- and tri-peptides as analytes. We observe that (1) most of the ions formed contain K^+, (2) $(M+K)^+$ is almost always present and is also the highest m/z product formed, and (3) low-energy decompositions of the peptides occur, for example, H_2O and CO_2 loss occurs and an $(M+K-CO_2)^+$ or $(M+K-H_2O)^+$ is observed.

While a number of possible mechanisms can be considered, a useful working model is as follows: A molecule thermally undergoes a decomposition to two (or more) smaller molecules on the surface. The K^+ being emitted from the surface beneath these species complexes with these species, "sampling" the molecules present on the hot surface. Figures 21-23 show representative spectra of a dipeptide and two tripeptides. Note that in each case an $(M+K)^+$ is observed. For each fragment, bond cleavage with a H shift can explain the observed species. For example, glycylglycine (Gly-Gly) can thermally decompose to form glycine.



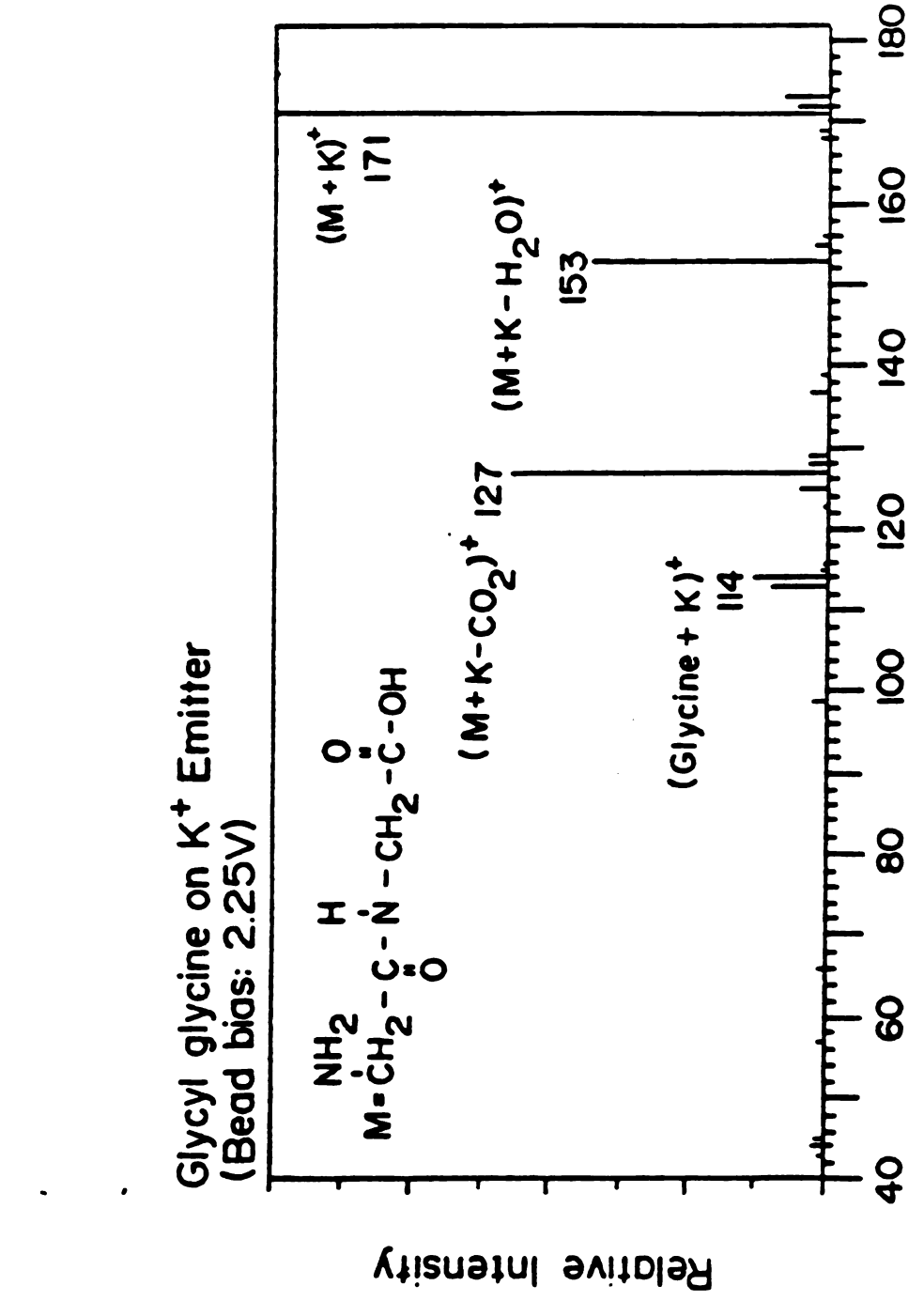


Figure 21. K^+Cl/Surface Ionization of Glycylglycine. Heating Current Was 2.0 A.

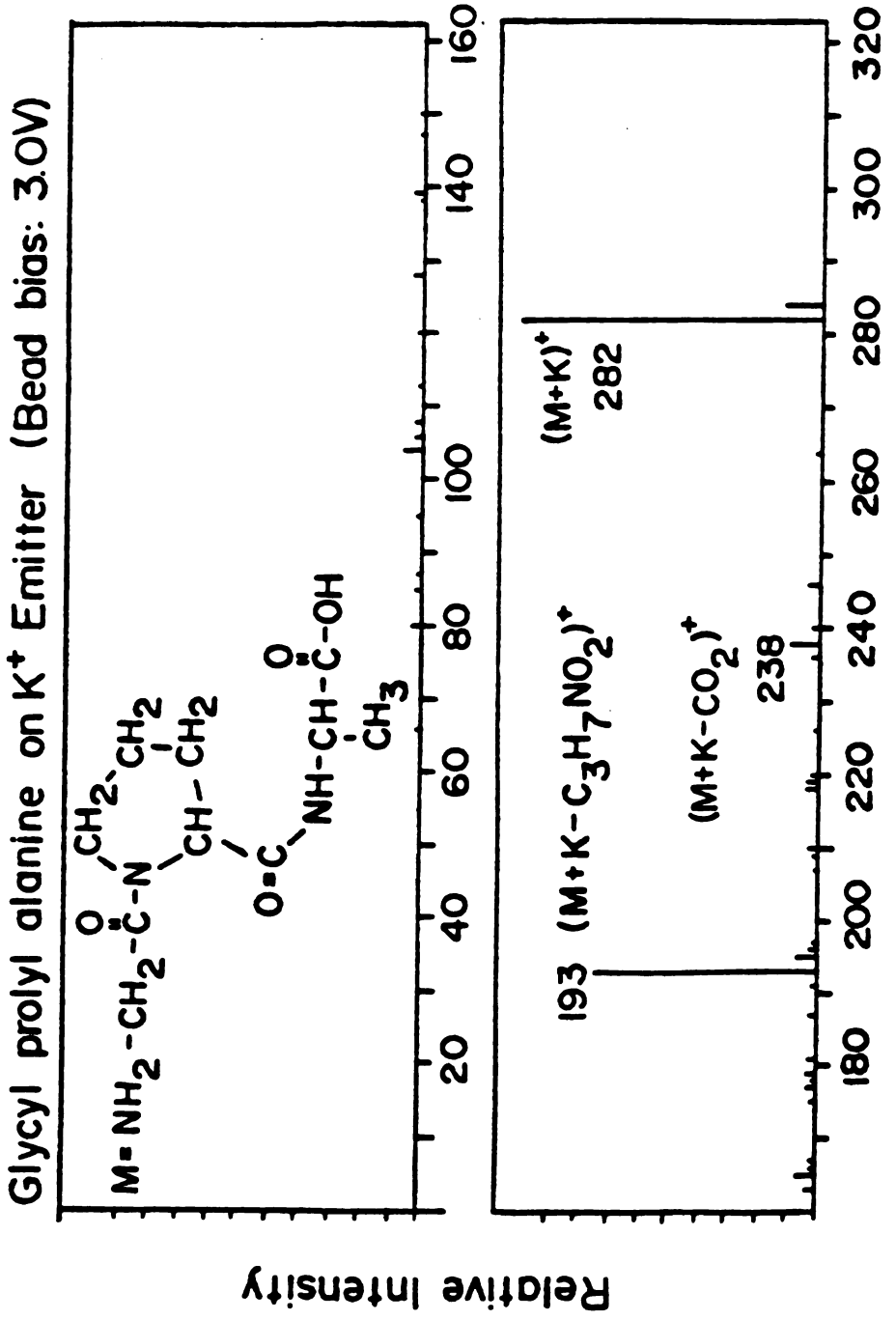


Figure 22. K^+Cl/Surface Ionization of Glycyl Prolyl Alanine.
Heating Current Was 2.0 A.

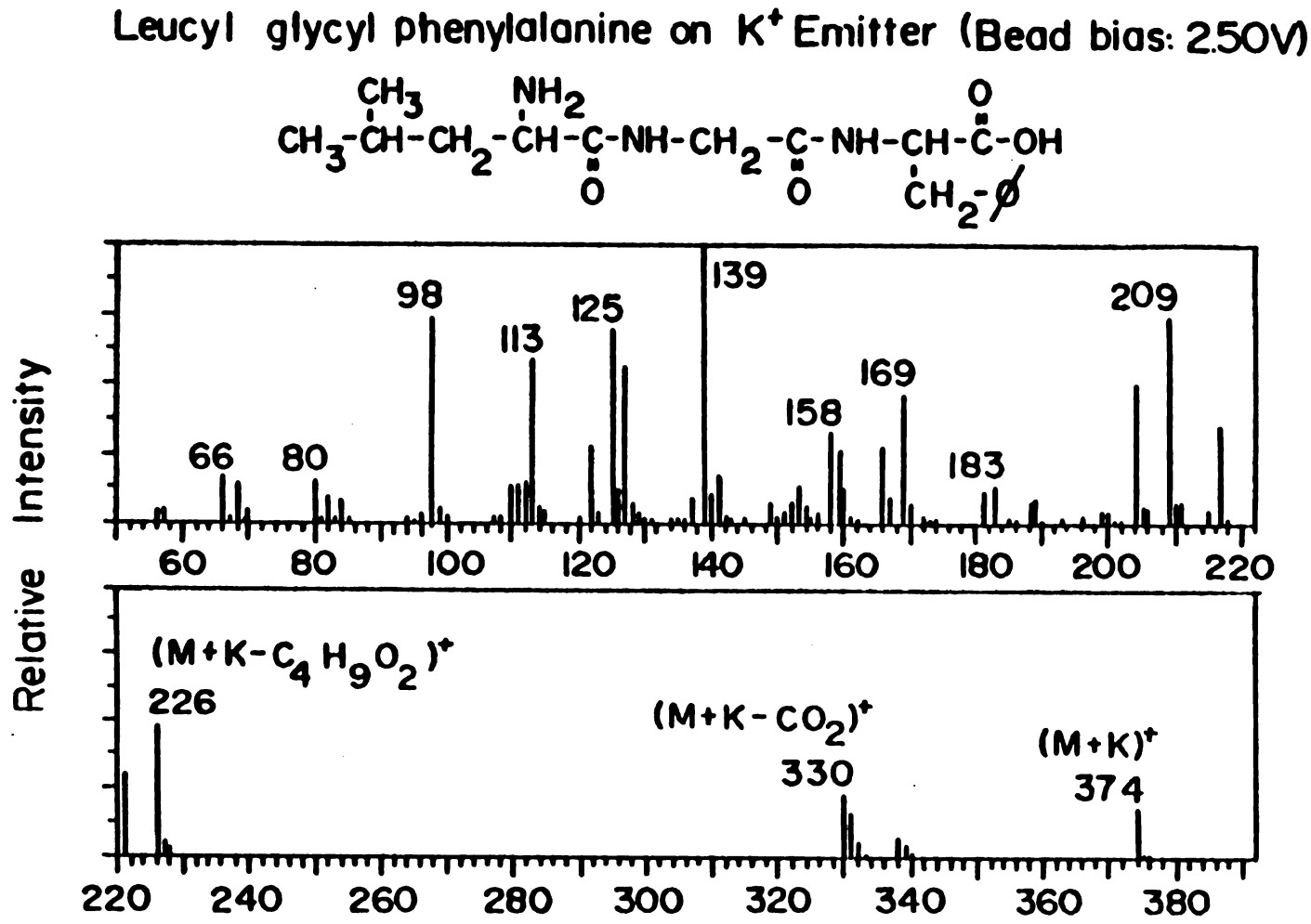
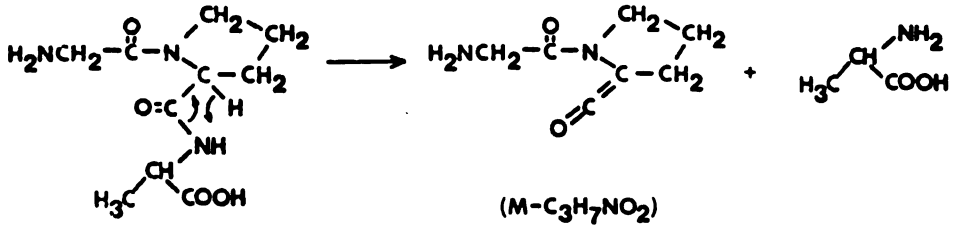
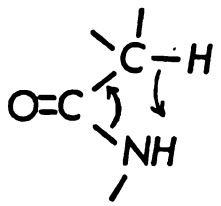


Figure 23. K^+Cl/Surface Ionization of Leucyl Glycyl Phenylalanine. Heating Current Was 2.0 A.

The spectrum of glycylglycine obtained in this way is fairly simple. A similar process can be postulated for the tripeptide glycyl-L-proyl-L-alanine (Gly-Pro-Ala), leading to the product at m/z 193.



Following this decomposition, K^+ complexes with these surface species to produce $[(M-C_3H_7NO_2) + K]^+$ at m/z 193. A similar process generates the m/z 226 product for Leu-Gly-Phe. Note that in all three cases, cleavage of the peptide linkage



dominates the decomposition pathways. Thus, the possible use of this technique for sequencing such species is worth pursuing. Note that DL-leucylglycyl-DL-phenyalanine (Leu-Gly-Phe) has a much more complex spectrum at lower masses. Many of the products do not contain K^+. Apparently, some bases are more susceptible to surface ionization.

Over a dozen di- and tri-peptides were included in this initial study with successful results. In all cases, an $(M+K)^+$ was observed, with cationized species indicative of low energy decompositions being common as well.

In some ways, this approach to analysis of nonvolatile/thermally labile compounds may be preferable to alternate methods such as FAB ionization, for a number of reasons. The most obvious advantage is cost. Secondly, the absence of a matrix (glycerol in FAB) and its associated spectral interferences is an advantage. Also, FAB frequently only produces an adduct ion of an analyte, $(M-H)^+$, with little structural information. Presumably, if this experiment could be performed with a K^+ bead which emitted potassium ions with no heating, peptides would only show an $(M+K)^+$ ion. The temperature at which potassium emission occurs appears to induce low-energy decompositions of such compounds into smaller molecules. The emitted potassium ion then samples these to generate simple, useful spectra. In some ways the technique is analogous to FAB or SIMS-the major difference being that K^+ is generated from the surface on which the species is deposited.

The last use of the potassium thermionic emitter probe (e.g., the analysis of nonvolatile and thermally labile compounds) was further investigated using a variety of compounds ranging from pharmaceuticals to saccharides. These investigations are included in Chapter 3 of this thesis. This technique was also applied to polymeric systems and will be presented in Chapter 4 of this work. In Chapter 3 further comments on the mechanism of this process will be included. The initial investigations of this probe to the analysis of nonvolatile/thermally labile compounds is included in this part to serve as an introduction to the technique.

CHAPTER 3. A NEW DESORPTION/IONIZATION MASS SPECTROMETRIC TECHNIQUE FOR THE ANALYSIS OF THERMALLY LABILE COMPOUNDS BASED ON THERMIONIC EMISSION MATERIALS

I. INTRODUCTION

The number of ionization techniques used in mass spectrometry is constantly growing, allowing for a wide variety of compound types to be studied. Early mass spectrometric analyses using electron impact, chemical ionization, field ionization (FI), and surface ionization required volatile analytes which could be introduced into the spectrometer source via a gas chromatograph or a direct insertion probe (DIP). Thermally labile compounds are frequently derivatized into volatile compounds in order to be analyzed by these methods.

A variety of ionization techniques are now available which enable mass spectrometry to be used for the direct analysis of thermally labile compounds. These include field desorption (FD) (77), FAB (78), secondary ion mass spectrometry (SIMS) (79), laser desorption (LD) (80), and plasma desorption (PD) (81). While these methods have greatly extended the range of chemical species which can be analyzed by mass spectrometry, each method has some limitations and/or weaknesses. Simply, there is no universal ionization method for thermally labile compounds which will provide both molecular weight and structural information in all cases.

Flash volatilization or rapid-heating techniques have been

recently used with ionization methods such as EI and CI in the analysis of thermally labile compounds. Rapid heating is useful due to the temperature dependence of evaporation and decomposition processes. It has been shown that at sufficiently high temperatures vaporization may be favored over degradation (82). Therefore if the analyte is rapidly heated, intact molecules may evaporate with little decomposition taking place. These intact molecules can then be analyzed by conventional EI or CI methods. It should be noted that the term "thermally labile" is rapidly replacing "nonvolatile", at least in context of mass spectrometric analysis. Compound classes such as peptides, sugars and salts were referred to as being nonvolatile because, on heating, gas phase intact molecules could not be generated due to their thermal lability, i.e., thermal degradation occurred before vaporization if the sample temperature was slowly increased. It has been shown that rapid heating can generate gas phase molecules of these compounds, hence they can no longer be considered "nonvolatile". The emphasis on the thermal lability is now more relevent than apparent volatility.

Another approach for the analysis of thermally labile compounds is pyrolysis mass spectrometry (Py-MS). There is ample literature documenting the methodology with which such compounds can be identified by the analysis of their pyrolyzates (83,84). Pyrolysis methods use no matrix and can be considered to be a universal method (i.e. most organic compounds thermally decompose to smaller, more volatile comounds). The weak aspect of Py-MS is the ionization step. Methods such as electron impact,

chemical ionization and field ionization have been utilized to ionize pyrolysis products. If, for example, a compound is heated and generates 10 volatile products in the source of the mass spectrometer, electon impact will yield the sum of the mass spectra of each compound. Such spectra are exceedingly difficult to interpret. Other ionization methods can yield simpler spectra (83).

In the plethora of methods listed above, the use of inorganic salts has introduced some new options. More specifically, techniques by which $(M+Cat)^+$ can be formed for thermally labile analytes (where cat= Na, Li, K, etc.) have been investigated and found to frequently simplify the spectra from techniques such as FAB. As early as 1975, it was shown that if salts were deposited on a field ionization emitter, alkali ion-organic molecule adducts could be formed in the presence of a moderate electric field (85). Such techniques were used for both volatile and thermally labile compounds (field ionization/desorption) (85-89). Alkali ion attachment can also be utilized in laser desorption techniques (90). Thermal desorption of ions such as $(M+Na)^+$ from heated mixtures of alkali salts and organic compounds on metal surfaces has also been reported (91, 92). The development of methodology leading to cationization of organic compounds as a method of ionization is largely due to the work of Rollgen and co-workers. Recently they have reported a technique using a two filament design (93). In a specially constructed ion source, two filaments are in close proximity, mounted on a common "push rod". The first filament is coated with a mixture of silica gel and alkali

salt which, when heated, emits alkali ions. Thermally labile compounds are present on the second filament. These molecules thermally desorb and form adducts with the alkali ions from the first filament. Cation-molecule adducts are apparently formed in the gas phase. This method produces simple mass spectra from which molecular weight information can be easily derived.

Earlier in Chapter 2 the methodology was presented by which a thermionic emitter could be introduced into the source of any mass spectrometer equipped with a direct insertion probe (see Figure 24). The last section of Chapter 2 introduced the use of this probe in the analysis of thermally labile compounds. This section of the dissertation will continue with this investigation. As will be discussed, this method appears to be a combination of pyrolysis and K^+Cl. Thus the technique is named K^+IDS (potassium ionization of desorbed species).

This method of desorption/ionization has a number of advantages. No matrix is involved. The technique has produced a mass spectrum from all of the compounds studied to date and has application in polymer and mixture analysis (will be presented in Chapter 4). This technique may not replace other ionization techniques, or that the compounds chosen as representative compounds cannot be identified by other ionization methods. What is presented is a simple, relatively inexpensive method which can be used to generate mass spectra from thermally labile species and mixtures. No investigation of alternate source designs were done since the goal was to develop a method which can be made available for limited cost and instrument

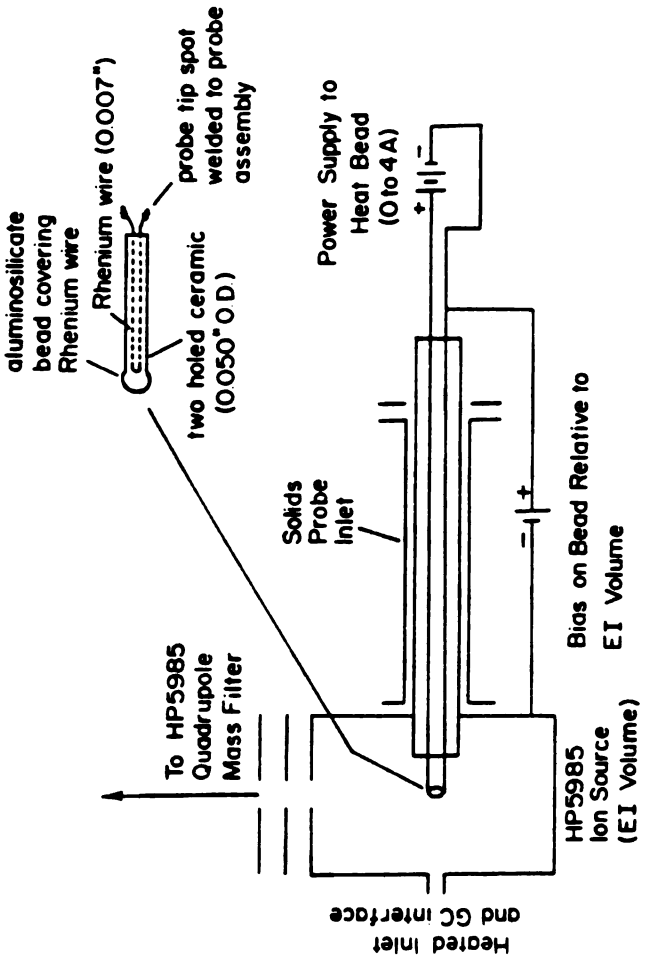


Figure 24. Schematic Diagram of Thermionic Emission Probe in the Mass Spectrometer's Source. The Structure of the Probe Tip is Shown Enlarged.

alterations. The single filament thermionic emitter probe has demonstrated analytical utility because it can be used to ionize gas phase species by K^+Cl and surface ionization and also be used for the analysis of thermally labile compounds. Included in this discussion is the apparent mechanism by which ions are formed in this technique, and the resultant spectra of various types of thermally labile compounds which have been targets for analysis by other desorption/ionization techniques.

II. EXPERIMENTAL

All experiments were performed on an unmodified Hewlett-Packard 5985 GC/MS/DS as before. The description and manufacture of the probe is given in Chapter 2. All experiments were performed using the EI source volume unless otherwise noted. Base pressures were typically 10^{-6} torr or less.

The thermionic K^+ glass was prepared as described in reference 17. A slurry of this mixture is made with acetone. A few drops of slurry are placed onto the rhenium wire loop of the probe tip (see Figure 24) and allowed to dry. The probe tip containing the glass mixture is lightly flamed over a bunsen burner to evaporate any solvent. This procedure also hardens the mixture about the rhenium wire, adding stability to the mixture covered probe tip. The probe tip containing the thermionic K^+ mixture is then conditioned within the mass spectrometer source for several minutes by passing 3 A through the filament. The final result is not a smooth glass as was before for K^+Cl but

resembles a ceramic-like matrix. A thin coating of this material about the rhenium wire produces the best result. A single thermionic K^+ probe tip typically can be used for the analysis of 30 to 40 compounds. Failure is usually due to oxidation of the rhenium filament.

The rhenium filament is held at a potential of +3 V with respect to the ion source using a 0-20 V, low-current power supply. This bias voltage corresponds to the "bias window". A final filament current of approximately 2 A is used to resistively heat the thermionic K^+ ceramic material. The initial temperature of the probe was 100 ^{0}C, the temperature of the ion source housing. The final temperature is greater than that needed for thermionic emission of potassium ions (800-1000^{0}C). Here 2 A and 4 A correspond to temperatures of 860 and 1270^{0}C, respectively. These temperatures were measured outside the mass spectrometer using a vacuum chamber and an optical pyrometer (Leeds & Northrup 8622-C). The temperature ramp is achieved manually and as reproducibly as possible. In general, less than 4 seconds are required before emission of potassium ions is observed. This time is a function mainly of the size of the thermionic K^+ bead on the probe tip.

Throughout this work the term rapid heating is used; this term and experimental specifics require some explanation. The term "rapid heating" may be interpreted as implying that the rate of heating is most important, dT/dt. Rapid heating experiments are useful because some high, final temperaure can be rapidly achieved. In this experiment, we need to rapidly achieve a

temperature at which desorption rates are high. We wish to spend a minimal time at lower temperatures such that, when the maximum temperature is achieved, most of the analyte is still present on the probe tip. The mechanics of this experiment is as follows: The power supply which heats the emitter is set such that, when the supply is turned on, it rapidly attains the preset current value. The time delay between turning on the supply and observing ions is approximately 4 seconds, independent of the final current (i.e., temperature) chosen. Therefore, when higher currents are chosen, the heating rate and final temperature achieved are higher. At this time, we have no accurate measurement of heating rate; the actual rate is not critical, although the experiment works best when the rate is on the order of 150-200^{0}C/sec or greater.

Solutions containing the analyte were prepared in an appropriate solvent depending upon the analyte. A drop of the solution was placed directly onto the thermionic K^{+} ceramic and allowed to dry. The sample was localized on the thermionic K^{+} ceramic tip in order to minimize spectral differences which may occur due to sample deposition at other locations on the probe shaft. Using this procedure several micrograms of the analyte were typically loaded onto the probe tip.

All (commonly available) chemicals were ACS reagent grade and used without further purification. The peptides, xanthines, and cholesterol were obtained from the Sigma Chemical Co. Sucrose and glucose were obtained from Mallinckrodt, Inc. Polyethylene glycol was obtained from the Aldrich Chemical Co.

Ampicillin was generously supplied by John L. Gower (Beecham Pharmaceuticals, Surrey, U.K.).

III. RESULTS AND DISCUSSION

Mechanistic Considerations. The first part of this discussion will focus briefly on the mechanism by which ions are formed in this technique. In this work, we consider a thermally labile compound deposited on the surface of the K^+ emission material, and heated to a temperature sufficient for thermionic emission of potassium ions. A proposed mechanism must explain the following observations. Usually, all the ions observed in the resulting mass spectrum contain K^+. In most cases, the ion of greatest m/z is the analyte-potassium ion adduct $(M+K)^+$. The appearance of the mass spectrum is dependent on the final temperature to which the thermionic K^+ ceramic is raised. Frequently at some temperature a large $(M+K)^+$ ion is observed, while lower m/z potassium-containing ions may dominate at other temperatures. Spectral lifetimes are dependent upon the analyte and usually do not last longer than approximately 30 seconds, although in some cases they last several minutes.

K^+IDS apparently involves two basic steps of desorption and ionization. Desorption of species is governed by the process of "rapid heating". Beuhler and co-workers (82) have used this process to enhance volatility. They have found that high heating rates favor vaporization of a thermally labile compound. In K^+IDS the final temperature to which the K^+ ceramic is stepped

apparently determines the heating rate. This is consistent with the observation that higher applied currents produce $(M+K)^+$ ions having higher relative intensities. In competition with vaporization is thermal degradation. Thermal degradation is thermodynamically a lower energy process than vaporization for the compounds studied here. Decomposition usually occurs via reactions such as the production of two molecules from one (frequently through 1,2 elimination reactions), loss of small neutral molecules (e.g., H_2O, H_2, CO_2), and cyclization reactions. The desorption process, the first mechanistic step in K^+IDS, gives a mixture of species (intact analyte and decomposition products) in the gas phase; the distribution of the species depends upon the temperature.

It is believed that the next step, ionization, takes place in the gas phase. Earlier gas phase studies in Chapter 2 revealed that addition of potassium ions to molecules in the gas phase was strongly energy dependent. If the potassium ions have too much kinetic energy, adduct formation does not occur. For this early work, a low bias on the emitter was used. The bias used in Chapter 2 was between 0.5 and 5 V. The dependence of bias volatage in these desorption experiments parallels the earlier work with gas phase analytes. The similarities between these two techniques strongly supports the concept that gas phase adduct formation is occurring in this desorption/ionization method. If adduct formation occurred on the surface of the thermionic material the ions could be extracted with any applied potential. This is not the case here.

Gas phase adduct formation is assumed to be the dominant ionization mechanism in other desorption/ionization methods. Cooks (94) has developed the concept of "selvedge" to explain cationized molecular ion formation in SIMS. Selvedge is the relatively high pressure region just above the surface. This concept is also useful for the understanding of other desorption methods. Regarding the concept of selvedge, adduct formation is generally accepted to be a termolecular process (from Chapter 2 and reference 68). More accurately, when K^+ and M react bimolecularly to form the excited adduct $(M+K)^+*$, the adduct must dispose of some energy or dissociate to reactants. Energy may be lost on collision with a third body or by infrared emission. This has been discussed for bimolecular adduct formation involving Li^+ and polar molecules by Beauchamp et al. (95). In K^+IDS a relatively high pressure region probably exists above the thermionic material and therefore adduct formation should be a tertiary process. The high pressure or selvedge region in K^+IDS would stabilize $(M+K)^+$. As will be seen shortly, adding a collision gas to the ion source increases the total ion intensity in this experiment. This behavior is consistent with gas phase, termolecular adduct formation. Similar experiments have been described in which adduct formation appears to occur bimolecularly without collisional stabilization of the adduct (93, 96-97). These complexes may be stabilized by emission of an infrared photon (95). A bimolecular reaction would be consistent with these low-pressure experiments.

There are a number of advantages in using potassium ions here

although it is not suggested that potassium is the optimum cation which can be used for such work (93). Allison and Ridge (61) have shown the capacity of an alkali ion to induce fragmentation following complexation decreases when going down the column in the periodic table. For potassium ions the dissociation energy [$D(M+K)^+$] is intermediate relative to other alkali metals. Therefore, a stable potassium adduct is produced with most polar organic compounds; it is highly improbable that this adduct will fragment to produce the other ions seen in the spectra resulting from this technique.

A summary of the mechanism of K^+IDS is as follows. Intact molecules and/or thermal decomposition products of the analyte desorb into the gas phase above the rapidly heated potassium thermionic ceramic. The thermal decomposition products produced are consistent with known thermal degradation pathways. Emitted potassium ions then "sample" these species in the gas phase to produce adducts.

Another possible ionization process which can occur in this experiment is surface ionization. Surface ionization occurs when an analyte or a decomposition product of the analyte has a sufficiently low ionization energy. Ions formed by SI do not contain potassium. Surface ionization has been well documented (28-31). Previous surface ionization experiments have been conducted using organic vapors, however, here the analyte is deposited directly onto the surface. This should make no difference if surface ionization is to occur. The potassium thermionic ceramic used in K^+IDS is very similar to materials

used in previous surface ionization experiments (31). Later in this discussion a situation will be presented in which surface ionization does occur. In these cases it is easily determined which ions are the result of SI since they do not contain potassium.

It should again be pointed out that this method is not optimized for source configuration and that the mechanism by which ions are formed may be complicated by other factors such as decomposition of described species on the ion source walls. However, this method does produce useful spectra from the analytes studied to date. K^+IDS appears to be analytically useful, inexpensive to utilize, and simple to perform. To demonstrate the utility of this ionization method, the following discussion presents K^+IDS spectra of several thermally labile compounds.

A. APPLICATIONS USING K^+IDS

1. Saccharides. The study of thermal decomposition reactions of saccharides continues to be an active area of research. A large amount of data has been collected on thermal decomposition of saccharides since they are present in foods, paper, and a number of other products (98, 99). It is not suggested that the saccharides shown here are difficult to analyze mass spectrometrically and in fact have been analyzed using other desorption/ionization methods (77, 90, 92-93). Saccharides were chosen for analysis by K^+IDS to compare previous thermal decomposition studies with the spectra obtained by this method.

It must be made clear that the conditions for thermolysis must be considered when comparing results. Early studies (98) identified over 70 products when glucose was subjected to high temperatures for a period of several hours. Curie-point pyrolysis of glucose however, showed 5 products (100) which are thought to arise from the decomposition of 1,6-anhydro-β-D-glucopyranose (levoglucosan). The variables which must be considered when comparing results include the amount of sample used, heating rate, heating time, and atmospheric conditions (composition and pressure).

When saccharides are deposited on the potassium thermionic emitter and heated, simple spectra are produced. The spectrum obtained for glucose ($M=C_6H_{12}O_6$, MW=180) is shown in Figure 25. The predominant peak in the spectrum is the potassium ion adduct of glucose at m/z 219 ($(M+K)^+$). The loss of water from glucose produces the largest fragment ion at m/z 201, $[(M-H_2O)+K]^+$. The fragment ion is most likely an anhydro sugar. Anhydro sugars are major decomposition products from the thermolysis of saccharides and polysaccharides (101). These thermal decomposition intermediates lead to the formation of lower molecular weight decomposition products (101, 102).

The peak intensities in the spectrum in Figure 25 are not unexpected since rapid heating is employed. If the heating rate were lowered, the intensity of the decomposition adduct, $[M-H_2O)+K]^+$, would be expected to increase relative to $(M+K)^+$. The high desorption rates of both M and $[M-H_2O]$ may account for

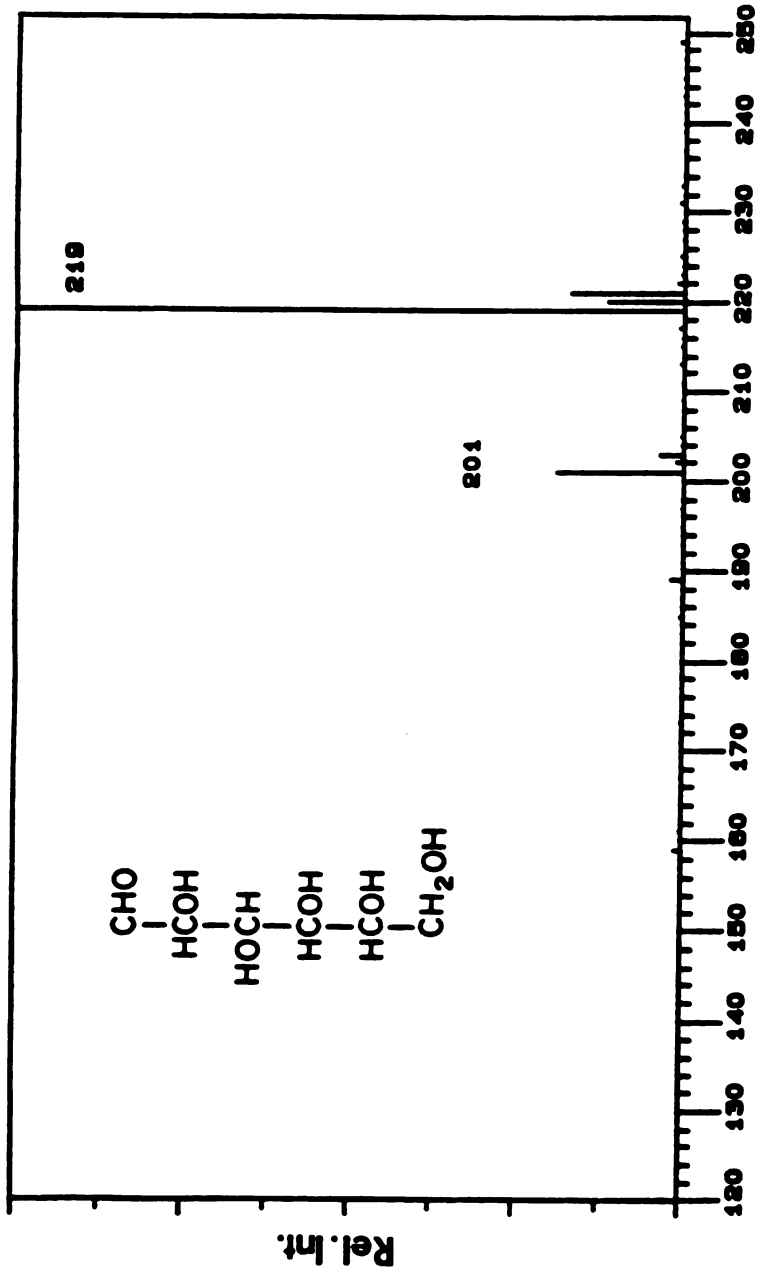


Figure 25. K^+ IDS Spectrum of Glucose.

the small amount of further decomposition products. If this were not true, low mass fragment adducts would be seen as suggested by some pyrolytic methods. Most decomposition products from sugars are produced from an intermediate such as an anhydro sugar, however this may not always be the case. The low intensity ions at m/z 189 $[(M-CH_2O)+K]^+$ and m/z 159 $[(M-C_2H_4O_2)+K]^+$ arise from neutral losses from glucose. This has been observed previously (102) and is also substantiated by the presence of formaldehyde (CH_2OD) and hydroxyacetaldehyde ($C_2H_4O_2$) in the pyrolysis of saccharides (102).

Figure 26 is a spectrum obtained when sucrose ($M=C_{12}H_{22}O_{11}$, MW=342) is deposited on the potassium thermionic emitter. The cationized molecule $(M+K)^+$ is observed at m/z 381. Fragment ions at m/z 363, 345, and 327 are adducts of the dehydration products of the sugar, i.e., $[(M-H_2O)+K]^+$, $[(M-2H_2O)+K]^+$, and $[(M-3H_2O)+K]^+$, respectively. In addition to dehydration, thermal decomposition of polysaccharides involves the cleavage of the glycosidic linkage in a 1,2 elimination process and has been well documented (103). The result of the cleavage is two products with the structures $C_6H_{12}O_6$ and $C_6H_{10}O_5$. This cleavage is evident here by the presence of ions at m/z 219 and 201 which are $[C_6H_{12}O_6+K]^+$ and $[C_6H_{10}O_5+K]^+$, respectively. Cleavage of the glycosidic linkage is an important process required for the sequencing of polysaccharides. From Figure 26 the molecular

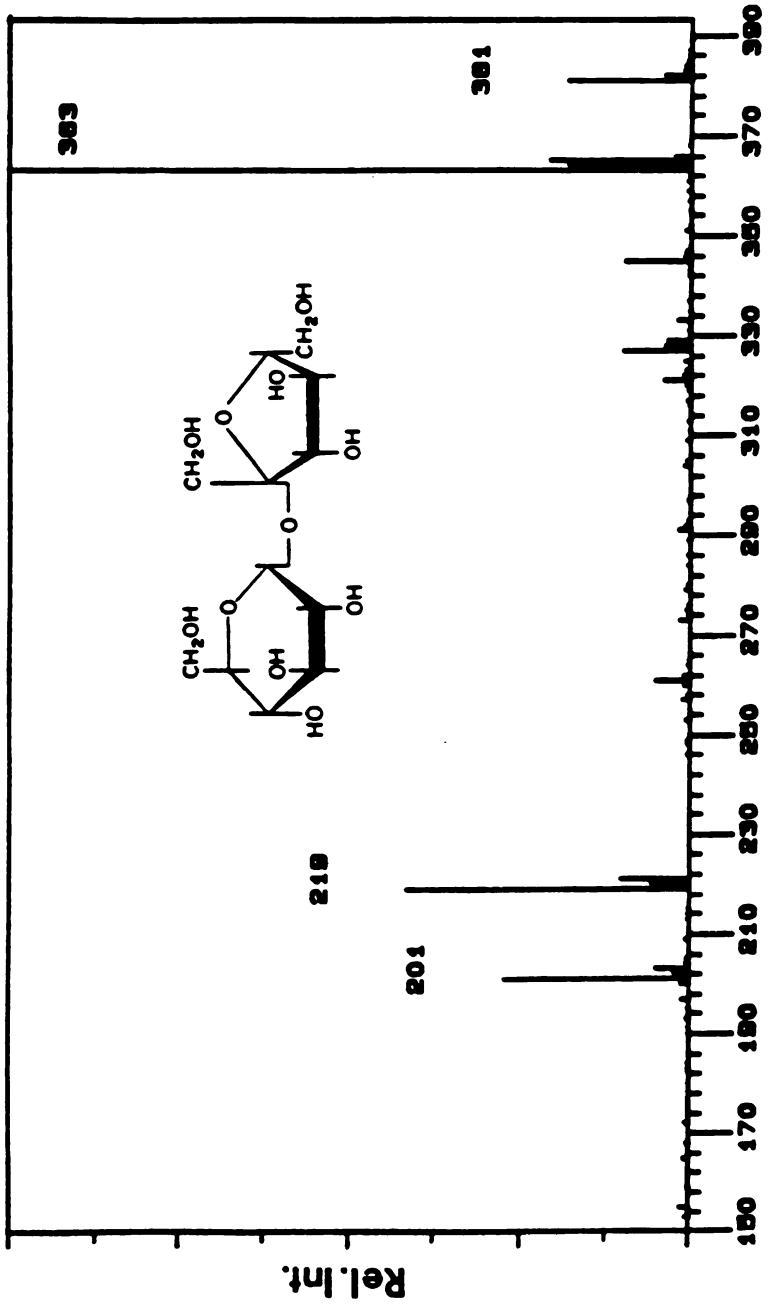


Figure 26. K^+IDS Spectrum of Sucrose.

weight of the sugar is obtained and, in addition, one can easily conclude that the molecule is comprised of two hexose units. Further work has been started to utilize this method for more complex systems such as gums, starches, and higher order polysaccharides.

2. Pharmaceuticals. A substantial amount of work has been done on the analysis of pharmaceuticals using pyrolysis techniques and desorption/ ionization methods. Most of these compounds are thermally labile. As an example, the β-lactam antibiotics have been studied by Py-MS (104) and by various DI methods (105, 106). Pyrolysis methods almost always lead to low molecular weight products and consequently compound identification relies upon matching pyrolysis mass spectra to known spectra. Desorption/ionization techniques have become the more popular tool for the analysis of these compounds, however, as yet there appears to be no optimum method for their analysis. For this reason the study of penicillins using K^+IDS was undertaken.

Figure 27 shows a K^+IDS mass spectrum of ampicillin ($C_{16}H_{19}N_3O_4S$, MW=349). The largest peak in the spectrum is that of the cationized molecular ion $(M+K)^+$ at m/z 388, which is not the case in the spectrum of this compound produced by other desorption methods (e.g., "in-beam" ionization (105)). In addition to the molecular adduction ion a large number of cationized fragments are present from the thermal decomposition of the ampicillin molecule. Major fragments can be identified by the cleavage of the lactam and thiazolidine ring as can be shown in

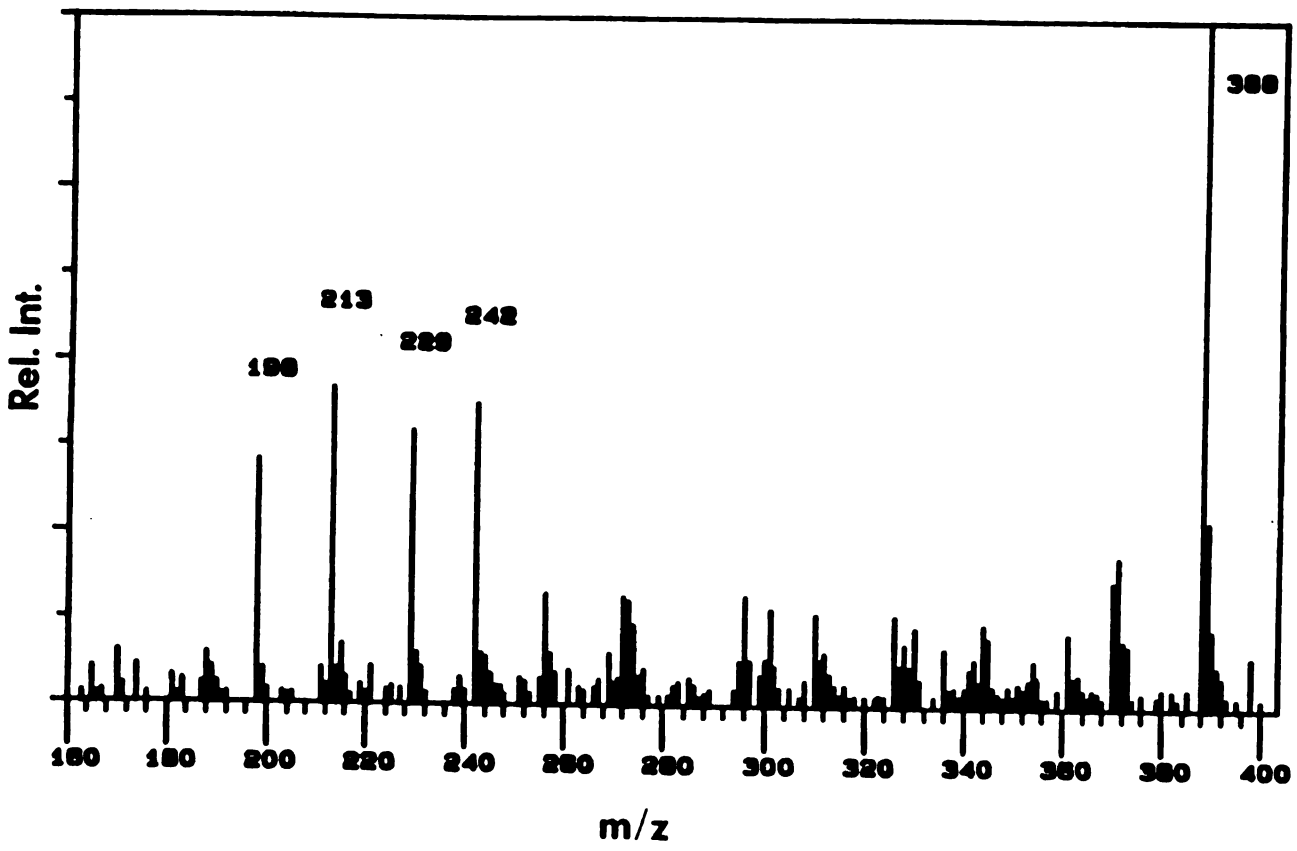
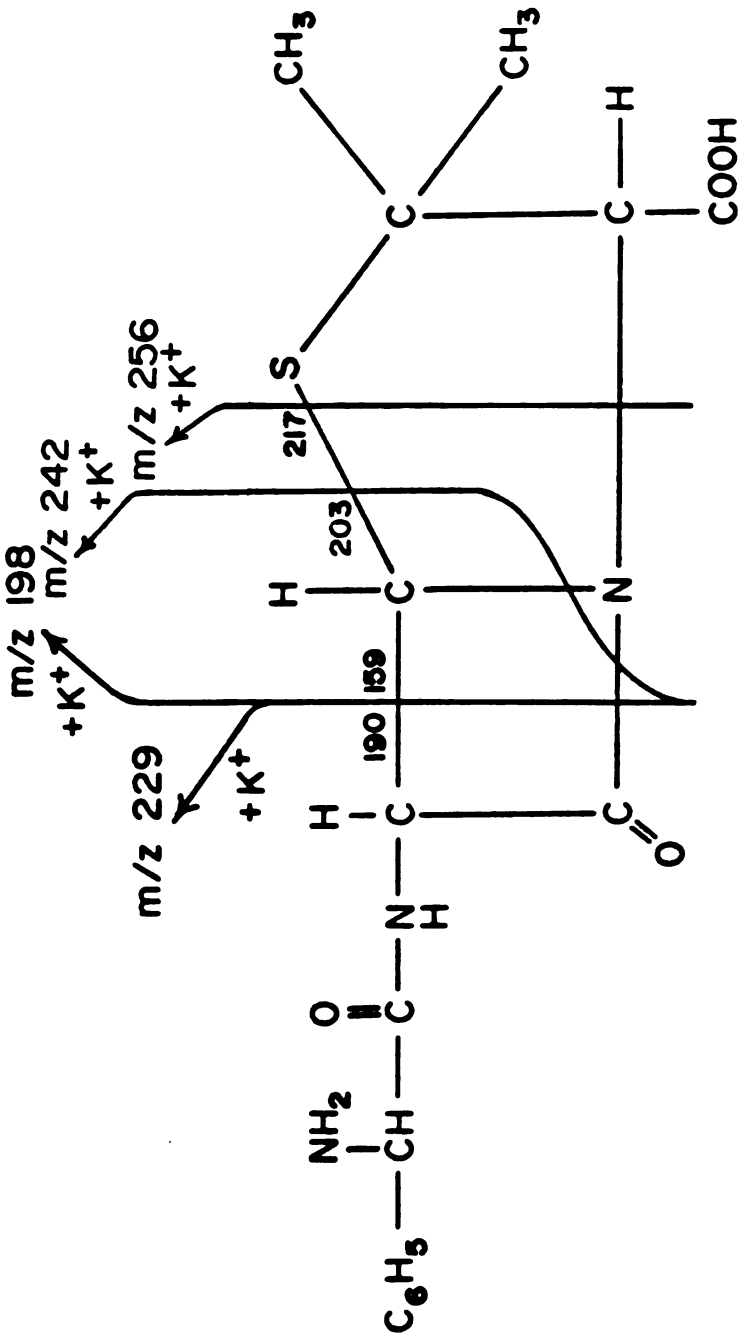


Figure 27. K^+IDS Spectrum of Ampicillin.


CH3
CH3
C
H
C
COOH
S
m/z 256
+K+
217
m/z 242
+K+
203
m/z 198
+K+
H
C
N
159
190
m/z 229
+K+
H
C
C
O
N
H
O
C
NH2
CH
C6H5

Scheme I

Scheme 1. The fragment adducts observed provide structural information on the molecule.

Two points can be made concerning Figure 27. The number of thermal decomposition products seen in the spectrum is substantially greater than that of the saccharides and account for a large proportion of the total ion intensity. Here the rate of decomposition on the thermionic material must be larger than the rate of desorption. Secondly, as will be shown later, cleavage at the amide functionality was expected. Cleavage of the strained lactam ring, however, appears to take precedence. This is substantiated by other desorption/ionization techniques in which intense fragment ions are observed corresponding to protonated species arising from the cleavage of the ß-lactam ring of the penicillin (106).

The free acid form of the penicillins studied to date by other DI techniques have given results comparable to those in Figure 27. However, also of interest are the salts of these compounds. In this case a cationized molecular ion is not obtained for the salt, however, adequate information is present for a structure analysis. Further results on such species will be the subject of future research.

3. Peptides. The sequencing of the amino acids in peptides has been of great interest in mass spectrometry. The thermal lability of the peptides has required extensive derivatization before a mass spectrometric analysis can be performed. Ionization methods requiring no derivatization, therefore, have been of considerable interest (107, 108). Pyrolysis processes of

amino acids have been studied and are well understood (109). Pyrolysis of polypeptides are not very well understood. A typical K^+IDS mass spectrum of a polypeptide, hexaglycine, is shown in Figure 28.

The spectrum of hexaglycine ($M=C_{12}H_{20}N_6O_7$, MW=360) is dominated by potassium adducts of thermal degradation products, however, an $(M+K)^+$ ion of small intensity is present at m/z 399. We can increase the relative intensity of $(M+K)^+$ by increasing the temperature to which the thermionic ceramic is stepped; the result is shown in the insert of Figure 28. Increasing the relative intensity of $(M+K)^+$ is done, however, at the expense of some of the decomposition adducts. A compromise is therefore needed and the result is the full spectrum in Figure 28. Scheme 2 shows the formation of the potassium adduct sequence ions arising from thermal degradation of hexaglycine. The majority of the adduct ions observed are a result of the 1,2-elimination reaction at the peptide bonds. This cleavage is a low energy process. This point can be illustrated using the decomposition of glycylglycine as an example.

$$\text{Glycylglycine} \rightarrow \text{glycine} + NH_2\text{-}CH{=}C{=}O$$

Using group equivalent values (110) this process is approximately 5 kcal/mol exothermic. This process is analogous to the cleavage of glycosidic linkages by a 1,2-elimination which was discussed earlier for the disaccharide. In addition, Scheme 2 shows the

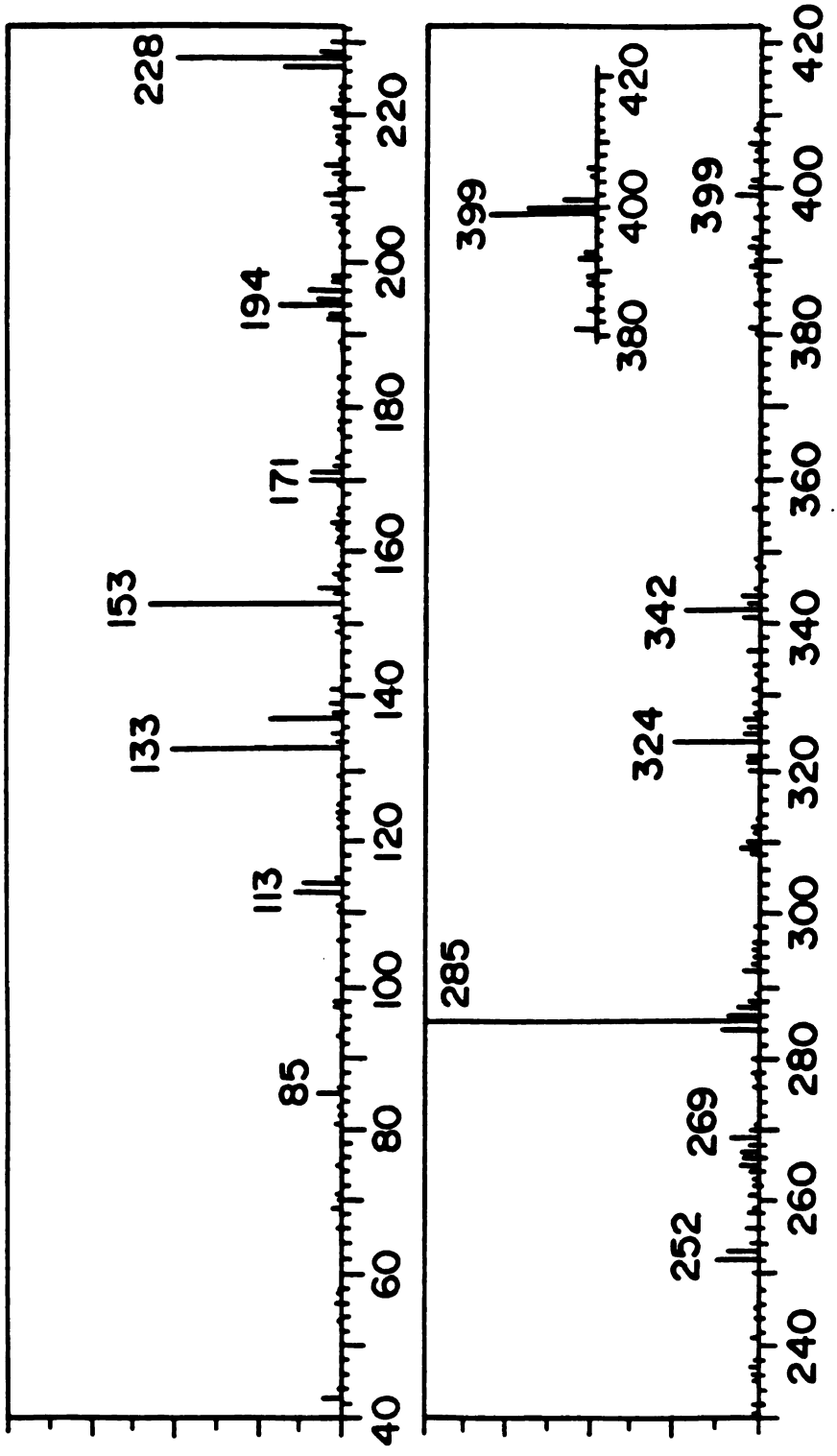
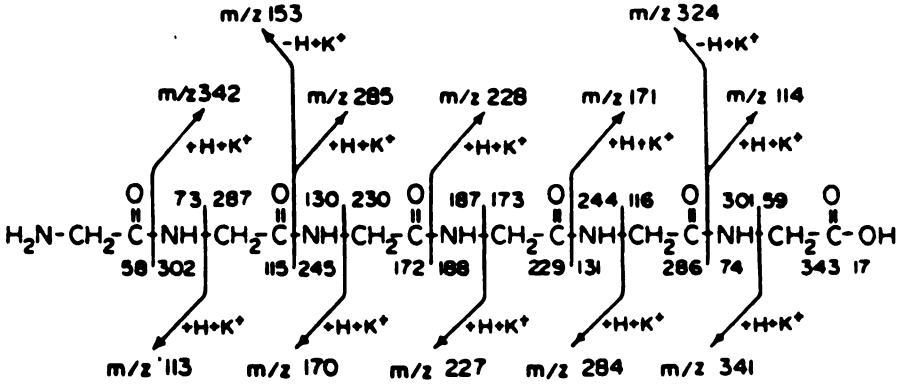


Figure 28. K^+IDS Spectrum of Hexaglycine. A Heating Current of 2 A Was Used. The Insert Shows the Molecular Ion Region For Which the Heating Current Was 2.5 A. The Relative Intensity In the Latter Case Was Approximately 2.5 Times That of the Previous (2 A) Spectrum.

Scheme 2


m/z 153
-H+K+
m/z 324
-H+K+
m/z342
+H+K+
m/z 285
+H+K+
m/z 228
+H+K+
m/z 171
+H+K+
m/z 114
+H+K+
H2N-CH2-C-NH-CH2-C-NH-CH2-C-NH-CH2-C-NH-CH2-C-NH-CH2-C-OH
73 287
130 230
187 173
244 116
301 59
58 302
115 245
172 188
229 131
286 74
343 17
+H+K+
+H+K+
+H+K+
+H+K+
+H+K+
m/z 113
m/z 170
m/z 227
m/z 284
m/z 341

rearrangements leading to the low intensity adducts observed from the cleavage of the RNH-CH_2R bond. This process is thermodynamically less favorable and this is reflected in the abundance of these ions.

Consider as an example, the sixth skeletal bond from the N-terminus in Scheme 2. If this C-N bond was cleaved, 2 radicals of masses 115 and 245u would be formed. However, as the skeletal bond is cleaved, a H shifts (1,2-elimination) to form two neutrals of masses 114 and 246u. The K^+ adducts of each are observed at m/z 153 and 285.

Here, most ions are a result of adduct formation from fragments arising from the C-terminal end. Ions at m/z 96, 210, and 267 should also appear in the spectrum. A more likely possibility is that the adduct at m/z 153 is the result of a cyclization reaction to give $\underline{\lceil CH_2\text{-}C(O)\text{-}NH\text{-}CH_2\text{-}C(O)\text{-}NH \rceil}$. Cyclization reactions were proposed previously from experiments in which depeptides were sublimed in a mass spectrometer to obtain EI spectra (111). The other ion at m/z 324 can be a dehydration product from the species at m/z 342. The reason for forming fragments from only the N-terminal end is not yet fully understood. Possibilities can include the particular interactions between the peptide and the surface of the thermionic emitter or the spatial configuration (conformation) of the peptide. Further research needs to be done on polypeptides to provide insights into this behavior. Finally, this desorption/ionization method is potentially useful for sequencing peptides and also provides

insights into their thermolysis. This information has not yet been obtained with other pyrolysis techniques.

4. Steroids. Steroids constitute a large class of compounds which continue to receive much attention due to their important role in plant and animal systems. In particular, cholesterol has been the steroid studied most extensively since it has been linked to human diseases such as atherosclerosis and cancer (112, 113). Methods in the analysis of cholesterol include wet chemical (113), chromatographic (114), and mass spectrometric techniques (113). The latter technique involves derivatization if used in conjunction with gas chromatography since sterols are often thermally unstable. Cholesterol will be used as a representative steroid.

When cholesterol (M=$C_{27}H_{46}O$, MW=386.6) was deposited onto the potassium thermionic material and heated the spectrum which resulted is shown in Figure 29. Potassium adducts of a large number of species appear at a higher mass than $(M+K)^+$ ion of cholesterol. The spectrum of Figure 29 was obtained from a cholesterol sample (U.S.P. grade) which was more than 20 years old. The K^+IDS mass spectrum of cholesterol from a newly opened bottle (Type CH-K, Sigma Chemical Co.) a much simpler spectrum resulted as shown in Figure 30. Here the peak at m/z 423 is the potassium adduct of dehydrogenated cholesterol $[(M-H_2)+K]^+$. These species are also observed in Figure 29.

The species present in Figure 29 are apparently the result of the autoxidation of cholesterol. A large body of literature exists

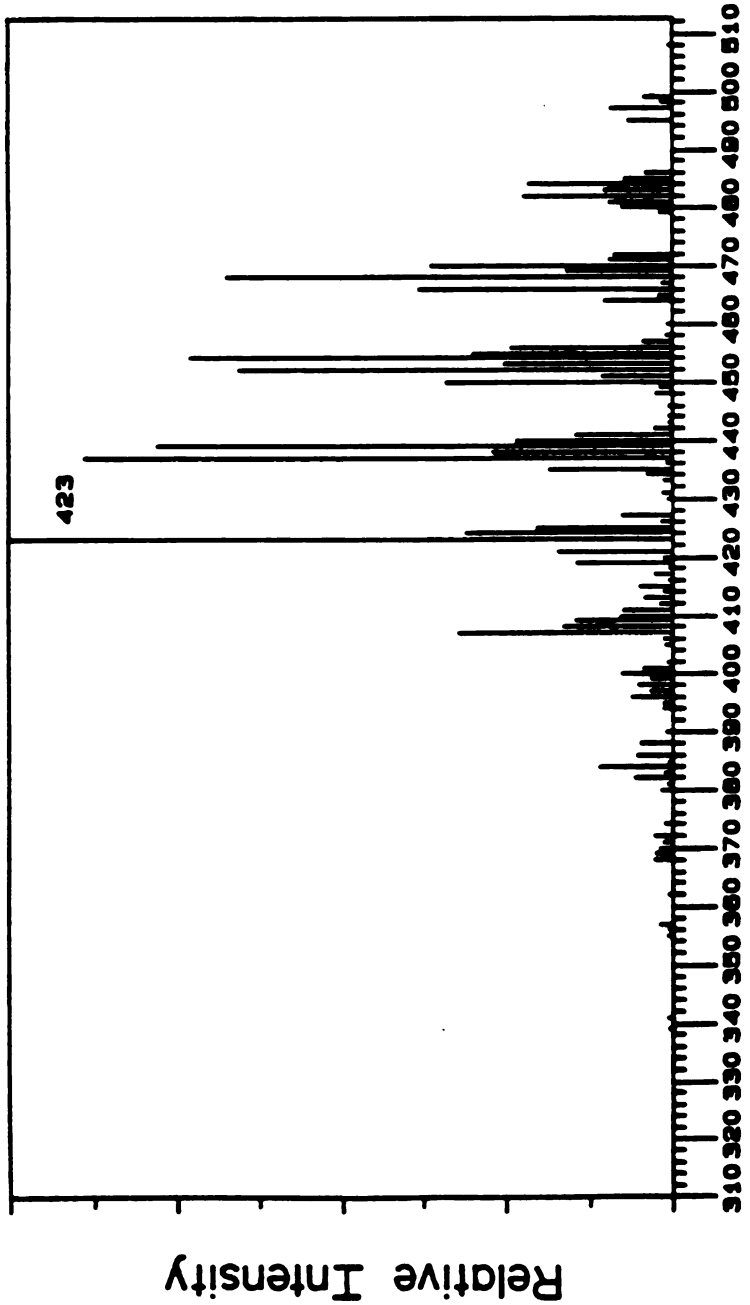


Figure 29. K^+IDS Spectrum of 20 Year Old Cholesterol.

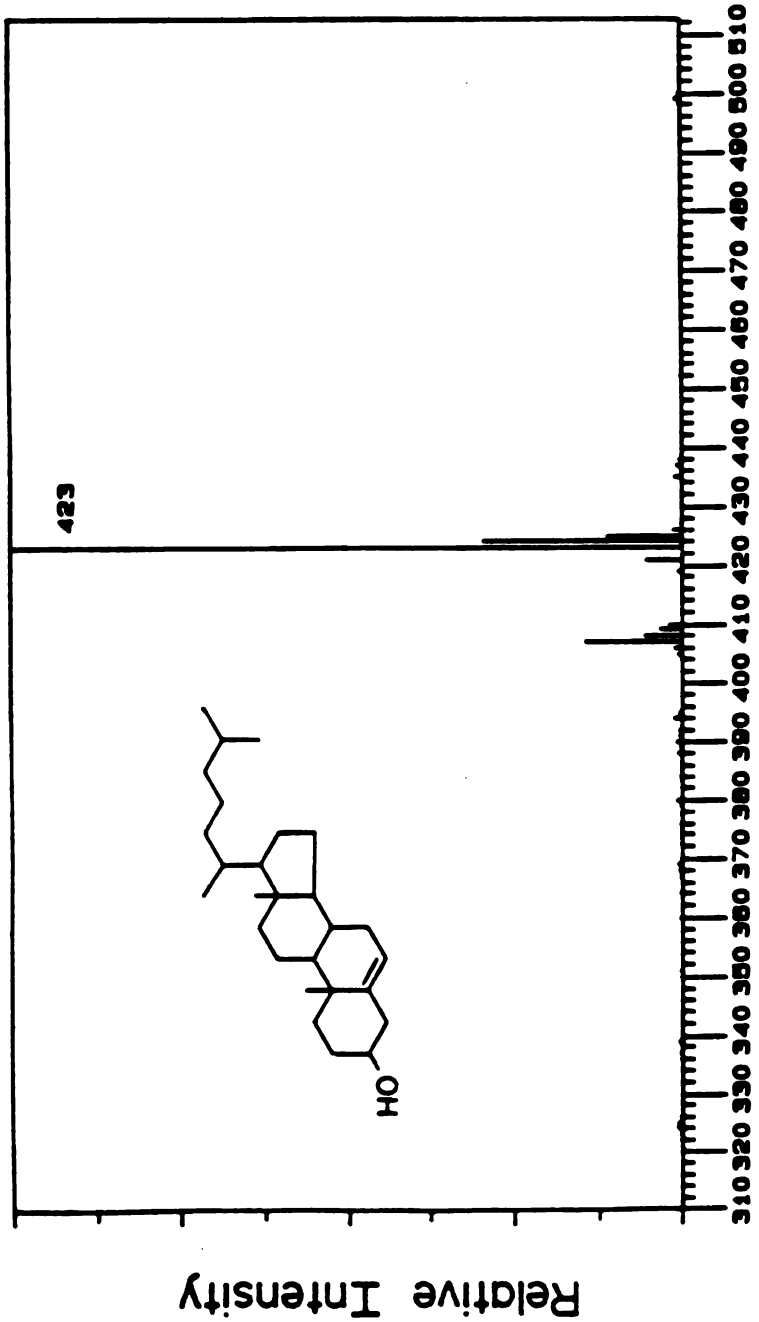


Figure 30. K^+IDS Spectrum of "Fresh" Cholesterol. Conditions the Same as in Figure 30.

concerning the autoxidation of sterols and in particular cholesterol (113). Nearly forty oxidation products have been isolated from cholesterol samples which have been merely stored in contact with air. The products include predomiantly C_{27} compounds however C_{24}, C_{22}, C_{21}, C_{20}, and C_{19} products were also isolated (113).

Two points can be made concerning the spectra in Figures 29 and 30. This ionization method presents a fast (less than five minutes) and simple method for determination of sample purity. In the case of cholesterol the "pure" sample is eassily recognized. The second point concerns the analysis of mixtures. The sample which lead to Figure 29 is actually a mixture of cholesterol and cholesterol derivatives. Mixture analysis often requires long and complex separation processes, however, here the analysis was performed rapidly using this method.

5. Mixture Analysis. Procedures for mixture analysis are often as complex as the mixtures to be analyzed. A particular class of compounds which can be considered in mixture analyses is polymers. Polymers can be categorized as synthetic or biopolymers and until recently (83) have received little attention in mass spectrometric analysis. Pyrolytic methods have been previously used however complex spectra often resulted, which required the use of pattern recognition or spectral matching for polymer identification. Figure 31 shows a typical K^+IDS spectrum of poly(ethylene glycol) having an average molecular weight of 1000 (PEG 1000). It should be emphasized that poly(ethylene

glycol) is a mixture of molecules having the formula $H(OCH_2CH_2)_nOH$. The average molecular weight of the polymer is determined by the distribution of the molecules in the mixture. This spectrum contains a wealth of information concerning the polymer but it must also be realized that the spectrum represents the analysis of over 70 different species or decomposition products derived from PEG 1000. Four series of ions in the spectrum for this polymer include $[H(OCH_2CH_2)_nOH+K]^+$, $[CH_3CH_2(OCH_2CH_2)_nOH+K]^+$, $[(H(OCH_2CH_2)_nOH-H_2O)+K]^+$, and $[H(OCH_2CH_2)_nOCH_3+K]^+$. (These are labelled A, B, C, and D, respectively, in Figure 31). These series are separated by 44 mass units which is indicative of the structural unit of the polymer (C_2H_4O). The first series of ions mentioned previously may also be used to determine the average molecular weight if the $H(OC_2H_4)_nOH$ molecules, to which K^+ is attached, are products of vaporization only (i.e., not thermal degradation products). An average molecular weight for a polymer would not be easily determined from vaporized decomposition products, therfore the relative amounts of certain gas phase species must parallel that of the bulk sample. This very important point suggests that quantitative information could be obtained for other types of mixtures. the determination of molecular weight distributions for polymers using K^+IDS will be addressed shortly.

In Figure 32 the same analysis was performed in which the potassium thermionic material was stepped to a current 0.5 A

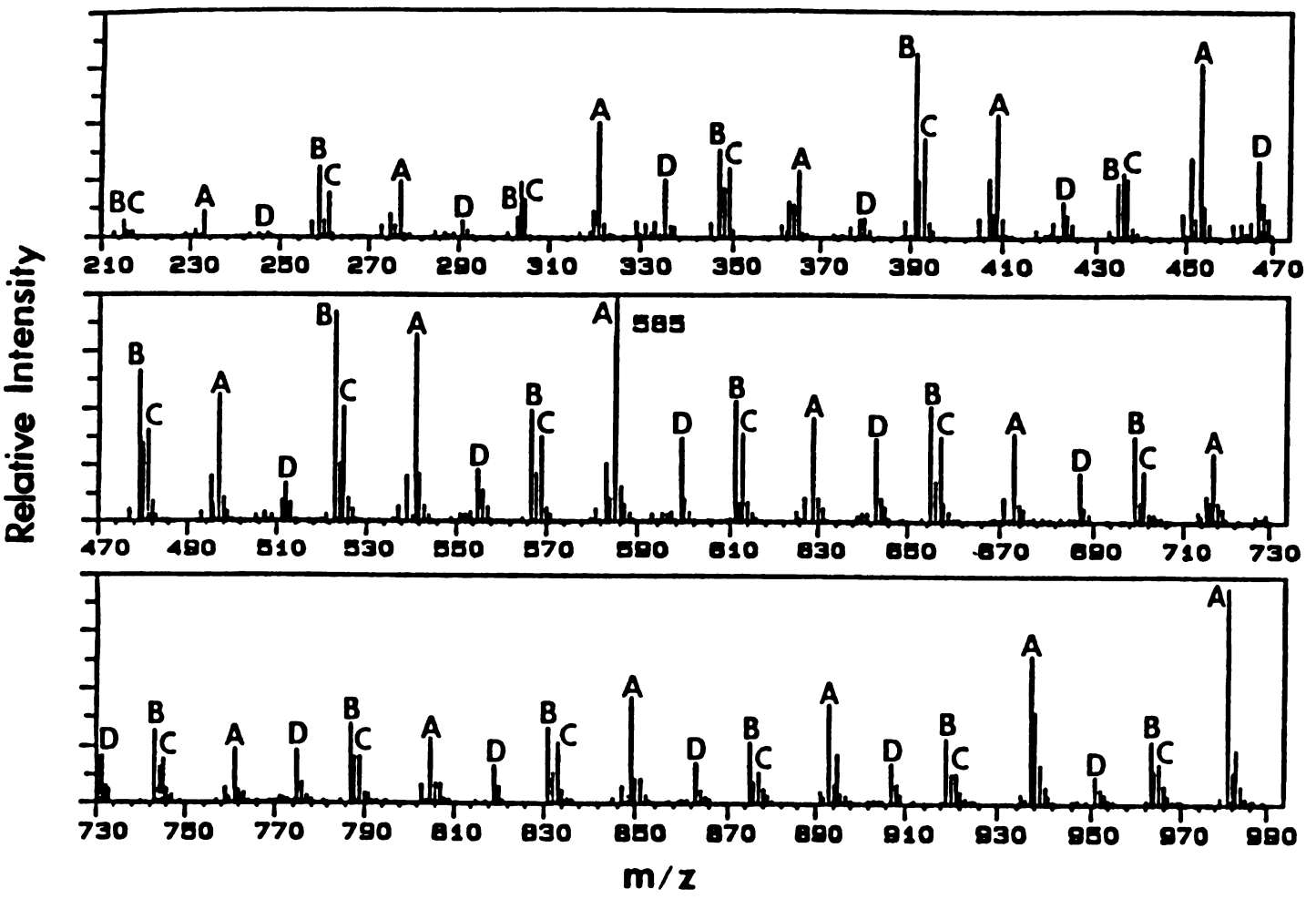


Figure 31. K^+IDS Spectrum of Poly(Ethylene Glycol) 1000 at a Heating Current of 2.5 A.

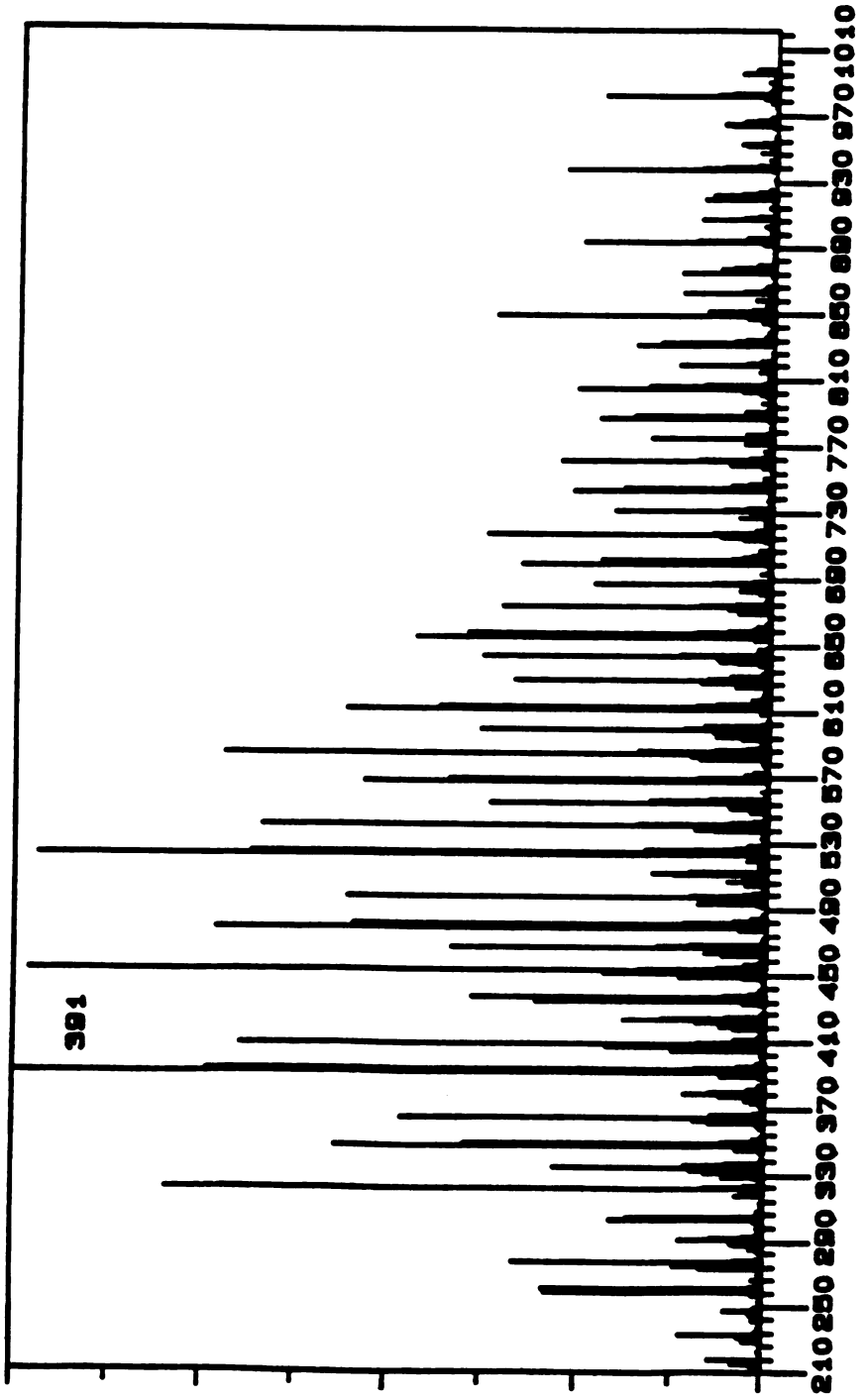


Figure 32. K^+ IDS Spectrum of Poly(Ethylene Glycol) 1000 at a Heating Current of 2.0 A.

lower than that used in Figure 31. The high temperature spectrum shows an increased abundance of higher mass ions (e.g. m/z 849, 893, 937, and 981) and in addition the relative intensities of decomposition product ions have increased. This observation seems to be in contradiction to earlier results (e.g., peptides) where increasing the heating rate diminished the intensity of decomposition products in the K^+IDS spectrum. However, another temperature related phenomenon of K^+IDS is the duration of time during which spectra representative of the analyte are produced. As an example of this behavior Figures 33 and 34 show the total ion intensity plots of PPG 725 and ampicillin respectively. When a single analyte produces a TII curve similar to Figure 34, an increased heating rate facilitates higher intensities for $(M+K)^+$ ions and less intense decomposition product-adduct ions. Behavior in Figure 33 occurs for some mixtures (e.g., PEG's and PPG's) in which an increased heating rate appears to facilitate both vaporization and decomposition. The difference in the two behaviors in Figures 33 and 34 must be a reflection of the thermal stability of the analyte, i.e., in Figure 34 no analyte is left after several seconds so that an increase in decompostion adduct ions cannot be observed.

In addition to structural analysis of polymers (e.g., the determination of the monomeric unit) molecular weight distributions are also of interest. Figure 35 shows a spectrum of poly(propylene glycol)725 (PPG 725) deposited on the potassium thermionic material and heated. Here the average molecular weight can be obtained from the sequence of

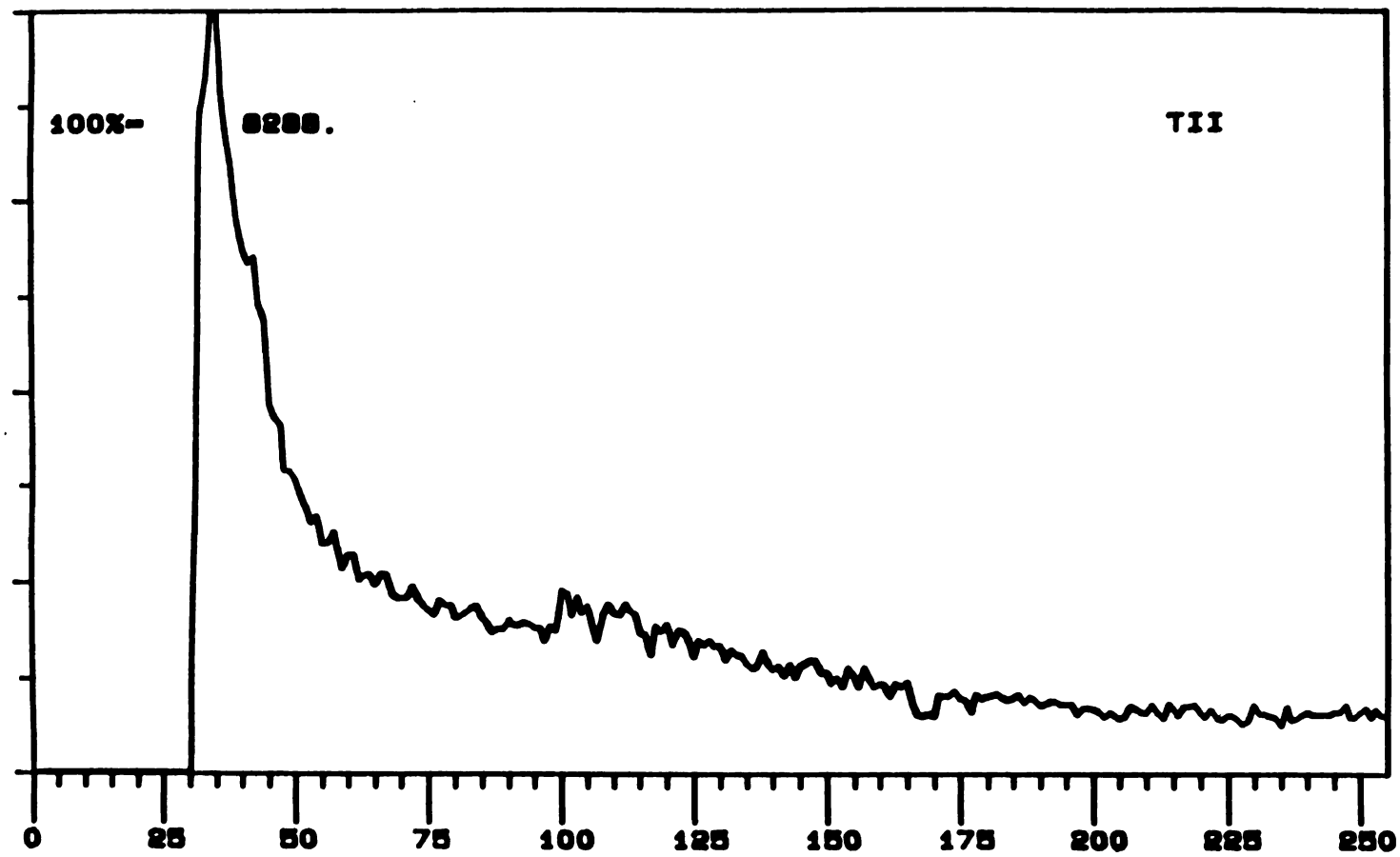


Figure 33. Total Ion Intensity vs. Scan Number of Poly(Propylene Glycol) 725. The Scan Rate Was 1.0 Scan/s.

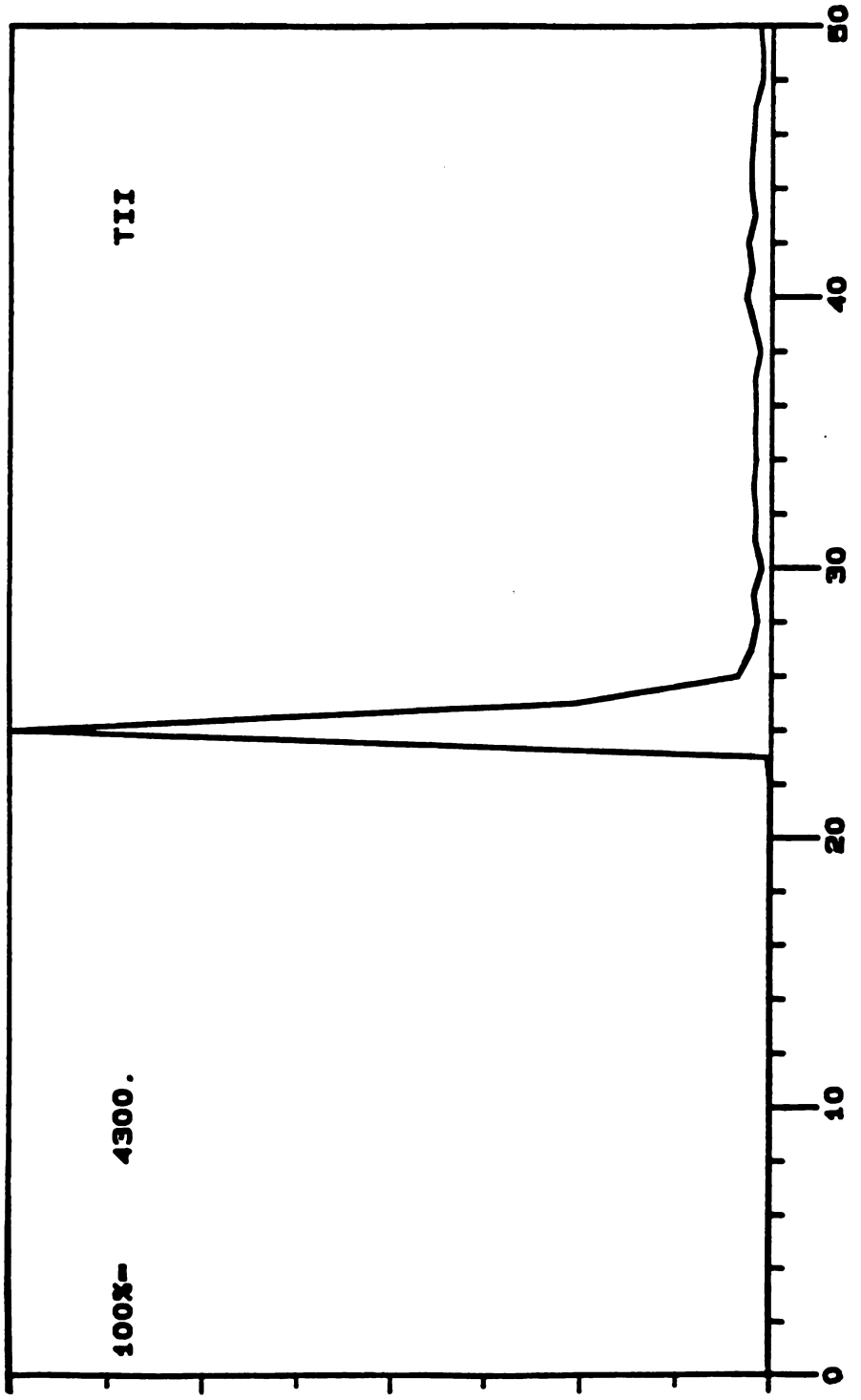


Figure 34. Total Ion Intensity vs. Scan Number of Ampicillin. The Scan Rate Was 0.6 Scan/s.

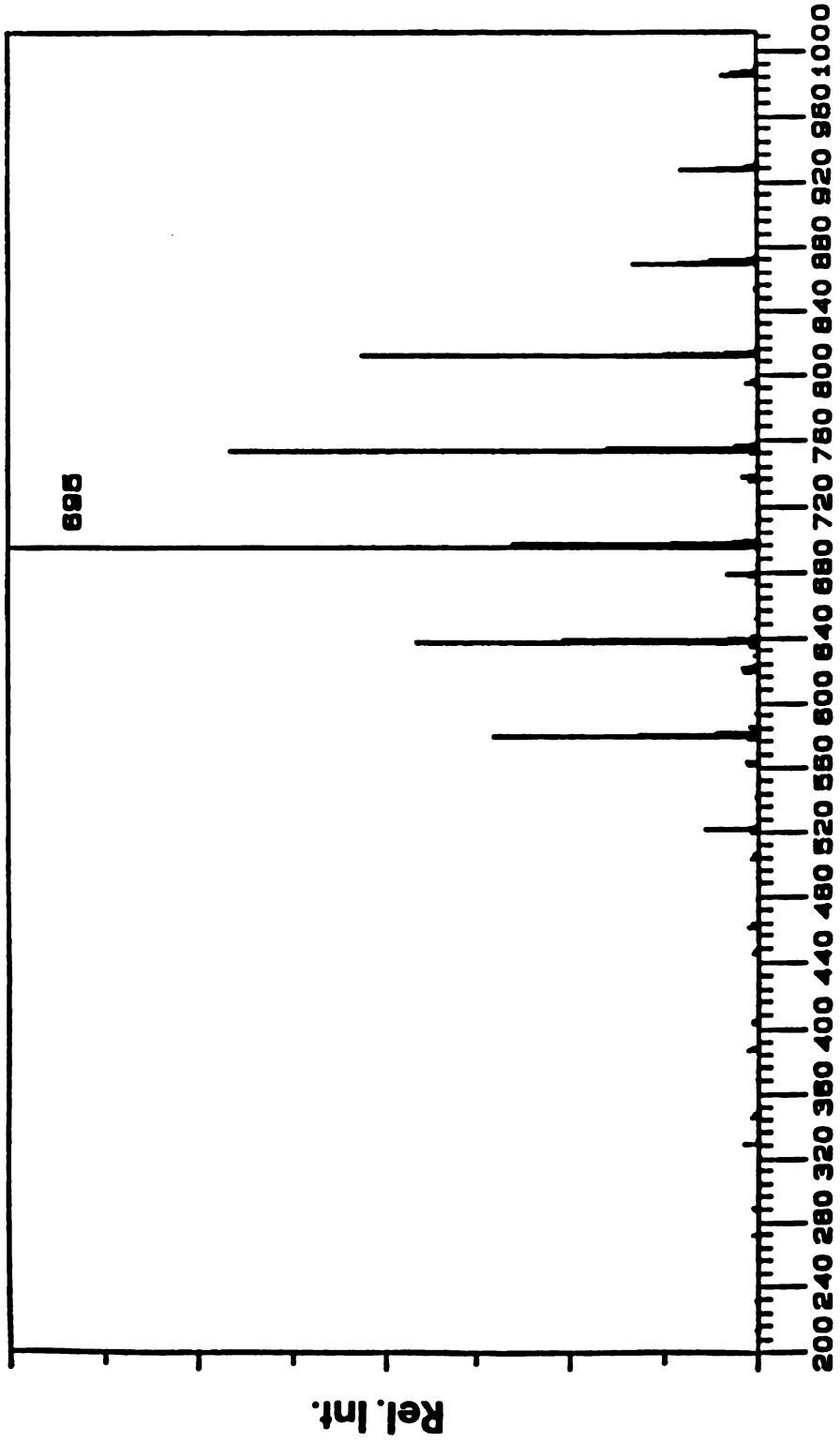


Figure 35. K^+IDS Spectrum of Poly(Propylene Glycol) 725. A Heating Current of 2 A Was Used.

$[H(OCH_2C(CH_3)HCH_2)_nOH+K]^+$ ions. From the spectrum shown the average MW is calculated to be 710. This ionization method appears to be a fast and simple method for determining the mean molecular weight in such mixtures. Unfortunately the mass range of the mass spectrometer used in these studies does not permit such analyses of higher molecular weight polymers. This ionization technique has been applied to a wide range of synthetic polymers and biopolymers. These results will be presented in Chapter 4 of this thesis.

B. SENSITIVITY

For polymer analysis the amount of sample used is usually large compared to trace analysis. Sensitivity of this DI technique however is of concern particularly in regard to trace components in complex mixtures. In Figure 36 the total ion intensity is plotted versus an amount of polyphenyl ether ($M=C_{36}H_{26}O_5$, MW=538) deposited on the potassium thermionic material. Polyphenyl ether (6 ring) is a compound which does not thermally decompose readily and therfore the spectrum produced from this ether using this technique consits of only the $(M+K)^+$ ion at m/z 577. A solution containing 239 ng/µl of the ether in acetone was prepared. The curve was obtained by applying the appropriate amount of solution on the probe tip, drying, and then heating within the mass spectrometer source.

Curve A in Figure 36 was obtained at the base pressure of the

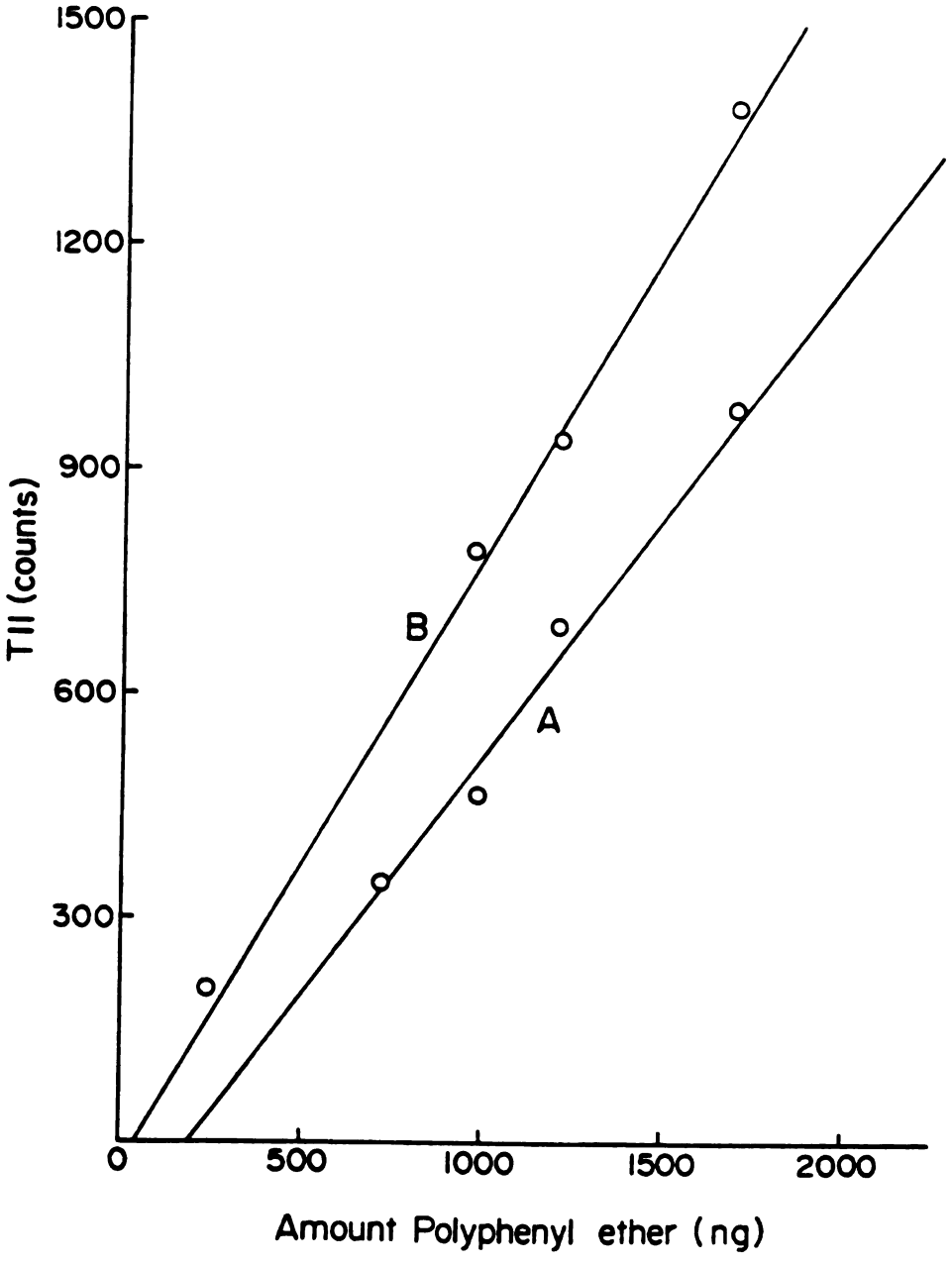


Figure 36. Total Ion Intensity at Peak Maximum of Polyphenyl Ether Plottes vs. Amount Deposited on the Thermionic Emission Material. A Heating Current of 2 A Was Used.

mass spectrometer ($2x10^{-6}$ torr). Here 500 ng of sample gave a peak ion intensity of 200 counts at a signal-to-noise (S/N) ratio of 20. Presently, attempts are being made to improve the sensitivity of this ionization method. If K^+IDS involves gas phase adduct formation the sensitivity would be enhanced by the addition of a neutral collision gas. As seen from earlier studies in Chapter 2 increasing the pressure facilitates adduct ion formation since this process is termolecular. Curve B in Figure 36 shows this experiment repeated at a pressure of $1x10^{-4}$ torr of N_2 within the mass spectrometer source. In this case approximately 250 ng of sample are required to obtain a peak ion count of 200 at an equivalent S/N ratio which is a factor of 2 improvement from the low pressure case. Further work is needed in this direction to improve sensitivity.

Polyphenyl ether was chosen for this study primarily for its simple spectrum. Other compounds may prove more or less sensitive using this ionization method however, for most analyses presently performed, sample sizes used were in the low microgram range.

C. SURFACE IONIZATION OF THERMALLY LABILE COMPOUNDS

To this point all of the spectra presented contain K^+ adducts of the analyte molecule or K^+ adducts of thermal decomposition products derived from the analyte. However, some organic compounds when analyzed using this ionization technique produce ions which do not contain potassium. Here two possibilities

exist: 1) direct thermal desorption of ions (as seen for quaternary salts (91, 92)) or 2) surface ionization. Thermal desorption has generally been accepted to occur for species which exists as "pre-formed" ions prior to the application of heat. Thermal desorption will not be applicable in the following discussion.

For surface ionization to occur the analyte molecule or a decomposition product of the analyte must have a low ionization energy. Amines generally have ionization energies less than 9 eV and have been observed to interact with heated surfaces (characterized by high work functions) to form positive ions (29). Ionization energies of 9 eV have been calculated for the thermally labile xanthines (115). Presently, however, only one study has determined these ionization energies. These authors find the ionization energies for the class of compounds containing the xanthines are greater than 9 eV (115). Figures 37 and 38 show the spectra of xanthine ($M=C_5H_4N_4O_2$, MW=152) and theophylline ($C_7H_8N_4O_2$, MW=180) respectively. Here an abundance of ions which do not containe K^+ are formed including the molecular ions of each compound. A mechanism for understanding the ions formed from theophylline is shown in Scheme 3.

This alternative ionization process is useful in this ionization method as can be seen from both spectra in Figures 37 and 38. Molecular weight information from the m/z of the M^+ and the $(M+K)^+$ ions is obtained as well as a number of fragment ions indicative of the molecule's structure. If the temperature of the

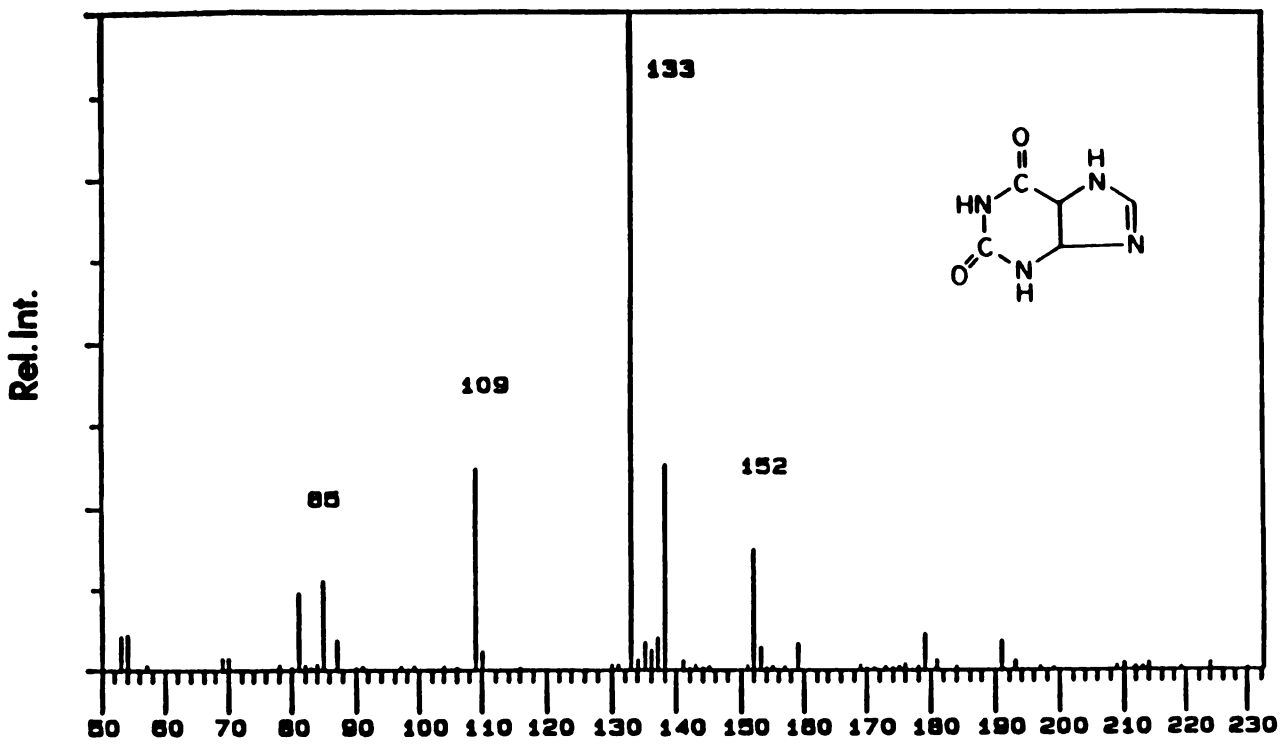


Figure 37. K^+IDS/Surface Ionization Spectrum of Xanthine. A Heating Current of 2.5 A Was Used.

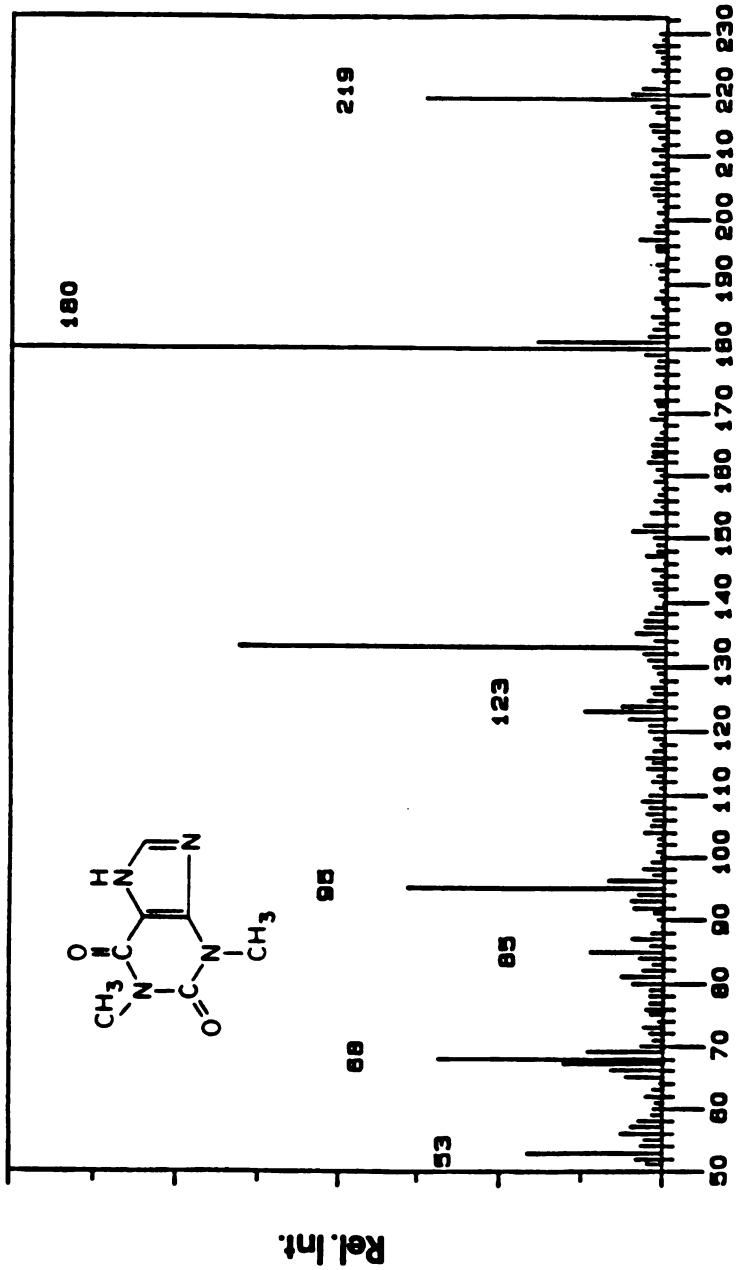
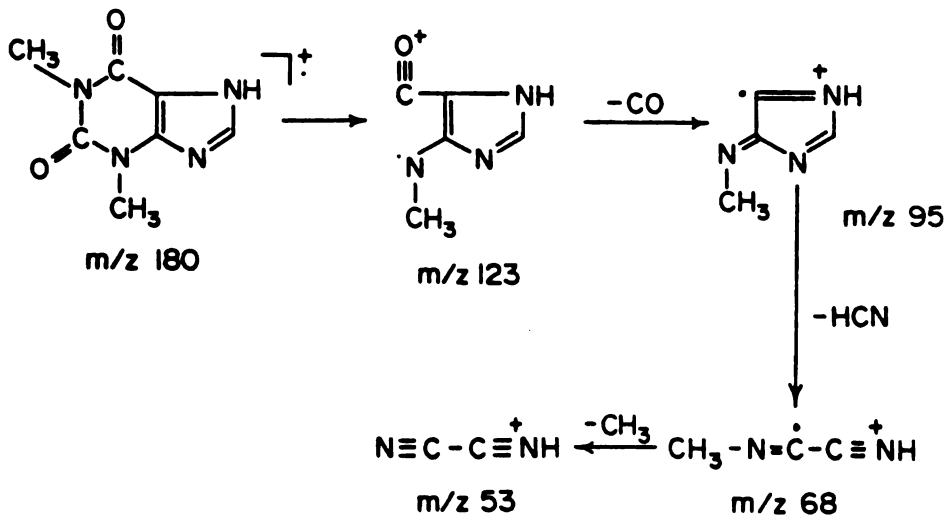


Figure 38. K^+IDS/Surface Ionization Spectrum of Theophylline. A Heating Current of 2.5 A Was Used.

Scheme 3



thermionic emitter is low enough to permit surface ionization a selective ionization process exists, that is, only species with low ionization energies will be ionized. Such a technique would be helpful in selectively ionizing components in a complex mixture.

In addition, the thermionic material can be used in a negative ion mode. Figure 39 shows the negative ion spectrum of L-methionylglycine (M=$C_7H_{14}N_2O_3S$, MW=206) when deposited on a cesium thermionic emitter and heated. The composition of the cesium thermionic emitter is $2SiO_2$:Al_2O_3:Cs_2O. Molecular weight information is obtained from the $(M-H)^-$ ion at m/z 205. The largest ion in the spectrum is that of CN^- which is not surprising due to its high electron affinity (a requirement for negative surface ionization). A cesium thermionic emitter was used since negative surface ionization is favored on low work function materials (30). For the alkali oxide thermionic material used in these studies the work function of alkali-containing material decreases as one goes down that column in the periodic table. Here, again, the use of negative surface ionization would offer selectivity in an analysis since only species with sufficiently high, positive electron affinities would be ionized.

IV. FINAL COMMENTS ON CHAPTER 3

The use of the thermionic emission probe has proven to be useful in the analysis of thermally labile compounds.

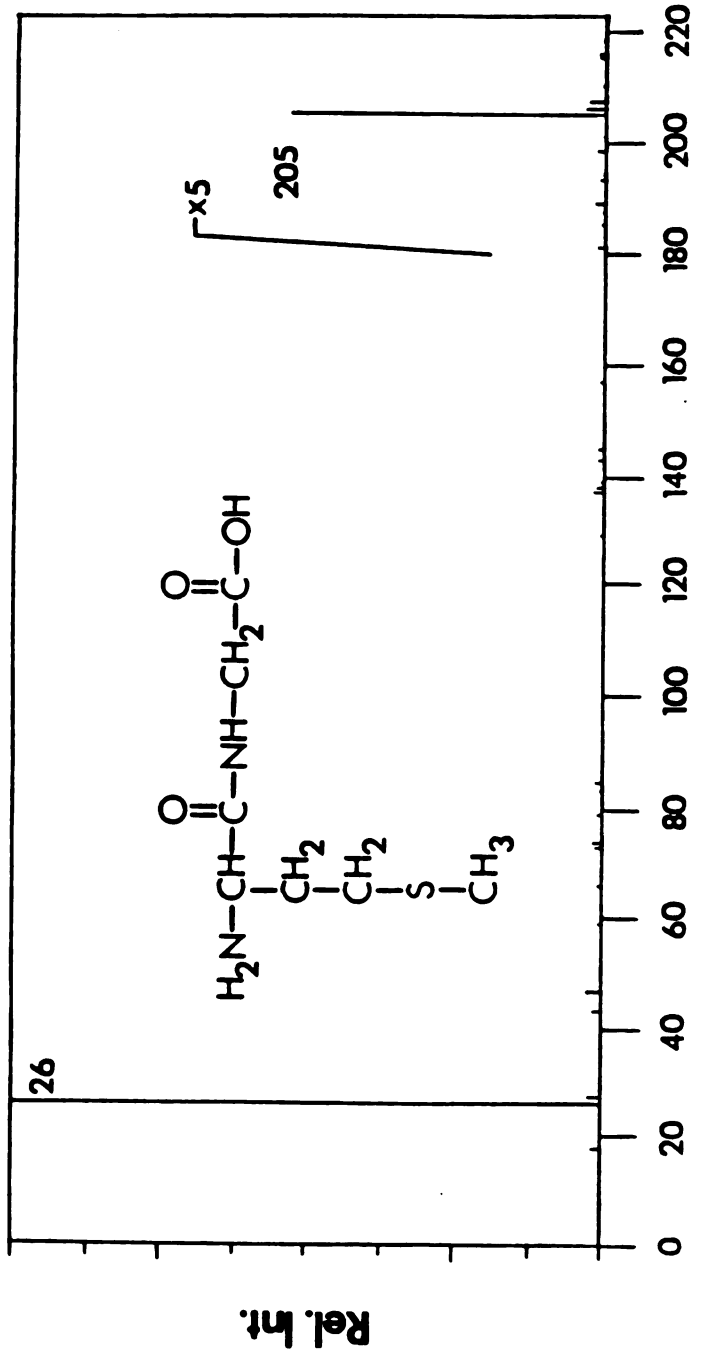


Figure 39. Negative Surface Ionization Spectrum of L-Methionyl glycine Deposited on the Thermionic Emission Material. The Bias on the Bead Relative to the Source Was -1.0 V. A Heating Current of 2.5 A Was Used.

Particularly enlightening was the success achieved for polymeric systems. This success led to further characterization of K^+IDS in polymer analysis which is the subject of the next part of this thesis. A number of other compounds have been tried using K^+IDS but have not been fully evaluated. The spectra for these compounds can be found in Appendix A of this work.

CHAPTER 4. MASS SPECTROMETRIC ANALYSIS OF POLYMERS USING K^+IDS

I. INTRODUCTION

Conventional analysis by mass spectromety involves the ionization and subsequent analysis of gaseous analytes. Polymeric systems, due to their nonvolatility, require either pyrolytic methods or desorption/ionization mass spectrometric techniques for their analysis. Pyrolysis methods are most often used for the MS analysis of polymers (83). These techniques generally involve thermally degrading the polymer followed by ionization using electron ionization, chemical ionization, or field ionization of the pyrolyzates. Pyrolysis can be achieved using resistively heated filaments, lasers, or by heating a ferromagnetic wire to its Curie point using a radio frequency field (Curie-point pyrolysis).

Pyrolytic methods of analysis can be divided into the two categories of pyrolysis-gas chromatography-mass spectrometry (Py-GC-MS) and pyrolysis-mass spectrometry (Py-MS). In the former thermal degradation products from a sample can be chromatographically separated and each qualitatively analyzed by conventional mass spectrometry. The mass spectrum from a Py-MS experiment can be used to identify degradation products or to produce a "fingerprint" spectrum that may be interpreted using pattern recognition techniques.

Pyrolytic techniques in the analysis of polymers can suffer

from several disadvantages. Secondary reaction products can be formed in the pyrolysis zone. These products are not desirable since they complicate the spectra and diminish the quantity of primary degradation products. The heating rate and final equilibrium temperature used are important factors since thermal decomposition processes of polymers are time and temperature dependent. The last disadvantage concerns the nature of pyrolysis products. Often, only low mass species are observed. These species are helpful when determining the structural subunits of a polymer, however, no molecular weight information can be derived.

These disadvantages suggest the need for alternate mass spectrometric methods for the analysis of polymers. The optimum method would be rapid and direct (i.e. the pyrolysis step and the MS analysis would be simultaneous). Most polymers are a mixture of oligomers consisting of a specific repeating unit (monomer). For the analysis of such mixtures, average molecular weight, the oligomer distribution profile, and structural information is desired. The advent of new ionization modes in mass spectrometry for nonvolatile/thermally labile compounds have made the analysis of some polymers possible. Various desorption/ionization techniques have been used for a number of polymeric systems with varied results. DI methods which have been used for polymer analysis include desorption CI (116), rapid-heating methods (117), laser desorption (80, 116) plasma desorption (118), secondary ion mass spectrometry (119), and electrospray (120). In most cases these DI methods produce

spectra reflecting the oligomer species and, when applicable, can make it possible to determine average molecular weights of polymeric mixtures. The mass difference between two consecutive oligomer ions in a mass spectrum allows the mass of the monomeric unit to be determined, however some of these DI methods only yield information of the mass of the monomeric unit. When the distribution of oligomer species is beyond the mass range of the mass spectrometer only structural information can be obtained. In this case pyrolysis techniques would be advantageous.

K^+IDS offers the advantages of other DI techniques and pyrolytic methods for the analysis of polymeric systems. The potential of this method has been demonstrated in Chapter 3. K^+IDS offers a number of advantages over pyrolysis methods and some DI techniques, due to the fact that the method utilizes rapid heating. Rapid heating allows for the rapid attainment of temperatures at which desorption rates are greater than competitive degradation rates. In polymer systems this is useful if molecular weight information is needed. In addition, rapid heating may tend to favor the production of larger mass fragments from the polymer chain. This type of information is often lacking in pyrolytic methods. For many polymers, the average molecular weight falls outside the mass range of current mass spectrometers. In these cases, the goal is to obtain structural information to identify the polymer. By adjusting the heating rate used in K^+IDS, spectra containing potassium adduct ions of thermal decomposition products are produced. Therefore

K^+IDS may be used in structural studies of such large polymers. Another advantage of K^+IDS is that the ionization process is in close proximity to the site of desorption. In general this feature is inherent in most DI methods but can be lacking in pyrolytic methods. It would appear that K^+IDS has some of the advantages of both pyrolytic and DI techniques. It should be noted that the use of alkali ions in the analysis of thermally labile compounds has been exploited in a number of related DI methods as pointed out in Chapter 3.

Examples of various polymeric systems analyzed by K^+IDS will be presented in this chapter. It is apparent that various polymers behave differently when analyzed by this technique. In the first section polymers with average molecular weights outside the mass range of the mass spectrometer will be discussed. Here K^+IDS provides structural information useful in identifying the polymer. The final section focuses on relatively low molecular weight polymers to highlight the utility of K^+IDS for molecular weight determinations.

II. EXPERIMENTAL

The polymer analyses were performed on the same GC/MS/DS system as before. This desorption/ionization technique and the operation parameters have been described in Chapters 2 and 3. The thermionic probe was the same used in the earlier studies. The temperature to which the thermionic probe was stepped determines the heating rate. In this case higher applied currents

produced higher heating rates. The mass spectrometer was set to begin scanning above m/z 42.

Appropriate solvents were used to dissolve the polymers. Several drops of dilute solution were applied to the thermionic K^+ ceramic and the solvent evaporated off. Typically, several micrograms of polymer were placed on the probe tip in this way. All (commonly available) chemical were ACS reagent grade. Nylon 6, polyvinylpyrrolidone, poly(ethylene glycol)s and poly(propylene glycol)s were obtained from Aldrich Chemical Co., and XF-1150 was obtained from Applied Science.

III. RESULTS AND DISCUSSION

A. General Consideration of Using K^+IDS For Polymer Analysis.

A particular polymer's behavior in K^+IDS will fall into one of two categories. These categories are differentiated solely by the length of time in which spectra characteristic of the polymer are produced during the K^+IDS experiment. The first class of polymers generates total ion intensity curves similar to that shown in Figure 40. The duration of useful K^+IDS spectra usually is less than 30 seconds. The second category of polymers show TII curves such as that shown in Figure 41. Here the duration of useful spectra often is longer than five minutes. Polymers in the former group will be referred to as "short-lived" and polymers in the latter group will be called "long-lived". The short-lived polymers are viscous, high average molecular weight polymers,

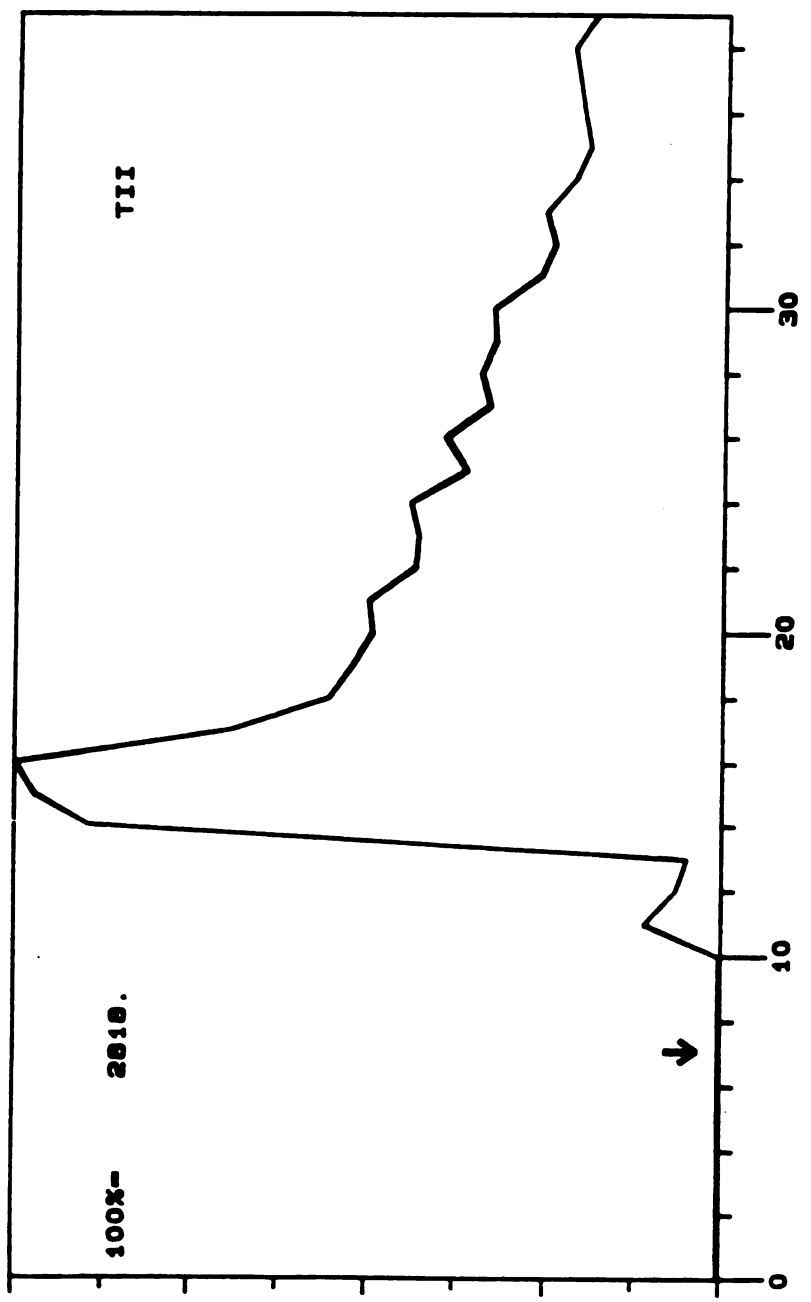


Figure 40. Total Ion Intensity For K^+IDS Analysis of Nylon 6.
Arrow Indicates When Current Was Applied.

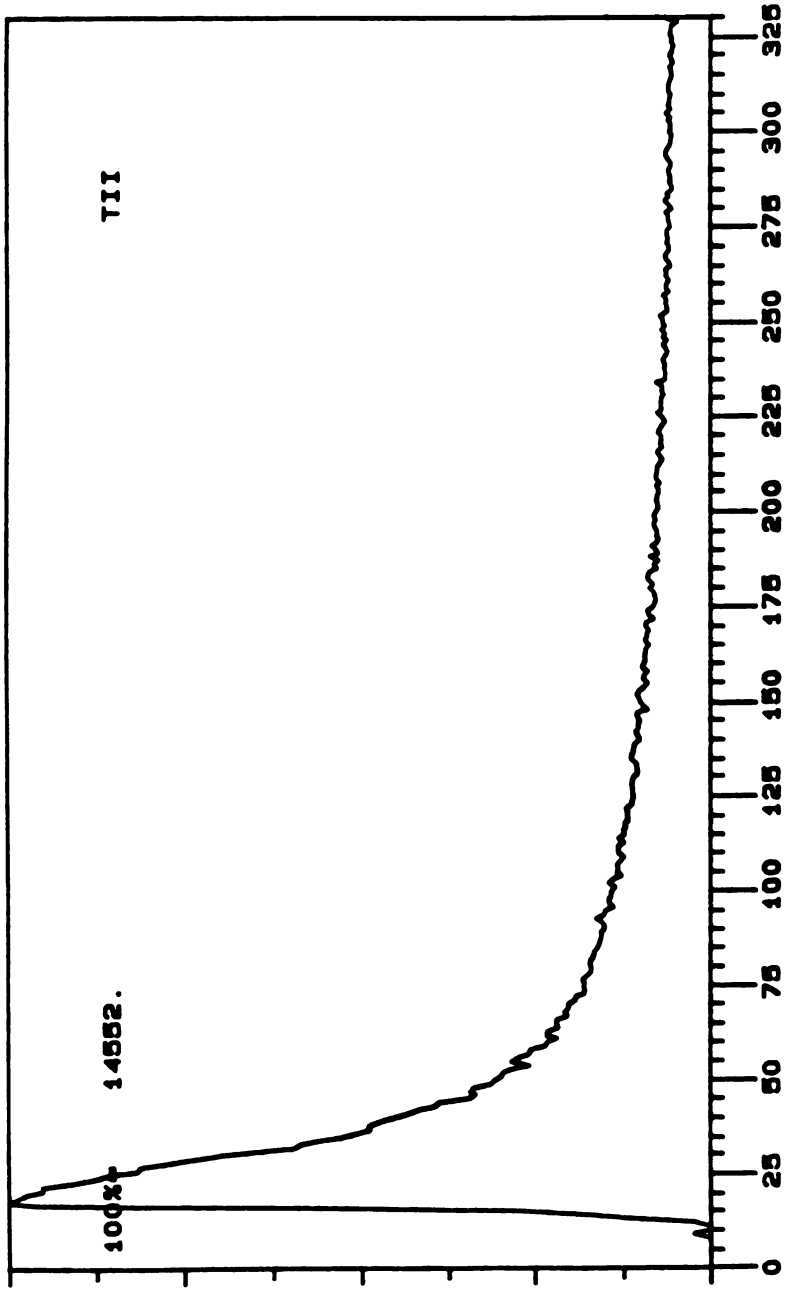


Figure 41. Total Ion Intensity For K^+IDS Analysis of Poly(Ethylene Glycol) 600. The Total Run Time Shown Here is Approximately 7 Minutes. Current Was Applied at Scan 7.

usually gums or solids. For these polymers, K^+IDS provides useful structural information. Long-lived polymers are of low viscosity, usually liquids. These polymers were chosen since their average molecular weights (M_w) fell within the mass range of the mass spectrometer used here. In this case K^+IDS can be evaluated for providing molecular weight information. Polymers representative of both groups will be discussed. For both cases suggestions on how to use the resulting K^+IDS spectra will be presented, that is, one purpose of this research is to provide the methodology for the analysis of polymers using K^+IDS. Once this methodology is established, polymer analysis can be performed, as will be demonstrated here.

The rapid heating of a thermally labile compound is an important aspect of K^+IDS. A short discussion of this topic is relevent here. Consider a case in which a thermally labile compound is deposited on the material and heated to a temperature at which potassium ions are produced (Figure 42). Until the emission temperature is reached, species desorb from the surface of the thermionic ceramic and no ions are formed. At the onset of potassium ion emission adducts will form with whatever is in the gas phase above the emitter. From Figure 42, spectra of the analyte will be formed only when the two curves overlap. Rapid heating leads to both vaporization of the sample, and the prompt production of potassium ions before the sample extensively decomposes. Pictorially, this leads to a greater overlap of the two curves in Figure 42. Figure 42 only applies to short-lived polymers and most other thermally labile compounds

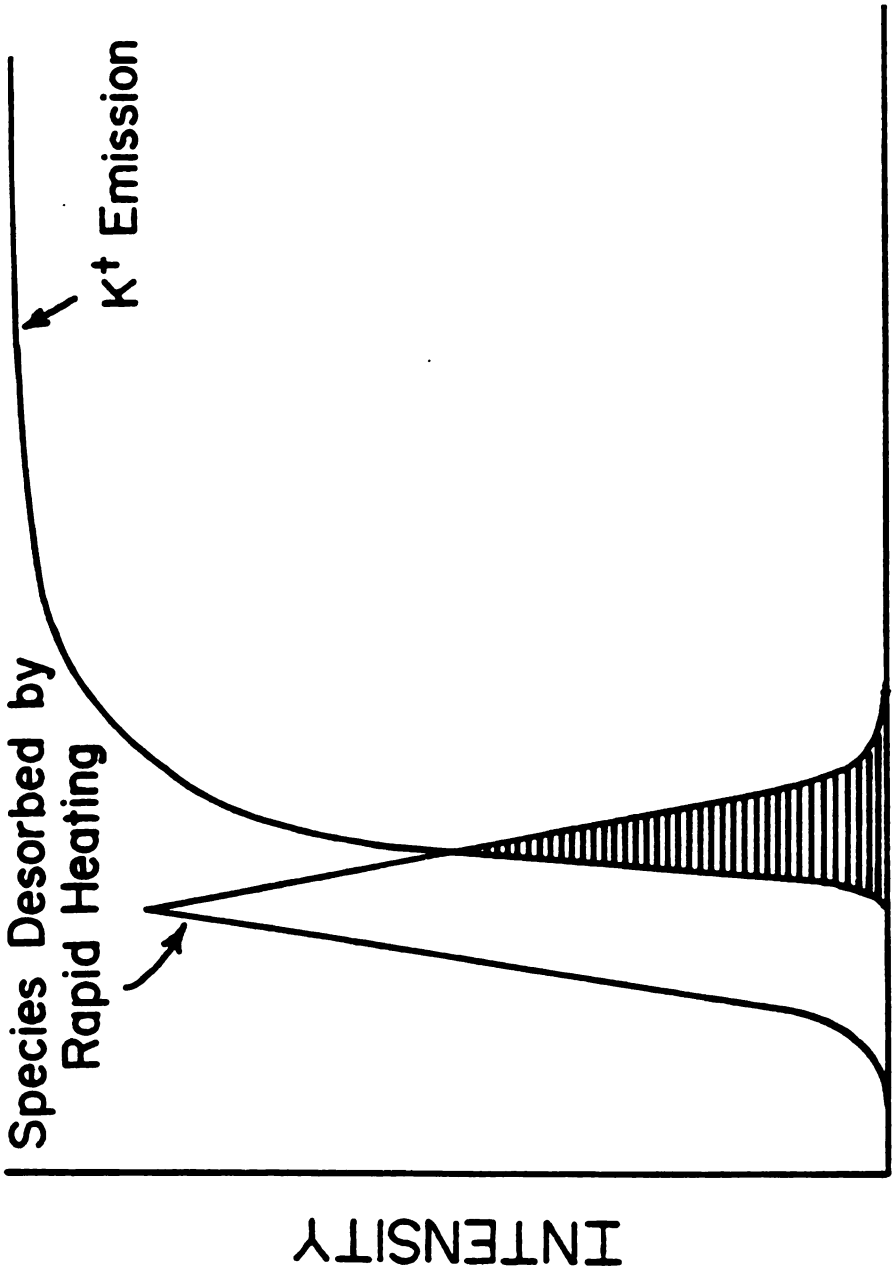


Figure 42. Intensity as a Function of Time for the Desorption of Species Due to Rapid Heating and the Emission of K^+. The Overlap Region Shows Where K^+ IDS Spectra are Produced.

which have been studied previously.

Desorption of thermally labile compounds by rapid heating has been performed using electron or chemical ionization (117). Friedman and co-workers (82) have previously found that desorption is favored at higher temperatures over decomposition. Simply, the heating rate and final temperature determine the extent of fragmentation. The K^+IDS spectra may be "adjusted" by altering the heating rate. Thus, the heating rate affects the cross section of the two curves in Figure 42, and also the types of neutrals which are being desorbed.

One factor which affects the heating rate is the amount of thermionic emission material on the rhenium filament. The amount determines the rate of heat transfer from the rhenium filament to the sample. A thin coating of the thermionic material on the filament allows for a sufficiently large heating rate. This is another variable in K^+IDS; the amount of thermionic material needed will depend upon the type of information (structural or molecular weight) which can be obtained for a polymer. Rapid heating of the probe applies to both short-lived and long-lived polymers. In short-lived polymers the heating rate is adjusted to maximize the overlap of desorbed species and potassium emission (Figure 42). However, due to the high molecular weights of these polymers, decomposition is required to provide structural information. Therefore the heating rate must not be too high, so that decomposition of the polymer will occur. What follows is a more detailed account of the short-lived polymers. This will then be followed by a discussion of long-lived polymers where

molecular weight information may be obtained using K^+IDS.

B. SHORT-LIVED POLYMERS

1. General Considerations

A typical example of a short-lived polymer's total ion intensity curve is given in Figure 40. Nylon 6 ($[NH(CH_2)_5CO-]_n$) will be used as a "model" polymer in explaining how the results of the K^+IDS experiment should be interpreted. For this figure the mass spectrometer scan rate was set such that each scan took 0.8 s. Past scan 40 the total ion intensity drops considerably and, in addition, pyrolysis proceeds to a point in which useful spectra are no longer obtained. Therefore there is little difficulty in deciding the useful "cut-off" point in the TII plot. Here, the cut-off point refers to the point in the curve in which information from the spectra is not useful for analyzing the polymer.

After the cut-off point is determined the next step is to decide which spectrum to choose for analyzing the polymer (in this case Nylon 6). Several questions need to be addressed before this decision can be made. Do the spectra change with time? If so, what should be considered as the K^+IDS spectrum of this compound? From Figure 40 the TII curve can be divided into two regions. One region is located between scans 11 and 20 and the other from scans 20 to 40. The first region encompasses the "peak" that is usually observed after the potassium thermionic

material on which the polymer is deposited is rapidly heated. The second region contains that part in the K^+IDS run where the total ion intensity is decreasing. Figures 43 and 44 are averaged spectra from each of these two regions in the TII curve of Figure 40. Only small differences exist between the two averaged spectra; they are very similar. Therefore, interpretation of polymers belonging to the short-lived group would begin by averaging all of the spectra up to the cut-off point. The total averaged spectrum for Nylon 6 is shown in Figure 45. This averaged spectrum is not markedly different than the averaged spectra from the two regions in the TII curve (Figures 44 and 45).

For short-lived polymers the procedure for selecting a spectrum for interpretation would involve:

1. Choosing the point in the TII plot where intensity diminishes to an unusable limit or to a point where potassium adducts of pyrolysis products create a "peak at every mass" situation. Usually the usable region of the TII curve for short-lived polymers is 30 seconds or less.
2. The averaged spectra from each region in the TII curve should be compared for gross differences. In most cases, for short-lived polymers there is little difference between these regions.
3. The K^+IDS spectrum is, then, an average over both of these regions. This final spectrum is suitable for interpretation.

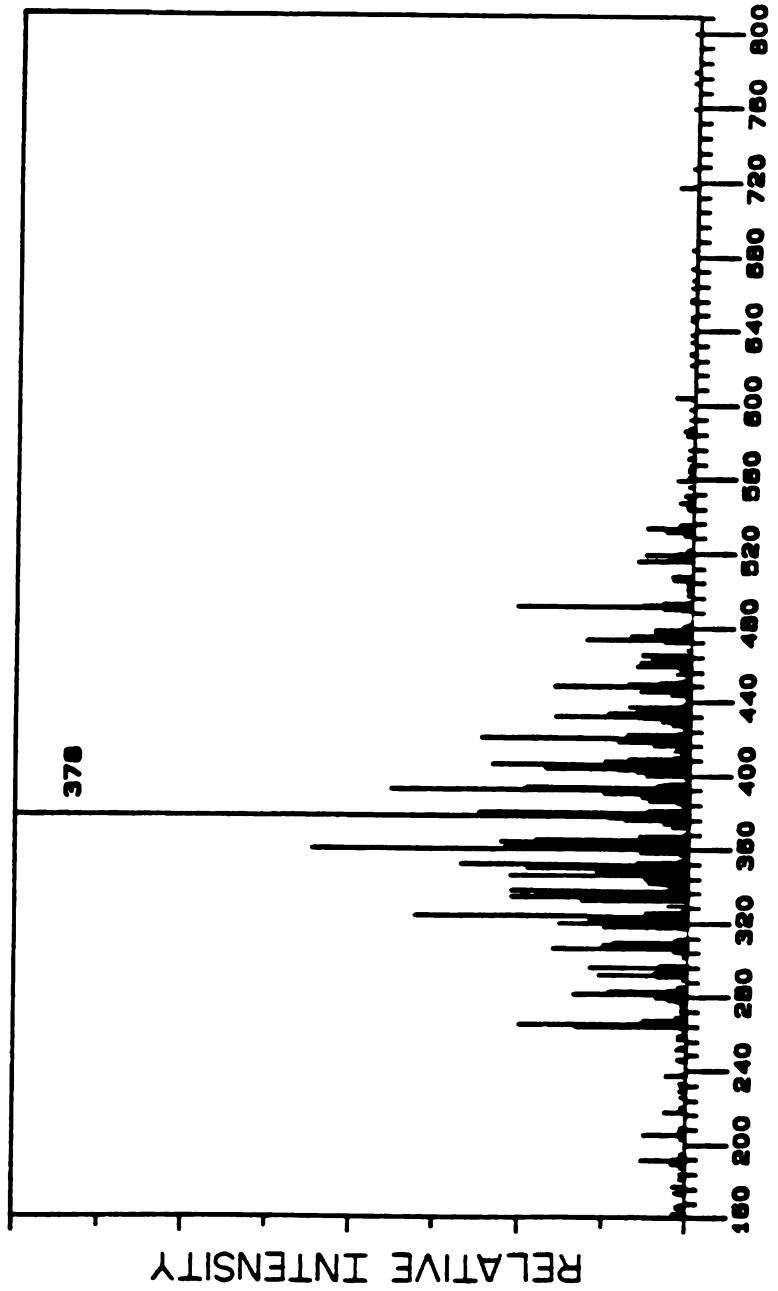


Figure 43. Averaged Spectrum of Nylon 6 From Scans 11-20 (See Figure 40).

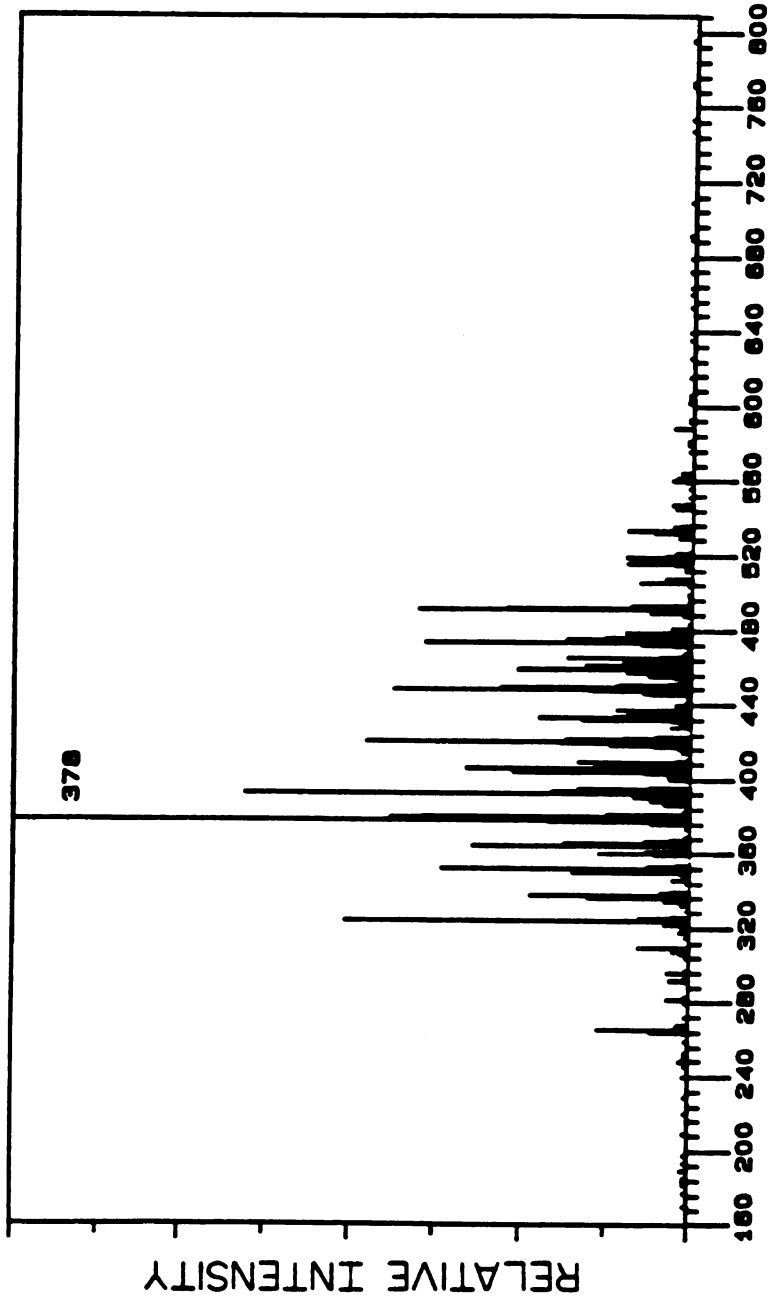


Figure 44. Averaged Spectrum of Nylon 6 From Scans 20-40 (See Figure 40).

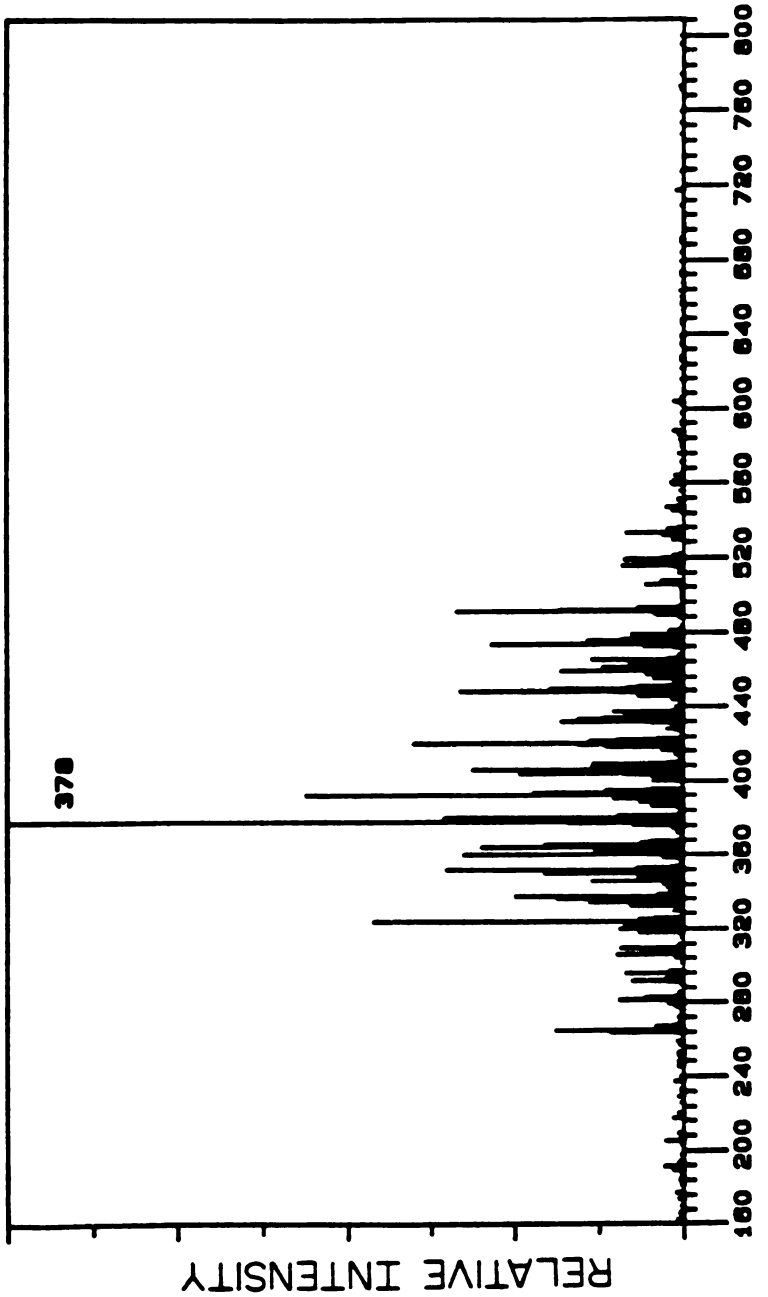


Figure 45. Averaged Spectrum of Nylon 6 From Scans 11-40 (See Figure 40).

Using this procedure a number of polymers which fall in the short-lived class will be presented here. The average spectrum of each polymer will be used to interpret the results. Several polymers will be presented which represent some of the more common polymer classes.

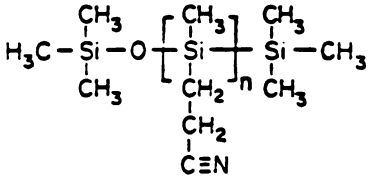
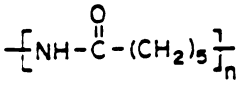
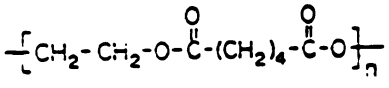
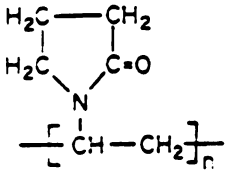
2. Cyanoethylmethyl silicone (XF-1150).

The structure of cyanoethylmethy silicone is shown in Table 2. Siloxane polymers have been used extensively as lubricants, chromatographic stationary phases, and in vacuum pump technology (121-123). In most cases these polymers are used in high temperature applications due to their nonvolatility and thermal stability. A number of thermal degradation studies have been reported for the silicones (124-126). These polymers were chosen for K^+IDS analysis so the results can be compared with earlier degradation literature.

Figure 46 shows an averaged K^+IDS spectrum of XF-1150 obtained in the manner which was described for short-lived polymers. Two ion series dominate the spectrum of this polymer. These series are shown in Table 3. The average molecular weight (M_w) of this polymer is unknown, however, in comparing M_w values of other silicones it would be safe to say that the weights of the cyanoethylmethyl silicone oligomers are outside the mass range (1000 amu) of the mass spectrometer used here. The major thermal degradation pathway in an inert environment (vacuum) is

Table 2

Formulas of the Polymers Used in the K^+ IDS Analyses

Polymer	Structure
XF-1150	
Nylon 6	
Poly(ethyleneadipate)	
Polyvinylpyrrolidone (PVP)	

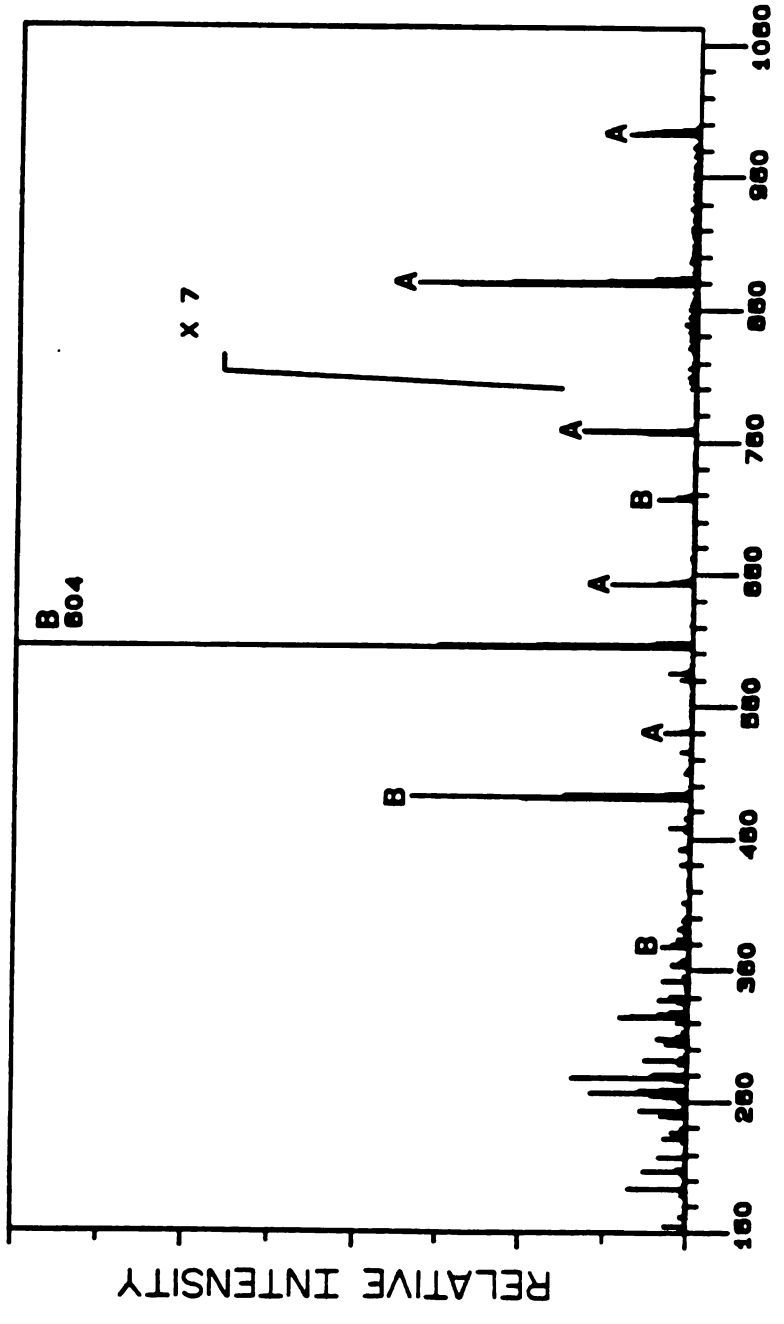


Figure 46. Average K^+IDS Spectrum of XF-1150.

Table 3

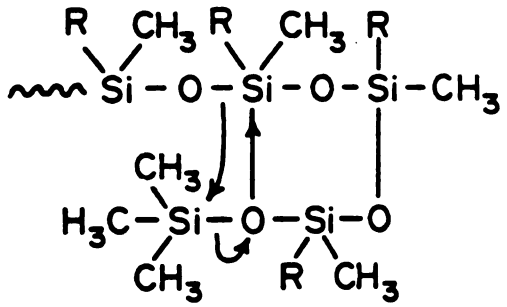
Potassium Ion Adduct Series for Cyanoethylmethyl Silicone (XF-1150)

Series	Proposed Structure of Degradation Product (M)	m/z of $(M+K)^+$
A	$(CH_3)_3SiO[Si(CH_3)(C_3H_4N)O]_nSi(CH_3)_3$	540 (n=2), 653 (n=3), 766 (n=4), 879 (n=5), 992 (n=6)
B	$[Si(CH_3)(C_3H_4N)O]_n$	378 (n=3), 491 (n=4), 604 (n=5), 717 (n=5)

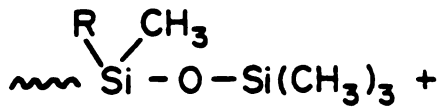
the formation of cyclic siloxanes and is believed to take place in either of the two ways shown in Scheme 4. The first possibility in Scheme 4 involves the formation of cyclic siloxanes through degradation at the terminus of the polymeric chain. This has been shown for hydroxy-terminated polymers (125) however here a much larger terminal group ($Si(CH_3)_3$) is involved. In this case the second possibility in Scheme 4 is favored. This mechanism proposes that formation of cyclosiloxanes occurs in the middle of the chain. This has been suggested by Grassie and Macfarlane (125). Either mechanism, however, explains the appearance of K^+ adducts of a series of decomposition products, $[(CH_3)_3SiOSi(CH_3)C_3H_4N)O]_nSi(CH_3)_3 + K^+]$, in the K^+IDS spectrum. It has been shown that the average molecular weight of silicone polymers decreases linearly due to the formation of such decomposition products (127). In addition to potassium adducts of these decomposition species, K^+ adducts of the cyclic siloxanes are observed in the K^+IDS spectrum. Their abundance is greater than that of the previous series of decomposition products. This is not surprising since, qualitatively, more cyclic siloxanes would be expected when a long silicone chain is degraded. These two series are labelled in Figure 46. Note that these species are all potassium ion adducts.

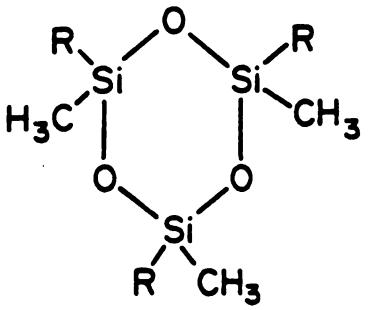
It is interesting to note that there is freedom of rotation about the silicone backbone allowing these polymers to coil helically (124). Substitution of larger groups on the backbone of the silicone affects the ability of the polymer to coil (124).

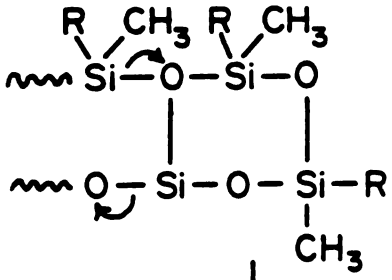
Scheme 4

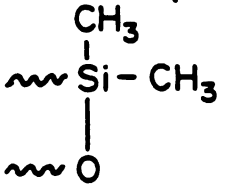


R= -CH_2 -CH_2 -C≡N

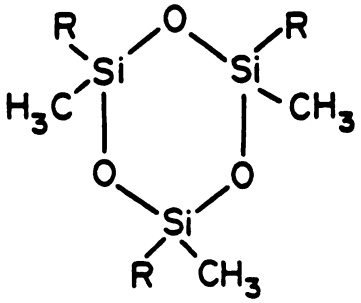








+



Larger groups hinder coiling more than small groups. The distribution of the potassium adducts of the cyclosiloxanes in the K^+IDS spectrum may be a reflection of this coiling ability. That is, for the larger backbone groups such as cyanoethyl, only larger coils are permitted leading to larger fragments such as tetramers and pentamers (n=4 and n=5 for cyanoethylmethyl silicone in Table 2). The large amount of the trimer found in thermal degradation studies of dimethylsiloxanes would also support this reasoning. Further work on other silicones will aid in the investigation of this behavior.

K^+IDS provides useful structural information for this silicone polymer. The potassium adducts of a series of decomposition products can be seen at m/z 540, 653, 766, 879, and 992 (see structure in Table 2; n=2 to 6). The potassium adducts of the cyclic siloxanes (m/z 378, 452, 604, 717) are indicative of silicone polymers. For both series the mass of the repeating unit of the polymer can be obtained. The large number of products seen in the low mass region of Figure 46 (below m/z 300) may arise from impurities and/or residual catalyst as is often the case in such polymers (122). Therefore one possible use of K^+IDS is as a screening method for silicones used in chromatography. Chromatographic applications of these polymers impart severe demands on the polymer purity since small amounts of impurities can dramatically affect the chromatographic behavior. K^+IDS can also be used for thermal decomposition studies of the silicones. Such studies are valuable due to the high temperature applications of the polymer class.

3. Polyvinylpyrrolidone

Figure 47 shows an averaged K^+IDS spectrum of polyvinylpyrrolidone (PVP) which also is in the short-lived category. It has an average molecular weight of 10,000. The structure for this polymer is given in Table 2. A number of series are observed for PVP, all of which are separated by 111 mass units, the repeating monomeric unit ([-CH(C_4H_6NO)CH_2-]). The major series in the spectrum contains the potassium adducts of the dimer (n=2), trimer (n=3), up to the octamer (n=8) at m/z 927. The value of n refers to the number of monomeric units in the structure of PVP (see Table 2). This series is labelled with an M in Figure 47. The oligomer series can arise from either low mass oligomers already present in the polymer or from the chain scission of the polymer backbone. Here the end groups of the PVP polymer are unknown and thus we are uncertain of the first possibility. From prior pyrolytic studies of polyolefins, however, it seems likely that the second possibility does occur (128). A likely mechanism proposed for the thermal degradation of polyolefins and polymers such as polystyrene involves a hydrogen transfer to the site of the chain scission yielding a saturated and an unsaturated (128). This is shown for PVP in Scheme 5. This intramolecular hydrogen transfer to the site of the scission can explain all but one of the series in the K^+IDS spectrum. Another possibility is an internal cyclization mechanism similar to that which accounted for the formation of cyclic siloxanes from the silicones. For this case end groups on the polymer are irrelevent

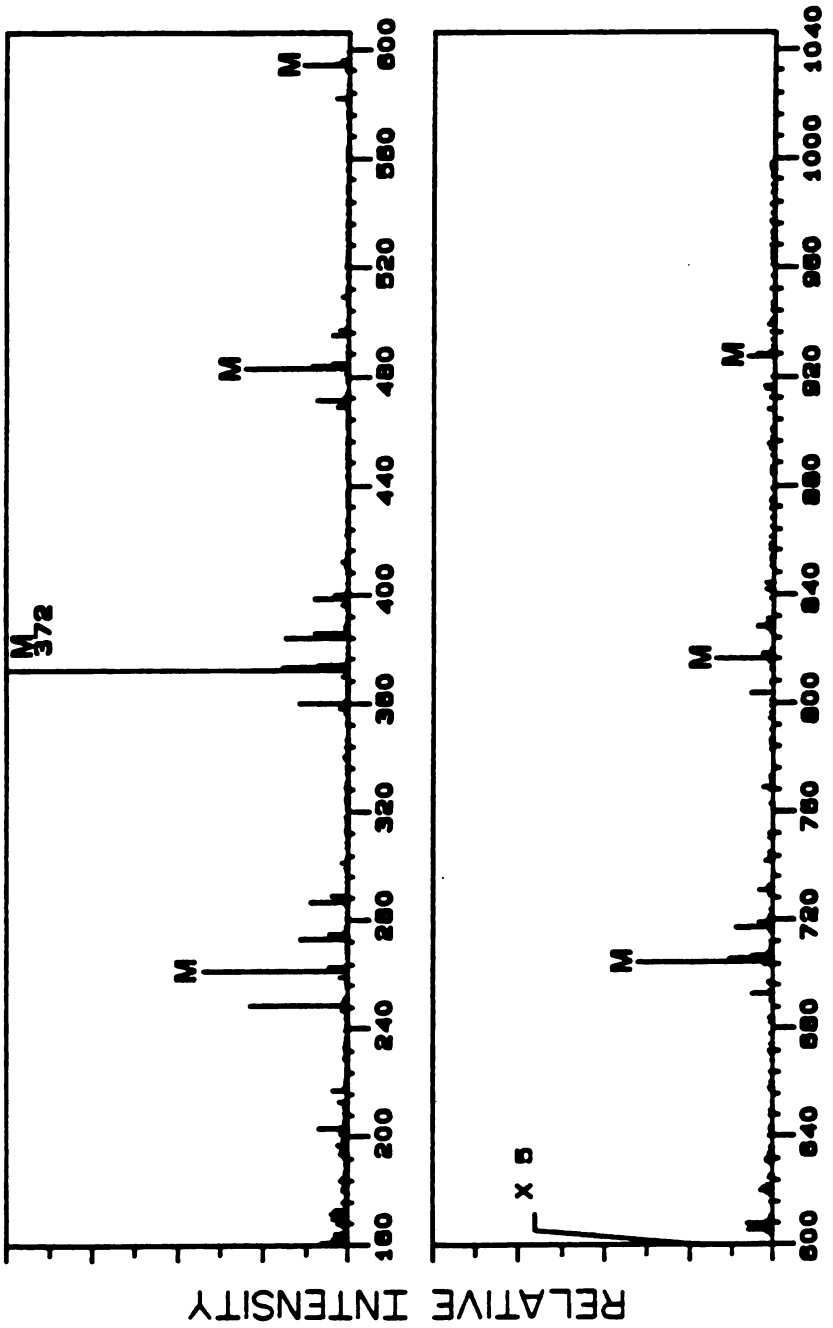
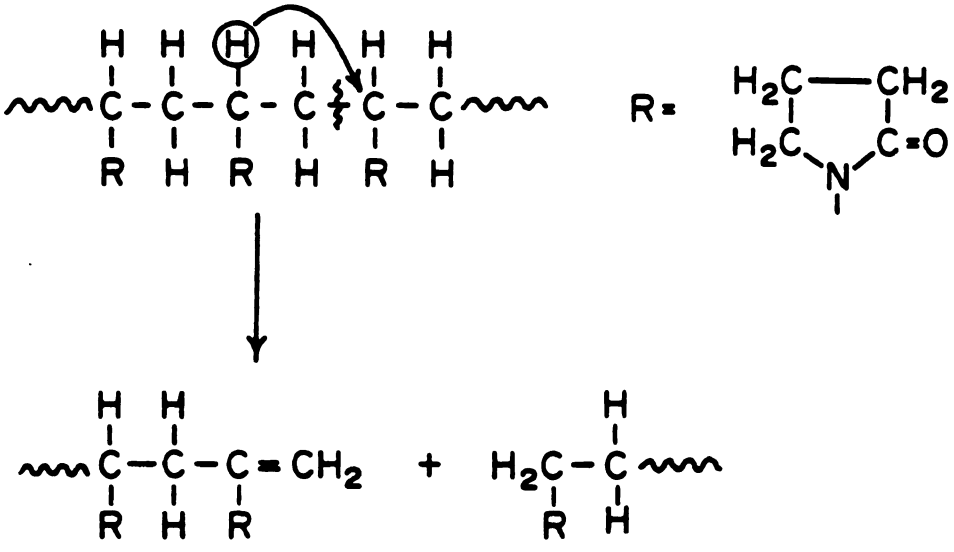


Figure 47. Averaged K^+ IDS Spectrum of Polyvinylpyrrolidone.

Scheme 5



to the production of decomposition series. A potassium adduct of the monomer of PVP is not evident in the K^+IDS spectrum. It should be noted that a free radical mechanism is a requirement for monomer (128); little evidence for radical mechanisms are present in K^+IDS.

The less intense series of K^+ adducts of decomposition products at m/z 287, 398, 509, 620, 731, 842, and 953 ($[H_2C{=}CH[CH(R){-}CH_2]_n{-}C(R){=}CH_2 + K]^+$, $R{=}C_4H_6NO$, n=1-7) may result from scission at the side chain. The loss of the side chain in PVP can be compared to the formation of benzene from polystyrene. Polystyrene is structurally similar to PVP, however the side chain is a phenyl group. Benzene was found to be a thermal decomposition product for polystyrene (128). For polystyrene intramolecular hydrogen transfer has also been considered for the formation of benzene. In a similar fashion this process may explain the previously mentioned decomposition series for PVP. The literature is rich with pyrolytic studies of polystyrene and polyolefins. Here the K^+IDS spectrum appears to be consistent with these earlier findings.

4. Polyesters

The next group of short-lived polymers reported here is polyesters. Polyesters are a major ingredient in paints, varnishes, and textiles. They are frequently used as polar stationary phases in gas chromatography. Thermal decomposition

studies of polyesters have been previously reported (129). From these studies it has been shown that the carboxyl group -C(O)-O- is the reactive center for the initiation of thermal degradation.

Figure 48 shows an averaged K^+IDS spectrum for poly(ethyleneadipate). In Table 4, the desorbed species which lead to the observed potassium adducts are listed. In one particular case a decomposition series has two proposed isomeric structures. The two structures cannot be distinguished since both are possible decomposition products. In addition to those products listed in Table 4 a number of unidentified peaks exist. These species are, like those identified, separated by 172 mass units which is the repeating unit of the polymer. The end groups for these decomposition species are consistent with those found in the Py-EI-MS study reported for this polymer (130). A comparison of the K^+IDS spectrum with other analyses of poly(ethyleneadipate) using FD, FAB, and negative FAB (131) is possible. Not one of these ionization techniques parallel the K^+IDS results, however, certain series from each of these methods can be found in K^+IDS. For example, oligomeric carboxylates (M^-) of the type

$$HO[CO(CH_2)_4CO_2(CH_2)_2O]_nC(O)(CH_2)_4CO_2^- \quad (n = 1\text{-}7)$$

appear in the negative FAB spectrum. In K^+IDS a similar series appears as potassium adducts of the protonated form ($M^- + H^+ + K^+$) and corresponds to the ions at m/z 185, 357, 529, 701, and 873 (n=0-4). Other correlations exist between the K^+IDS and the FD

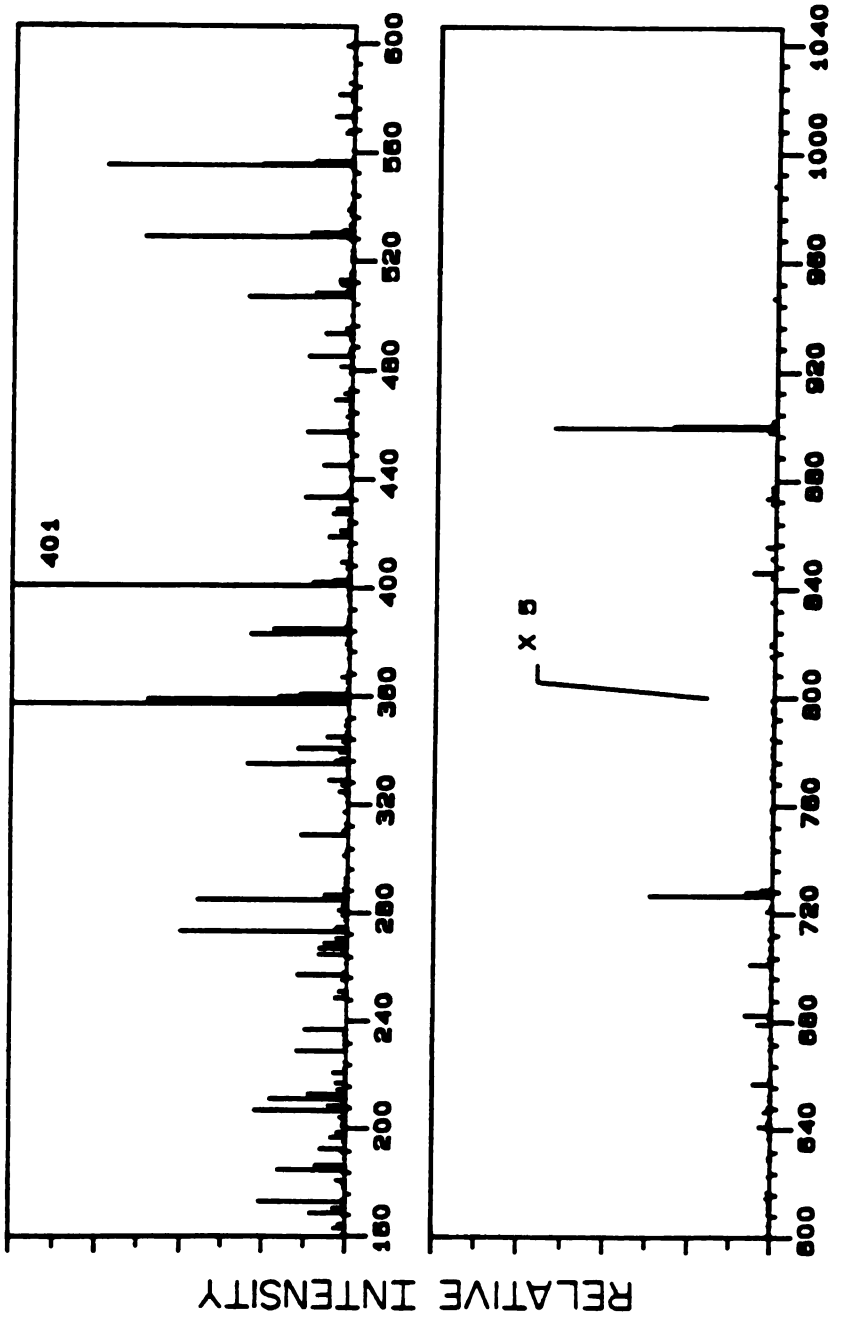


Figure 48. Averaged K^+ IDS Spectrum of Poly(Ethyleneadipate).

Table 4

Potassium Ion Adduct Series For Poly(Ethyleneadipate)

Proposed Structure of Degradation Product (M)	m/z of $(M+K)^+$
$H[O(CH_2)_2CO_2(CH_2)_4C(O)]_nO(CH_2)_2OH$	273 (n=1), 445 (n=2)
$HO[(CH_2)_2CO_2(CH_2)_4CO]_n(CH_2)_2CO_2(CH_2)_3CH=C=O$ $H_2C=C(H)CO_2(CH_2)_4C(O)[O(CH_2)_2CO_2(CH_2)_4CO]_nOH$	211 (n=0), 383 (n=1), 555 (n=2), 727 (n=3), 899 (n=4)
$H[O(CH_2)_2CO_2(CH_2)_4C(O)]_nO(CH_2)_2CO_2(CH_2)_4CO_2H$	229 (n=0), 401 (n=1), 573 (n=2)
$HO[C(O)(CH_2)_4CO_2(CH_2)_2O]_nC(O)(CH_2)_4CO_2H$	185 (n=0), 357 (n=1), 529 (n=2), 701 (n=3), 873 (n=4)

spectra. From earlier results obtained for FAB and FD the two ionization methods appear to be complimentary and are useful in characterizing the polymer by identifying diagnostic degradation products (131). K^+IDS appears to compliment these two ionization techniques and can also be used to characterize this polymer by identifying diagnostic thermal decomposition products.

5. Polyamides

The K^+IDS spectrum of a polyamide (Nylon 6) is shown in Figure 45. The Nylon 6 sample was used for characterizing K^+IDS; it also demonstrates the utility of the method for the analysis of aliphatic polyamides. Aliphatic polyamides such as Nylon 6 have been studied previously by mass spectrometry (132-134). From Py-MS it has been shown that the main thermal decomposition pathways of polyamides are the cleavage of the amide bonds and the elimination of methylene units (134). At lower temperatures cyclic oligomers are formed. In a recent SIMS study (135) six nylons were analyzed in which high mass adducts were seen with Na^+, K^+, and Ag^+. Here potassium adducts are observed for the dimer ($[-NH-C(O)-(CH_2)_5]_n$, n=2) to the hexamer (n=6). In the SIMS study the highest fragment ion containing potassium was that for the tetramer, while for Na^+ it was the 24-mer. It was proposed that Na^+ stabilizes long chains of polymers more effectively than potassium or silver, as suggested by Röllgen and co-workers (93). Initial investigations from this laboratory

using sodium emitters for K^+IDS type work suggest that sodium cationization (Na^+IDS) may be advantageous in mixture analysis.

In the case of Nylon 6, we cannot be sure of the site of cleavage along the polymer chain. From previous work with peptides it would seem a 1,2- elimination at the amide bond would be favorable. However we have also shown that NH-CH_2 and CH_2O bonds cleave as well for the peptides. As can be seen from Figure 46, Nylon 6 undergoes extensive fragmentation. This is consistent with earlier studies (135) in which cleavage of C-C, C-C(O)-, and C-N bonds occur. Essentially every bond in the monomeric unit may be broken down giving rise to two different species. For example, equation 63 shows cleavage of CH_2-CO; equation 64 shows cleavage of NH-CH_2, and equation 65 shows cleavage of CH_2-CH_2 bonds.

$$\sim CH_2\text{-}CH_2\text{-}C(O)\text{-}NH\text{-}CH_2\sim \rightarrow CH_2\text{-}CH_3 + O{=}C{=}N\text{-}CH_2\sim \quad (63)$$

$$\sim CH_2\text{-}CH_2\text{-}C(O)\text{-}NH\text{-}CH_2\text{-}CH_2\sim \rightarrow$$

$$\sim CH_2\text{-}CH_2\text{-}C(O)\text{-}NH_2 + CH_2{=}CH \quad (64)$$

$$\sim CH_2\text{-}CH_2\text{-}CH_2\text{-}C(O)\text{-}NH\sim \rightarrow \sim CH{=}CH_2 + H_3C\text{-}C(O)\text{-}NH\sim \quad (65)$$

An important question is, why do the oligomer series stop at the hexamer in K^+IDS? A number of possibilites exists which include cationization efficiency of potassium ions, intermolecular hydrogen bonding (135), heating rate, and sample

introduction (the sample was evaporated onto the potassium thermionic probe tip from solution using a heat gun). More work is needed to answer the above question.

C. LONG-LIVED POLYMERS

The last section of this discussion focuses on "long-lived" polymers; those polymers are characterized by long lasting total ion currents in excess of approximately 45 seconds. Long-lived polymers exhibit characteristics different than those of short-lived polymers. The two largest differences are the duration of spectra, and spectral differences which arise during various portions in the TII curve. The two polymer types which are included here are the poly(ethylene glycol)s (PEG) and the poly(propylene glycol)s (PPG). Their behavior is illustrated in Figures 49 and 50 using PPG 725 as an example. PPG 725 has an average molecular weight of 725. In Figure 49 the spectrum shows a distribution of oligomer-potassium ion adducts which yields an average molecular weight of 710. Here only the oligomer-potassium ion adducts, $(HO[CH_2CH_2O]_nH+K)^+$, are used for the calculation of molecular weight. This averaged spectrum was obtained late in the TII curve. In Figure 50 an averaged molecular weight is shown early in the TII curve. The apparent average molecular weight in this case is much lower. In contrast to short-lived polymers, these spectra vary with time. Since this is the case an averaged spectrum should not be taken over the entire TII curve. If this were done the spectrum would not be

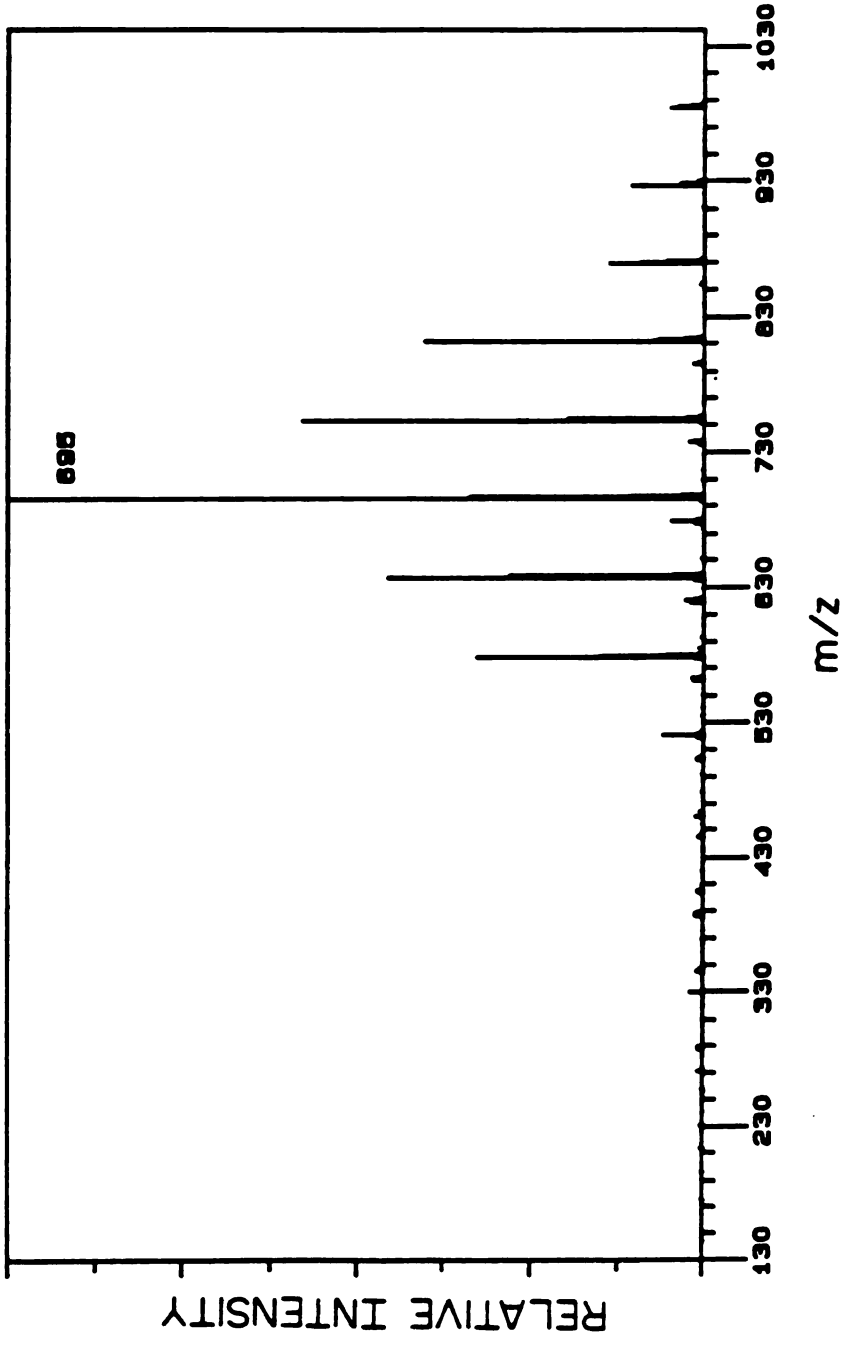


Figure 49. Averaged K^+IDS Spectrum of Poly(Propylene Glycol) 725 Using Spectra Late in the K^+IDS Analysis.

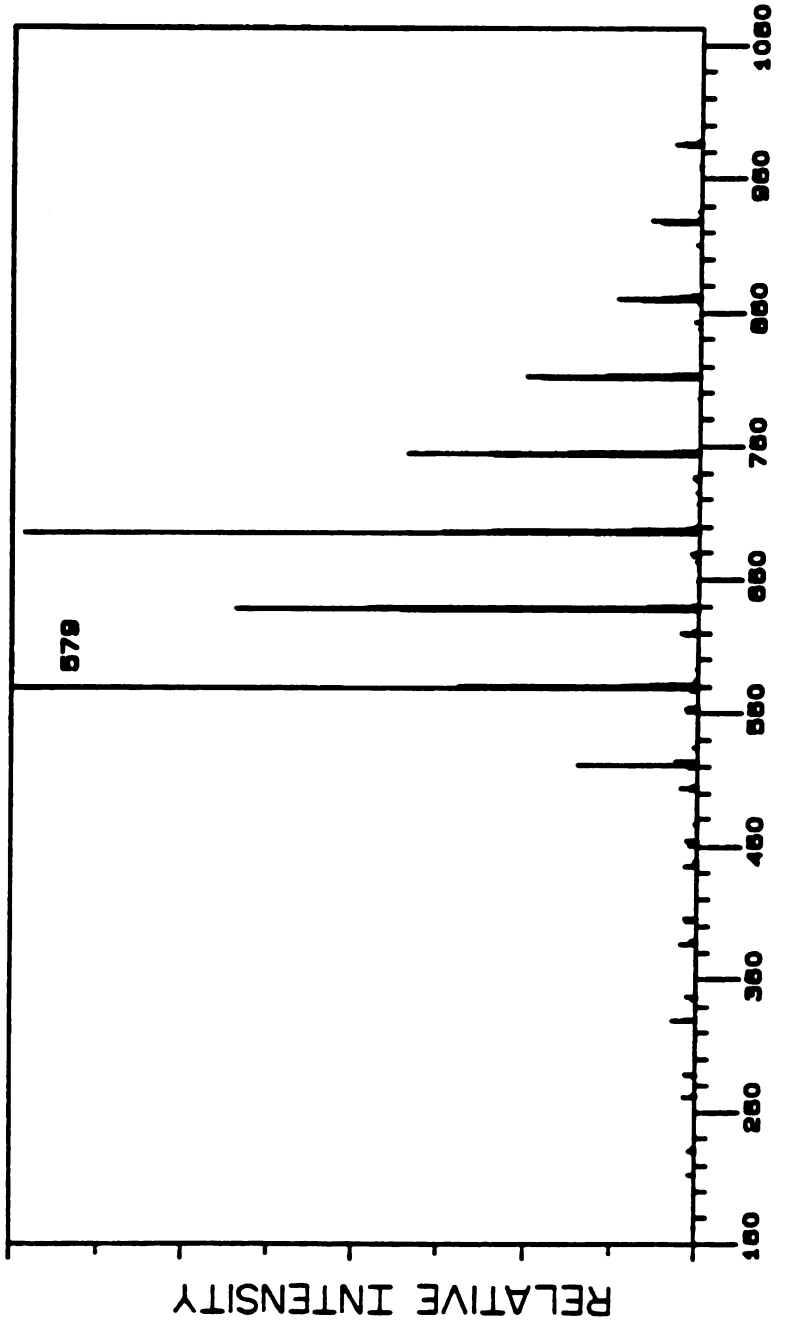


Figure 50. Averaged K^+IDS Spectrum of Poly(Propylene Glycol) 725 Using Spectra Early in the K^+IDS Analysis.

truly representative of the polymer's behavior in the K^+IDS experiment.

To explain this behavior we propose the following mechanism. In the K^+IDS experiment, immediately after current is applied to the thermionic probe tip, a number of thermal regions are produced. These are labelled A, B, and C in Figure 51 which is a schematic of the thermionic probe inside the mass spectrometer. Region A is the hottest and reaches some final temperature (T_{max}) rapidly. It is this region in which species are quickly desorbed into the gas phase. As a consequence it is this region where analyte is depleted first. Regions B (the probe shaft) and C (the source walls) are colder than A. Here region B is continually proceeding to T_{max} and the temperature of region C, while experimentally set, slowly increases when the probe is hot. (In most cases the source temperature was 100^{0}C). Gas phase species originating from regions B and C would be formed over longer time periods since these regions are at lower temperatures. This behavior accounts for the long-lived total ion currents seen for the PEG and PPG polymers. The following is a discussion how this behavior affects the analysis of these polymers, in obtaining both structural and molecular weight information.

What region of the TII curve should be analyzed for polymers which produce continuously varying spectra during the K^+IDS analysis? Similarly, is there a spectrum which we can consider as "the K^+IDS spectrum" of the polymer? To answer these

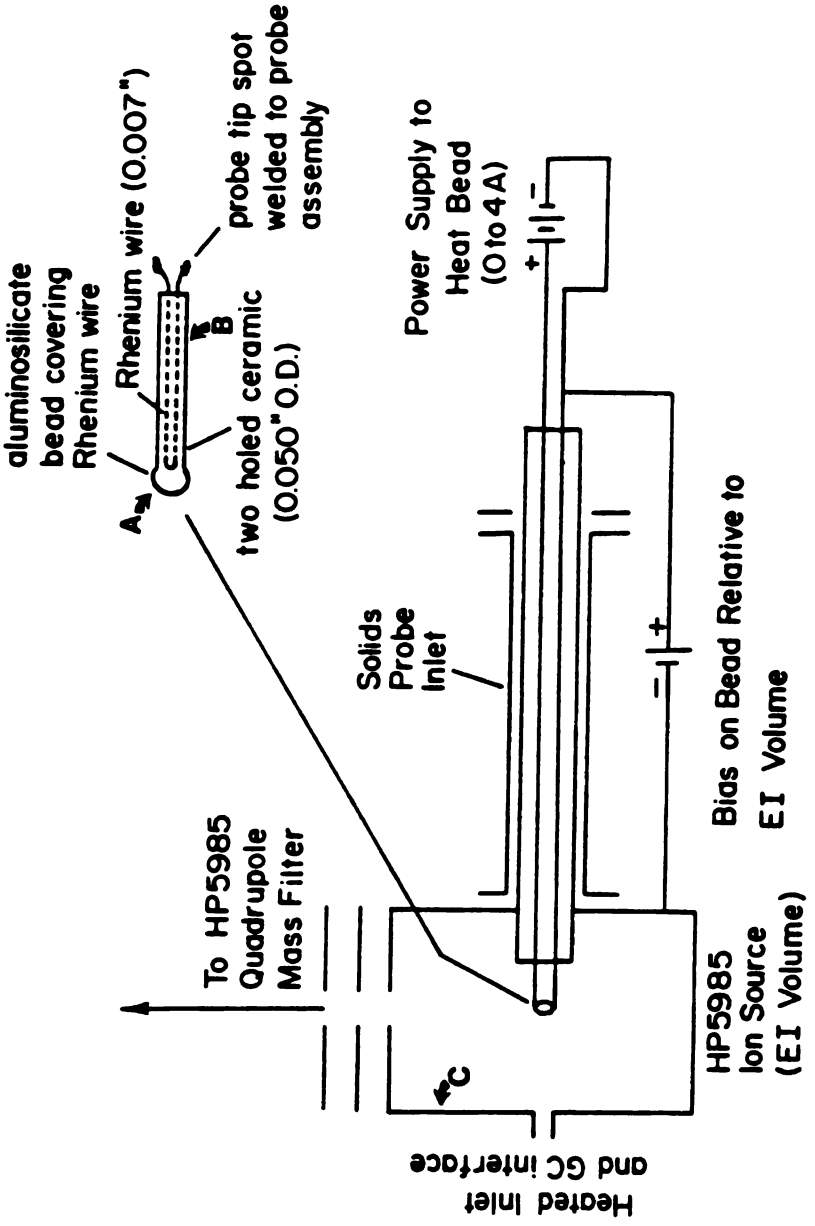


Figure 51. Schematic Diagram of Potassium Thermionic Emission Probe in the Mass Spectrometer's Source Showing Various Thermal Regions.

questions Figure 52 shows a curve of apparent average molecular weight as a function of time (scan number) for poly(ethylene glycol) 400 (PEG 400). It appears from this curve that three regions exist in the K^+IDS analysis. The minimum in this curve corresponds to approximately the correct molecular weight for PEG 400, fortuitously. Figure 53 provides a means of investigating the behavior of these long-lived polymers during K^+IDS analysis. Here the relative intensities of the oligomer-potassium ion adducts are plotted as a function of scan number for PEG 400. Each ion is shown to behave similarly during this experiment, that is, early in the K^+IDS run a maximum value for each ion is reached. At some time later in the same run the ion reaches another maximum value. Apparently two discrete sources of desorbed neutrals are responsible for this behavior. These two regions occur from a temperature gradient which is produced immediately after current is passed through the filament which contains the thermionic K^+ ceramic.

This behavior is analogous to the proposed mechanism which identifies the cationizaion process in laser desorption (91, 97). Investigators (91, 97) have concluded that emission of alkali metal ions occurs from the region directly irradiated by the laser. Cooler regions, away from direct laser irradiation, are responsible for analyte desorption. Cationization is a gas phase process between the emitted alkali metal ions and the desorbed species. Similarly in K^+IDS, although the K^+ thermionic ceramic is resistively heated, a range of temperatures exists along the emitter probe. It should be noted that the laser in LD appears to

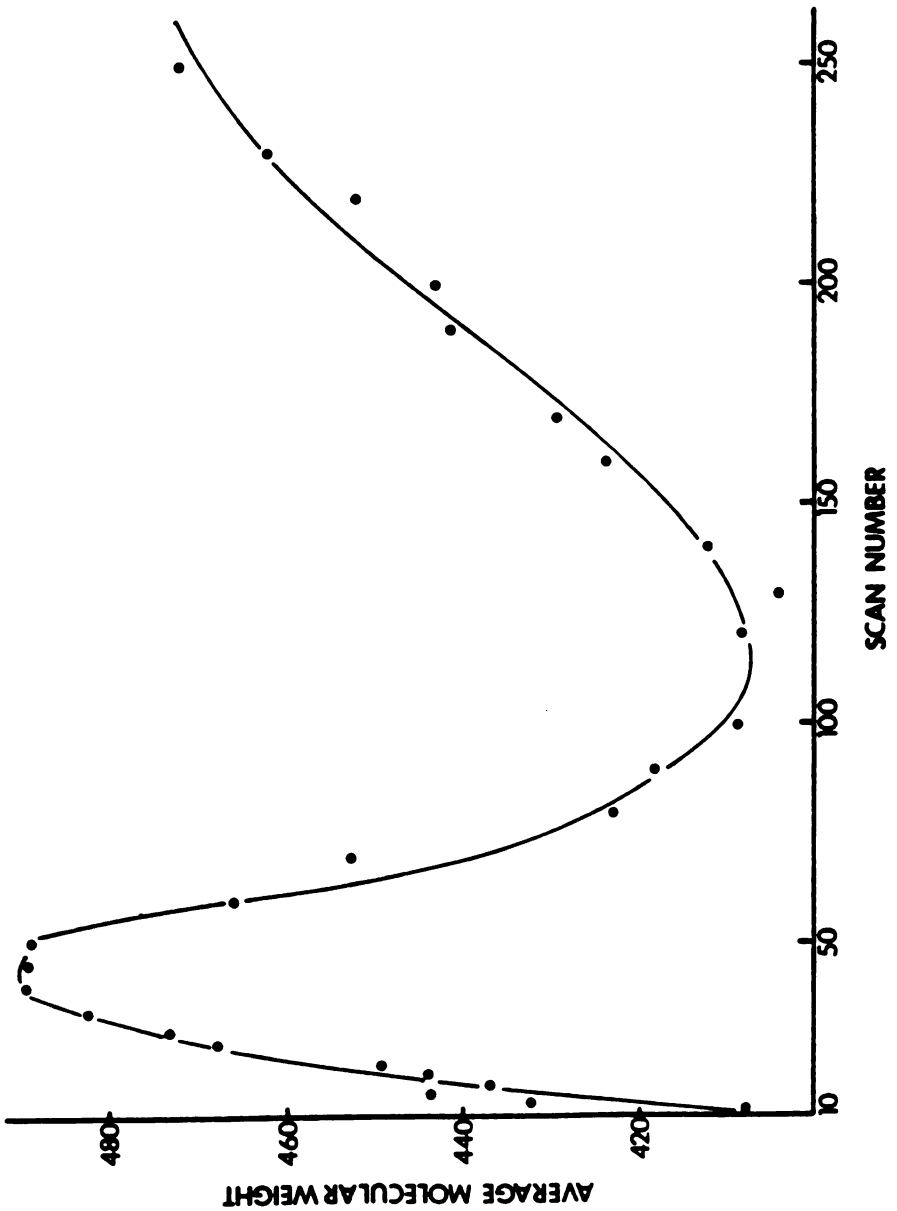


Figure 52. The Apparent Average Molecular Weight of Poly(Ethylene Glycol) 400 as a Function of Scan Number.

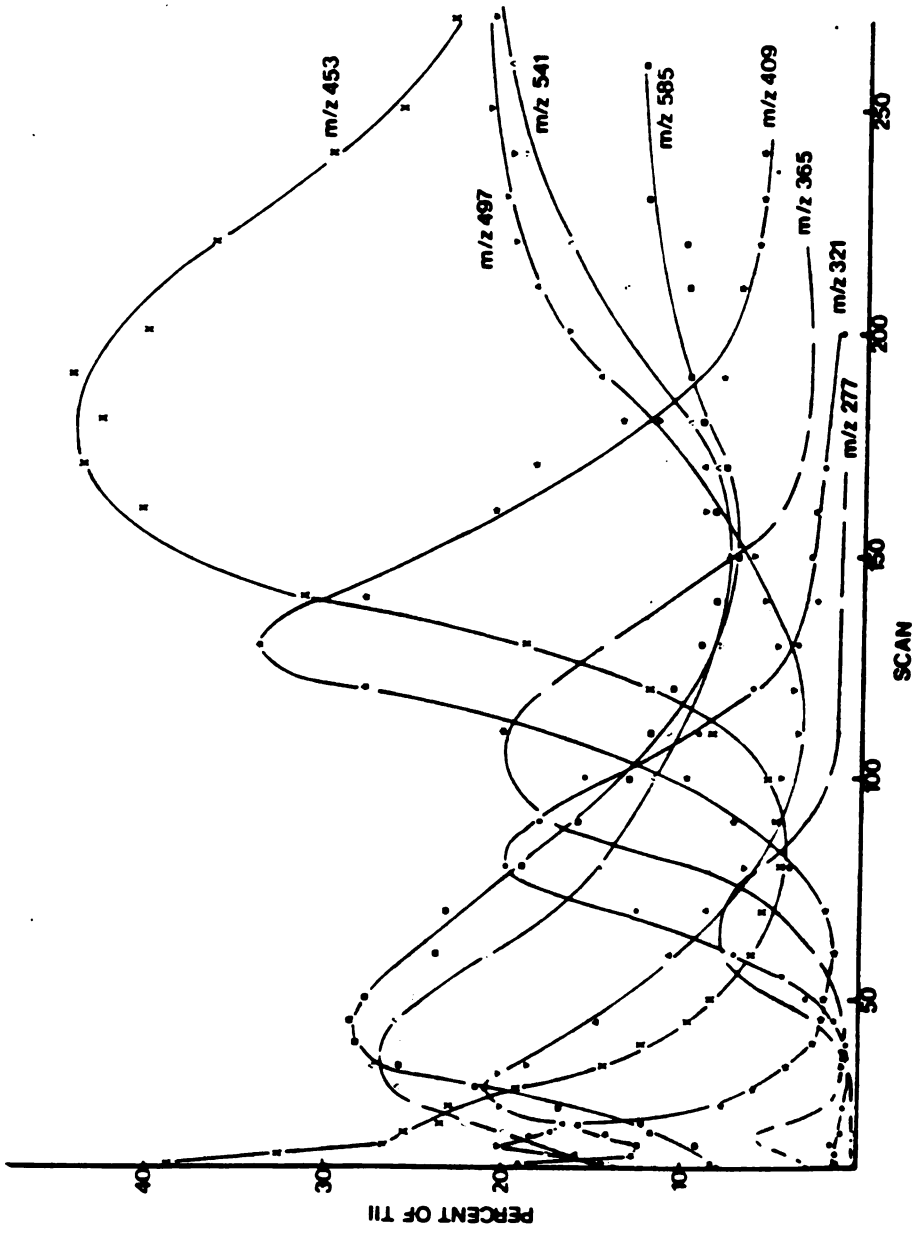


Figure 53. The Relative Intensities of the Oligomer-Potassium Ion Adducts of Poly(Ethylene Glycol) 400 Plotted as a Function of Scan Number.

serve the purpose of heating, i.e., LD is a thermal process (91, 97).

The hot and cold areas create two distinct thermal processes which are responsible for the release of analyte into the gas phase. Figure 54 shows this behavior. Curve A in Figure 54 parallels the behavior of short-lived polymers (Figure 42). Curve B shows the slow distillation of species from the colder regions of the experiment. The longevity of the total ion intensity can be easily visualized from this figure. Decomposition species would be expected to be more abundant from these cooler regions since decomposition is generally favored at lower temperatures (82). It would be difficult to differentiate between a rapid heating process and the slow distillation process using Figure 52. In Figure 53 it becomes clearer that the results of rapid heating are seen early within the K^+IDS run. The relative intensities of a number of ions (e.g. m/z 409 and 453) decrease immediately after the experiment begins. Higher m/z oligomer-potassium ion adducts show a maximum shortly after the run is initiated. Increasing the heating rate affects these higher mass oligomer adduct ions be decreasing the time at which their maxima are observed. After scan 50 in Figure 53, the curves for ions at m/z 277, 321, 365, 409, and 453 may reflect the evaporation from the cooler regions in the K^+IDS experiment. This behavior is analogous to what is observed if one were to analyze PEG from a direct insertion probe which is slowly heated and the compounds are distilled off. If the amount of decomposition products formed during the K^+IDS run is monitored with time, a distinction should

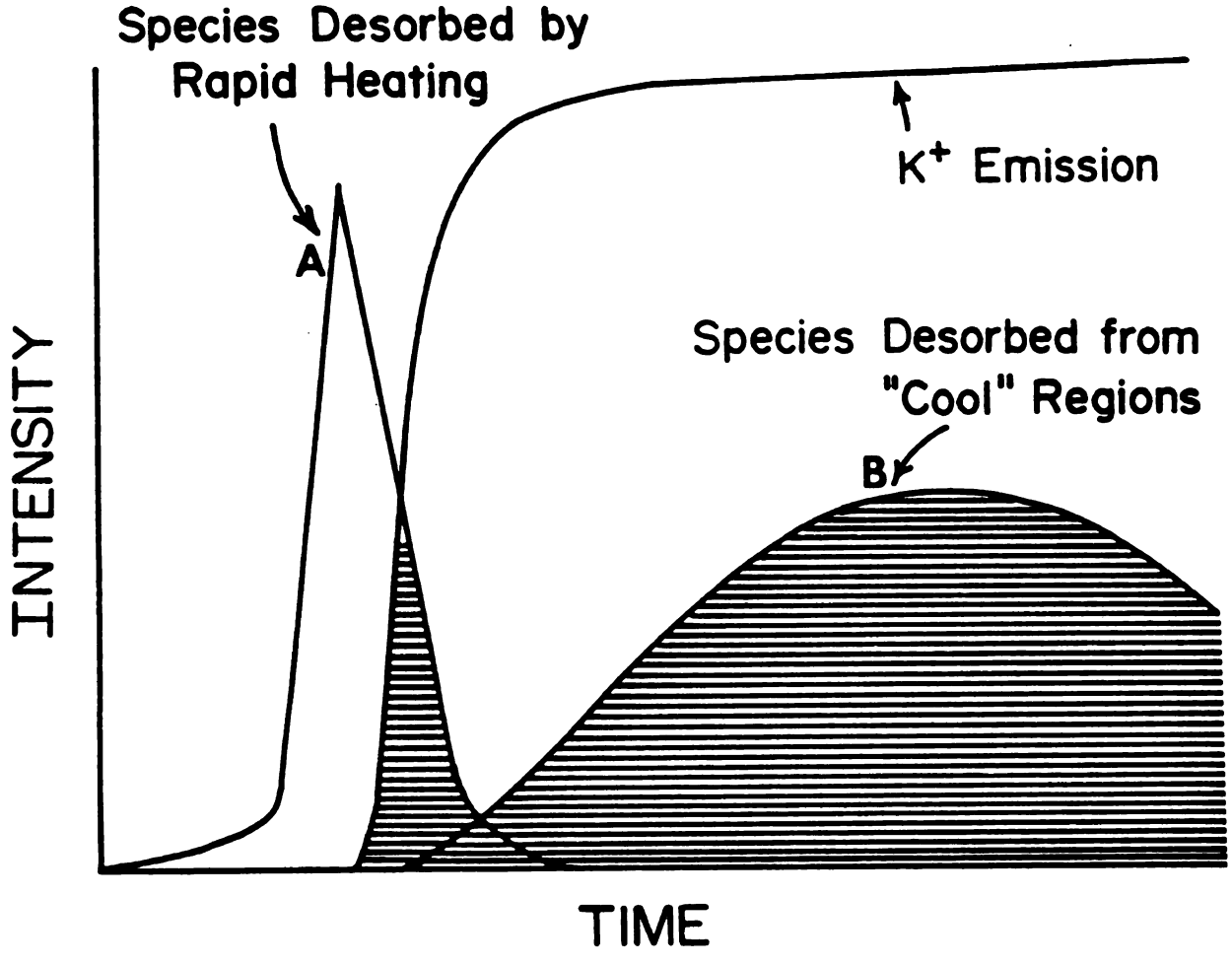


Figure 54. Intensity as a Function of Time for the Desorption of Species Due to Rapid Heating; the Distillation of Species From "Cold" Regions; and the Emission of K^+ Ions. The Overlap Region Shows Where K^+ IDS Spectra are Produced.

become evident. This distinction arises from the areas affected most by rapid heating and the area of slow heating which results in distillation and decomposition. Figure 55 shows the percentage of the total ion intensity due to decomposition products as a function of time (scan number) for PEG 600. The two curves reflect the differences between two current settings, i.e., the effect of heating rates. There exists two well-defined portions in these curves. There is a lower abundance of decomposition products early followed by a rise to a second region which shows a constantly increasing amount of the decomposition species. This increase is not as apparent for curve B. Figure 55 complements Figure 53, supporting two thermally different regions.

In addition to the above behavior the apparent effect of decreasing the heating rate (lowering the current passed through the filament) is to diminish the abundance of decomposition products late in the run. While the profile of curve B is similar to curve A, the difference between the two desorption processes (rapid heating and distillation) is less defined. The extent of decomposition of the polymer is less in curve B than A since the heating current used in curve B is considerably less than in curve A.

Earlier in this section of the discussion a mechanism was proposed for the long-lived polymers. This behavior can now be summarized for these polymers in K^+IDS which leads to this mechanism. The polymer's viscosity allows the polymer to move to regions in the experiment other than the tip of the probe

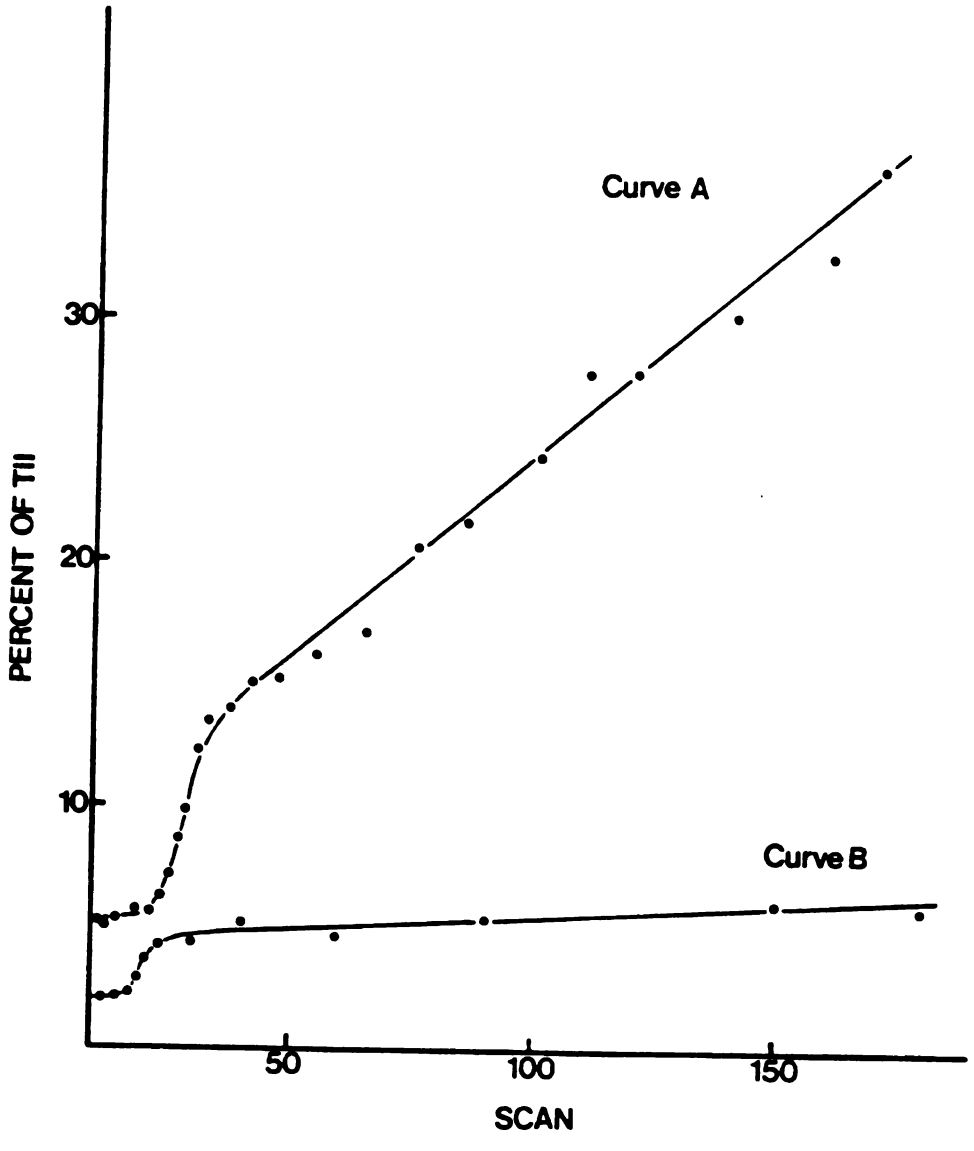


Figure 55. The Percent of the Total Ion Intensity as a Function of Scan Number For the Potassium Ion Adducts of Decomposition Species of Poly(Ethylene Glycol) 600. The Heating Currents Used are 2.5 Amps for Curve B and 3.5 Amps for Curve A.

containing K^+ thermionic ceramic. These regions can be the source walls or the shaft of the probe. K^+IDS experiments were performed where a PEG was deposited at the base of the probe tip near the spot weld (Figure 51). In this case behavior paralleled that of the potassium-oligomer adducts in the late scans of Figure 53. This behavior would be consistent with a distillation process from a cooler region. These polymers produce long-lived total ion currents because of these two thermal regions. In the hot region, analyte is depleted rapidly. This can be shown in all cases for the high viscosity polymers discussed previously. the "cold" regions are responsible for the long runs simply because the analyte takes longer to distill off. Decomposition is more likely to occur from the areas of slow heating and is consistent with Figure 55. This observation is also consistent with what is known about rapid heating processes.

The question that arose earlier as to which spectrum or spectra should be taken as representative of the polymer can now be addressed. It becomes clear that with these two regions in which different processes are occurring, there is no answer. From Figure 55 it would appear that approximately the first 10 scans of the K^+IDS run is that portion of the TII most influenced by rapid heating. Rapid heating has been used to determine molecular weight information from polymer systems (117). Table 5 lists the calculated average molecular weights using the first ten scans for the PEG and PPG polymers studied here. (It should be noted that all of the glycols studied behaved similarly to those used as examples in Figures 52-54). What is demonstrated here

from Table 5 is that low molecular weight glycols give artificially high averages while higher molecular weight glycols give lower averages than what is expected. This behavior is consistent with the proposed processes. Oligomers from the colder areas are influencing these averages.

Figure 49 shows an average of spectra obtained after approximately 40 scans. The calculated molecular weight is in good agreement with the actual value. This would suggest that taking an averaged spectrum late in the run is useful. This can be the case for the higher molecular weight polymers. From Figure 53, the region to select to average would be difficult to determine. For PEG 600 and PPG 725 the choice is more clearly defined due to a smaller amount of low mass oligomers present in the polymer. An accurate molecular weight determination would depend upon how long the ion intensity lasts. As can be seen in Figure 41 the ion intensity drops slowly with time. Therefore in the cases of PEG 600 and PPG 725 an adequate amount of sample was used to generate spectra for a molecular weight determination. In addition the heating current used must be low enough to prevent decomposition of the analyte. Decomposition products do not parallel the oligomer species in the gas phase. Decomposition of long chains of the polymer would not be expected to produce a distribution similar to that of the intact oligomer species. This observation became clear when only the decomposition adduct ions are plotted in a similar fashion as Figure 53. The conclusion here is that the heating current must be kept low to prevent decomposition, however, low heating

Table 5

Apparent Average Molecular Weights Using the First Ten K^+IDS Spectra For the PPG and PEG Polymers.

Polymer	Average Molecular Weight (M)	ΔM*
PEG 200	323	+ 123
PEG 300	358	+ 58
PEG 400	445	+ 45
PEG 600	514	- 86
PPG 425	466	+ 41
PPG 725	650	- 75

* ΔM refers to the absolute error calculated from the known average molecular weight of each polymer.

currents may be insufficient for the distillation of higher mass oligomers.

Before summarizing the behavior of the long-lived polymers it should be stated that K^+IDS can be useful in providing structural information about the polymer. This was demonstrated in earlier studies and is important due to the limited mass range of existing mass spectrometers. K^+IDS showed promise in being able to provide molecular weight information for PEG 600 and PPG 725. The PEG and PPG polymers below 600 in molecular weight did present difficulties for K^+IDS analysis, due to their low viscosity. Perhaps in molecular weight determinations using K^+IDS with solid polymers these difficulties would not be present. Although polymers of average molecular weights of less than 600 are uncommon, small changes in the K^+IDS experiment can be made to determine their average molecular weights. These changes may include the use of less sample. Minimizing the sample quantitiy reduces the amount migrating to colder spots. A second alternative would be using a larger diameter ceramic probe tip. Here the larger mass would reduce the heat transfer from the rhenium filament to the ceramic post. Any other alternatives suggested must reduce the desorption of species from the cooler thermal regions in the experiment. A variety of modifications need to be investigated.

IV. FINAL COMMENTS ON CHAPTER 4

I have discussed the use of the thermionic probe in performing K^+Cl and in K^+IDS. In the latter technique a number of compounds were tested and characterized including polymers. The next part of this thesis will also make use of the thermionic probe to some extent. In the last investigation that will be discussed the thermionic probe will be used to evaluate the gas chromatographic thermionic ionization detector. In addition to using the thermionic probe a number of gas chromatographic studies will be described. Both mass spectrometric and gas chromatographic results will then be used to evaluate the GC-TID and aid in elucidating the TID response mechanism.

CHAPTER 5. MASS SPECTRAL AND GAS CHROMATOGRAPHIC INVESTIGATIONS INTO THE RESPONSE MECHANISM OF THE THERMIONIC IONIZATION DETECTORS FOR GAS CHROMATOGRAPHY

I. INTRODUCTION

The need for and use of selective gas chromatographic detectors has increased in recent years primarily due to the necessity of performing trace analyses on complex mixtures. Selective detectors, responding only to chemical species containing specific heteroatoms, functional groups or structural features, have had a tremendous impact in chromatography (136). A number of selective detectors have been developed but few have reached the commercial market. One commercially available selective detector which has become popular is the thermionic ionization detector (TID).

Thermionic ionization detectors are primarily used to detect compounds which contain nitrogen or phosphorus. Selectivities of these detectors are approximately 4×10^4 gC/gN and 7×10^4 gC/gP (137). Detection limits for the TID are in the range of 10^{-13} gN/sec and 10^{-14} gP/sec (137). Most commercial TID's offer a linear dynamic range of greater than 10^4. Other advantages such as the ease of adaptation of existing flame ionization detectors (FID) to accommodate the TID and the capability of utilizing the detector over a prolonged period make the TID the detector of

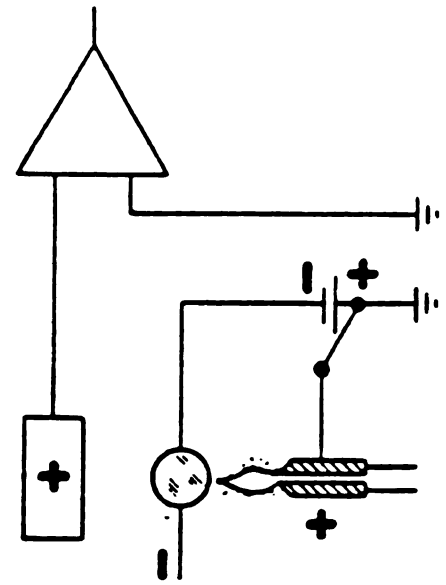
choice for the analysis of nitrogen and phosphorus containing compounds. The need to perform analysis on complex samples of biological, pharmaceutical and toxicological importance has led to extensive usage of the thermionic ionization detector (138-143). While the utility of the TID has been well documented, work needs to be done to better understand the TID's response. Presumably, once a chemical process is understood, it can be optimized and further developed.

In brief, the TID contains a heated bead (the "source"). Certain types of compounds (containing nitrogen and phosphorus atoms), when introduced into the detector, produce gaseous charge carriers which are detected. For many molecules (e.g. alkanes) a greatly reduced response is observed. The heated bead in thermionic ionization detectors is normally composed of materials which are good thermionic emitters. However, most proposed mechanisms do not involve the emission of metal ions from the materials that comprise the source. Proposed mechanisms which are based on thermionic emission suffer from a number of contradictions (144). As the following discussion will indicate, thermionic ionization detectors are actually misnamed. This is indicative of the fact that a unified and proven response mechanism needs to be established.

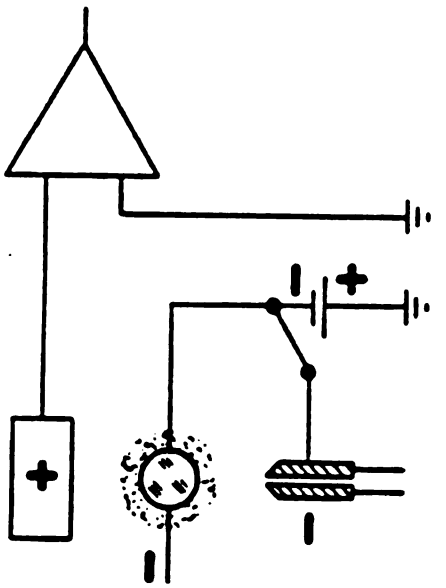
The origins of the TID lie in the gc detector first described by Karmen and Guiffride (145), which used the thermionic behavior of an alkali salt when heated. In their design, a common flame ionization detector was used and the thermionic source (a salt

"bead") was placed over the flame. In later models an alkali salt reservoir placed around the flame was used. These designs incorporating a flame are called alkali flame ionization detectors (AFID). Several mechanisms (144) for AFID's have been proposed but a unified mechanism has yet to be realized. A detailed discussion of AFID designs and operating parameters has been published by Brazhnikov et al. (144).

Recently, due to the disadvantages of AFID's a new type of nitrogen/phosphorus detector has been developed by Kolb and Bischoff using a flameless design (146). It is this particular design which is now called the thermionic ionization detector (TID). Kolb and Bischoff described two modes of operation in their design as can be seen in Figure 56. The NP-mode is capable of detecting both nitrogen and phosphorus compounds. In the P-mode, a signal results from only phosporus compounds. The NP-mode operates with flow rates of 1-3 ml/min for hydrogen and approximately 100 ml/min for air. Under these conditions it has been suggested that a "cold flame" is produced around the resistively heated alkali bead (146). The need for fine adjustment of distances between flame tip, collector, and bead is not necessary, (as is the case in AFID's) since the cold flame/plasma "adjusts itself" accordingly around the bead (146). This particular configuration is designed to collect negative charge carriers which are responsible for the detector response. The phosphorus mode differs from the NP-mode by two factors. First, the air and hydrogen flow rates are the same as in a



P-mode



NP-mode

Figure 56. The Two Modes of Operation in the Kolb-Bischoff TID.

standard FID so a true flame is maintained. Secondly, the flame tip is at a potential which is positive with respect to the bead so that the normal hydorcarbon signal from FID's does not interfere with the signal arising from the region around the bead and the collector electrode. The end result is that two signals, phosphorus and normal FID response, can be separated giving the detector specificity toward phosphorus compounds. As in the NP-mode, the P-mode detects negative charge carriers formed from phosphorus compounds.

Recently Patterson et al. (71) developed a TID which features a ceramic core coated with an alkali-ceramic material. The source is negatively biased with respect to the collector electrode as in earlier designs. Patterson used a number of gases to elicit responses for different compounds.

Burgett et al. (147) devoloped a TID designed much like that of Kolb and Bischoff however, the collector is positively biased and therefore responds to a positive ion current.

Kolb and Bischoff (146) were the first to propose a mechanism to explain the response of the thermionic ionization detector. They suggest that the signal results from the production of cyanide ions (CN^-). Cyanide ions are produced as follows: nitrogen compounds decompose in the region around the bead to form CN. Rb atoms (the source contained nonvolatile rubidium silicate) are vaporized from the source and react with the cyano radicals. An electron transfer reaction occurs from Rb to CN resulting in a rubidium cation and a cyanide ion. The Rb cation

can be captured by the negatively biased source. A major problem in this mechanism lies in the fact that the difference between the ionization energy of rubidium (4.16 eV) (146) and the electon affinity of a cyano radical is too large for the reaction to occur. It was postulated that an excited state rubidium atom (IE(Rb*) = 2.57 eV) must be produced from the surface for this to occur (146). The mechanism for response due to phosphorus-containing compounds according to Kolb is similar, with PO_2^- being responsible for the signal (generated, presumably, in an analogous process).

Olah et al. (70) proposed a mechanism which was not based on gas phase reactions. Their mechanisms proposed that the signal arises due to a surface reaction. In this mechanism the N-containing compound is adsorbed onto the surface of the bead upon which degradation occurs to produce adsorbed cyano radicals. The CN radical can either desorb from the surface to degrade or react further to form CO_2 or N_2, or produce adsorbed cyanide ions resulting from the ionization reaction:

$$Rb(surface) + CN(adsorbed) \rightarrow Rb^+(surface) + CN^-(adsorbed).$$

The cyanide ion can then be emitted from the surface and this ion current detected. The rubidium cation can recombine with an electron (migrating through the glass from the internal platinum wire used for heating and biasing) to regenerate the neutral

alkali species.

Patterson (148) is in agreement with Olah, suggesting that ionization takes place at the surface rather than in the gas phase, and that a surface mechanism must take three factors into consideration. These include the temperature of the bead, the environment around the bead, and the composition and concentration of materials contained in the bead. The concentration and composition of the thermionic material determines its work function which in turn determines the ease of extracting an electron from the surface.

The surface ionization mechanism seems to be preferred over the gas phase mechanism proposed by Kolb. However, the response of the TID designed by Burgett and coworkers, which detects positive charge carriers, cannot be explained by either proposal. The following several points should be included in the formulation of a mechanism:

1. Should be based on known and physically consistent results.
2. Should explain the role of the various gases used in TID's.
3. Should be consistent with the fact that TID's are available which detect positive and negative charge carriers.
4. Should explain the ability of the detector to operate for extended periods of time.
5. Should explain the response for phosphorus compounds as well as nitrogen containing molecules.

Presently all of the above points have not been incorporated into one mechanism. These investigations take a fundamental approach to the problem. To date the exact nature of the charged species being formed in the TID has not been established.

Mechanisms have been proposed which suggest two reactive zones; one in the gas phase and the other on the surface of the bead. If a reactive gas phase zone exists, it is likely to be composed of radical species, which may assist in degradation and possibly ionization. Both processes could also occur on the surface. It seems unlikely that degradation and ionization occurs in the gas phase since this would give a mechanism which is completely independent of the surface. In addition, ionization by gas phase mechanisms is thermodynamically unlikely at the temperatures used in the TID. There is a substantial amount of literature on surface ionization mass spectrometry which appears to be absent in any discussion of the TID. In this technique molecules decompose and form positive or negative ions on a heated surface. Such studies may suggest that the TID is merely a surface ionization detector. This mechanism is attractive since a majority of N- and P-containing compounds can easily surface ionize. This mechanism, however, appears to ignore the effects due to detector gases in the TID. Also, surface ionization is typically performed on heated metal and metal oxide surfaces, not traditionally on alkali aluminosilicates. Apparently, for the TID to operate, two processes must be operative-decomposition and

ionization. Ionization is apparently a surface process. Decomposition can occur in a reactive gas phase zone about the bead, on the surface of the bead, or both. Perhaps a mechanism involving either region could adequately explain the observed response.

The question as to where decomposition occurs is reflective of a more basic question: What role do detector gases play in the TID response mechanism? This paper discusses these possibilities in light of experiments performed and relevent prior work. In an effort to determine the mechanism(s) which are operative in the TID, an investigation of the interactions of nitrogen and phosphorus containing compounds with a heated alkali aluminosilicate surface in the source of the mass spectrometer wil first be discussed. This will allow for the identification of surface-only processes. An investigation of how the introduction of gases into the ion source affect the response will be included. This will suggest the possible role of detector gases in the response mechanism, realizing that the ion source cannot be operated at the actual pressures which are used in the detector. The behavior of a variety of compounds in the low pressure mass spectrometric experiment, and in the GC-TID analysis will be discussed to provide insights into the response mechanism.

The organization of the discussion for Chapter 5 will be as follows. A number of investigations were performed which can be categorized into three questions. These questions attempt to

answer important concepts in the response of the TID. Each of these questions will serve as a separate section of this discussion. In each section (question) several experiments will be discussed which attempt to clarify the question. The three questions are:

1) What happens to an analyte in the TID in the absence of any other detector gas?
2) What role do gases have between an analyte and the hot surface?
3) What are the similarities between the mass spectrometric experiment and the gas chromatographic TID. Here we attempt to simulate the TID in the mass spectrometer source. I will refer to these two types of experiments as the GC-TID and the MS-TID.

Keep in mind the MS-TID is not a chromatographic detector but a simulation of one inside the mass spectrometer's source.

II. EXPERIMENTAL

Experiments were performed on an unmodified Hewlett-Packard 5985 GC/MS/DS. The thermionic probe is the same one used in Chapters 2-4 of this dissertation. Care was taken to ensure that the bead material entirely covered the rhenium wire that was used for heating the bead. By

encapsulating the rhenium wire in this manner two possible processes leading to ionization was avoided, i.e., 1) surface ionization on the hot rhenium wire and 2) positive/negative ion formation due to electron impact from electrons emitted by the hot rhenium wire. The surface area of the aluminosilicate bead was approximately 0.01 cm^2.

The same power supplies and experimental set-up were used here as in the earlier studies with the thermionic probe. The thermionic material however, was comprised of 15% by weight of rubidium nitrate in a high temperature cement (D-10 Dacron Industries, Inc.). This material was chosen from a study that selected a material similar in properties to the thermionic material which comprised the bead in the GC-TID. This material was placed on the rhenium filament as a slurry and allowed to dry overnight. It was conditioned for at least one hour in vacuum at approximately 3 A and at a bias of +3 V. Unless otherwise noted any mass spectrometric results reported used the 15% by weight $RbNO_3$ bead. The gas chromatographic results presented here used the thermionic bead supplied with the gas chromatograph which was also the one used in the comparison study.

Organic samples were introduced through the "capillary direct" port of the GC/MS interface. Additional gases were introduced through the "CI direct" port of the interface. The pressures given for all spectra refer to the pressure within the CI volume and were typically between 50 and 100 mtorr.

The gas chromatograph used was a Varian Vista 6000 series

supplied with the Varian thermionic ionization detector. The column used was either a 18 inch OV-101 or a 6 foot Pennwalt 23+2%KOH column purchased from Applied Science Laboratories. In most cases the flow rate of carrier gas was 30 ml/min He unless otherwise noted. The column temperature varied depending upon the analytes used. All chemicals were ACS reagent grade and were used without further purification.

III. RESULTS AND DISCUSSION

A. What Happens to an Analyte in the TID in the Absence of Any Other Gases?

The first part of this section will discuss what happens to an analyte in the MS-TID. This experiment will allow us to determine the response of a compound on the hot alkali thermionic material in the absence of any gases. Since most GC-TID's are designed to detect negatively charged species we will begin with negative ion formation. The following discussion will also attempt to apply the principles of SI to the results obtained when organic compounds are exposed to the hot thermionic material.

1. Negative Ion Formation.

When an organic compound is in the presence of a hot alkali aluminosilicate bead which is at a negative potential with respect to the collector or in this case, the surrounding mass spectrometer source, negative ions are produced. Figure 57 shows the negative SI mass spectrum of acetonitrile on the alkali aluminosilicate bead. The simple mass spectrum is composed of the cyano ion, CN^- (m/z 26) and a low intensity ion at m/z 25, C_2H^-. The abundant amount of cyano ions produced would seem to support earlier mechanisms which suggested that the negative charge carrier responsible for the response of N-containing species is the cyano ion. Cyclic N-containing compounds such as pyridine have also been shown to produce CN^- in these studies.

As discussed in the introduction of this thesis, for negative SI to occur, an absorbed species must have a positive electron affinity in order to surface ionize. The ionization efficiency is largest when a high electron affinity species is adsorbed to a low work function surface. For this reason the alkali salt or oxide most often used in the TID is either a rubidium or cesium one. Recall the work function of alkali aluminosilicate materials decrease as the ionization energy of the alkali metal used in their preparation decreases.

To predict whether a compound will surface ionize to produce negative ions depends upon its decomposition behavior. Only species with positive electron affinities can surface ionize.

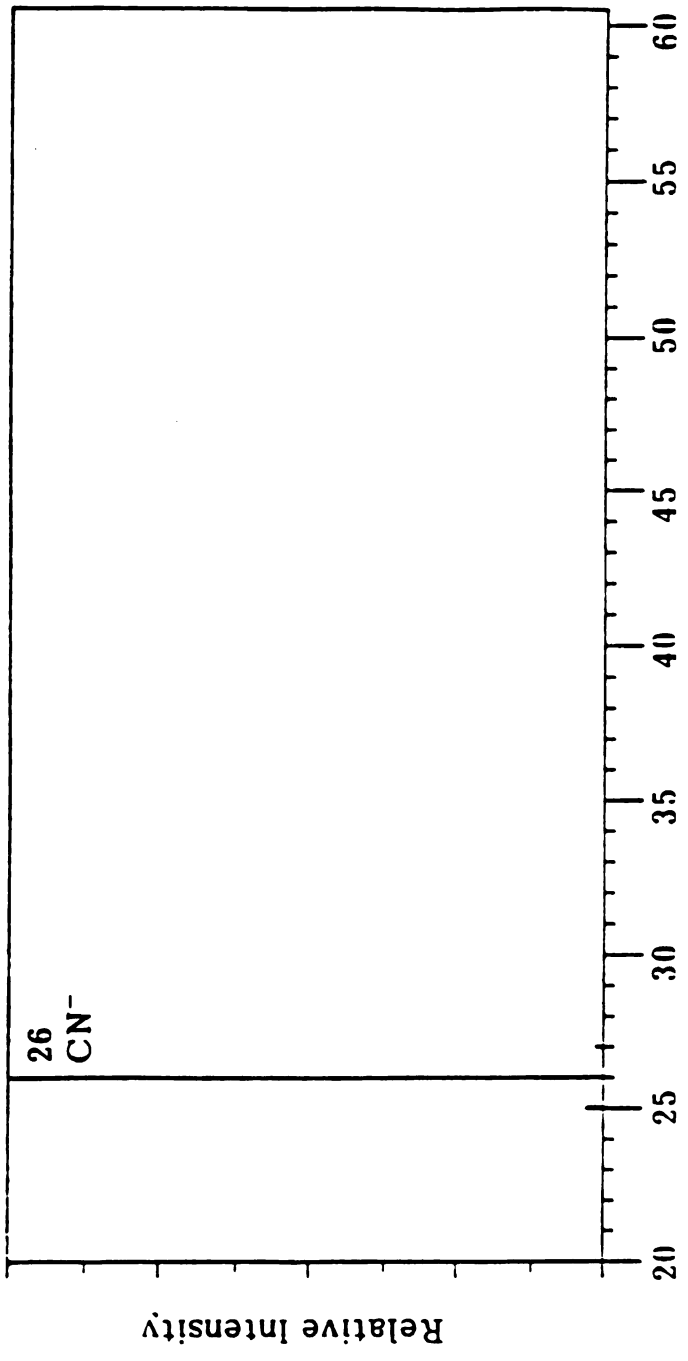


Figure 57. Negative SI Spectrum of Acetonitrile Obtained Using the Alkali Aluminosilicate Bead.

The use of available electron affinities and known thermal decomposition pathways would provide a framework for predicting an organic compounds behavior in the TID if a surface-only mechanism is accountable for the TID's response. Known decomposition pathways and EA's do provide a means of predicting an organic compounds response on the hot alkali aluminosilicate surface used here.

Other organic compounds when ionized on the alkali aluminosilicate bead produce ions other than CN^- (Figure 58). The spectrum of nitromethane contains an ion at m/z 46 which corresponds to NO_2^-. Also observed are $CH_2NO_2^-$ (m/z 60), CNO^- (m/z 42), and CN^- (m/z 26). The high NO_2^- ion intensity is not unexpected due to the electron affinity of NO_2 (4.0 eV) (57). Thermal decomposition studies of nitroalkanes suggest that NO_2 is a major product even at temperatures as low as 240°C. (149). The most intense ion in the negative SI spectrum of n-butyl nitrite is the alkoxy anion $C_4H_9O^-$ at m/z 73. In this case CN^- and NO_2^- are not evident (see Figure 59). Thermal decomposition of alkyl nitrites does lead to the production of alkoxy radicals (149). It is clear from these studies that N-containing molecules do not necessarily produce CN^-. In addition, alkoxy radicals can have relatively high electron affinities (57). Alkoxy radicals such as $C_4H_9O^-$ have relatively high electron affinities (57), thus the two conditions are met-species which have positive EA's are

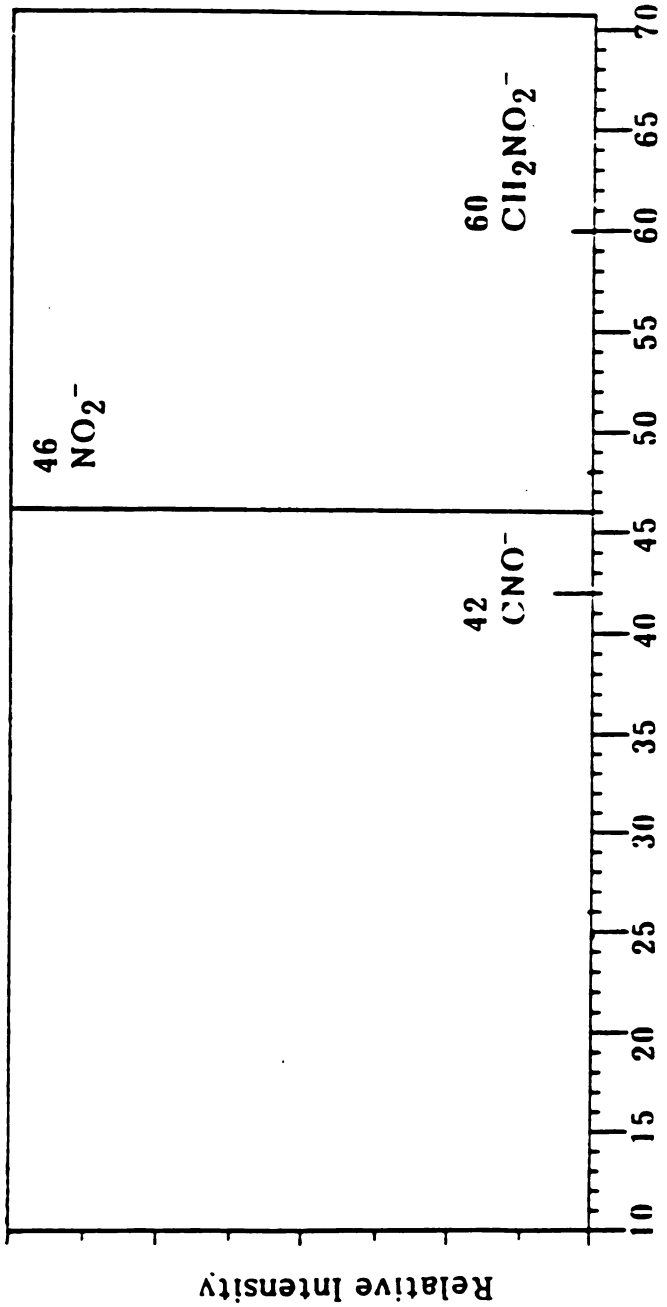


Figure 58. Negative SI Spectrum of Nitromethane Obtained Using the Alkali Aluminosilicate Bead.

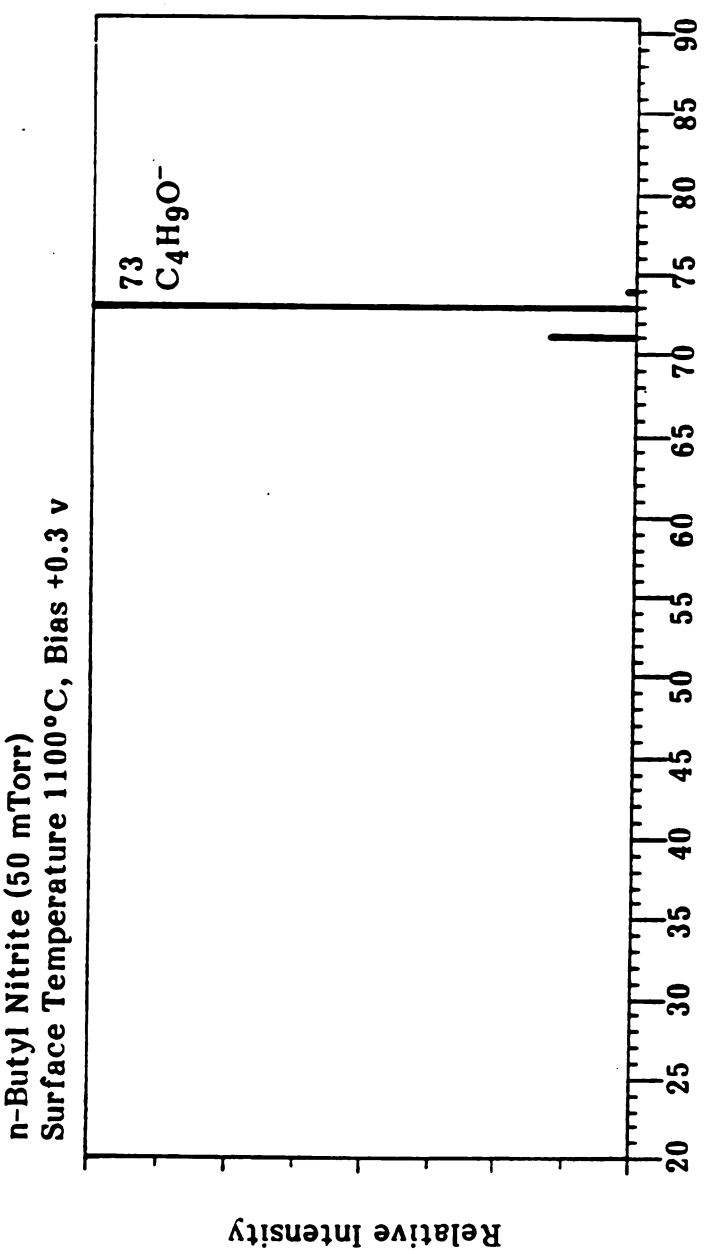


Figure 59. Negative SI Spectrum of n-Butyl Nitrite Obtained Using the Alkali Aluminosilicate Bead.

formed in thermal degradation pathways.

The response from phosphorus compounds in the TID has been neglected. Speculation has led to the popular belief that PO_2^- is the charge carrier causing the response in the TID due to P-containing compounds (144). Figure 60 shows the negative ions produced from tri-n-butyl phosphate on the hot alkali aluminosilicate bead. The most intense ion in the spectrum is at m/z 79, PO_3^-. The PO_2^- anion is not observed. The phosphate presumably adsorbs on the surface via the lone electron pairs of the oxygen atoms or the electron donating capibilities of the surface. Similar behavior has been observed for the adsorption of organophosphates, organophosphites, and organophosphines on metal oxides (150).

Hydrocarbons elicit a response in the TID which is often 3 or 4 orders of magnitude lower than that of N- and P-containing molecules. While the response of the hydrocarbons is small in the TID, there is a response. Figure 61 shows the negative charge carriers produced when hexane comes into contact with the hot alkali aluminosilicate bead. The ion series of C_nH^- stands out in this mass spectrum. Hydrocarbon decomposition studies on metals and metal oxides have shown that a carbonaceous layer (so called "surface carbide") is produced at high temperatures which is severely dehydrogenated (56). C_nH fragments have also been shown to have high electron affinities (57). These observations would support the appearance of the hexane SI spectrum in Figure

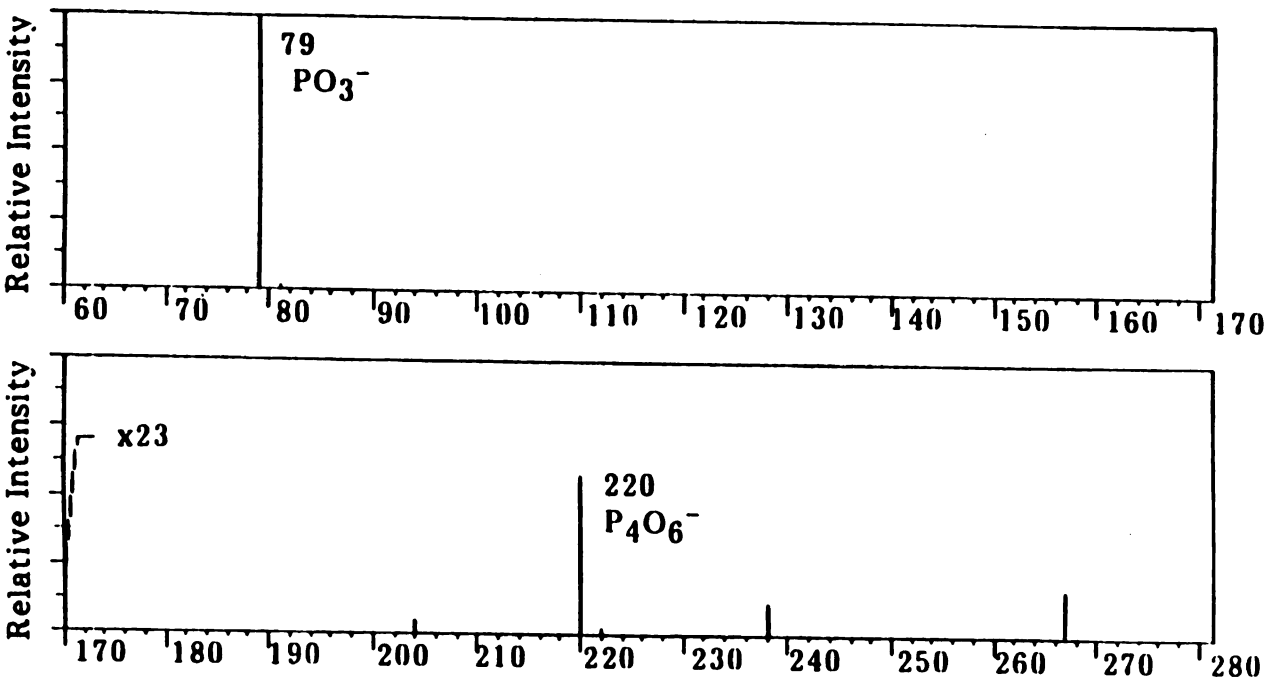


Figure 60. Negative SI Spectrum of Tri-n-Butyl Phosphate Obtained Using the Alkali Aluminosilicate Bead.

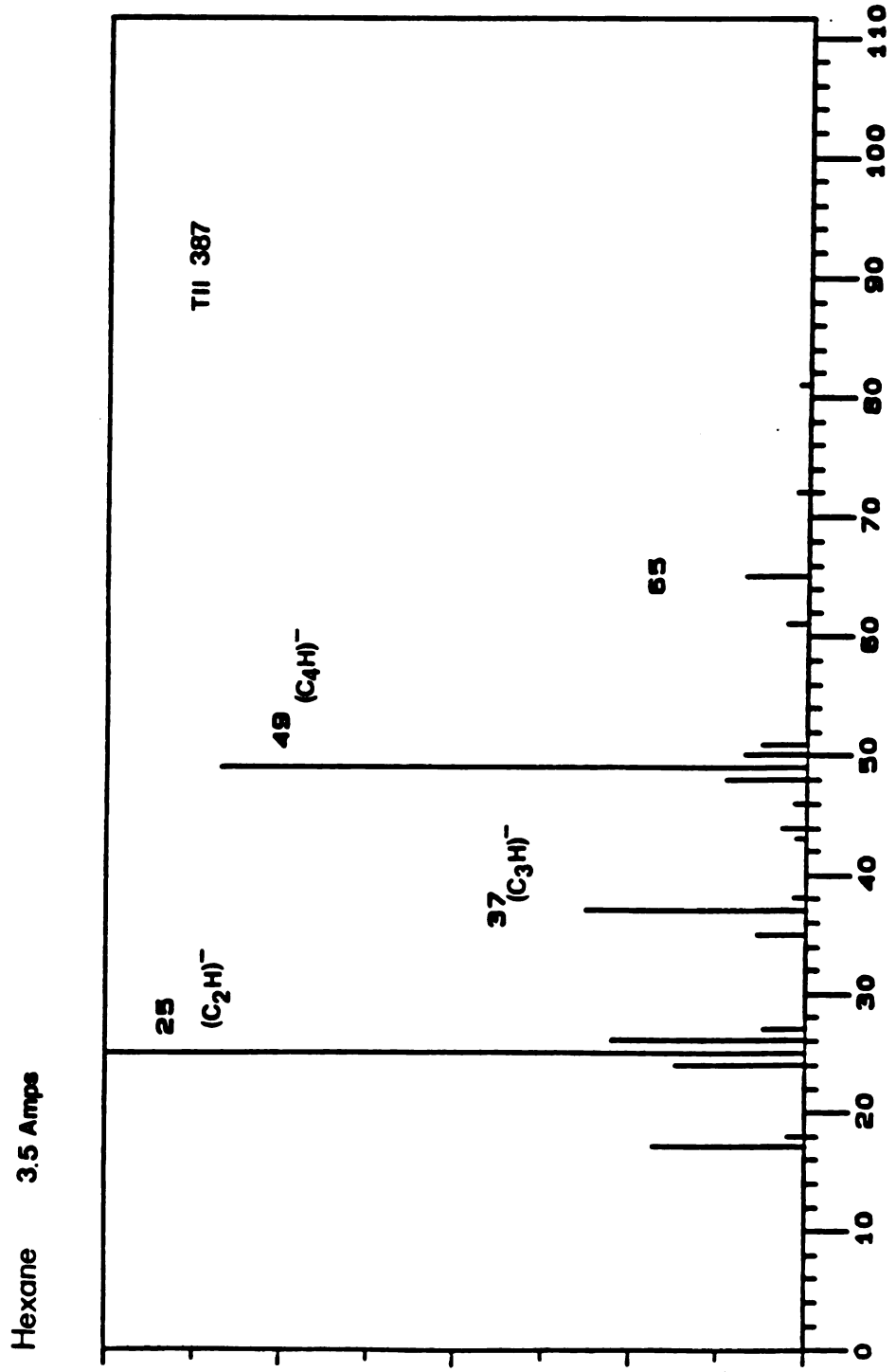


Figure 61. Negative SI Spectrum of Hexane Obtained Using the Alkali Aluminosilicate Bead.

61. Our experience is that, in our NSI experiment the overall process of ion formation for alkanes is 100-1000 times less efficient than that for N- and P-containing compounds. This behavior is consistent with the selectivity of the TID and could support a surface-only mechanism.

2. Positive Ion Formation

A TID mechanism must account for both types of detectors, i.e., those that collect positive species as well as negative charge carriers. The results that are presented here are consistent with a surface ionization mechanism for the positive ion mode of the TID. For positive surface ionization the ionization efficiency is largest when the difference between the work function of the surface and the ionization potential of the adsorbed species is small, i.e. when a high work function solid interacts with an atom/molecule fragment with a low ionization energy. When nitrogen and phsophorus compounds are used with favorable work function materials this condition can exist. High temperatures also favor ion formation in two ways, because of the temperature dependence in those expressions for negative surface ionization efficiency (see Chapter 1) and since thermal degradation products (having sufficiently low ionization energies) are formed at elevated temperatures.

Triethylamine is used here to demonstrate the possible routes that a molecule adsorbed on the hot alkali aluminsilicate bead can

take. A typical positive SI mass spectrum of triethylamine using our experimental approach is shown in Figure 62. Molecules are in equilibrium between the gas phase and adsorption sites on the surface. Triethylamine (and in general most N-containing molecules) can adsorb on the surface via the lone electron pair on the nitrogen atom. A similar process can be visualized for P-containing molecules. Once the species are adsorbed decomposition products can form. These newly formed species are also adsorbed on the surface and may exist in equilibrium with their precursors. An induced partial positive charge can cause a weakening of the β-bonds relative to the nitrogen atom. Evidence exists for this behavior (151). Thus for triethyamine, the radicals $[H\cdot+(C_2H_5)_2N\text{-}CH\text{-}CH_3]$ and $[\cdot CH_3+(C_2H_5)_2N\text{-}CH_2]$ are produced. Strong bonds between the radicals and surface atoms can make this a low energy process.

The adsorbed species can follow three possible pathways: (1) an ion can be formed; (2) the neutral product can desorb from the surface; and (3) the species can further decompose. For an ion to form the adsorbed neutral must have a low IP. The selectivity of the TID can be explained in this way. Many compounds decompose on hot surfaces (e.g. hydrocarbons) however, these decomposition products have relatively high ionization energies, leading to undetectably small signals. An example of an adsorbed neutral undergoing further decomposition is shown in equation 66.

$$CH_3\text{-}CH\text{-}N(C_2H_5)_2(s) \rightarrow (C_2H_5)NH\text{-}CH\text{-}CH_3(s) + C_2H_4(s) \qquad (66)$$

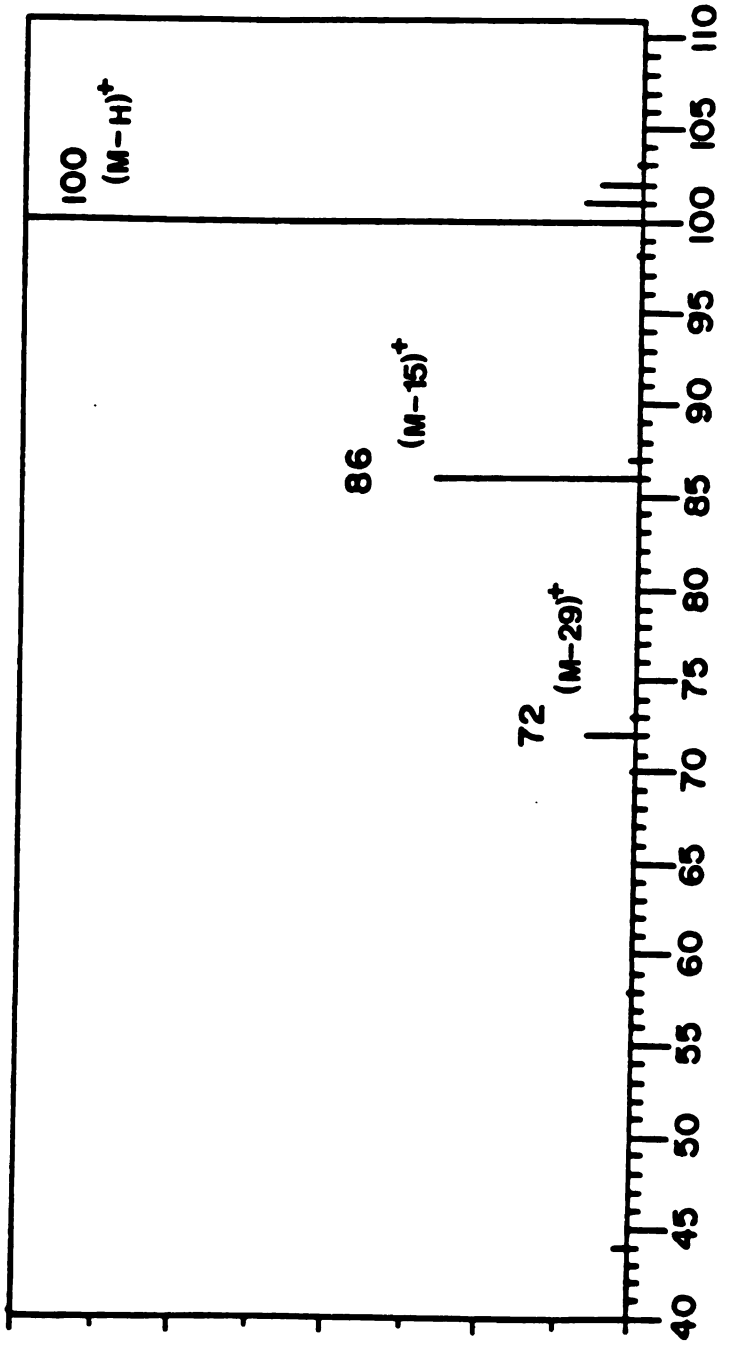


Figure 62. Positive SI Spectrum of Triethylamine Obtained Using the Alkali Aluminosilicate Bead.

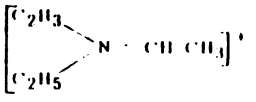
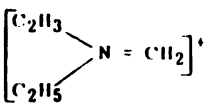
Similar reactions have been reported to be the intermediate steps leading to neutral products from amines on metal surfaces (152). From equation 66 the new decomposition products can form the ion $[(C_2H_5)NH=CH-CH_3]^+$ (m/z 72) or perhaps decompose further.

Table 6 shows the parallels between these results of positive surface ionization on alkali metal aluminosilicates with prior surface ionization results obtained on oxidized tungsten. The surface temperatures in both methods are comparable. Clearly our results are in good agreement with those reported earlier with only small variations. We do not necessarily expect the surface ionization products in this experiment to precisely match those previously reported since the two systems are chemically different in a variety of ways.

The previous discussion supports surface ionization as the dominant ionization mechanism in the TID. Decomposition can occur on the hot alkali aluminosilicate. In a surface-only mechanism, decomposition on the surface is highly important for the production of species with low ionization energies. A large body of literature exists for positive SI of organic compounds and has been recently reviewed (see references cited in Chapter 1). In most cases this literature refers to studies involving metal or metal oxide surfaces. Results using the alkali aluminosilicate thermionic bead closely parallel positive SI experiments on metal and metal oxides. It would appear from the surface ionization studies (both postive and negative) on the alkali aluminosilicate bead a surface-only mechanism is a possibility.

Table 6

Comparison of Positive Surface Ionization of Some Amines on Heated Alkali Aluminosilicate and Oxidized Tungsten Surfaces.

Compound	Ions Formed on Potassium Aluminosilicate Bead	m/z	Ions Formed on Oxidized Tungsten	IP of Desorbing Species (eV)	Postulated Structure
Ethylamine MW=45	$(M+H)^+$	46	$(M+H)^+$	~ 7.8	$[(C_2H_5)NH_3]^+$
	$(M-H)^+$	44	$(M-H)^+$	~ 8.3	$[CH_3-CH = NH_2]^+$
Diethylamine MW=73	$(M+H)^+$	74	$(M+H)^+$	~ 7.2	$[(C_2H_5)_2NH_2]^+$
	$(M-H)^+$	72	$(M-H)^+$	~ 7.2	$[CH_3-CH = NH-(C_2H_5)]^+$
	-	70	$(M-3H)^+$	~ 7.4	$[CH_3-CH = NH-CH-CH_2]^+$
	$(M-CH_3)^+$	58	$(M-CH_3)^+$	~ 7.8	$[CH_2 = NH-(C_2H_5)]^+$
	$(M-C_2H_5)^+$	44	-	~ 8.3	$[CH_3-CH = NH_2]^+$
Triethylamine MW=101	$(M+H)^+$	102	$(M+H)^+$	-	$[(C_2H_5)_3NH]^+$
	$(M-H)^+$	100	$(M-H)^+$	~ 6.9	$[(C_2H_5)_2N = CH-CH_3]^+$
	$(M-3H)^+$	98	$(M-3H)^+$	-	
	$(M-CH_3)^+$	86	$(M-CH_3)^+$	~ 7.1	$[(C_2H_5)_2N = CH_2]^+$
	$(M-CH_3-2H)^+$	84	$(M-CH_3-2H)^+$	-	
	$(M-C_2H_5)^+$	72	-	~ 7.2	$[CH_3-CH = NH-C_2H_5]^+$
	$(M-C_2H_5-CH_3-H)^+$	58	-	~ 7.8	$[CH_2 = NH-C_2H_5]^+$
	$(M-C_4H_9)^+$	44	-	~ 8.3	$[CH_3-CH = NH_2]^+$
Aniline MW=93	M^+	93	M^+	~ 7.7	$(C_6H_5)NH_2$

3. The GC-TID in the Absence of Gases.

The compounds studied in the above surface ionization experiments on the alkali aluminosilicate material can behave differently when introduced in the GC-TID. No reponse is observed for these compounds when the GC-TID is operated using no detector gases (other than 30 ml/min He) and high current settings. It would seem that if a surface-only mechanism is operative a response should be seen in the TID for these compounds. This may not necessarily be the case since detector gases not only influence the gaseous environment surrounding the bead but can also influence the surface. Next we will attempt to answer the next question: What is the role of detector gases in the TID? We will discuss the influence of several gases on the response of N- and P-containing compounds in the MS-TID. The low pressures used in the mass spectrometric experiments would not likely support a "reactive zone" near the hot bead. (However, high flow rates in the TID may not allow a "static" reactive zone to be maintained either). The mass spectrometric studies would be useful in identifying what surface effects these detector gases have on the hot thermionic bead. This behavior then will be compared to results using the GC-TID.

B. What Role Do Gases Have Between an Analyte and the Hot Surface?

The lack of response in the GC-TID in the absence of other gases (other than the analyte) suggest that the gases are extremely important to the response mechanism. The following investigation in this reaction will be divided into the categories of mass spectrometry (MS-TID) and gas chromatography (GC-TID).

1. The Effects of Gases in the MS-TID.

Initially the effects of introducing air with the organic vapor into the ion source containing a hot alkali aluminosilicate bead was studied. The introduction of air in the mass spectral experiment had three effects on the results: 1)changes in the total ion intensity (increase or decrease of product ions); 2) change in the product ion distribution; and 3) a "renewal" of the surface ionization characteristics of the thermionic bead. In general, the compounds giving the largest increase in total ion intensity were halogenated compounds. These compounds generally give responses 20 to 30 times higher when the pressure in the CI volume was doubled by using air while keeping the pressure of the organic compound constant. The increased response shows an increase of each ion signal in the spectrum without any change in the relative abundances. Other compounds such as acetonitrile and triethylamine yielded reduced responses

on addition of air. This behavior at higher pressures may be in part due to the cooling of the alkali aluminosilicate bead since the bead is heated under constant current conditions. To investigate what role an additive gas (e.g. air) has on a surface-only mechanism, consider the simple model which is represented by equations 67-69.

$$A(g) + M \rightarrow A{\cdot}M \quad (67)$$

$$A{\cdot}M \rightarrow B{\cdot}M + C{\cdot}M \quad (68)$$

$$B{\cdot}M,\ C{\cdot}M \rightarrow B^{+}(g) + C^{+}(g) \quad (69)$$

Equation 67 considers the adsorption of molecule A to some surface site M located on the thermionic ceramic. In 68 decomposition of A on the surface forms adsorbed decomposition products (B·M and C·M). If the electron affinities of the adsorbed decomposition products are sufficiently high these products can surface ionize. When the thermionic emitter is correctly biased gas phase ions are observed. Using this simple model the effects of adding air to the mass spectrometer will be investigated particularly focusing on each step in this process.

In a surface-only mechanism the addition of air may influence the surface by changing the work function. In our model the work function would be only important in equation 69. It has been shown that on metals (e.g. tungsten) the addition of O_2 increases the work function of the surface (7). Some positive SI methods in mass spectrometry are performed with the addition of O_2 into the

source (35). Here the addition of air appears to lower the work function of the surface which would favor the production of negative ions. This apparent reversal in behavior upon the addition of air is likely due to differences between the surface characteristics of metals and of the alkali aluminosilicates. If the addition of air to the SI experiment discussed here only served the purpose of lowering the work function of the surface we would expect to enhance the response for compounds such as triethylamine. This is not the case, triethylamine has a reduced response upon the addition of air. Evidently air can influence the surface in a manner other than changing the work function.

The adsorption of O_2 (air) on the surface can affect the adsorption of other species. This behavior pertains to equation 67 in our model. For surface ionization to occur the neutral species (molecule A) must be adsorbed onto the surface. Adsorption of two different neutrals can influence the adsorptive behavior (ref). This behavior results in either interactions between the two coadsorbed species or one species blocking adsorptive sites (M) thus decreasing the concentration of the other adsorbate on the surface. Coadsorption is one phenomenon which can influence the adsorption behavior of a molecule on the thermionic ceramic. Other factors are the thermodynamics of adsorption (heats of adsorption) and types of adsorptive behavior (molecular or dissociative). Additive gases such as O_2 may alter the surface here as well to change these adsorbate-surface interactions.

Figure 63 shows the effect of adding air with tri-n-butyl phosphate. The rich chemistry of phosphorus compounds in general causes difficulty in certain peak assignments, however it is important to note the change in the relative intensity of each ion in the spectrum. Changes in the adsorptive behavior or work function of the surface would only serve to change the intensity of the ionic species. Compounds such as CCl_4, a halogenated hydrocarbon, in the presence of air shows an increased total ion intensity without any changes in relative intensities of the observed ions (Cl^-, Cl_2^-, CCl_2^-, CCl_3^-, CCl_4^-). The change for this P-compound would seem to indicate a process other than those implicated in equations 67 and 69. It would appear that the environment at the surface of the bead has changed so that it is taking a chemically active role in the production of ionic species. This process would be described best by equation 68. The effect of surface oxidation or catalytic combustion is well documented (153). This process is often facilitated on surfaces by the addition of air. Catalytic combustion GC detectors were commercially available during the 1960's (153-154). At the time their ionization mechanism was a subject of debate. It is beyond the scope of this work to discuss in detail these detectors, however their behavior parallels our results in the mass spectrometric experiments involving the addition of air.

The addition of air appears to affect a variety of processes-adsorption, decomposition and surface ionization. It may not be possible only to get a change in work function without

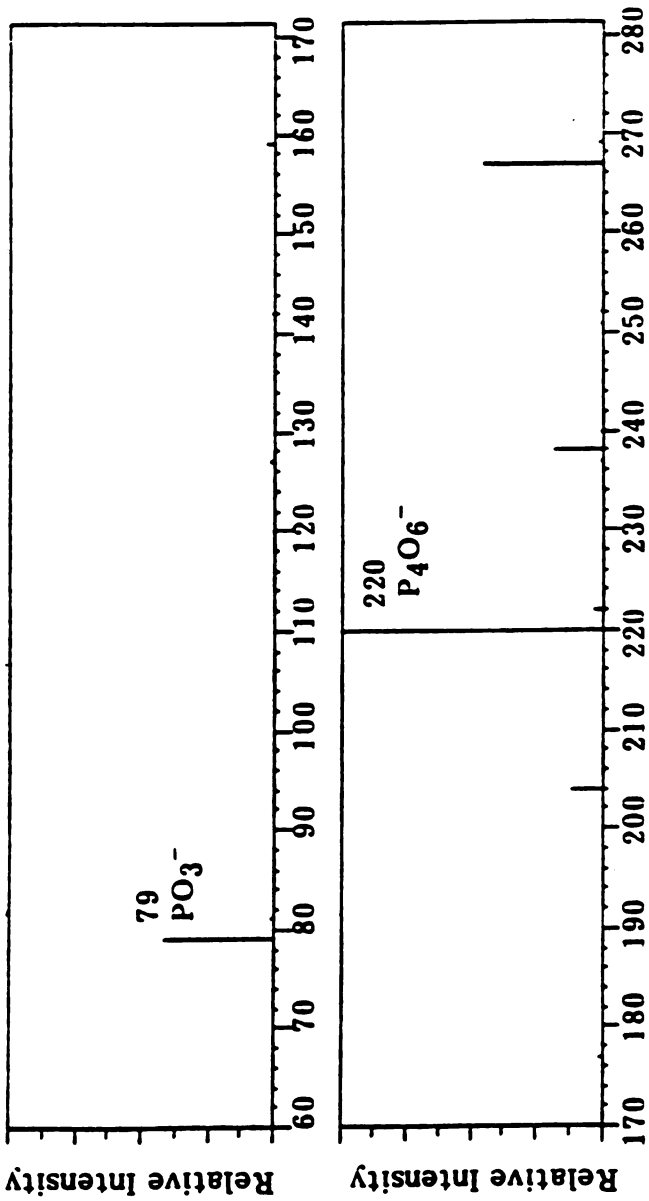


Figure 63. Negative SI Spectrum of Tri-n-Butyl Phosphate Obtained Using the Alkali Aluminosilicate Bead. This Spectrum Was Obtained With a Source Pressure of 100 mTorr of Air.

a corresponding change in the adsorptive behavior of the surface to a compound. Qualitatively however, the simple model as suggested by equations 67-69 does well to explain our findings.

The GC-TID is most widely used with hydrogen and air as detector gases. These gases, by themselves, only produce an ion current at very high bead currents (>5 A) within the mass spectromter. The lifetime of the thermionic probe tip housing the alkali aluminosilicate is short at this current setting and no useful information can be obtained. The ion current at this high bead current consists solely of OH^- ions. The background current in the TID has been surmized to be due to the hydroxyl ion and our results would seem to support this view.

When N-, P-, and chlorinated compounds are introduced with these two gases the behavior is identical to that obtained upon the introduction of air. Phosphorus and chlorinated compounds show an enhanced response and any spectral changes (e.g., trimethyl phosphate) are the same as with the addition of air. At no time was the OH^- ion seen with the other product ions in the spectra. The lifetime of the bead is short at high currents so that no conclusions can be made at higher temperatures. The observations here are nothing more than those obtained for air. Apparently the effect on the response of any compound in the presence of radical species of hydrogen and oxygen cannot be studied here at these pressures. While this is discouraging the importance of pressure becomes evident. Pressures greater than 1 torr are needed for the combustion of H_2 at reasonable bead

currents (<5 A) and as will be shown later the combustion of H_2 must in some way take part in the production of charge carriers in the GC-TID. Next we will characterize the GC-TID in terms of detector gases. This is necessary in order to make a comparison between the MS- and GC-TID's.

2. The Effects of Gases in the GC-TID

Before discussing the role of various detector gas systems the role of <u>any</u> gas on the bead temperature will be discussed. This can be done here since the gases' affect on the temperature of the bead was independent of the gas used as will be seen. In addition, detector gas-bead temperature phenomenon will be needed in later separate discussion of detector gas systems.

<u>a. Temperature of the Bead.</u> The detector block in all the GC-TID experiments is 300^{0}C. as suggested in the operation manual supplied with the TID. Figure 64 shows the effects of changing flow rates of various detector gases on the temperature of the bead. The temperature was measured with an infrared thermometer and occasionally checked with an optical pyrometer when applicable (above 750^{0}C). The data used in Figure 64 varied by no more than 10^{0}C. Figure 64 shows that the temperature of the bead changes with flow rate <u>independent</u> of the nature of the gas used. Only the top of the TID bead is visable and it was this location from which the temperature was measured. This would suggest that this phenomenon is physical and not chemical. In

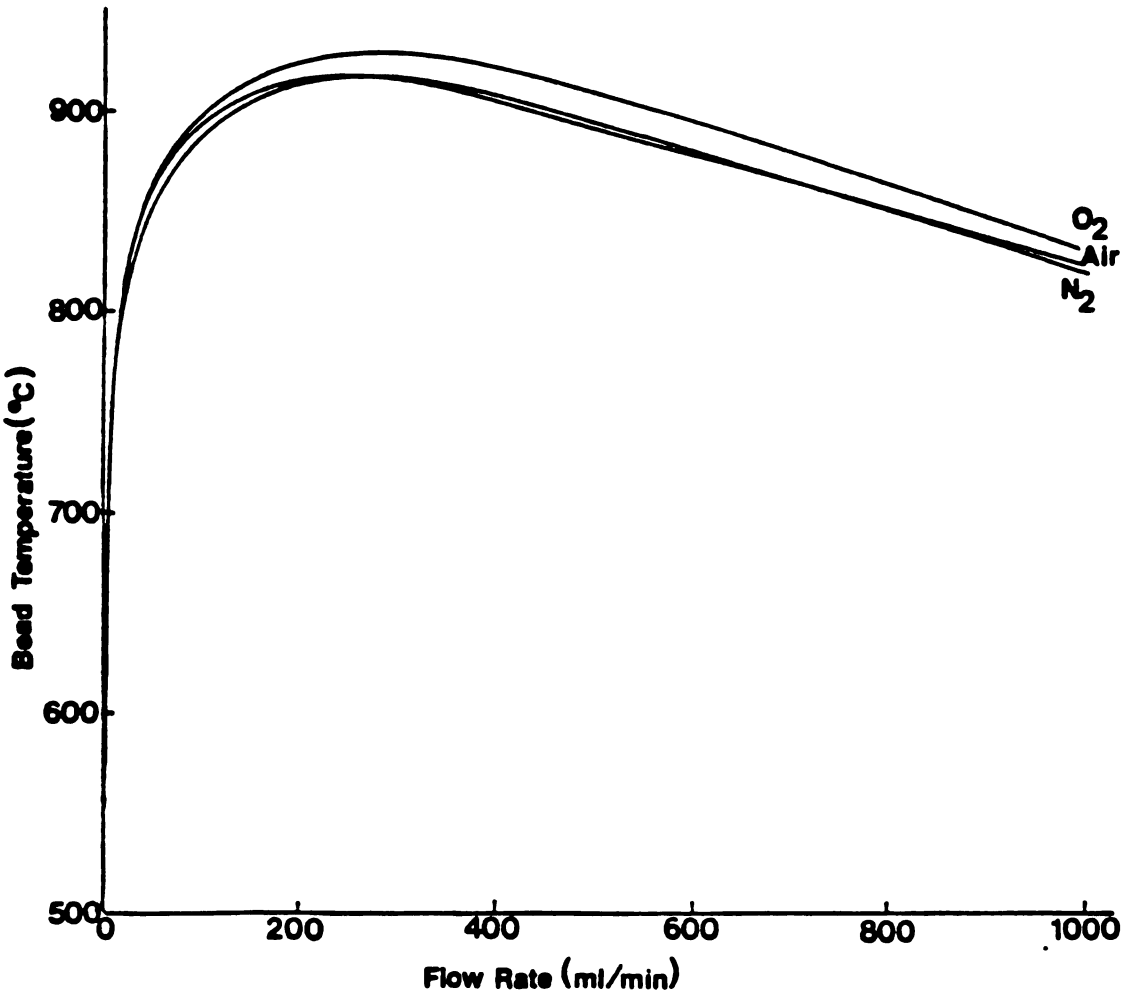


Figure 64. Bead Temperature as a Function of Detector Gas Flow Rate.

addition, when various pressures of H_2 are used with air or O_2 no change is observed for either curve. This is not true when sufficient H_2 is added to bring the H_2-O_2 system above the explosion limit. At this point a true flame is established. As can be seen from Figure 64 the temperature of the beade is below 600^{0}C. when no detector gases are used (except for ~30 ml/min He as carrier gas). Under these conditions no response is observed from all the test compounds used here. These observations would suggest that, in part, one role of the detector gas appears to in some manner increase the bead temperature.

A physical explanation which would support our observations involves laminar flow of the detector gases around the TID bead. Consider the configuration of the TID used in these studies (see Figure 65). The TID bead is located within the detector cylinder. The TID bead is directly above the flame tip and separated by a distance of approximately 3 mm. The sample, carrier gas, and H_2 are introduced through the flame tip. Other detector gases (e.g. O_2, N_2, and air) are introduced through small holes at the base of the flame tip. A schematic of the TID used here is shown in Figure 65. The flow of any gas into the detector via the flame tip has no influence on the bead temperature. This is not true however, when the flow exceeds 80 ml/min. (The bead temperature decreases). It is the flow of gases introduced at the base of the flame tip which affects the temperature. For this case laminar flow would produce areas of low pressure around the

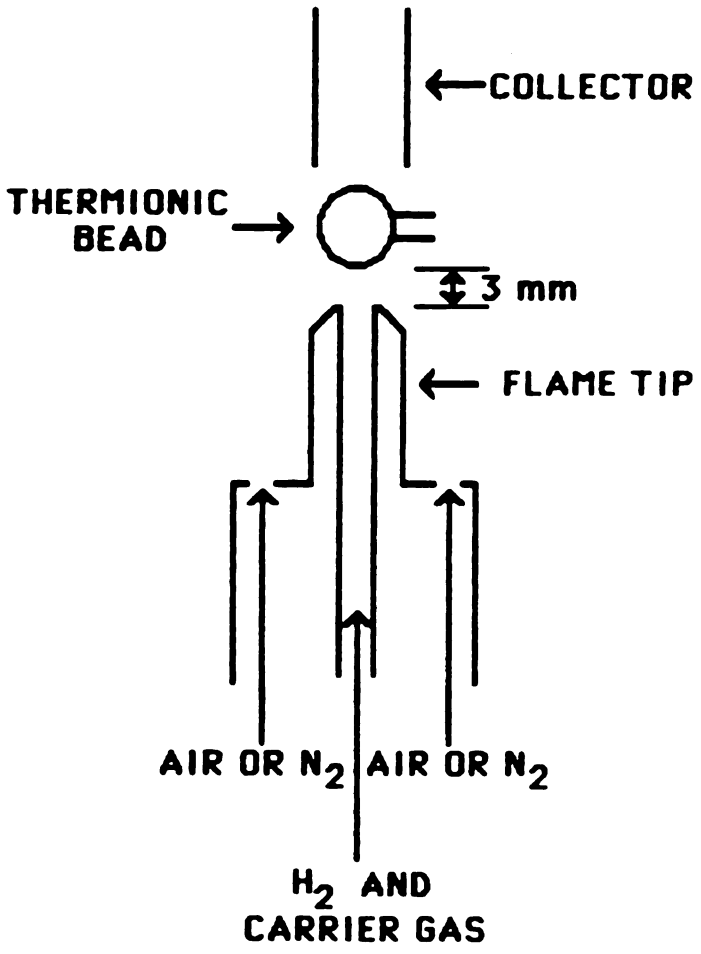


Figure 65. A Typical Configuration of a TID.

bead. Collisional cooling of the bead would produce areas of low pressure around the bead. Collisional cooling of the bead would diminish in these areas of low pressure which results in an increase in temperature.

The detector configuration does not permit observation of the entire bead. One would expect however, the bottom of the bead would be cooler due to its bombardment by the effluent from the flame tip. This would suggest that the temperature at the surface of the bead is not uniform and may vary by several hundred degrees Celsium. How can these different temperature regions affect the TID response? The adsorption, decomposition, and surface ionization of neutral species are all temperature dependent in a surface-only mechanism. Varying temperature zones could also affect a gas phase decomposition mechanism by dictating the concentration and composition of the reactive gas phase boundary surrounding the bead. It will be shown shortly that the TID response is dependent upon the flow rates of the detector gases. In addition to changes in bead temperature, flow rates can alter the composition of atmosphere surrounding the bead. Both these factors (temperature and composition) must be jointly discussed with changing flow rates of the detector gases since they cannot be separated. It will be shown that in some cases the temperature of the bead or the composition of the atmosphere surrounding the bead is more important to the detector response.

Several experiments and definitions must be clarified before

discussing the behavior of the TID with respect to different detector gases. In these experiments the response will be reported as peak height (Amps) per mole compound injected. The selectivity (response of one compound relative to another) will be determined by the ratios of the response of the two compounds in question. Generally the selectivity of the TID is calculated with respect to a hydrocarbon. Here the units of selectivity will be a mole ratio. There are three types of experiments which will be used in these behavioral studies: 1) response as a function of flow rate keeping bead current constant; 2) response as a function of bead current keeping flow rate constant; and 3) response as a function of injection number. The first two types of experiments are self explanatory; the third involves injecting an analyte repeatedly with constant time intervals in between each injection (typically 1-2 minutes). These intervals are timed from the point after elution of a compound to the next injection. In addition to these three experiments a compound may show irregular behavior in regard to peak shape. These experiments will serve to characterize the TID response for various compounds with respect to different detector gases. The first detector gas which will be discussed is air.

b. Air in the GC-TID. Throughout these studies several model compounds are used typically having one functional group which contains the N or P atom. Molecules such as malathion, methyl parathion, and azobenzene have been used previously to characterize the TID (71). Here simpler molecules are used. For

some of these simpler molecules data such as electron affinities and decomposition (surface and gas phase) are more likely to be found.

In Figure 66 the behavior of several test compounds in the constant flow rate study is shown. Here the air flow rate is a constant 160 ml/min. No other gases are used. A plot of response versus current, when plotted logarithmically, is linear. It is important to note that heating current is used instead of temperature due to the likely existence of a temperature gradient along the bead. Therefore the relationship between current and bead temperature is unclear. What is known is that bead current is proportional to bead temperature is unclear. What is known is that bead current is proportional to bead temperature; further increasing the current increases the average temperature of the entire bead. Several observations can be made from the curves in Figure 66. The slope of the lines for the functionally similar compounds (p-nitrophenol, p-nitrotoluene and C_{12}-C_{17}) are nearly the same. This would suggest the role of air as a detector gas is dependent upon the functional groups on the molecule. . As a consequence each compound with a different functional group should have a different slope as is the case here. The different slopes are responsible for the change in selectivities over the current range shown. For example, p-nitrophenol has a higher response at lower currents than tributylamine; after 3.6 A this behavior is reversed. The influence of temperature can be large as is the case for tributylamine where the response changes over

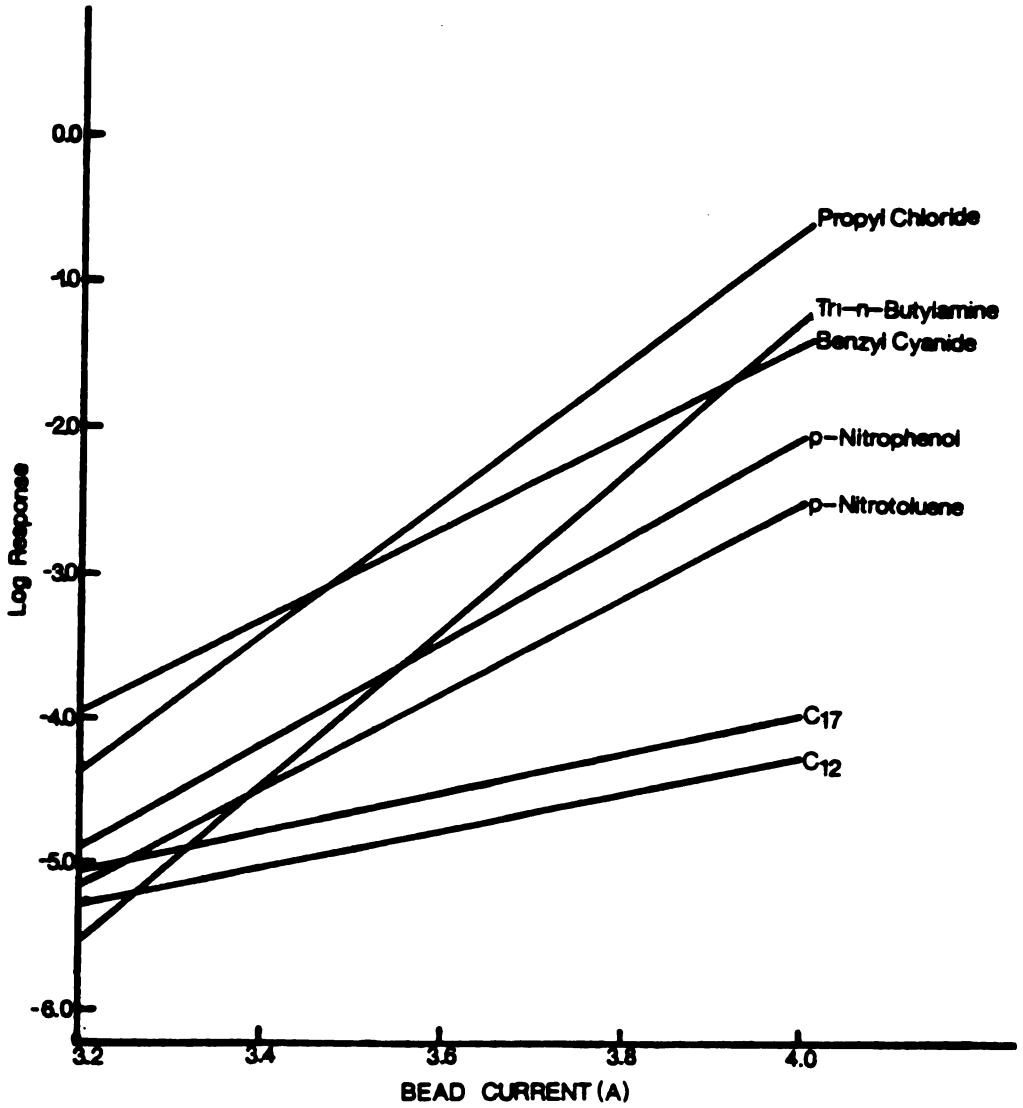


Figure 66. Plot of Log Response as a Function of Bead Current For Several Compounds at a Constant Air Flow Rate of 160 ml/min.

4 orders of magnitude. As shown temperature has a profound effect on response.

One test compound, trimethyl phosphate, could not be plotted in Figure 66 since the response varied upon repetitive injections of the compound. The peak shape of this compound was symmetrical over a large range of sample sizes. It was concluded that this behavior is not a column effect but is detector related. Response for trimethyl phosphate is plotted as a function of injection number in Figure 67. These results are obtained at 3.2 A bead current and a 160 ml/min air flow rate into the detector. The elution of trimethyl phosphate is equally spaced by approximately 2 minutes. The increase in response for this compound is nearly linear up to 14 injections where a plateau is reached. After 3.6 A bead current trimethyl phosphate shows no dependence upon injection number. We believe this behavior is a surface phenomenon. The possibility that reactive gas phase species (created when the compound is introduced into the detector) could remain in the detector for several minutes is small. At this flow rate (160 ml/min) and considering the design of the TID, a species remaining in the gas phase after eluting from the GC column would reside within the detector for no longer than 5 seconds. The time interval between each introduction of trimethyl phosphate into the detector was 2 minutes.

The modification of oxide surfaces by phosphorus compounds has been recently studied (150). It was observed that

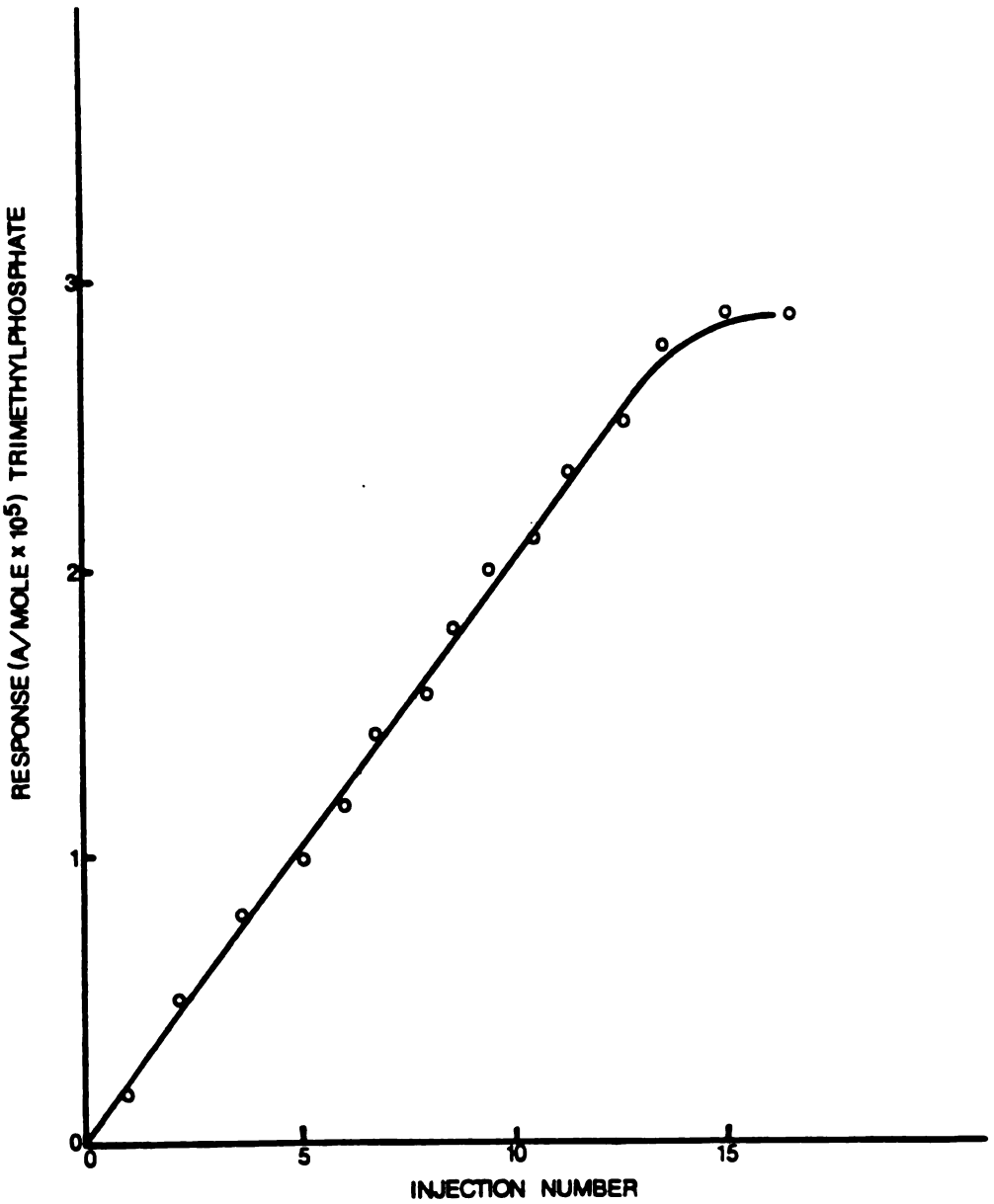


Figure 67. Response as a Function of the Number of Injections For Trimethyl Phosphate.

decomposition of these P-compounds on the surface led to gas phase species such as ethers and hydrocarbons. No gas phase P-containing molecules were found. Decomposition therfore, led to a modification of the surface by various phosporus compounds which are mostly oxides. Above a particular bead current, repetitive injections have no enhancing effect. Apparently high surface temperatures serve to keep the surface "clean" by not permitting any build-up of P-containing species. The modified surface has an effect on the response of other compounds. Compounds eluting after trimethyl phosphate show a diminished response. Conditioning the bead at higher bead currents apparently "rejuvenates" the surface to the test solutes' original responses.

The chlorinated compound used here (propyl chloride) also shows behavior similar to trimethyl phosphate. Below 3 A bead current the response increases with repetitive injections similar to that shown in Figure 67. In contrast to trimethyl phosphate the other test solutes show an enhanced response on elution after propyl chloride. With air as the only detector gas the use of chlorinated solvents has been suggested as a response enhancer in the TID (148). Increasing the bead current for this case also rejuvenates the surface to its original condition. The opposite effects that propyl chloride and trimethyl phosphate have on sample response is most likely a reflection upon the various ways a modified surface can change a compounds response in the TID. For example, a decrease in response would suggest the

obstruction of adsorptive surface sites or an increase in work function. An increase would suggest a decrease in work function. In light of these results, care must be taken in quantitative analyses of a singular component from mixtures where a calibaration curve is used. It is advisable to use internal standardization.

In Figure 68 several test compounds are plotted against air flow rate at a constant 3.6 A bead current. The dependence of response on flow rate can be categorized into three groups. Tributylamine and nitrobenzene produce curves which have a definite maximum. Trimethyl phosphate shows an exponential decrease in response with flow rate. Not shown but similar to trimethyl phosphate is propyl chloride. Dodecane exhibits the third type of behavior in which response is nearly linear with flow rate over an extended range. (Response for dodecane falls rapidly at very low or high flow rates). In general, the degree to which the sensitivity changes with flow rate is smaller than with bead current.

The curves for tributylamine and nitrotoluene in Figure 68 would suggest a temperature dependence. The shape of these curves parallels the temperature dependence on air flow rate shown in Figure 64. The response for all compounds studied depend upon temperature. For instance, below approximately 50 ml/min air no response (i.e. response is less than $5x10^{-6}$ A/mole) is observed. The response for trimethyl phosphate and propyle chloride would appear to depend upon more than the temperature

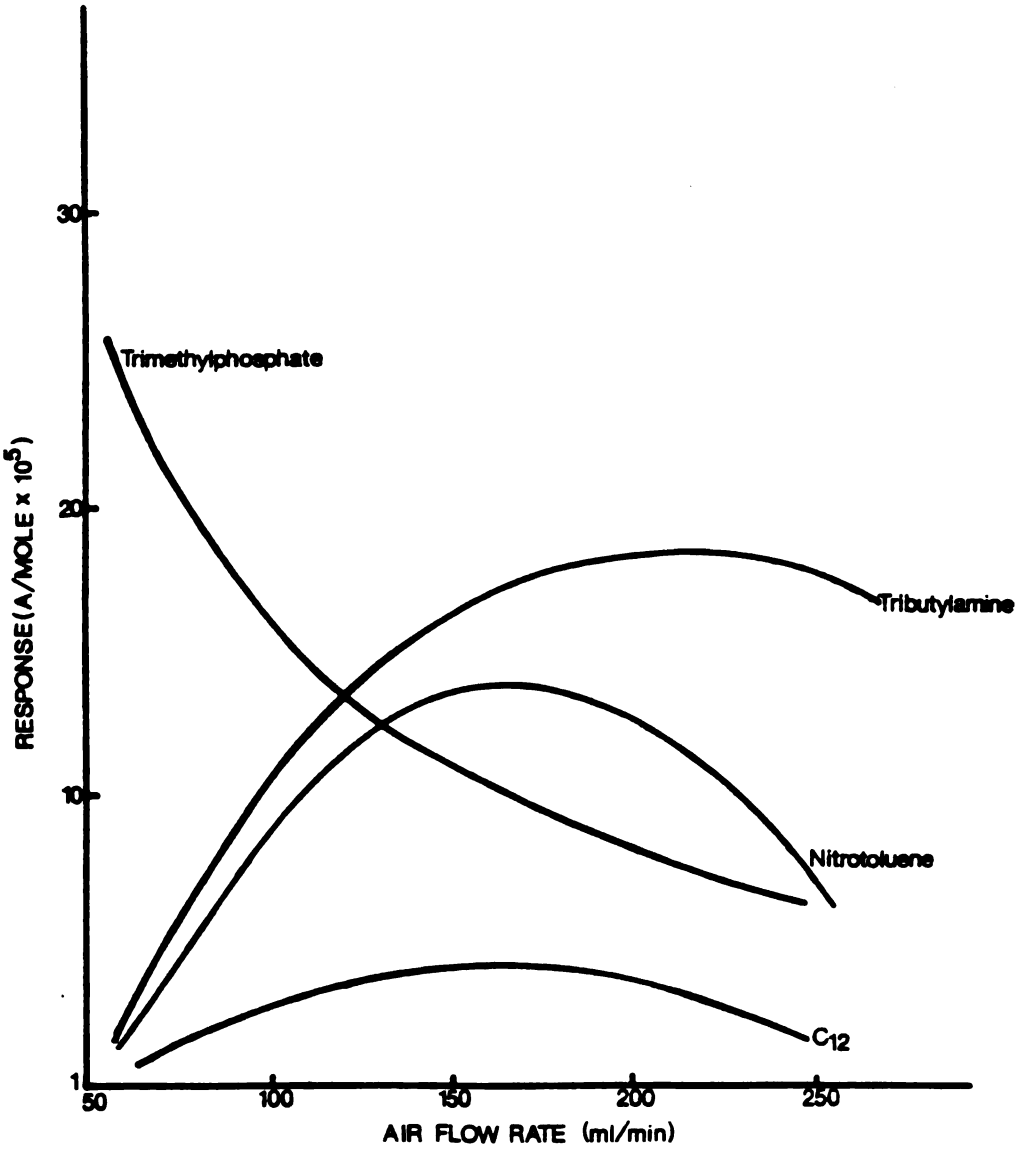


Figure 68. Response as a Function of Air Flow Rate For Several Test Compounds.

of the bead. What this suggests is that trimethyl phosphate and propyl chloride's response is dependent upon the concentration of detector gas (most likely O_2). For the phosphate, as stated earlier, oxides of phosphorus can form. The chloride's response may be increased by a reactive mechanism such as that for the phosphate or perhaps O_2 can increase the sticking probability of this compound on the surface. In the case of dodecane it is unclear what effect causes the behavior in Figure 68. The steep fall-off region suggests temperature is important. It also appears once a particular bead temperature is reached the dodecane response is independent on air flow rate.

Several important points can be made in summarizing the characteristics of the TID when air is used as the only detector gas. Temperature appears to have more of an effect on the test compounds' responses than the flow rate of air. Selectivity can vary greatly with bead current (bead temperature) with a reversal of selectivity observed for some compound pairs. It is also apparent that the TID response can be dependent upon the surface species on the bead. Trimethyl phosphate and propyl chloride when injected can change its own or other compounds responses in subsequent injections. This behavior diminishes with increasing bead currents therefore one role of temperature may be a cleansing mechanism which maintains a constant response. Finally, the sensitivity of all these compounds are much higher when a mixture of H_2 and air is used as the detector gas. The

H_2/air system will now be discussed.

c. The H_2/Air System in the GC-TID. The TID is most often used with a mixture of air and H_2 as detector gases. In the detector used here H_2 is introduced to the thermionic bead via the flame tip (see Figure 65). If H_2 is introduced along with air into the detector at the base of the flame tip a much different response is obtained. For example, a higher H_2 flow rate is needed for optimum response. These experiments involve some changes in the "normal" TID design. These experiments will not be discussed here however, since they are incomplete. These experiments are justified since such changes do bring about different responses and can be used to aid in elucidating the TID mechanism. Here we are concerned only with an unmodified commercial detector.

The optimum response of the H_2/air system at a given flow rate and bead current is strongly H_2 dependent. Figure 69 shows the response of a number of test compounds plotted versus H_2 flow rate at a constant bead current and air flow rate. Very small changes in H_2 dramatically change the sensitivity of the detector. It appears that for the compounds studied here there are two different optimum H_2 flow rates that depend upon whether the compound contains nitrogen or phosphorus. The nitrogen containing compounds reach a maximum value and then

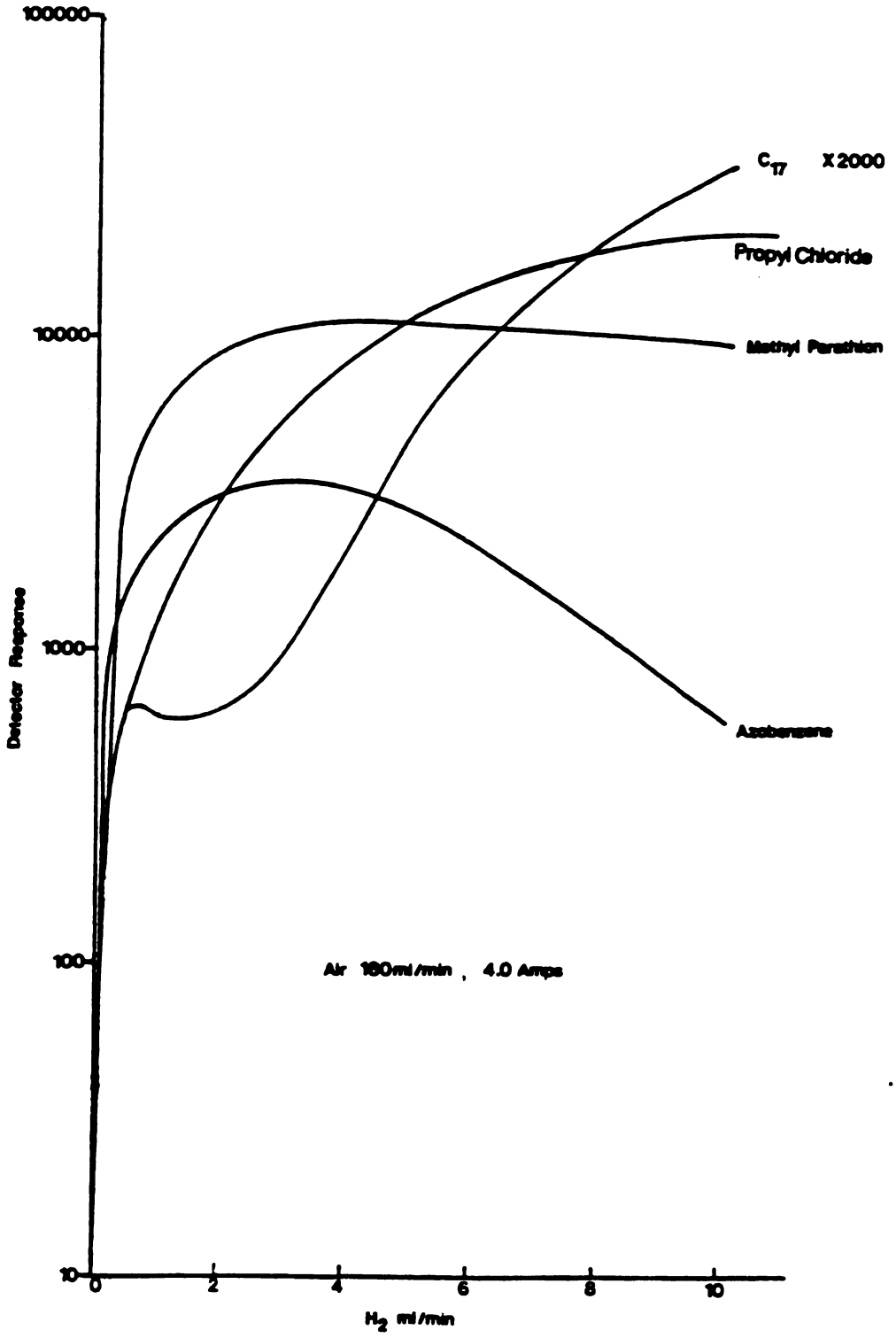


Figure 69. Response as a Function of H_2 Flow Rate For Some Test Compounds at Constant Current and Air Flow rate.

decrease. In contrast to this behavior the phosphorus, hydrocarbon, and chloride compounds show a plateau or no maximum at all. All the test compounds show a substantial increase after a small addition of H_2 into the detector. Above 8 ml/min hydrogen all compounds begin to increase in response. With the additon of H_2 above this limit a true flame is produced and the background of the detector increases to a point at which useful information cannot be obtained.

In addition to an increase in sensitivity H_2 can influence the peak shape of particular compounds. Figure 70 shows two chromatograms which are obtained under identical condition except for different H_2 flow rates. Once again only a small difference in hydrogen flow rate has a profound effect on the results. Here higher flow rates favor symmetrical peak shapes for the two compounds containing phosphorus. After 1 ml/min H_2 the peak shapes for these two compounds become symmetrical and baseline resolution is obtained. No effect is seen on azobenzene or the hydrocarbon when changing the flow rate of hydrogen. The same type of behavior, comparable to the P-compounds, is observed for propyl chloride (not shown). Column effects are unlikely since the chromatographic conditions are identical. Apparently at particular H_2/air mixtures P-containing molecules and chlorinated compounds interact at the surface of the bead which causes the tailing in their respective peaks. It would seem

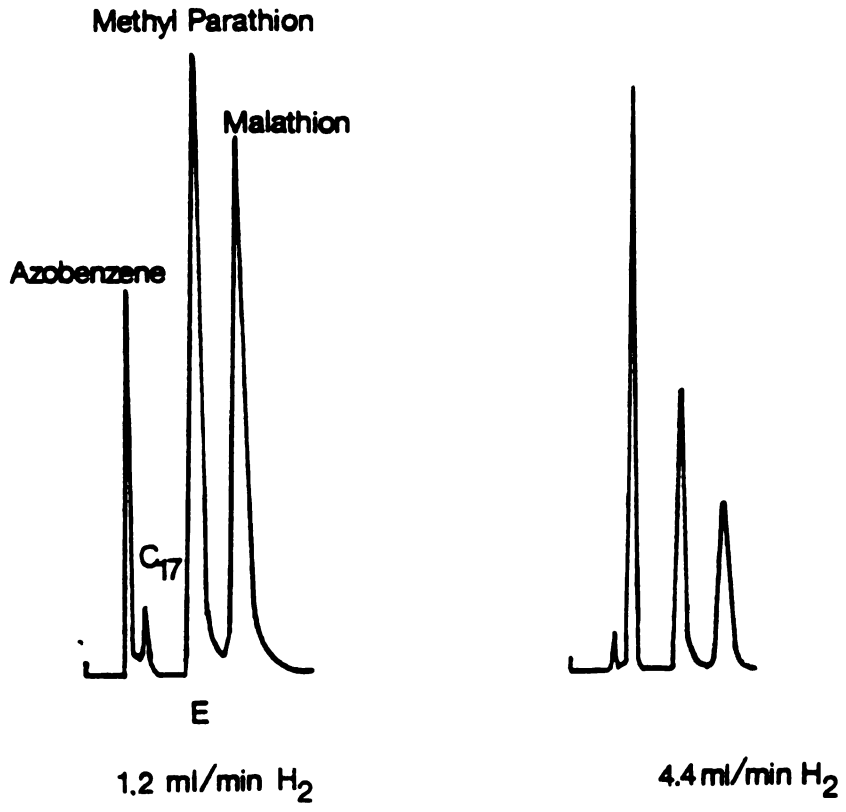


Figure 70. Chromatograms of Test Mixture at Two Different H_2 Flow Rates.

that one role of hydrogen/air is to keep the surface clean and this can only occur at the appropriate ratio of H_2 to air.

Changing the air flow rate while keeping H_2 and bead current constant does have a small effect on the sensitivity of the test compounds (Figure 71). As for air in the absence of H_2 the flow rate would appear to follow the temperature of the bead shown in Figure 64. Unlike before, when air alone was used, all compounds show the same behavior. The response curves for P- and Cl-containing compounds are similar to those of the N-compounds. This behavior can be observed for all H_2 flow rates and bead currents used here. The presence of H_2 therefore, radically changes the response of P- and Cl-compounds in the TID. The optimum air flow rate in the presence of H_2 approximately corresponds to the maximum temperature observed (see Figure 64).

Bead current has the largest effect on all the test compounds responses as can be seen in Figure 72. The response of a compound using the H_2/air detector gas mixture can vary by over 2 orders of magnitude when the bead current is increased. From Figure 72 it is apparent that hydrogen enhances the TID's response by several orders of magnitude when compared to the air-only case. Two distinct differences between H_2/air and air are evident from Figure 72. For hydrogen/air the curves are no longer linear but are curved. As suggested by Patterson et al.

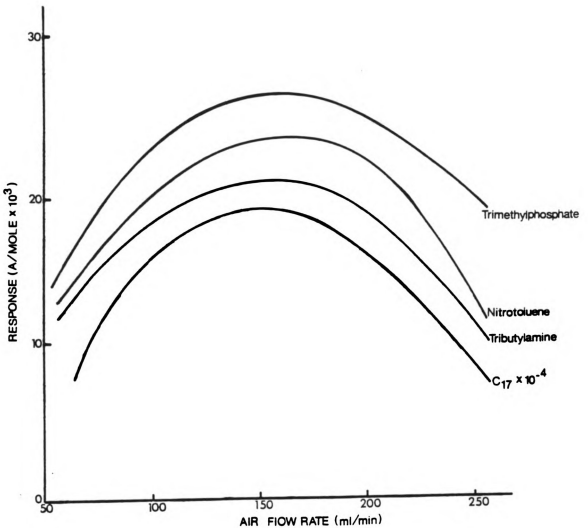


Figure 71. Response as a Function of Air Flow Rate For Some Test Compounds at Constant Current and H_2 Flow rate.

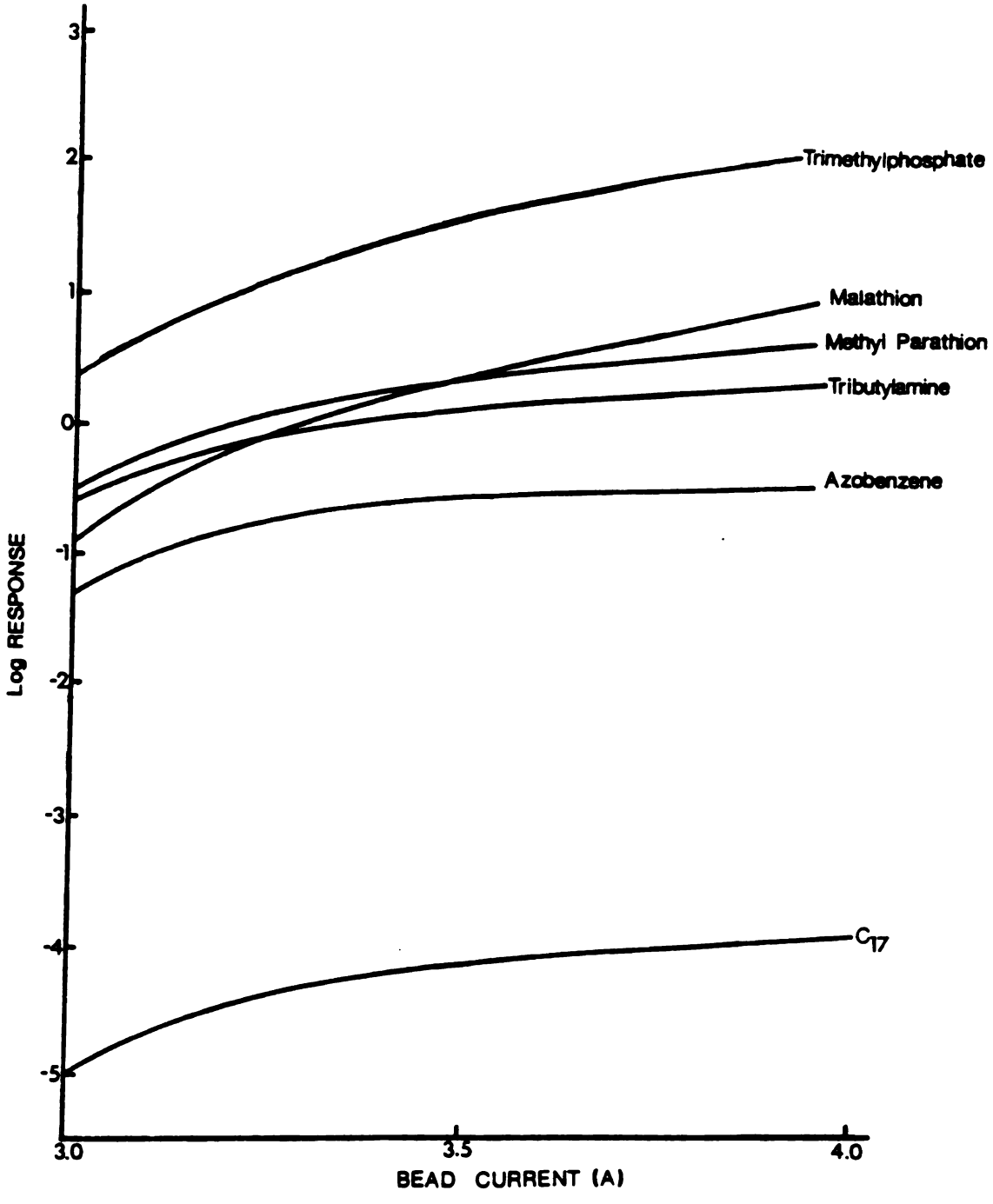


Figure 72. Log Response as a Function of Bead Current For Several Test Compounds.

(148) under these conditions the response should have a Amp^{-2} dependence upon current, i.e., a plot of response (detector current) versus $1/(amp)^2$ (bead current) should be linear. This was suggested when the heat transfer properties of the TID was compared to the thermal conductivity detector. Their findings are based upon the bead being of uniform temperature and also that current showing a nonlinear relationship with temperature. Our results (when H_2/air is used) is in agreement with Patterson's. With air only, the response is linear with current. Adding H_2 does not affect the bead temperature (measured at the top of the bead) and the same temperature dependence (at the top of the bead) on current is observed. From the two kinds of curves produced it would seem that two different processes can occur depending upon the composition of the detector gases. We cannot say presently that this is evidence supporting decomposition on the surface of the bead or in the gas phase but that more than heat transfer properties must be considered in the TID.

The second major difference in the constant flow rate experiment between the two detector gas systems concerns selectivity. When H_2/air is used the selectivity remains nearly constant with bead current. This occurence is due to all compounds having similar response curves. The selectivity is much different when only air is used due to each compound (with different functional groups) having different slopes. (Tributylamine (NR_3) behaves differently than benzyl cyanide

(RCN) with air but their response in hydrogen/air is nearly the same). There is also a dependence on flow rates on selectivity with both detector gas systems. For air only the P-compound's selectivity (mole trimethyl phosphate/mole C_{17}) continually decreases contrary to the N-compounds. With H_2/air all compounds show a maximum value for selectivity (compared to the hydrocarbon). This behavior along with the other experiments from both detector gas systems suggest a very important point concerning the behavior of the TID. When air is used the response appears to be very compound (i.e. functional group) related, i.e., the environment in which the N or P atom is located in the molecule determines the TID response. For the H_2/air system this structure dependence no longer exists. All P- or N-compounds behave nearly in the same fashion.

In summarizing the H_2/air detector gas system we must consider the fate of these gases in the TID when they come near or in contact with the hot surface of the thermionic bead. The production of radicals from these gases occurs. This simple verification that water is produced can be performed by holding a cold finger over the exit port of the TID. In order for water to be formed the combustion of H_2 must take place. The combustion of H_2 involves the production of a number of radicals such as H, O, and OH. Among these radical species the OH radical has a sufficiently high electron affinity to surface ionize on the bead.

Even at low pressures in the mass spectrometric studies the OH^- species was observed. The background current is highest in the TID when the H_2/air system is used which may suggest that it is OH^- responsible for this background emission.

The influence of these radical species on any analyte introduced into the detector is unclear. The decomposition of any compound usually begins by the formation of a radical species. Decomposition can take place by pyrolysis (strictly a thermal process), combustion (gas phase or surface) or by a catalytic process on an appropriate surface. These radicals can influence any of these processes and as yet one process cannot be singled out to explain the TID response. We have shown that the H_2/air mixture can apparently influence the surface to affect peak shapes for P- and Cl-containing species. While this is true we cannot claim that decomposition of these compounds takes place solely on the surface. Coupling these possibilities with a thermal gradient along the bead complicates any explanation of the TID response. Low or high temperature processes can occur in both the gas phase or the surface. For example, the gas phase process of autoxidation (which leads to the production of radical intermediates) can occur at temperatures below 300°C. Surface processes such as pyrolysis or catalysis can occur at temperatures even below this, e.g., the pyrolysis of nitromethane which produces NO_2 (E.A. 4.0 eV) can occur at 200°C (149). At best, what can be said about the hydrogen/air system is that

decomposition is likely a combination of all three processes (catalysis, combustion, and pyrolysis). It should be said that regardless of the decomposition mechanism, the production of electronegative species in the H_2/air system is also more efficient than when N_2 is used as a detector gas as will be seen from the following discussion of this system.

d. Nitrogen in the GC-TID. Consider the role of the earlier detector gas systems. Air and H_2/air can produce chemically reactive species or modify the surface of the TID bead. The gases, regardless of the action on the response via the surface or the gas phase, appear to actively participate in the response mechanism. Nitrogen, contrary to these gases, is nearly inert and no such participation can be envisioned. The role of nitrogen is to maintain an inert environment on and around the TID bead. In this case, the behavior a compound exhibits is mainly due to its interaction on the various thermal regions of the thermionic bead. Here the pyrolytic behavior and the compound's electron affinity would be extremely important. The inertness of nitrogen would also suggest that the behavior of the GC-TID should parallel our results obtained in the MS-TID (no added gases). As will be shown from the following discussion this is typically the case.

Under constant current conditions the results using N_2 as a detector gas were similar to that of H_2/air. Each compound studied had a maximum value which nearly coincided with the maximum temperature obtained (Figure 64). As would be expected

no dependence on the gas is observed. Here, temperature should be the dominant factor determining the response of the TID using nitrogen.

Figure 73 shows the dependence of several compounds under constant flow rate conditions. The optimum flow rate corresponding the maximum in Figure 64 was chosen. It should be noted that the curves are linear similar to the air-only case discussed previously. In addition the magnitude of the response is on the same order as that of the GC-TID when air is used. At low currents the response parallels the electron affinity. That is tetracyanoethylene>dinitrobenzene>chloronitrobenzene which have respective electron affinities of 66.5, 43.5, and 27.5 kcal/mole. The response of these compounds also parallel the total ion intensities obtained in the MS-TID. For the most part, at low currents with the mass spectrometer, molecular anions or ionic species which have not undergone substantial decomposition (M-H, M-NO, and M-OH) are observed. When the current is increased this no longer holds true and species such as CN^- begin to increase in the mass spectra. Similarly in the GC-TID when the current is increased the response may no longer depend upon the electron affinity as can be seen for chloronitrobenzene. At higher currents this compound shows a greater response than dinitrobenzene. The selectivity using the nitrogen mode of the GC-TID depends upon which current is used. At low currents response parallels the electron affinity of the molecule. At high currents response depends upon how decomposition takes place to

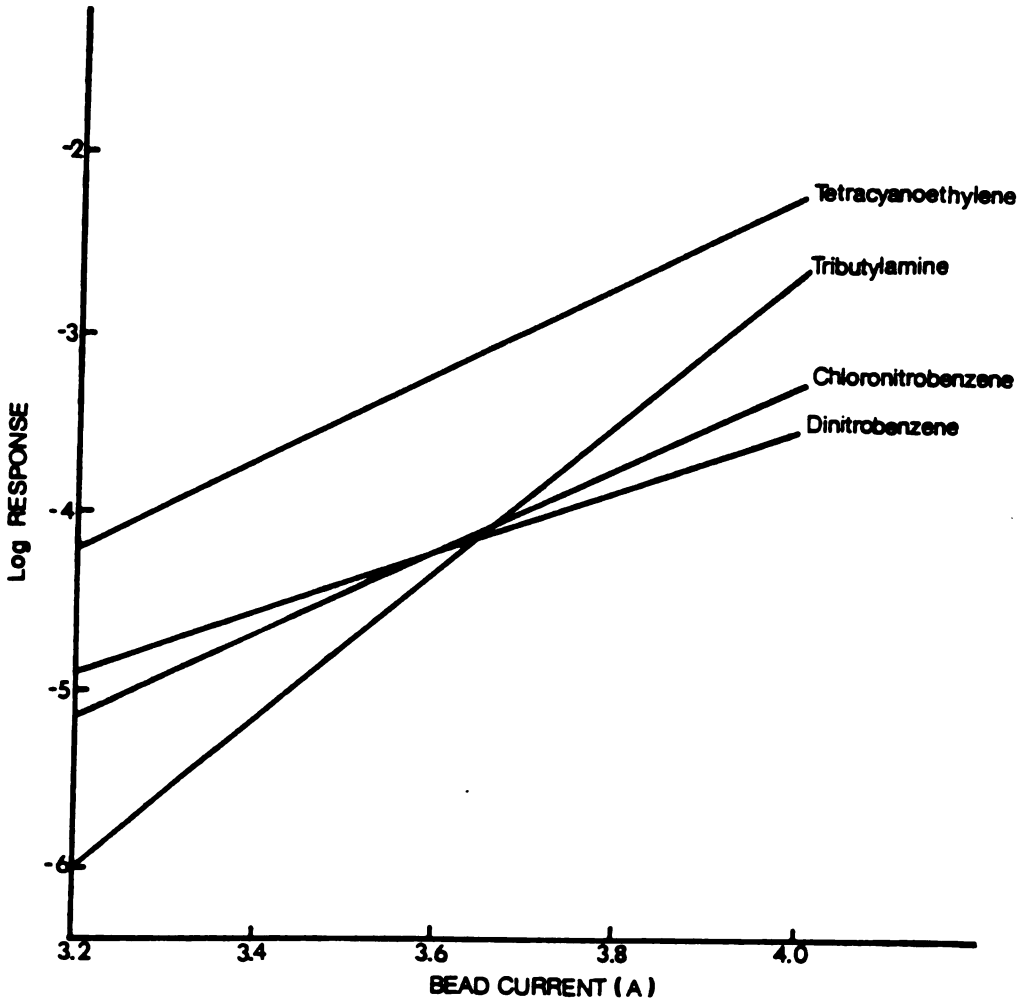


Figure 73. Response as a Function of Bead Current For Several Test Compounds With a Constant 160 ml/min N_2 Flow Rate.

produce fragments with high electron affinities. Hydrocarbons can elicit a response at very high currents and it has been shown that two isomers of octane (n-octane and iso-octane) behave differently in this mode of the GC-TID.

The nitrogen only mode of the GC-TID can be used to increase the selectivity between various analytes. At low currents responses are only obtained for compounds which have a high molecular electron affinity. In this case the selectivity of the GC-TID can be very large (e.g. substituted nitrobenzenes compared to hydrocarbons). When the current is increased the molecular structure and any functional groups on the molecule determine how it will decompose and to what species. If these fragments have a favorable electron affinity they will surface ionize and give a response. Therefore the response is decomposition dependent. Hydrocarbons can have an observable response here since supposedly upon decomposition can form species such as C_n and C_nH which have high EA's.

We have discussed our results in the two systems (the mass spectrometer and the GC) under a number of various conditions. The following question attempts to coordinate these results and make conclusions as to the mechanism of the gas chromatographic thermionic ionization detector.

C. What are the Similarities Between the MS-TID and the GC-TID?

We believe that presently there would be no argument as to the ionization process within the TID. It appears that surface ionization can be the only possibility over any proposed gas phase ionization mechanism. Thermodynamically, gas phase ionization is improbable at the normal operating temperatures of the GC-TID. The pertinent question is how a molecule behaves prior to ionization? Does the molecule decompose and if it does where; the gas phase or the surface? The following is a summary of the results obtained here.

A concern between the two studies is the pressure differential of the mass spectrometer and the GC. The pressure within the mass spectrometer (<1 torr) favors surface phenomena since a high pressure region surrounding the thermionic bead cannot be formed. We have shown the responses of a number of N-, P-, and Cl-containing compounds on the hot alkali aluminosilicate material within the mass spectrometer. These studies, by themselves, suffest that a surface-only (ionization and decomposition) mechanism can occur.

We have studied, both in the mass spectrometer and in the GC, the effects of adding gases to the hot alkali aluminosilicate material. The dependence of bead temperature upon flow rate is an important point to consider when devising a response mechanism. It was shown that this dependence is independent upon the gas used. As is seen for a number of compounds in all

three detector gas systems, the response parallels this temperature dependence. We propose a thermal gradient along the thermionic bead. At the bottom of the bead, directly above the flame tip, the temperature is most likely at a minimum. The thermal gradient should have the same dependence on gas flow rate as is seen at the top of the bead. For phosphorus or chlorine containing compounds using air as a detector gas the response is atypical when compared to all other systems. Here it was shown that air has pronounced effects on these compounds' responses and the results suggested that air can modify the surface of the TID bead.

The mass spectrometric results indicated that air can effect a compound's response by increasing the total ion intensity (presumably by modifying the surface) and by participating reactively with the compound on the surface. The same compounds (P- and Cl-compounds) which responded in this fashion behaved differently than the N-compounds in the TID. Low flow rates of air (which we believe increases the concentration of O_2 to the surface) and the adsorptive nature of P- and Cl-compounds suggest that a surface-only mechanism can be in operation.

All compounds showed a linear dependence with bead current at a constant air flow rate. It appears that the slope of these lines indicate that the response in the TID with air is compound dependent. Compounds with unlike functional groups had different slopes, however, those having a common functional group had the same slope.

Similarities between the MS and GC experiments also occurred when nitrogen was used as the detector gas and when no gas is added to the mass spectrometer. This is not totally unexpected due to the inertness of nitrogen. Under constant current conditions the behavior parallels the temperature dependence on flow rate. Under constant flow rate conditions the behavior was similar to that of the air experiment. The sensitivity of the compounds studied was similar in both the MS and the GC and appeared to follow the compound's electron affinity. At higher temperatures, decomposition of the compound is more prevalent and behavior in both the GC and MS depend upon the efficiency of decomposition, i.e., the molecule's electron affinity becomes less of a factor. Using nitrogen in the TID also indicates that a surface-only mechanism can be used to explain the response.

The H_2/air system is the most complicated. In the mass spectrometric experiment, OH^- was observed at high bead currents. This anion may be partly responsible for the background in the TID. It is likely that radicals containing O and H do occur in the TID. These radicals can actively participate in the decomposition of a molecule. We cannot compare the MS results with those obtained in the TID, however, it can be said that the higher pressures in the GC are necessary for the response in this particular mode. The sensitivity of the H_2/air system is by far the greater than any other detector gas system. The selectivity of N- and P-compounds is high when compared to hydrocarbons. The selectivity amongst two nitrogen compounds or two phosporus

compounds is much less than that of the other two detector gases. Under constant flow rate conditions it was observed that the curves for all nitrogen and phosporus compounds are similar and nonlinear. Apparently in this detector gas system a N- or P-compound must decompose into fundamentally similar fragments which can surface ionize. It is unclear from these studies whether this process occurs on the surface of the bead or in the gas phase. It is evident, as was observed for the P-compounds of malathion and methyl parathion, that interactions with the surface do occur but as to what extent these interactions account for the entire response cannot be determined here. It is clear that with the H_2/air system additional information is needed to pinpoint the location of decomposition in the TID. Continuing investigations in this direction is necessary to answer these questions.

APPENDIX

APPENDIX A

The K^+IDS spectra in this appendix are those which do not appear in the main body of this work. They are included here to serve as a guide in future K^+IDS work. The spectra may not be the optimum that can be obtained, but are representative of the compound. No attempt is made here of identifying the major peaks which appear in the spectra. The spectra were obtained at heating currents of 2.5 A or higher. The bead bias was within the K^+ addition window.

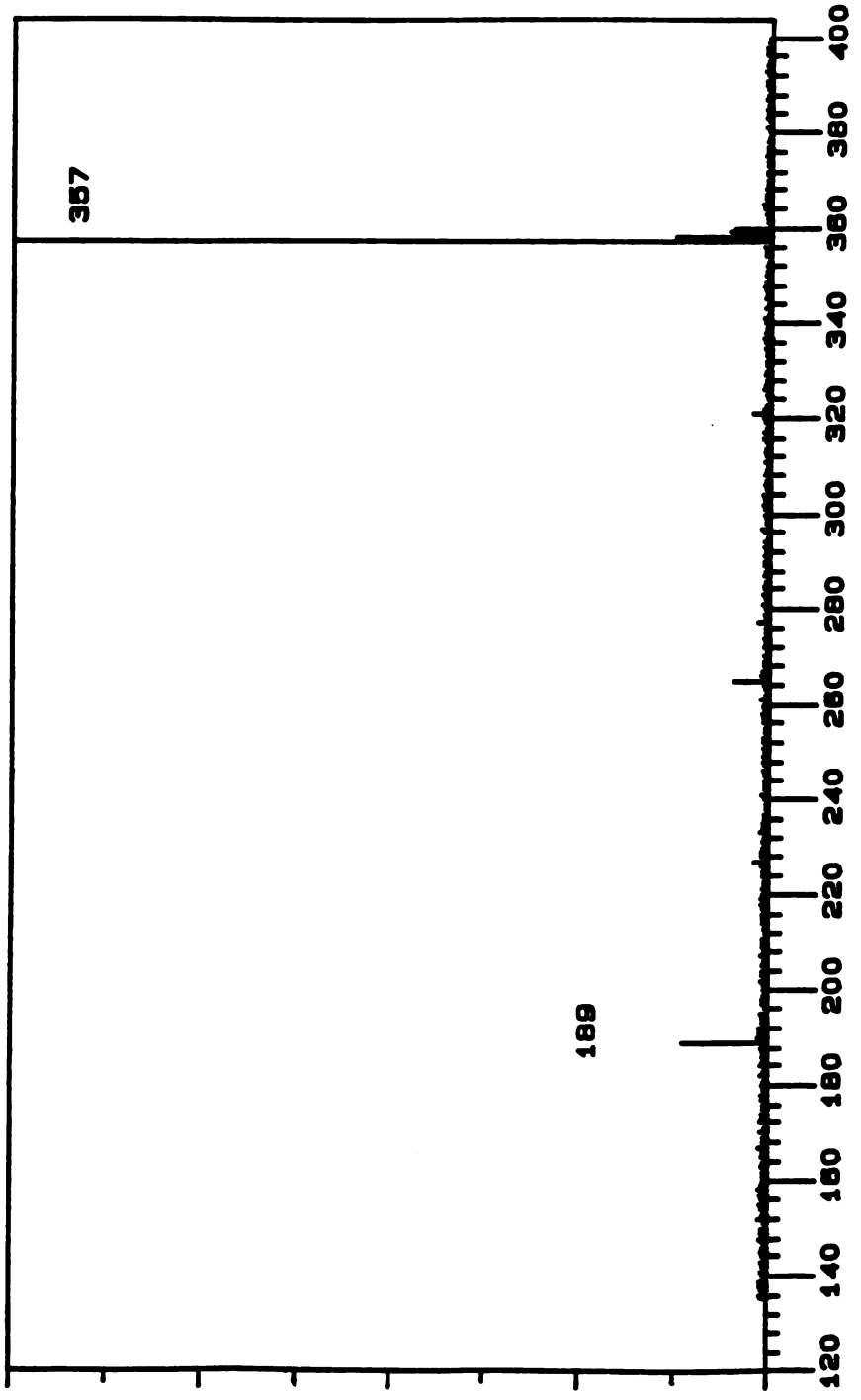


Figure 74. K^+IDS Spectrum of Phenolphthalein.

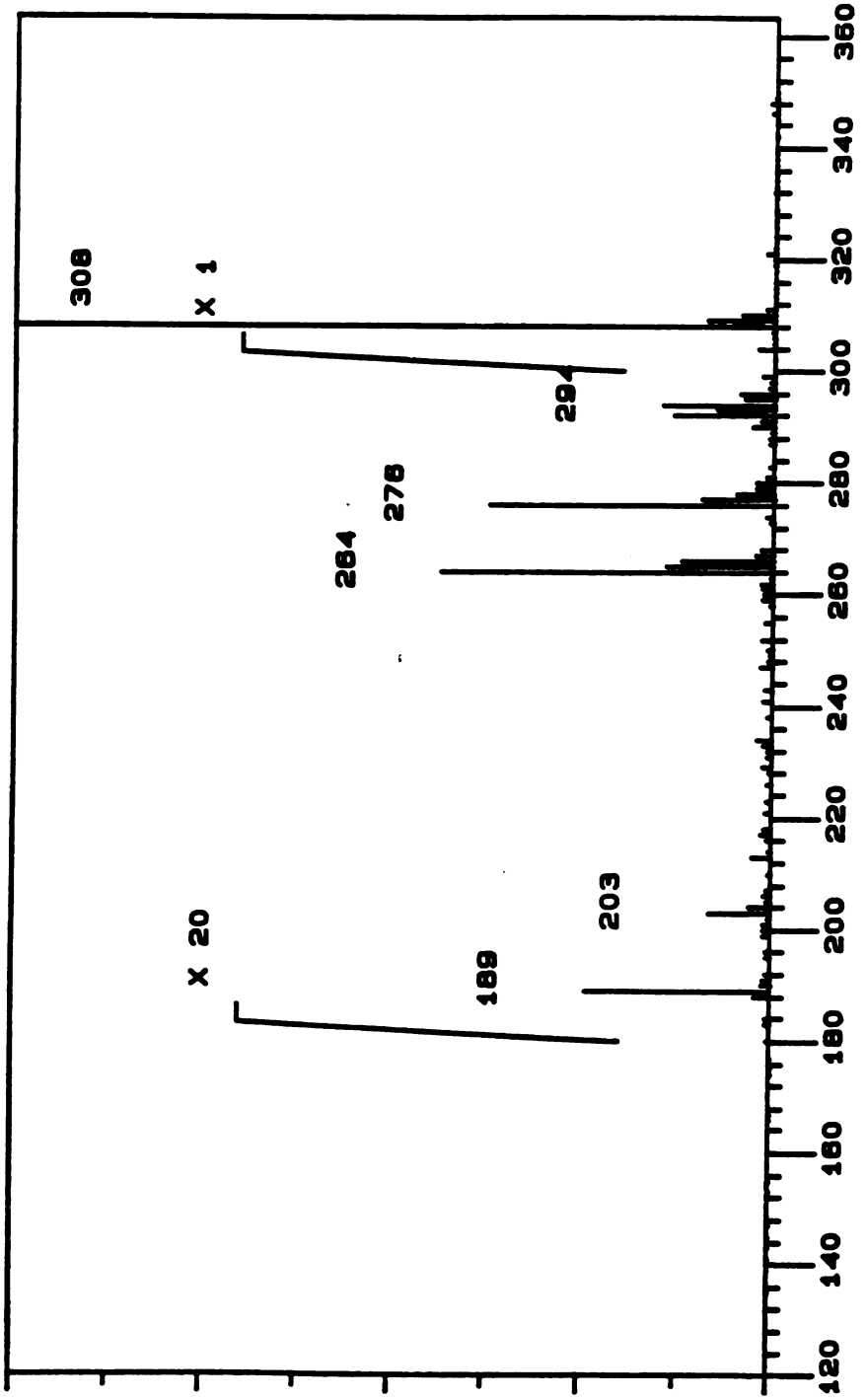


Figure 75. K^+IDS Spectrum of Methyl Red.

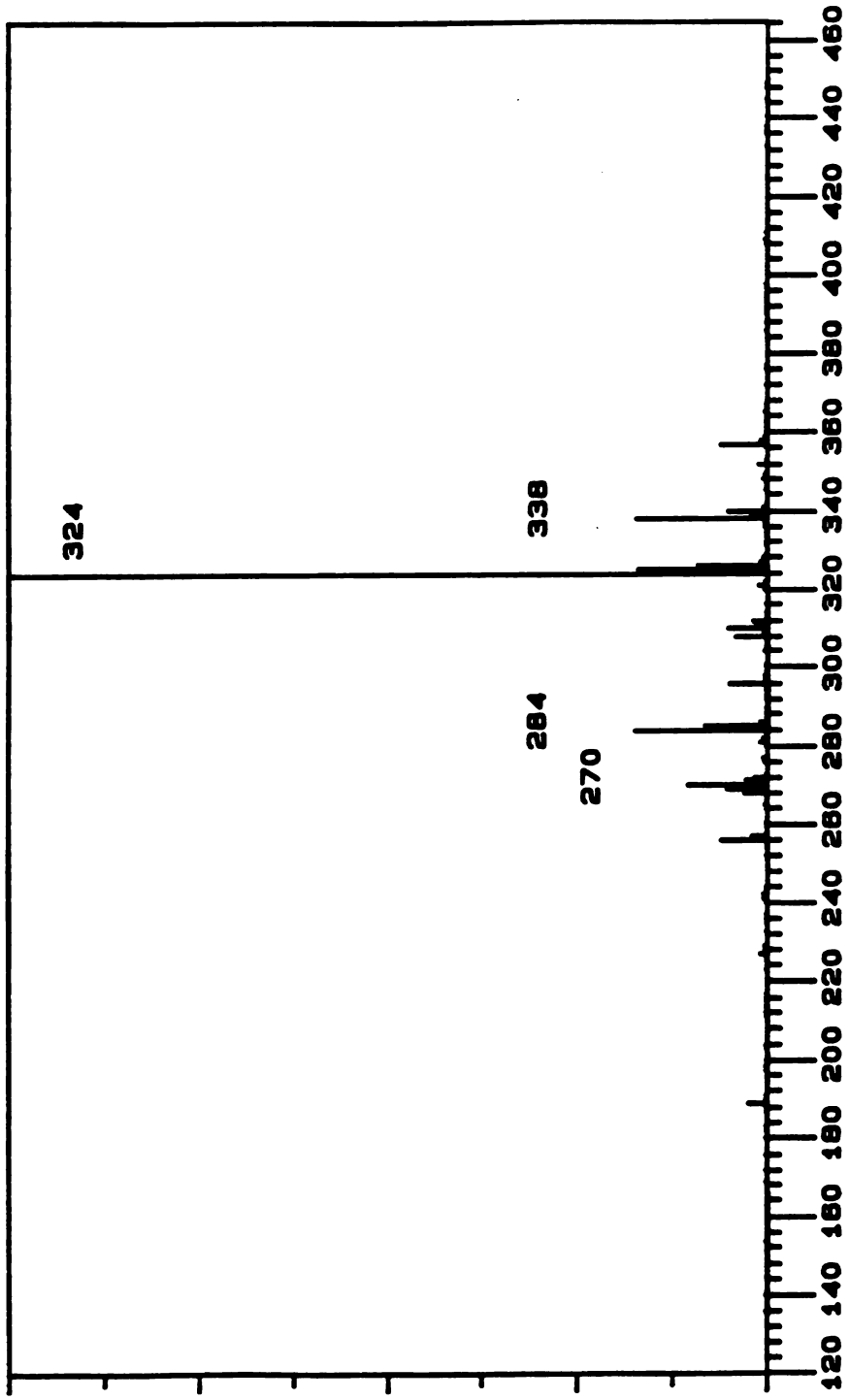


Figure 76. K^+IDS Spectrum of Methylene Blue.

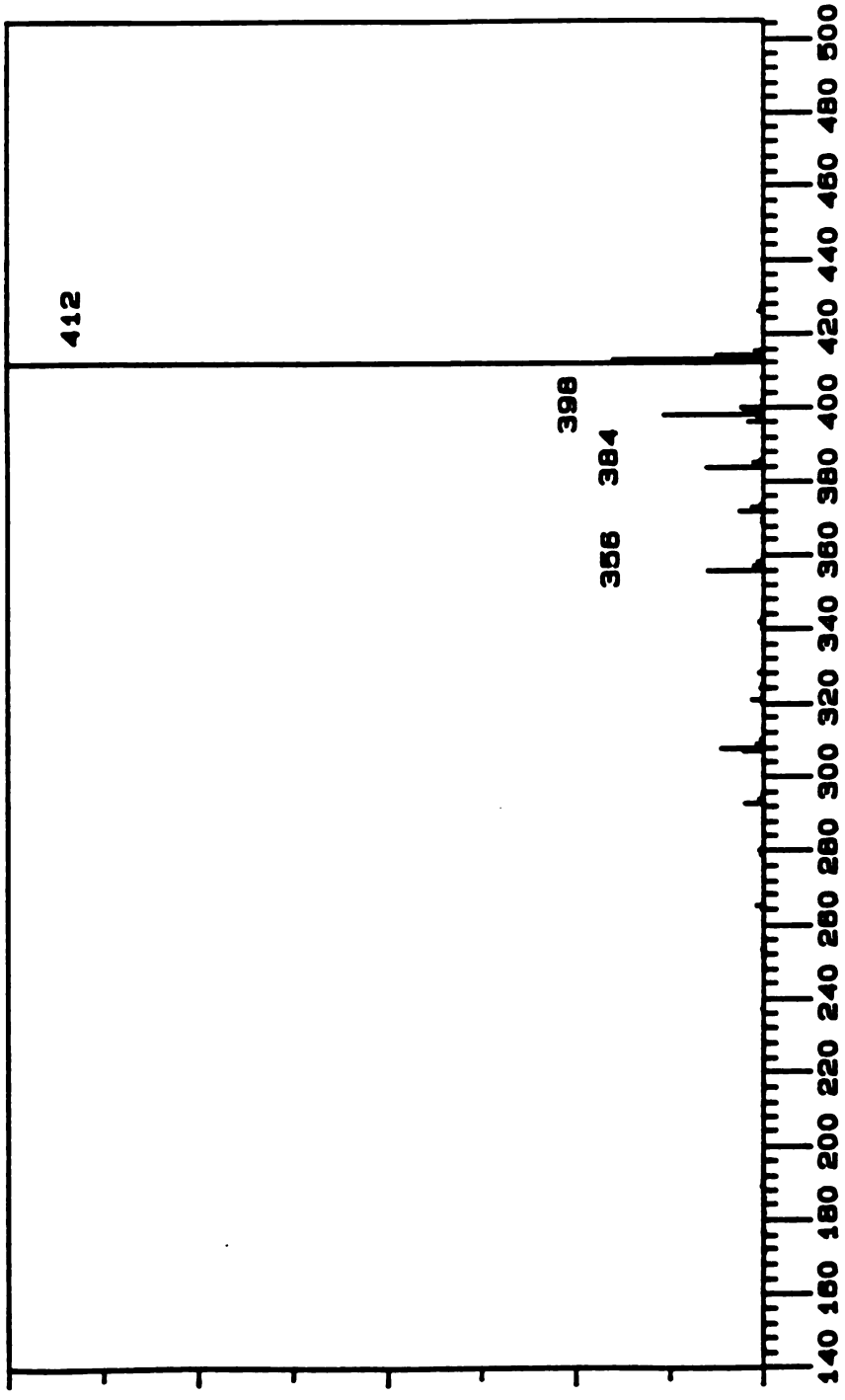


Figure 77. K^+IDS Spectrum of Methyl Violet.

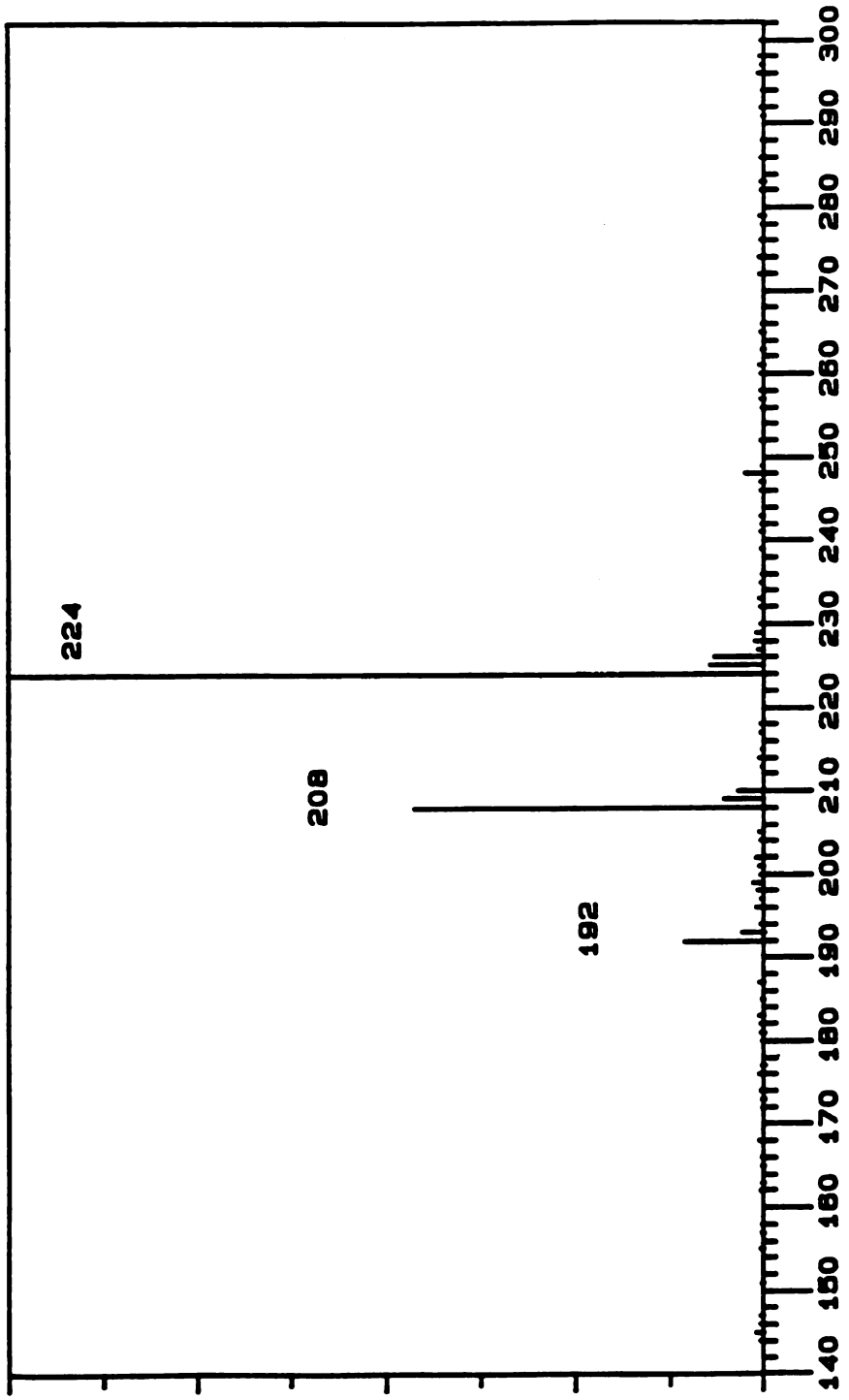


Figure 78. K^+IDS Spectrum of Martius Yellow.

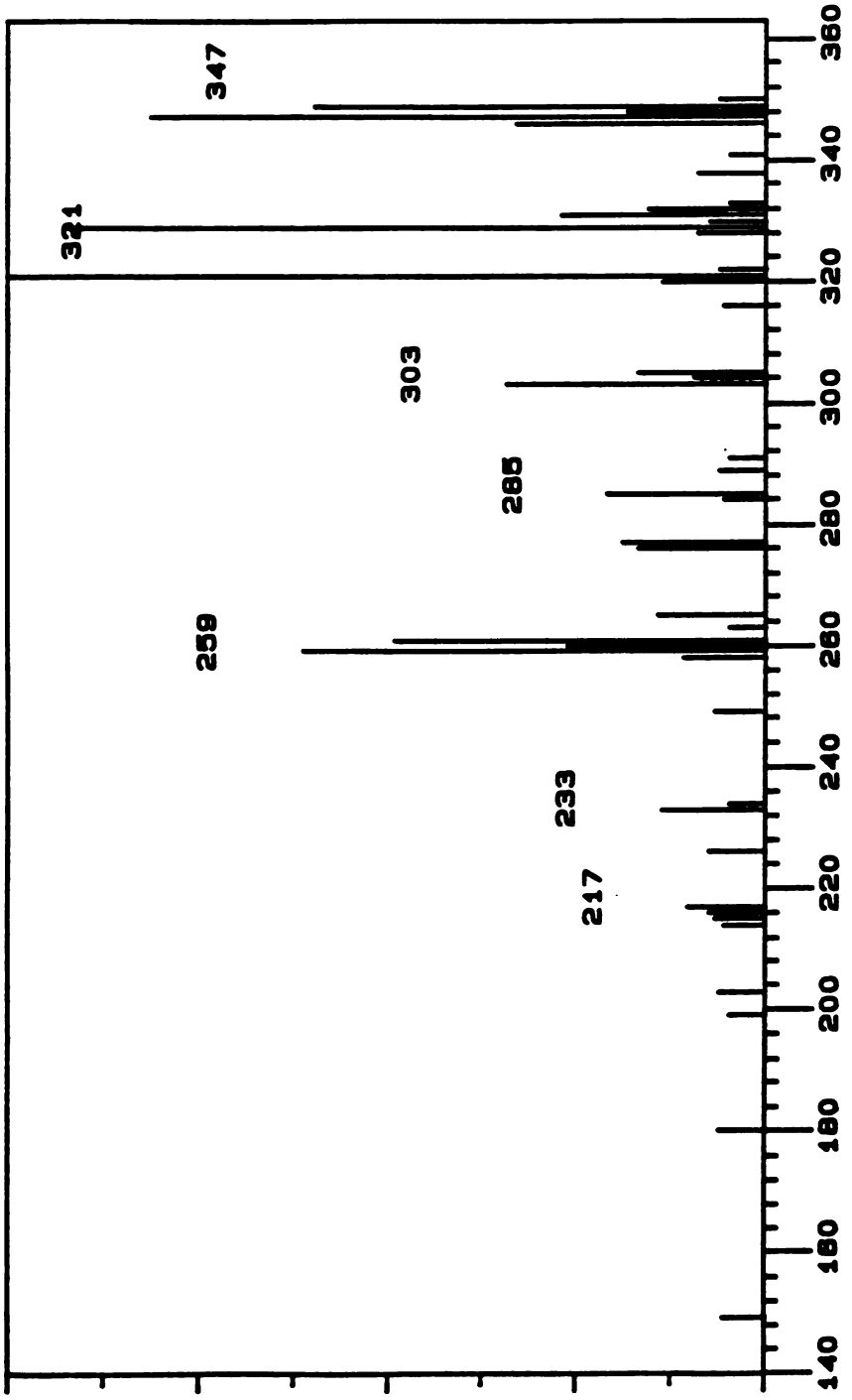


Figure 79. K^+IDS Spectrum of Murexide.

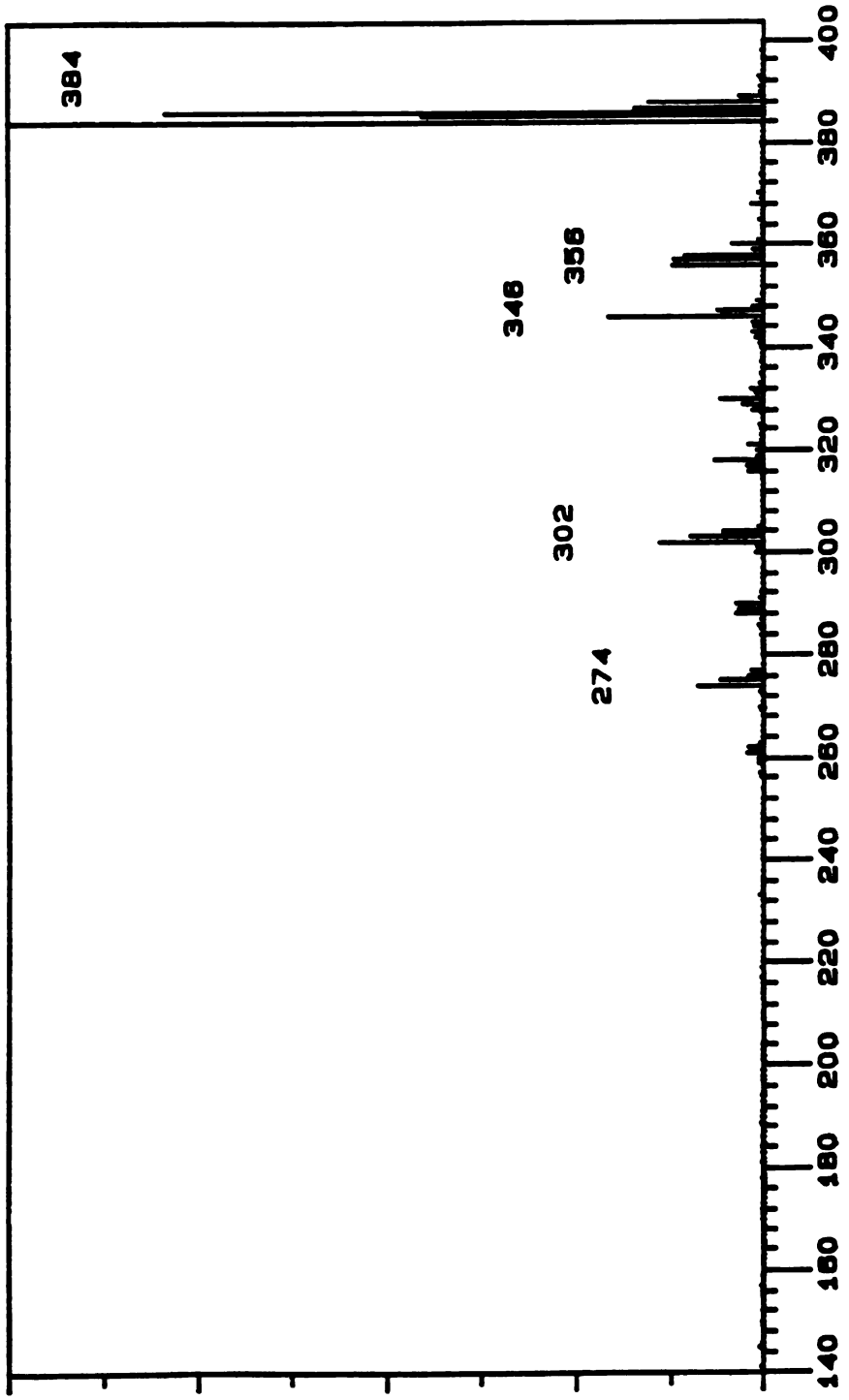


Figure 80. K^+IDS Spectrum of Nile Blue A.

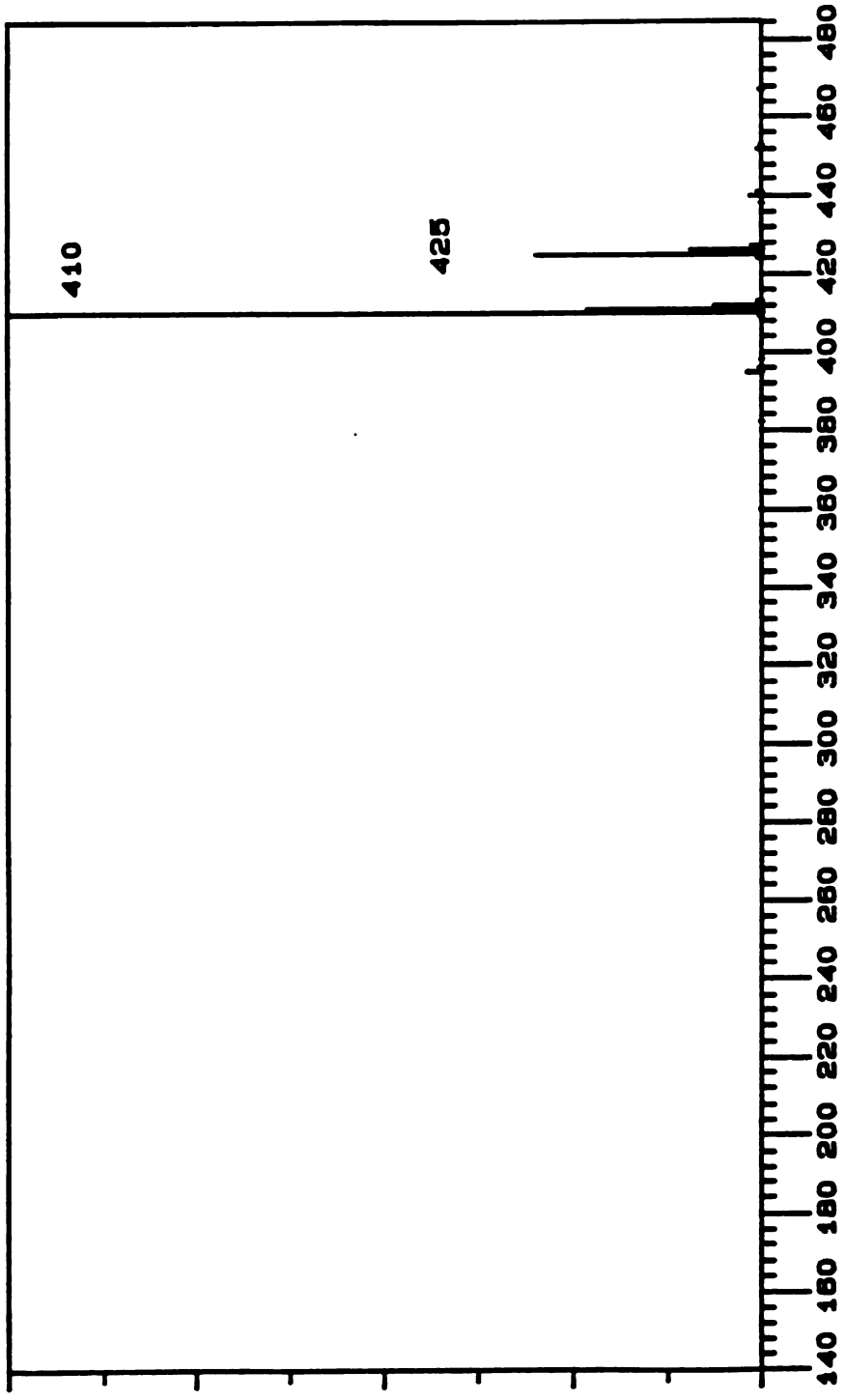


Figure 81. K^+IDS Spectrum of Magdala Red.

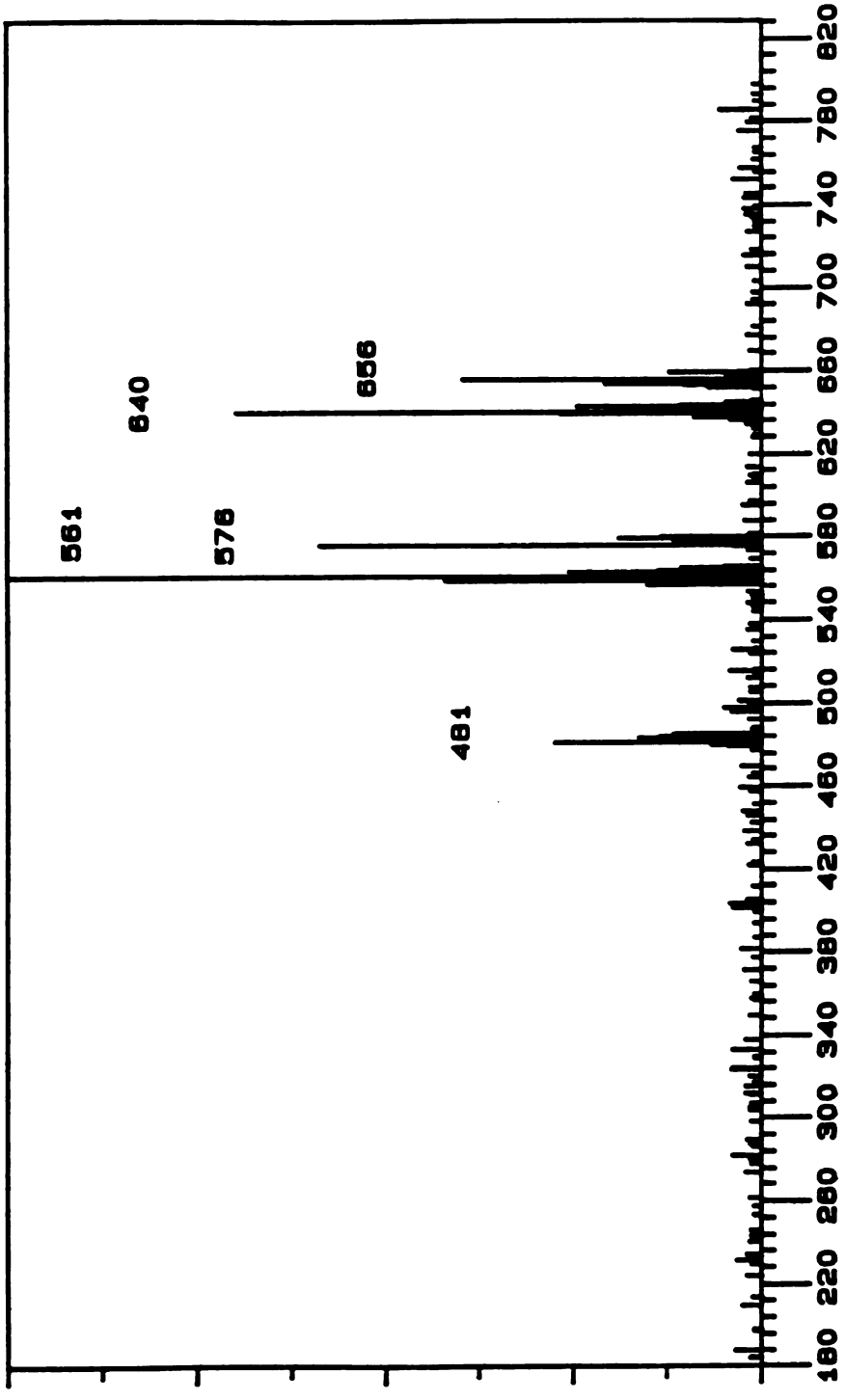


Figure 82. K^+IDS Spectrum of Bromocresol Green (Na Salt).

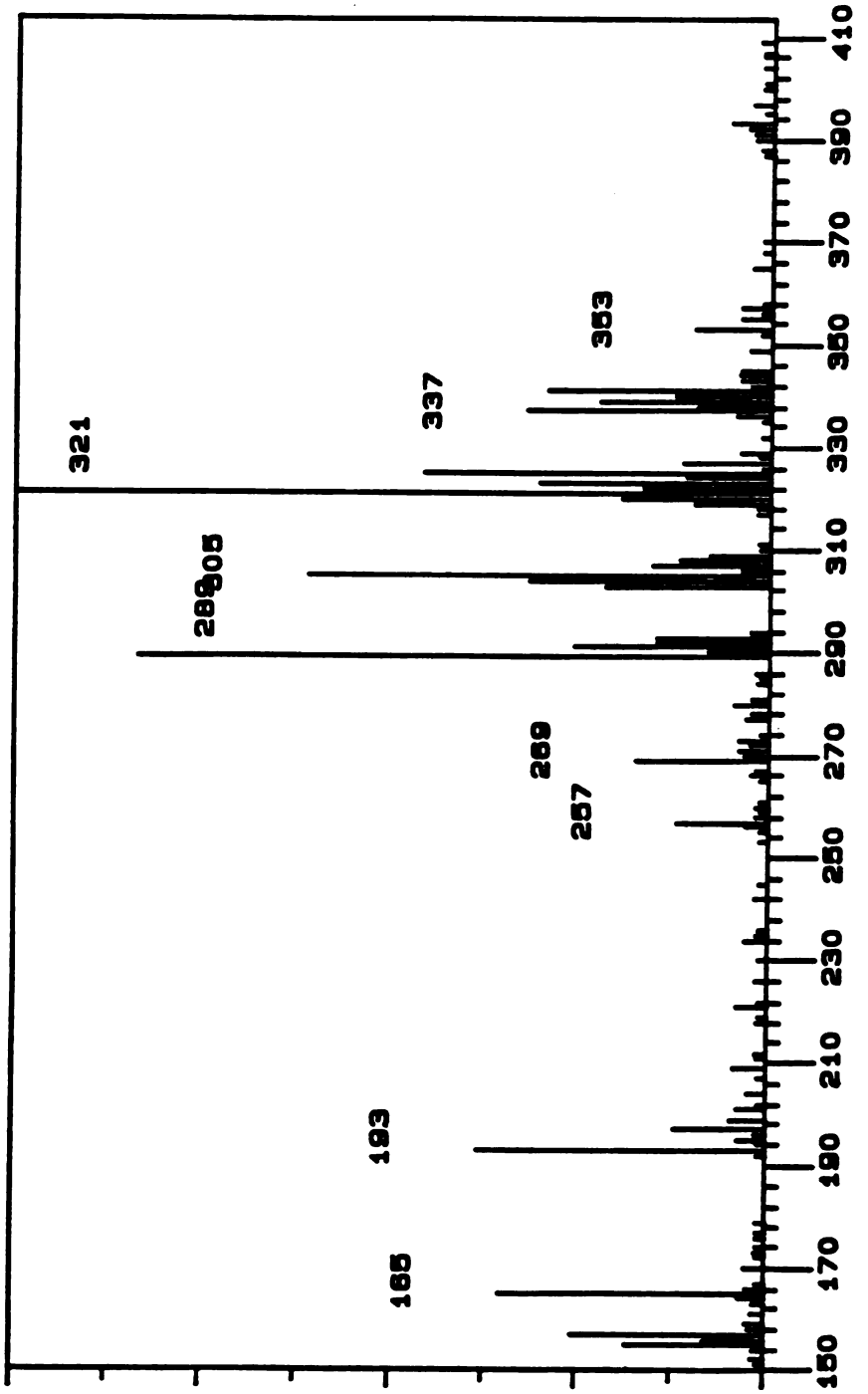


Figure 83. K^+IDS Spectrum of Chlorophenol Red.

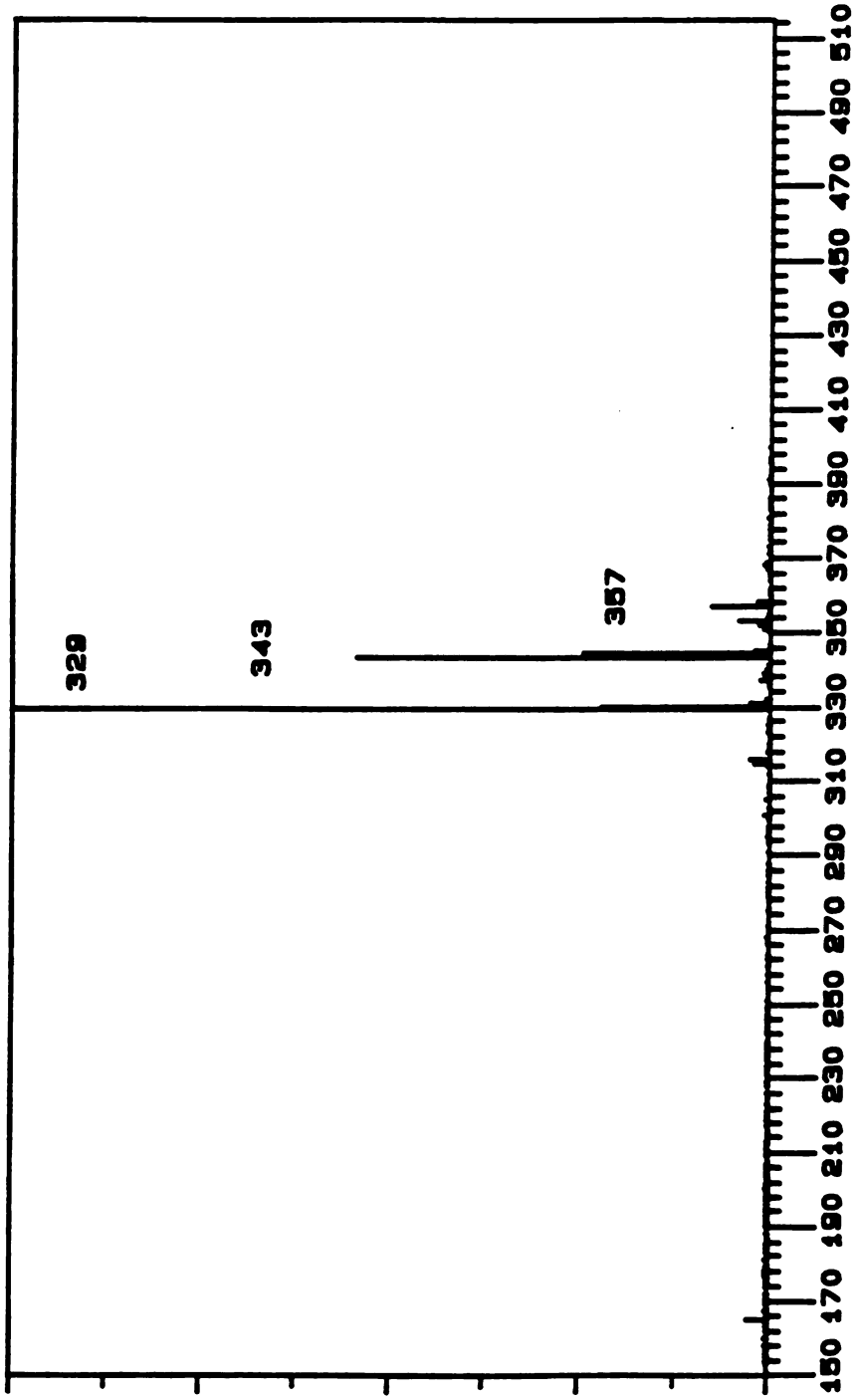


Figure 84. K^+IDS Spectrum of Phenosafranine.

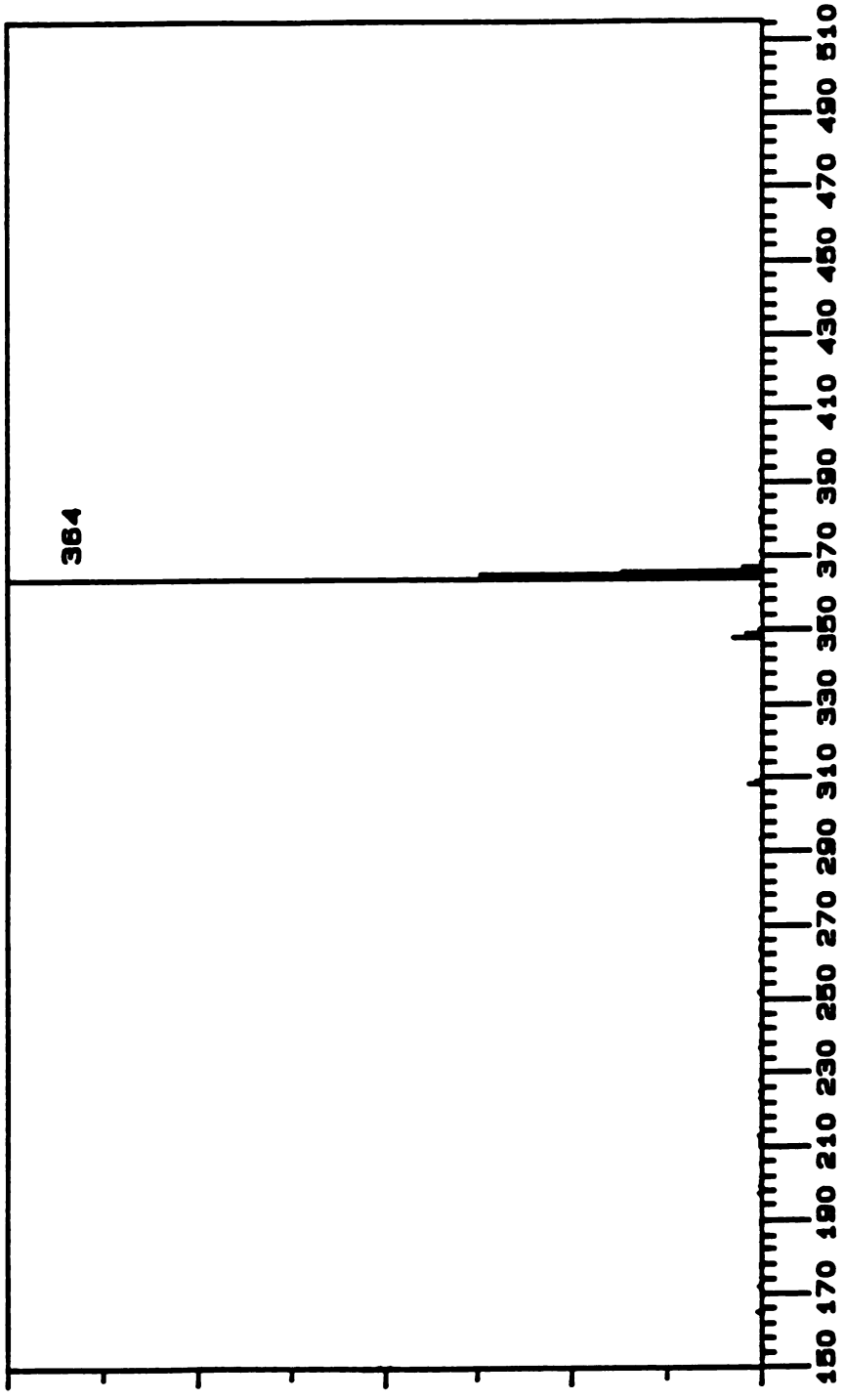


Figure 85. K^+IDS Spectrum of Quinine.

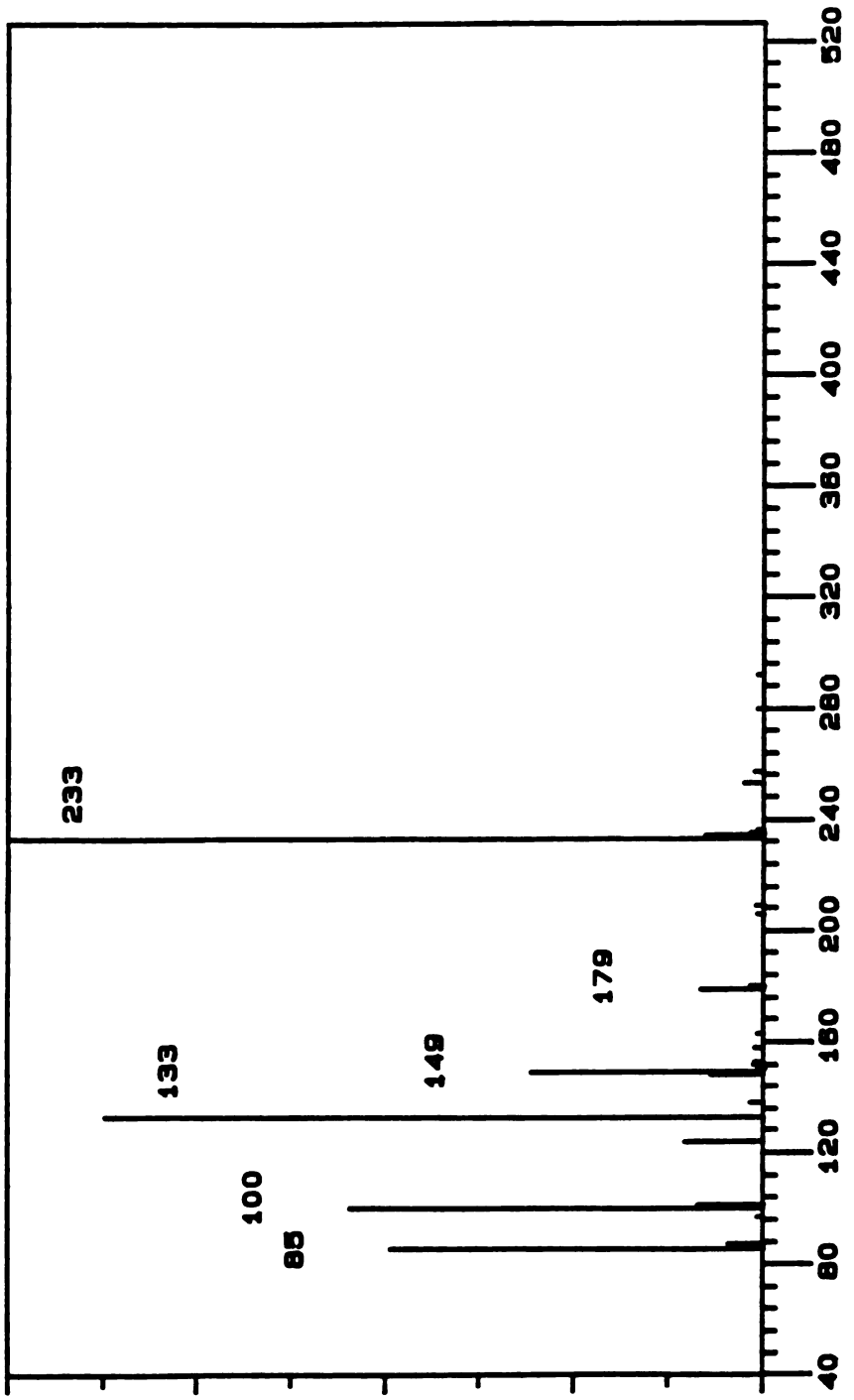


Figure 86. K^+IDS Spectrum of Caffeine.

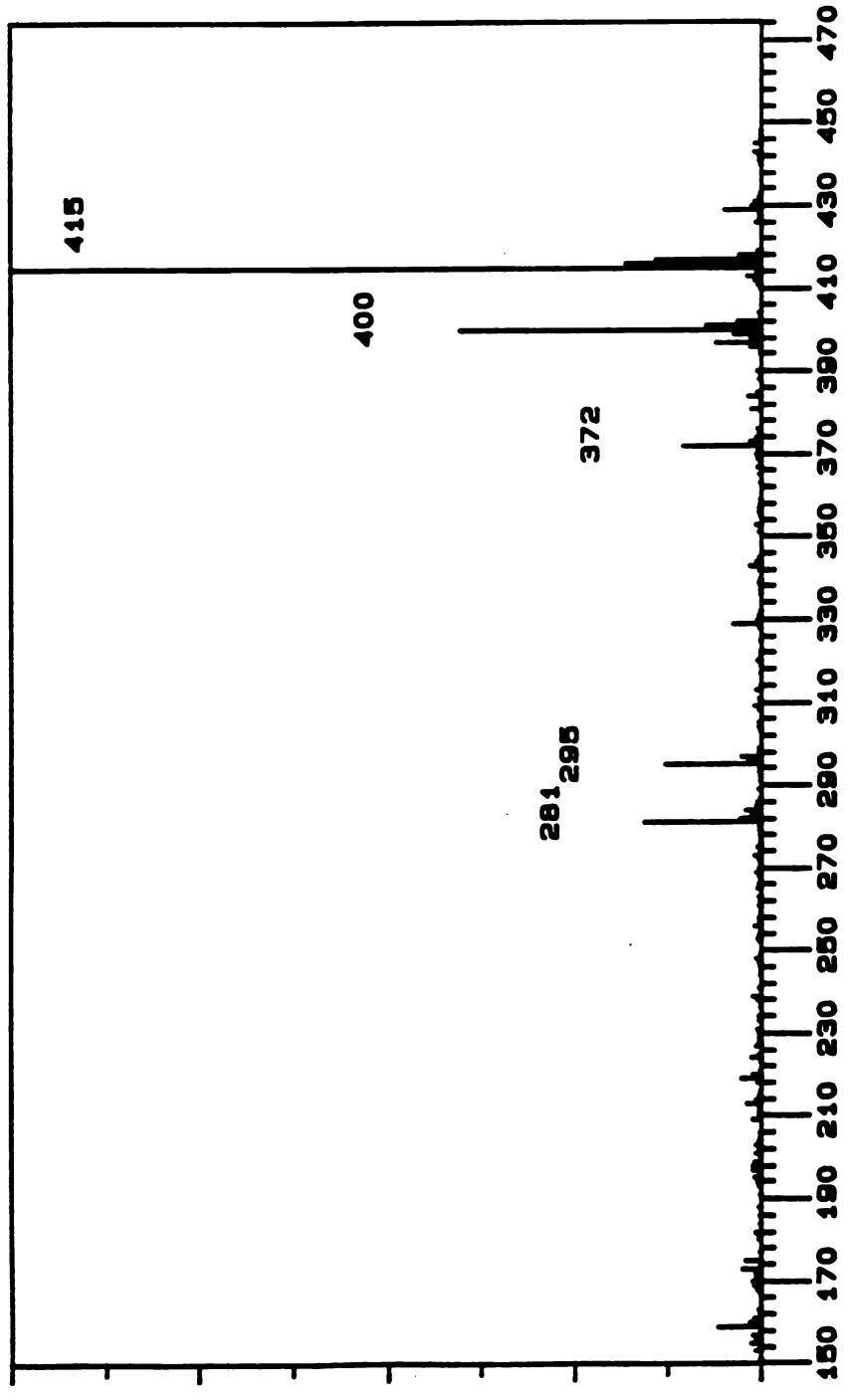


Figure 87. K^+IDS Spectrum of Riboflavin.

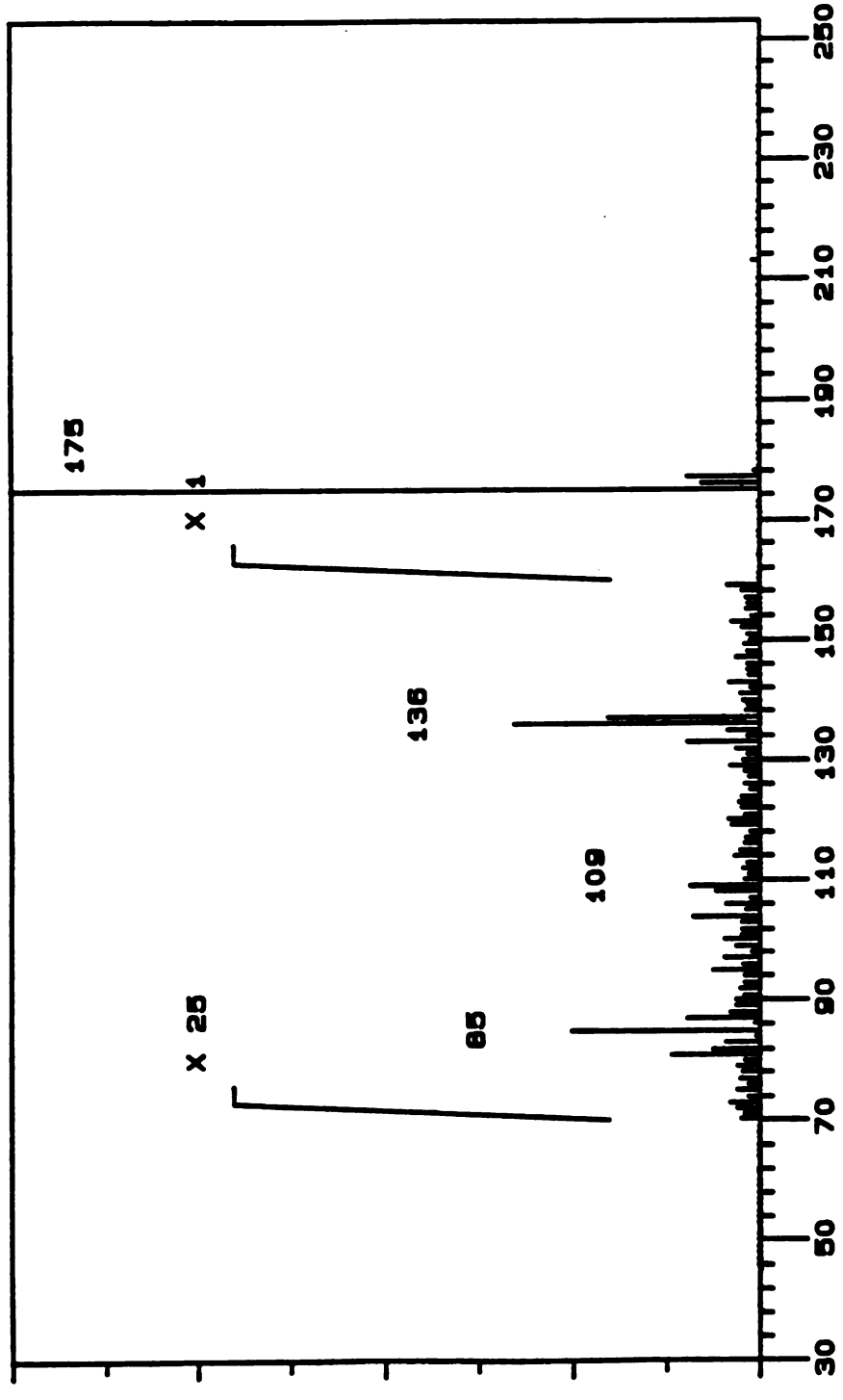


Figure 88. K^+IDS Spectrum of Hypoxanthine.

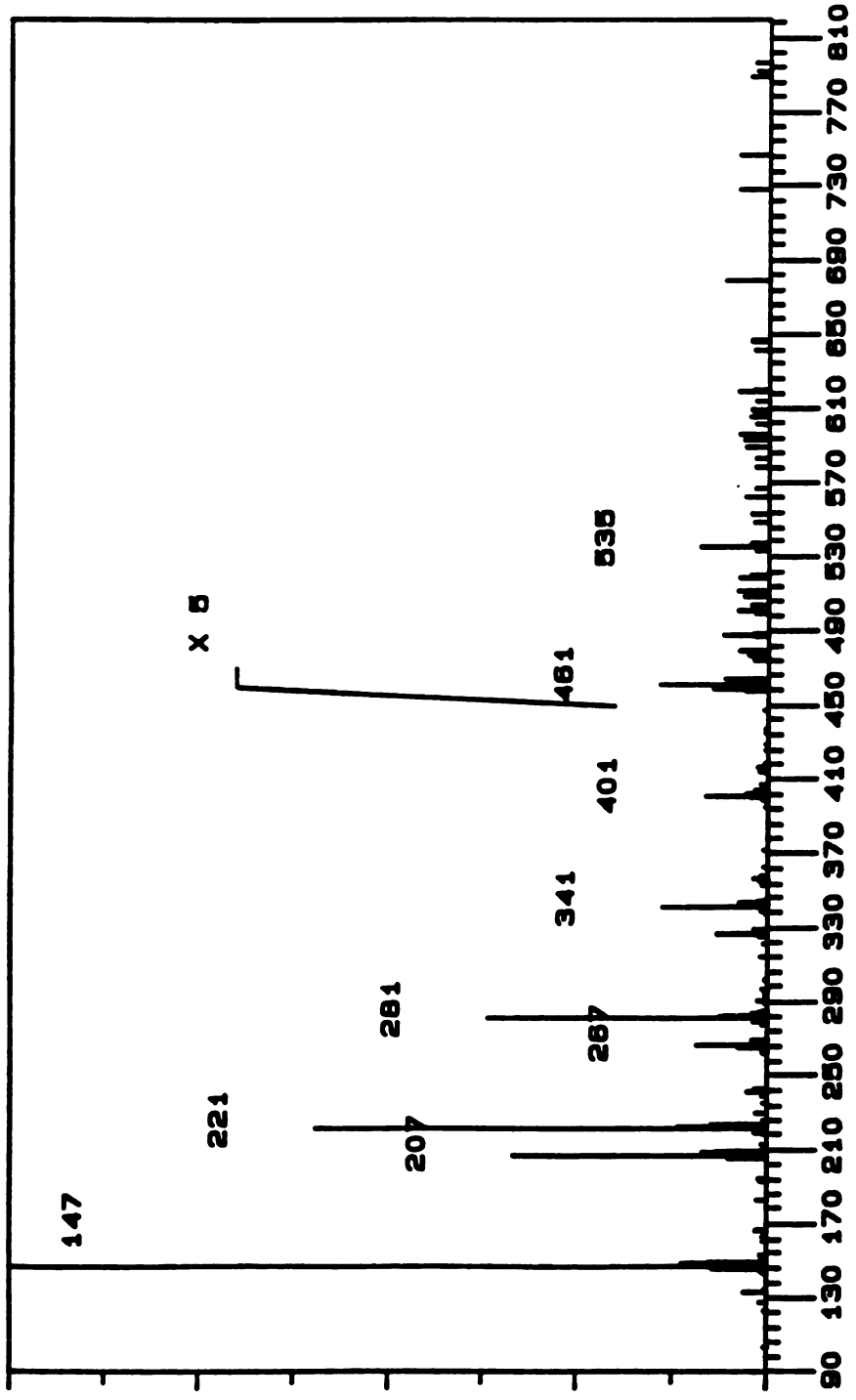


Figure 89. K^+IDS Spectrum of F-50 (Methyl Silicone).

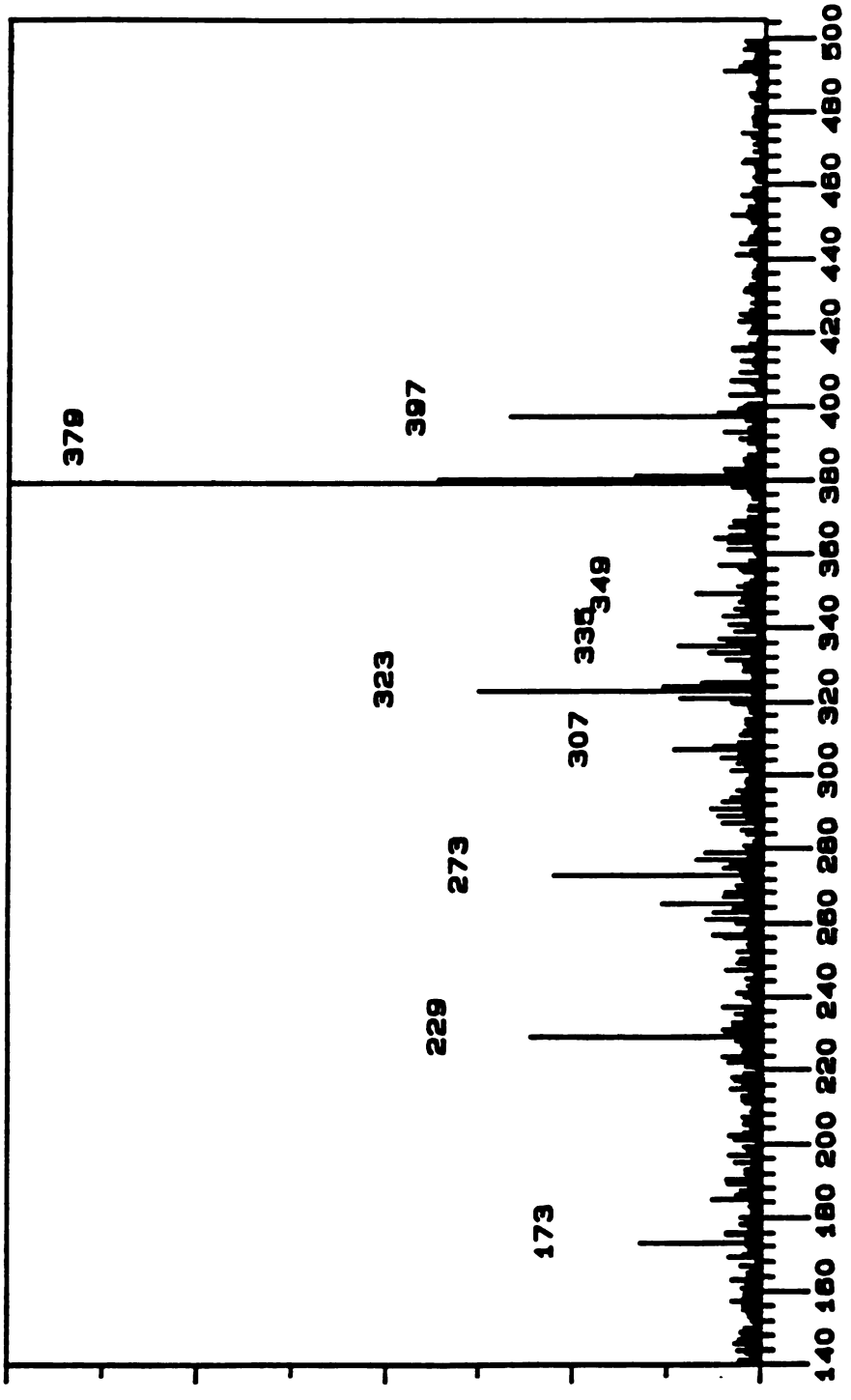


Figure 90. K^+IDS Spectrum of EPON 1001.

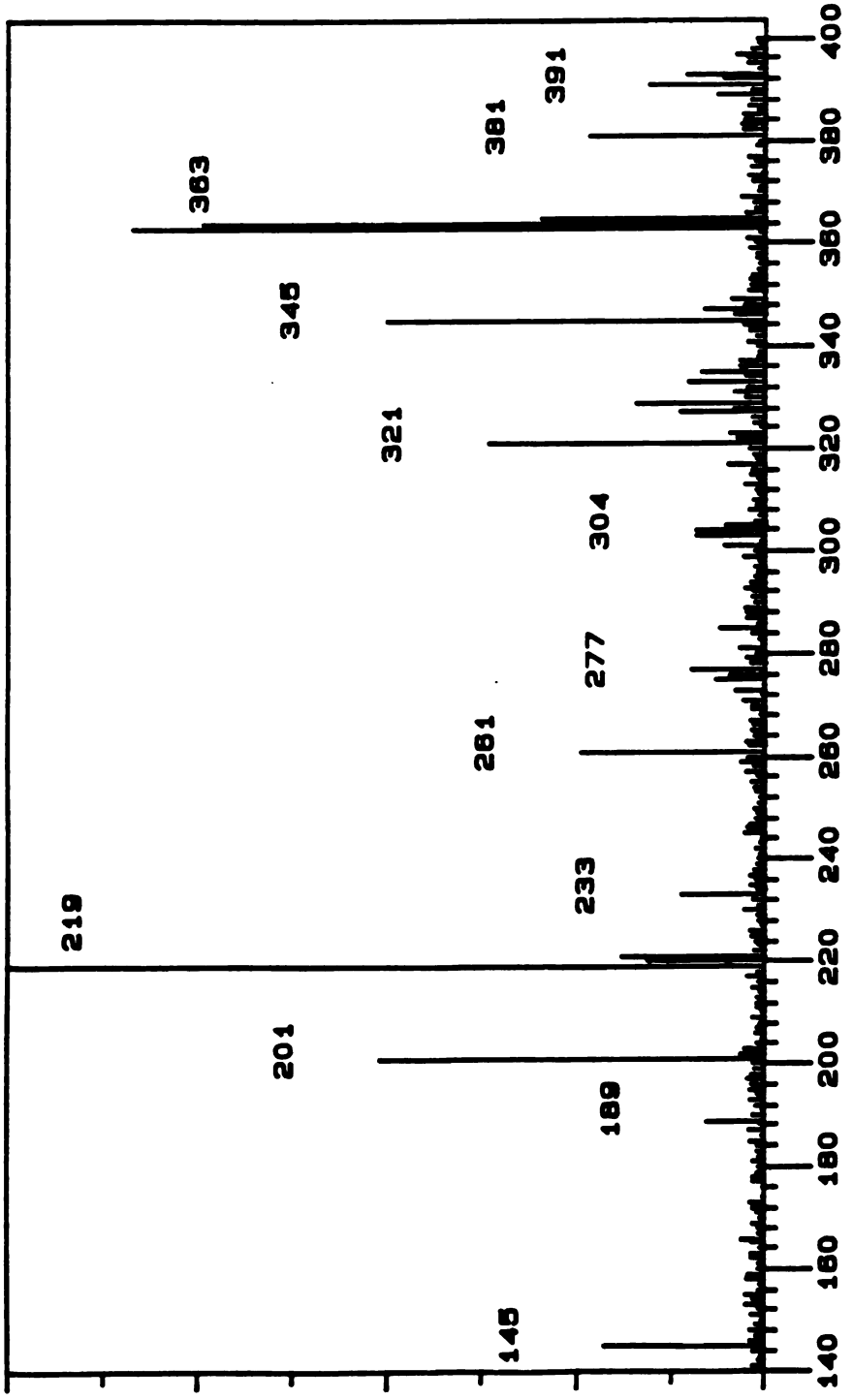


Figure 91. K^+ IDS Spectrum of Maltose.

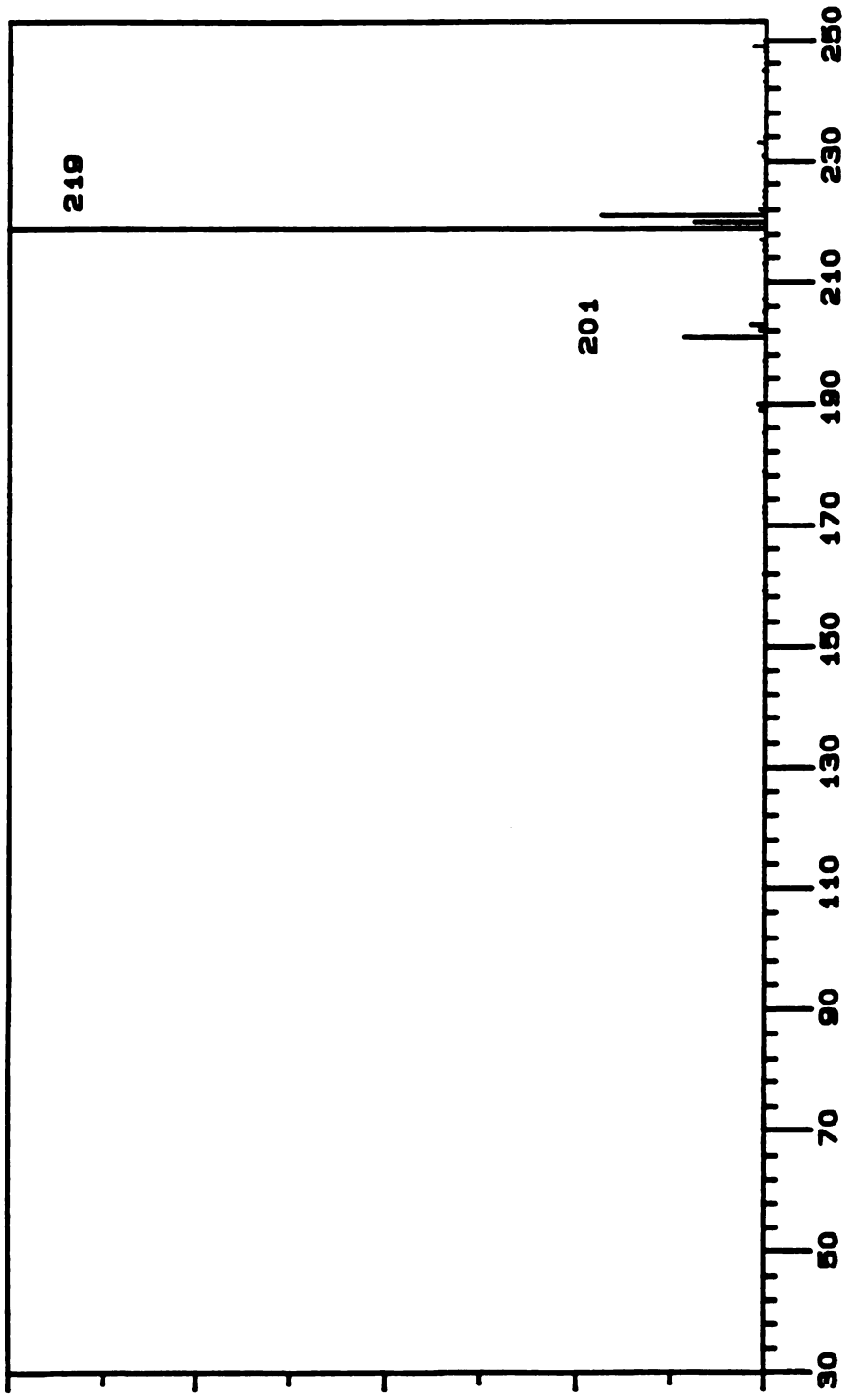


Figure 92. K^+IDS Spectrum of Fructose.

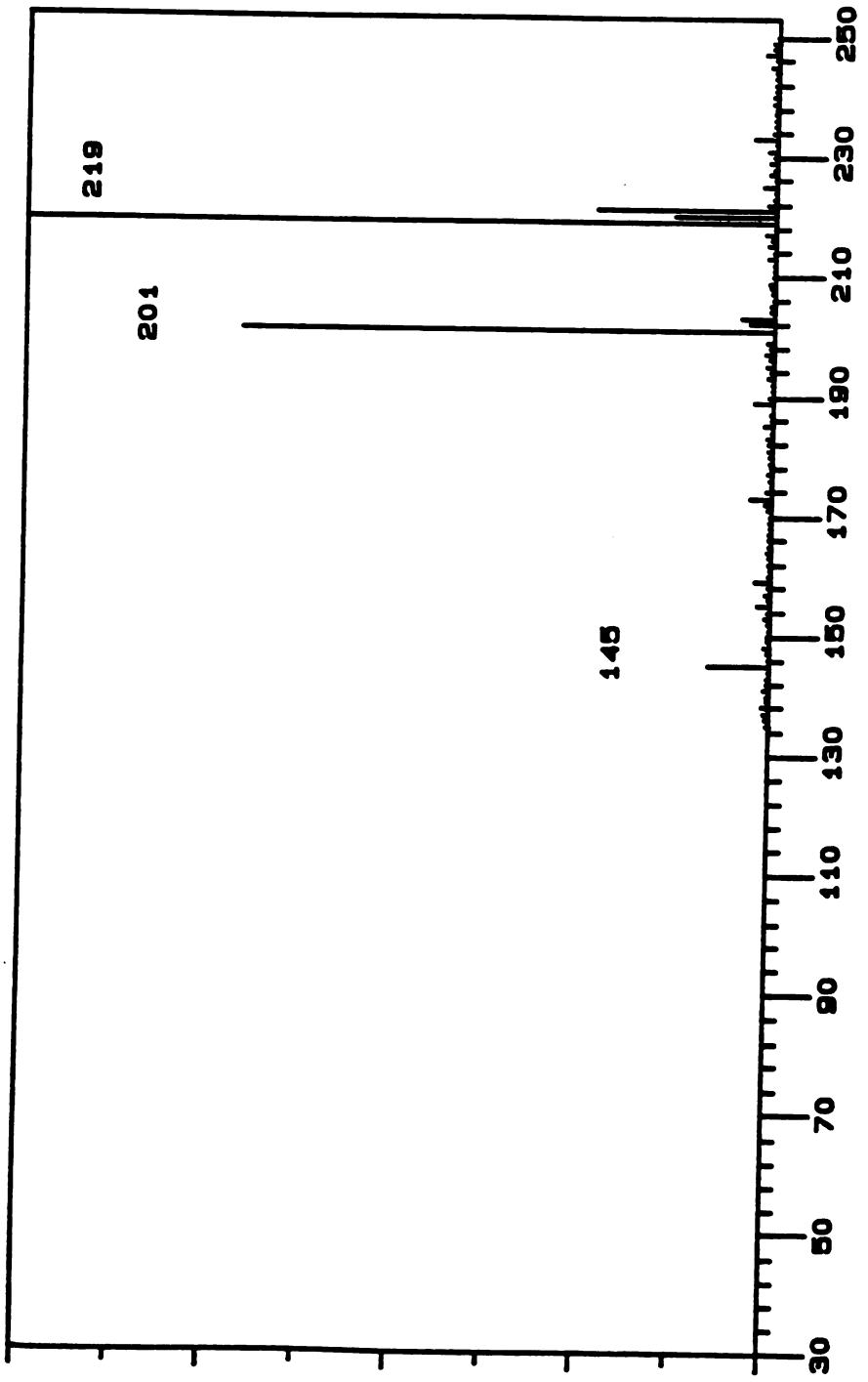


Figure 93. K^+IDS Spectrum of Lactose.

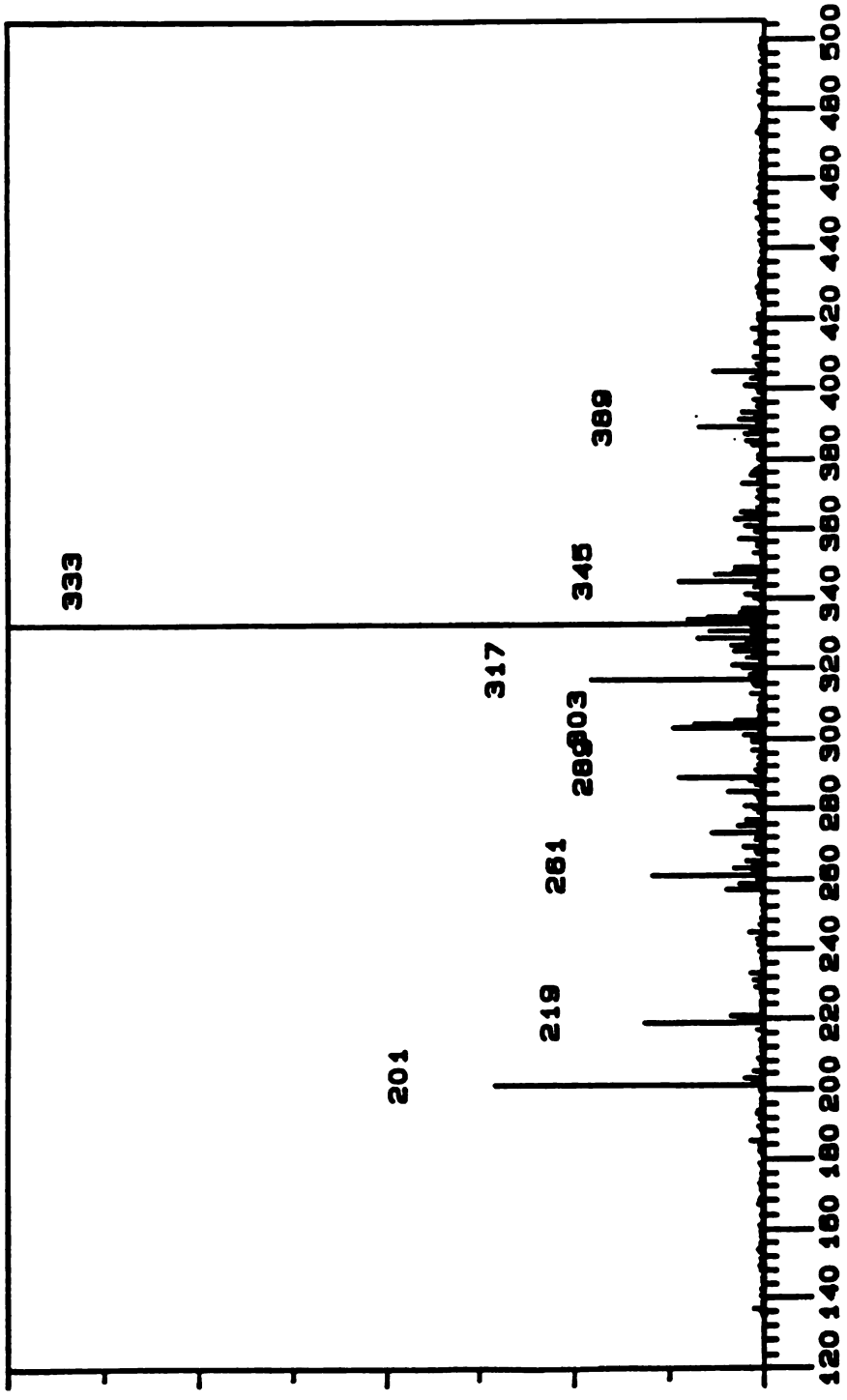


Figure 94. K^+IDS Spectrum of Gum Arabic.

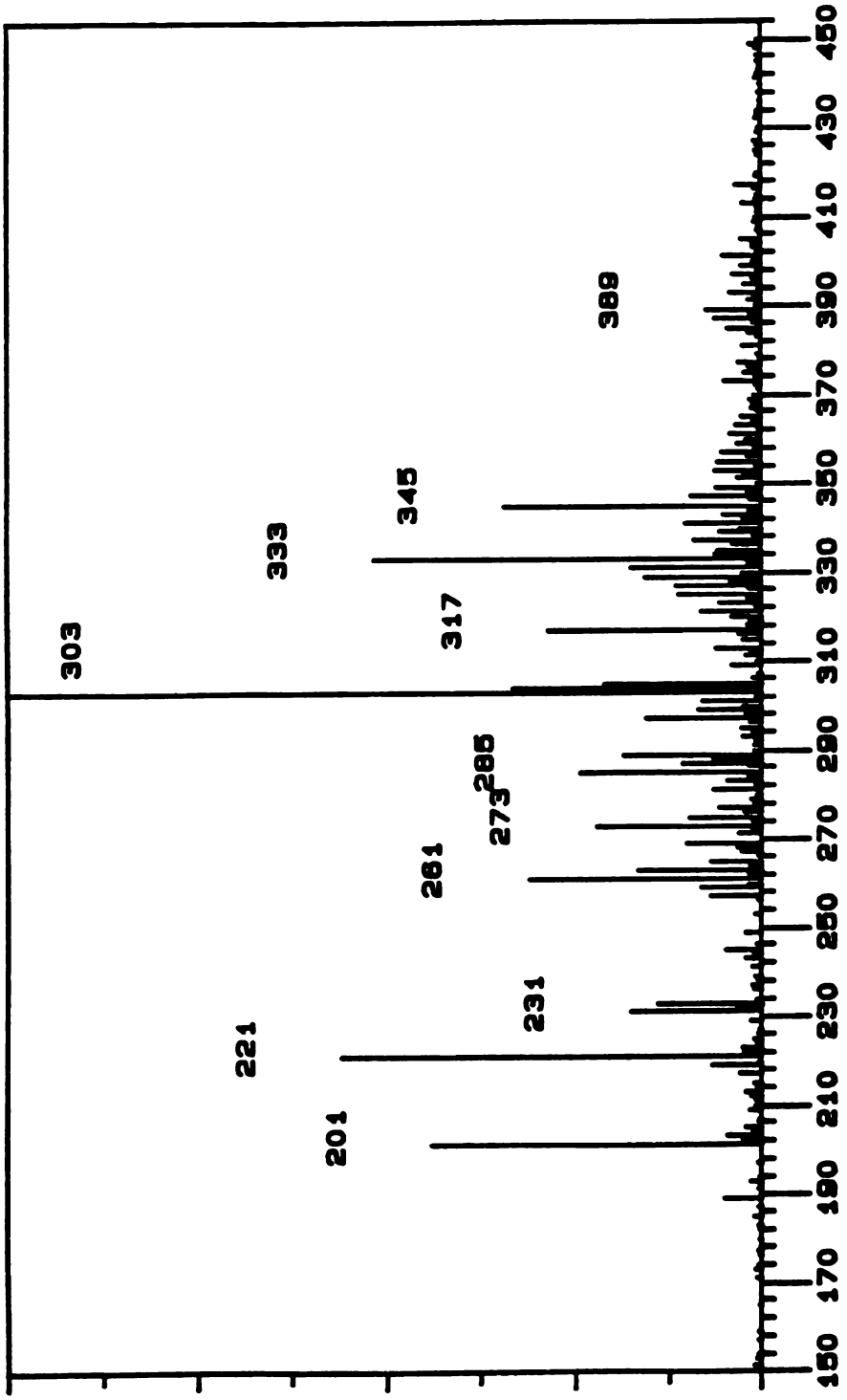


Figure 95. K^+ IDS Spectrum of Gum Ghatti.

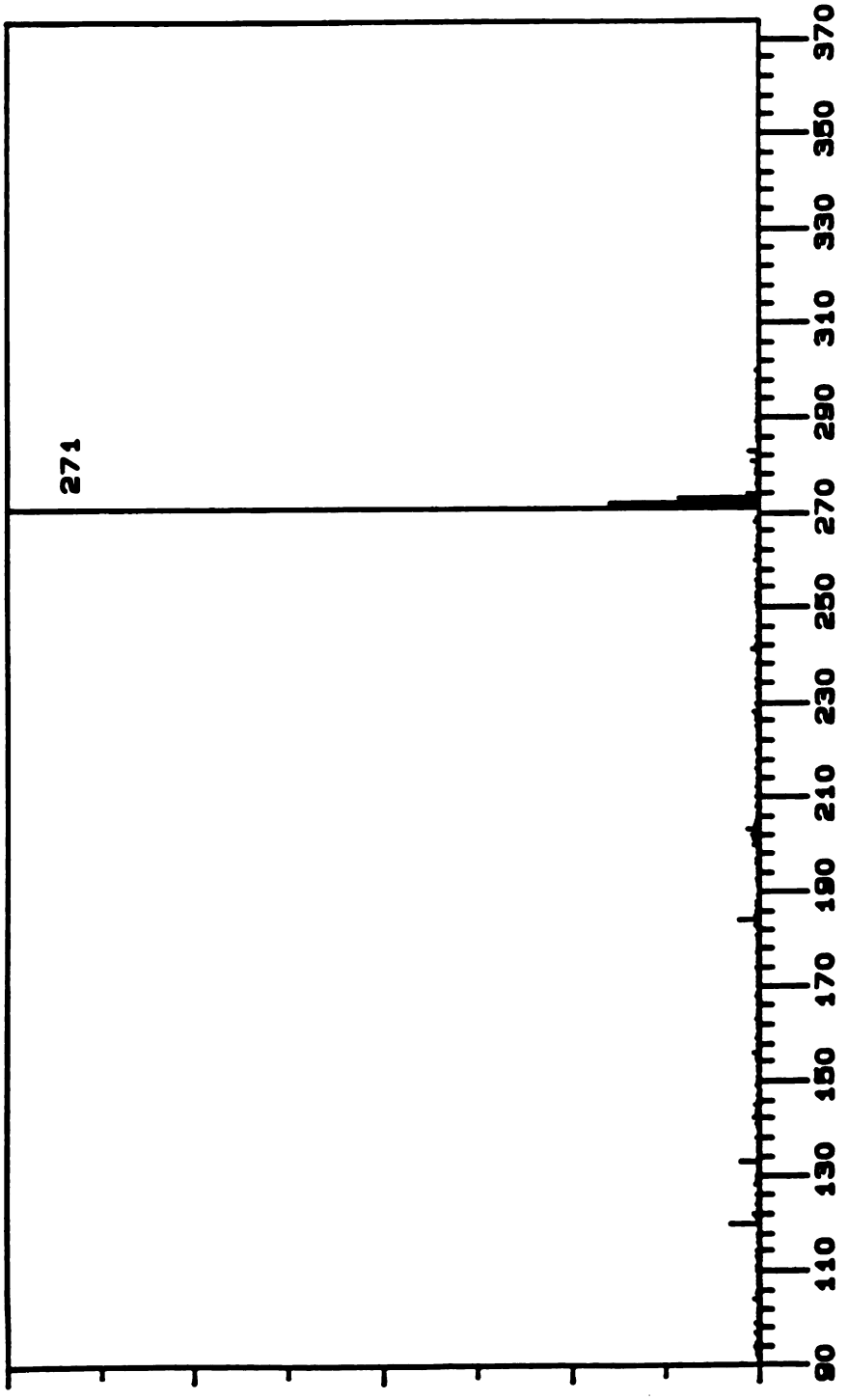


Figure 96. K^+ IDS Spectrum of Phenobarbital.

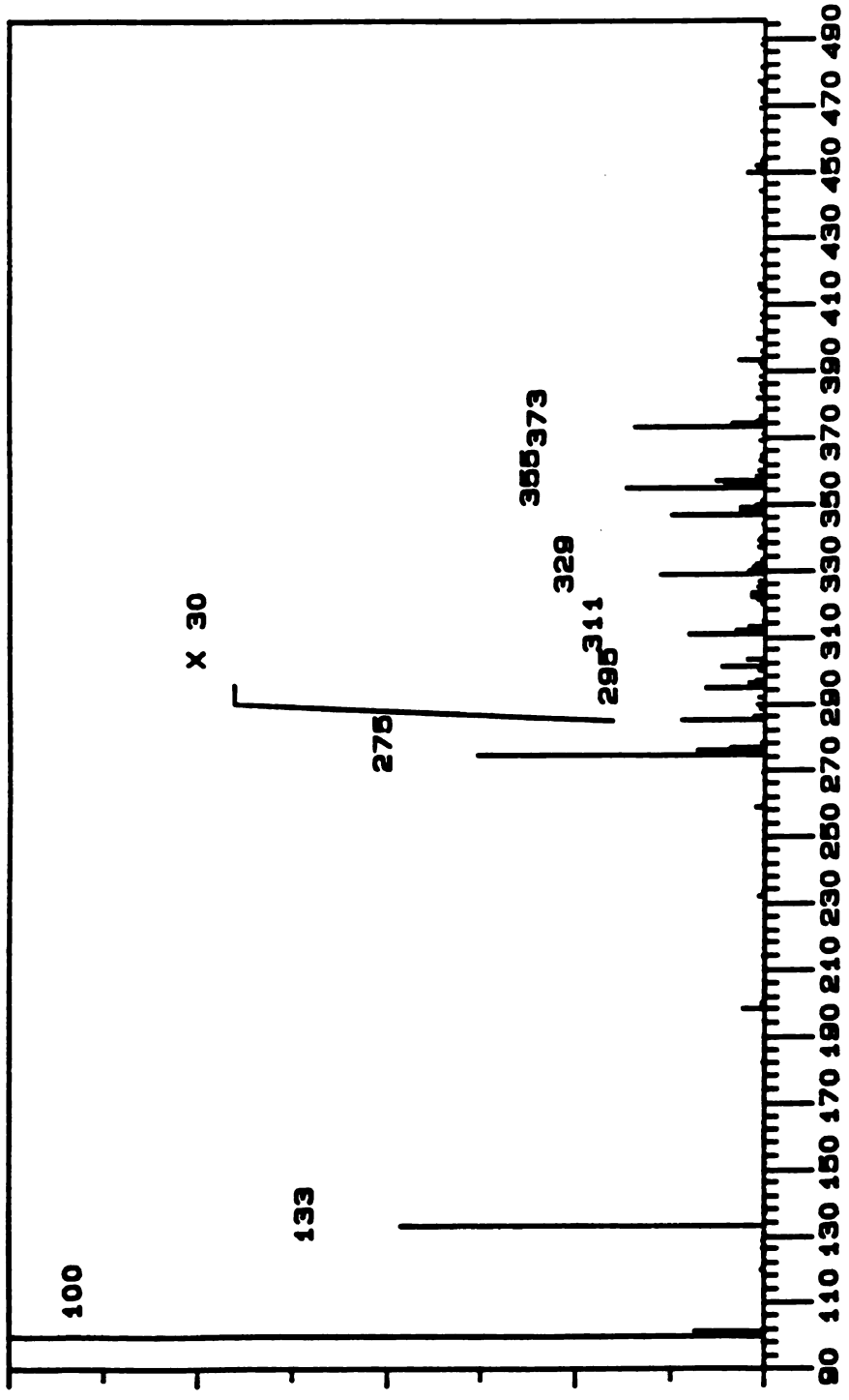


Figure 97. K^+IDS Spectrum of Penicillin G.

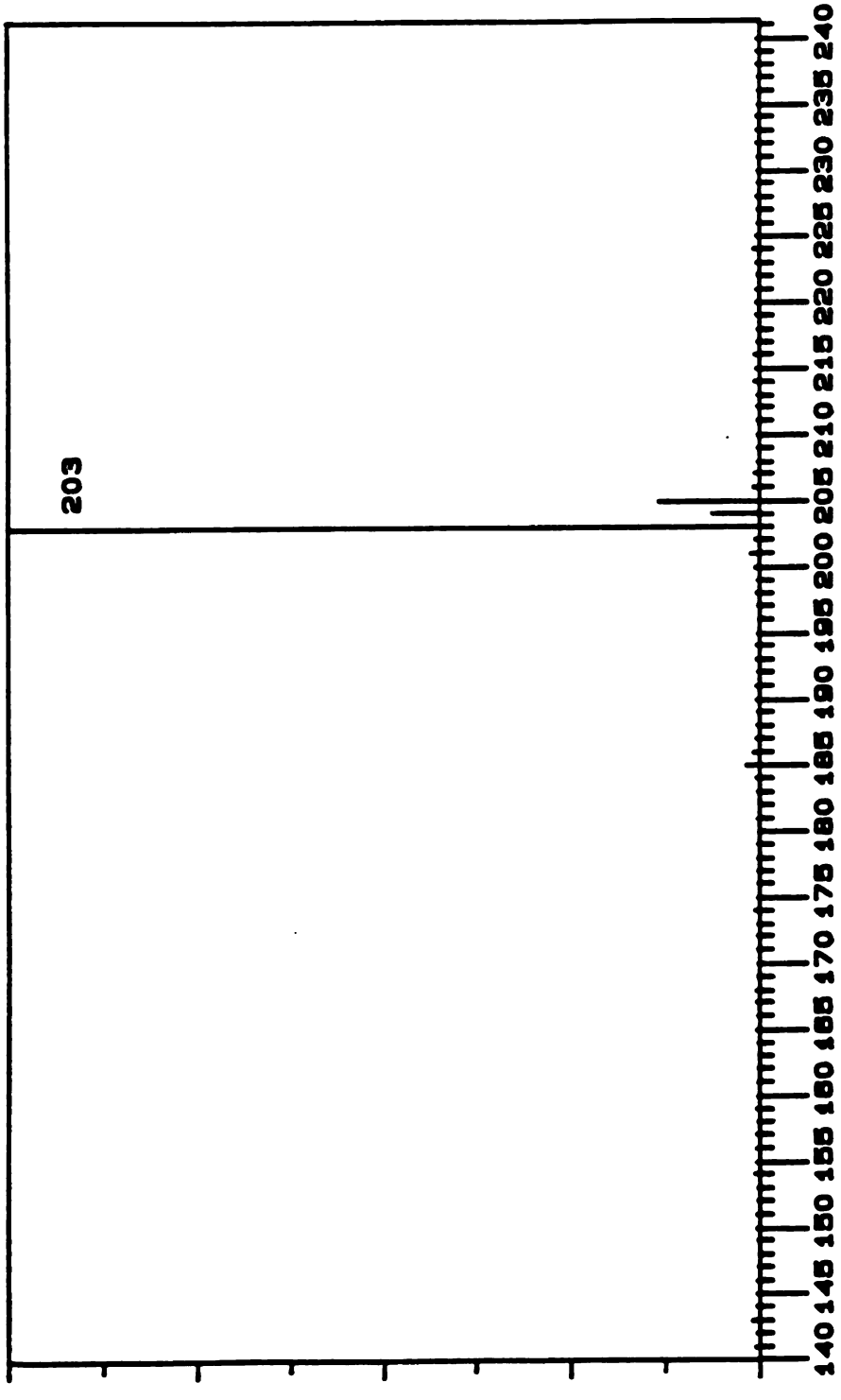


Figure 98. K^+IDS Spectrum of Rhamnose.

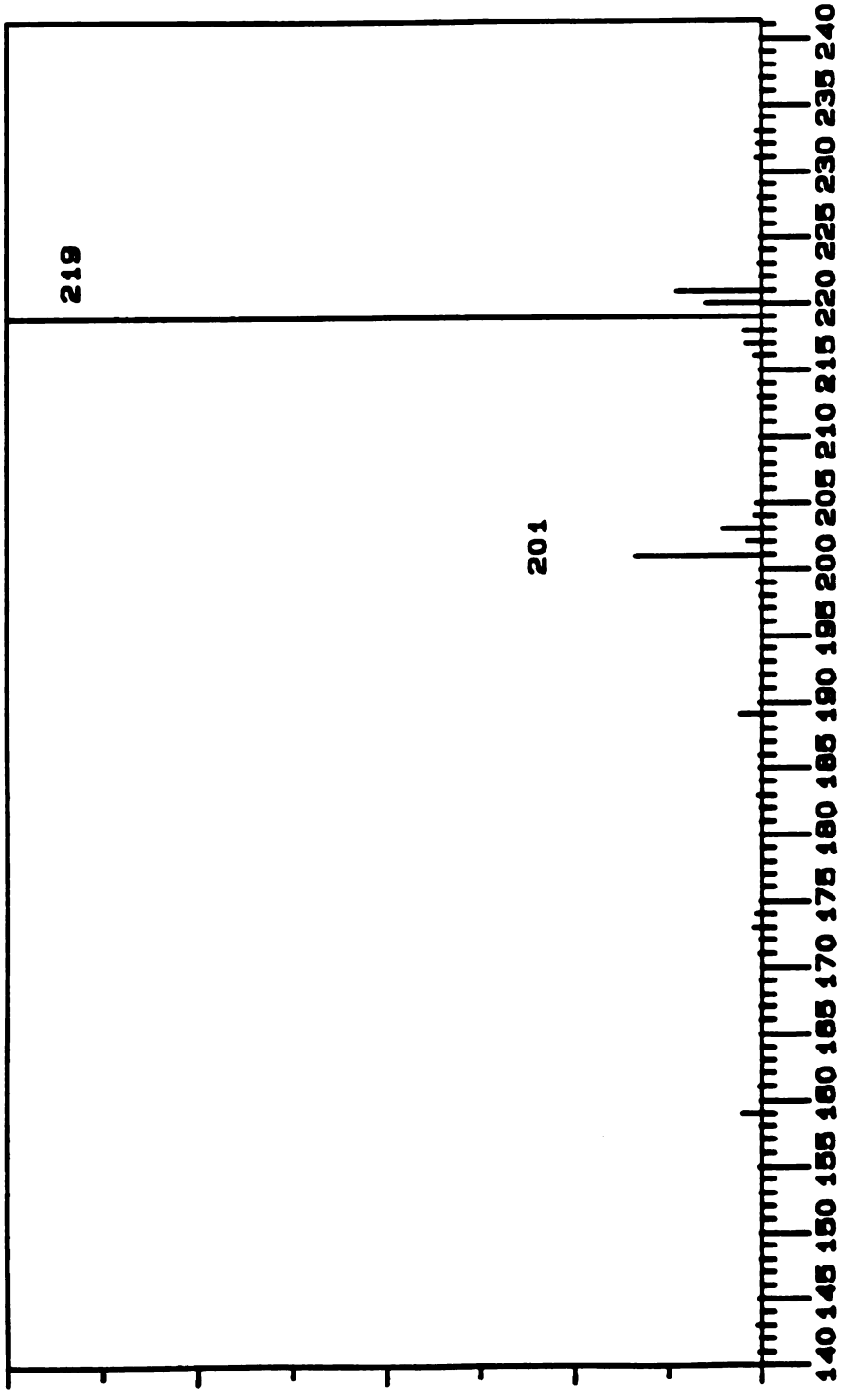


Figure 99. K^+IDS Spectrum of Sorbose.

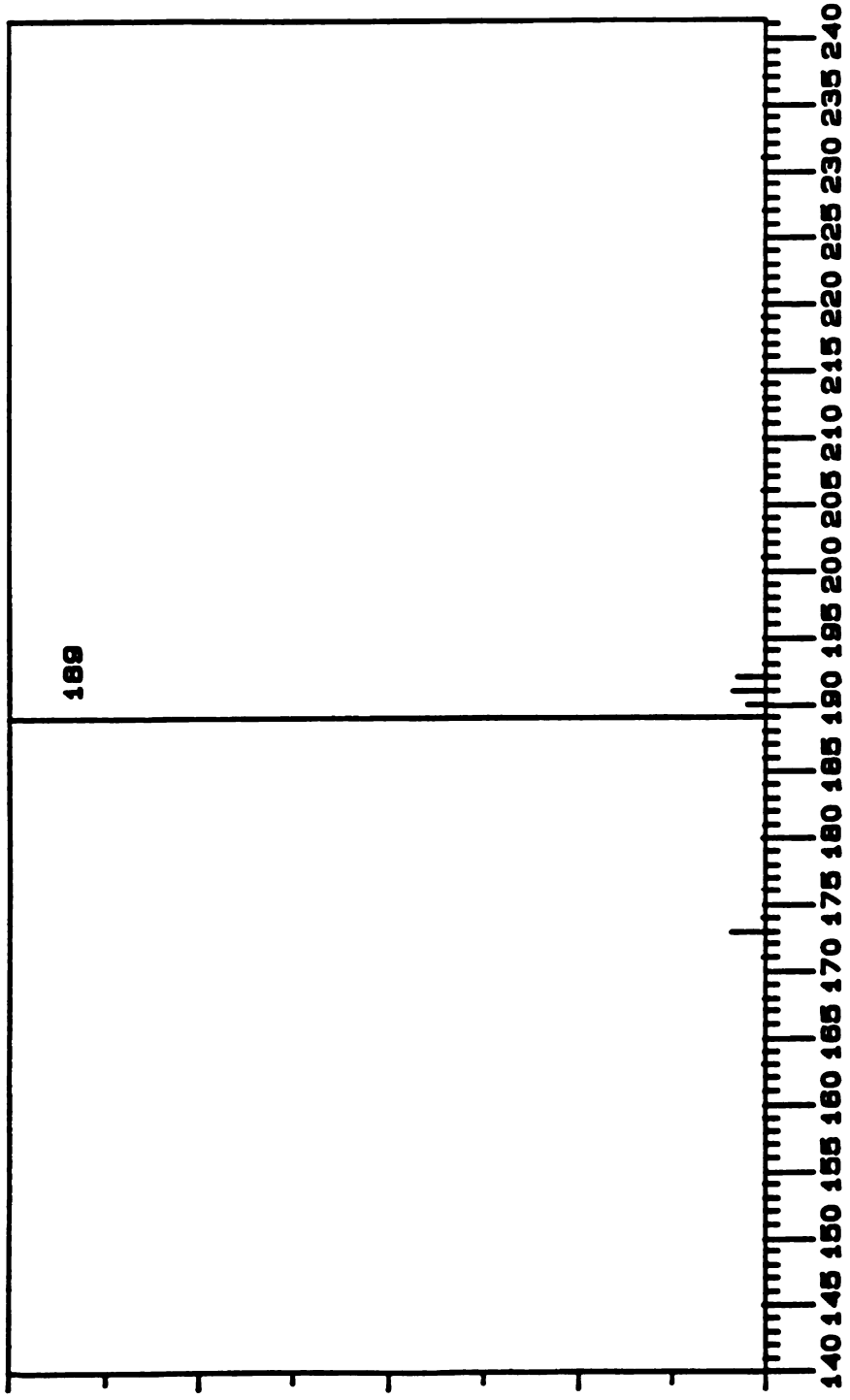


Figure 100. K^+IDS Spectrum of Ribose.

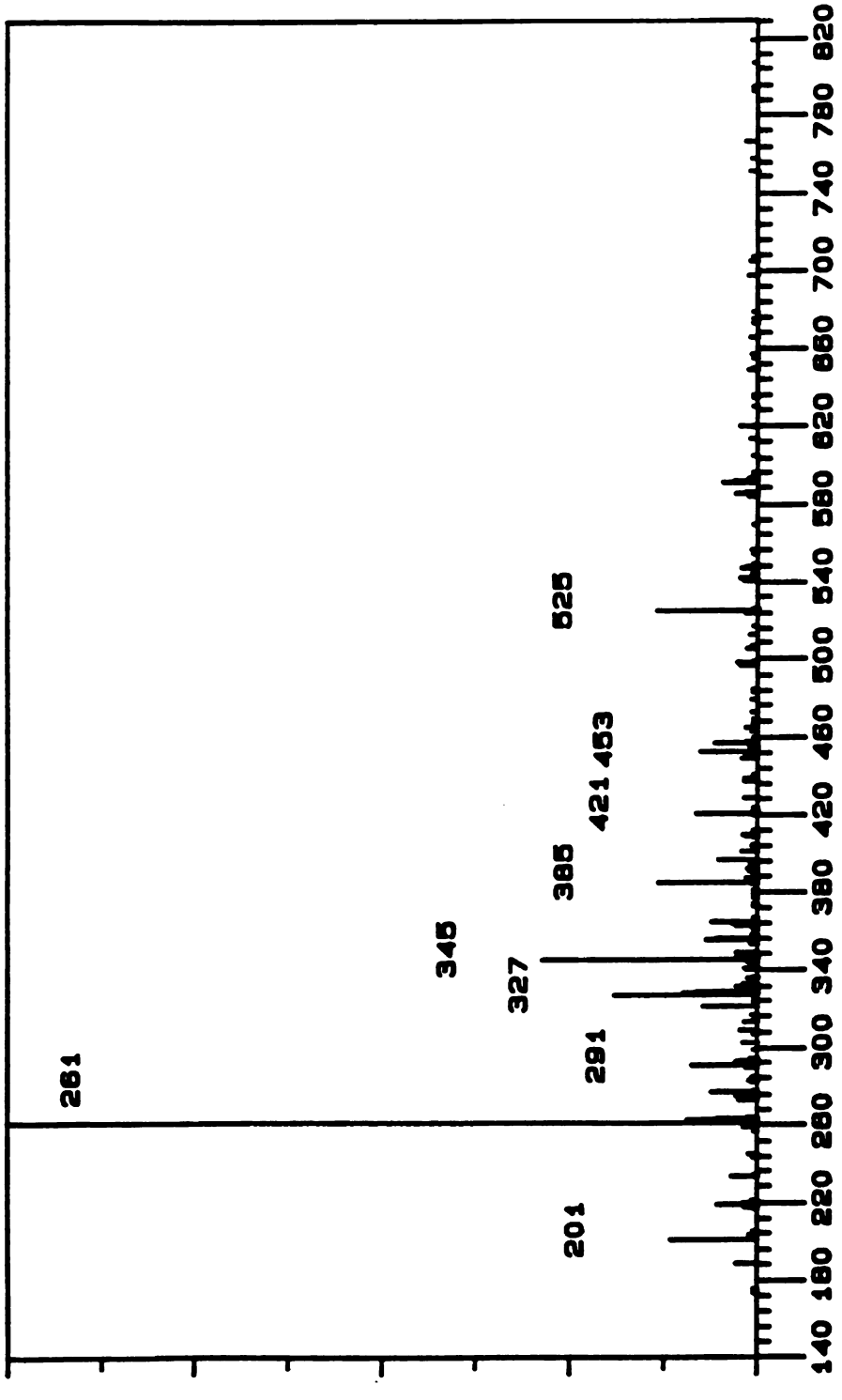


Figure 101. K^+IDS Spectrum of Dextran.

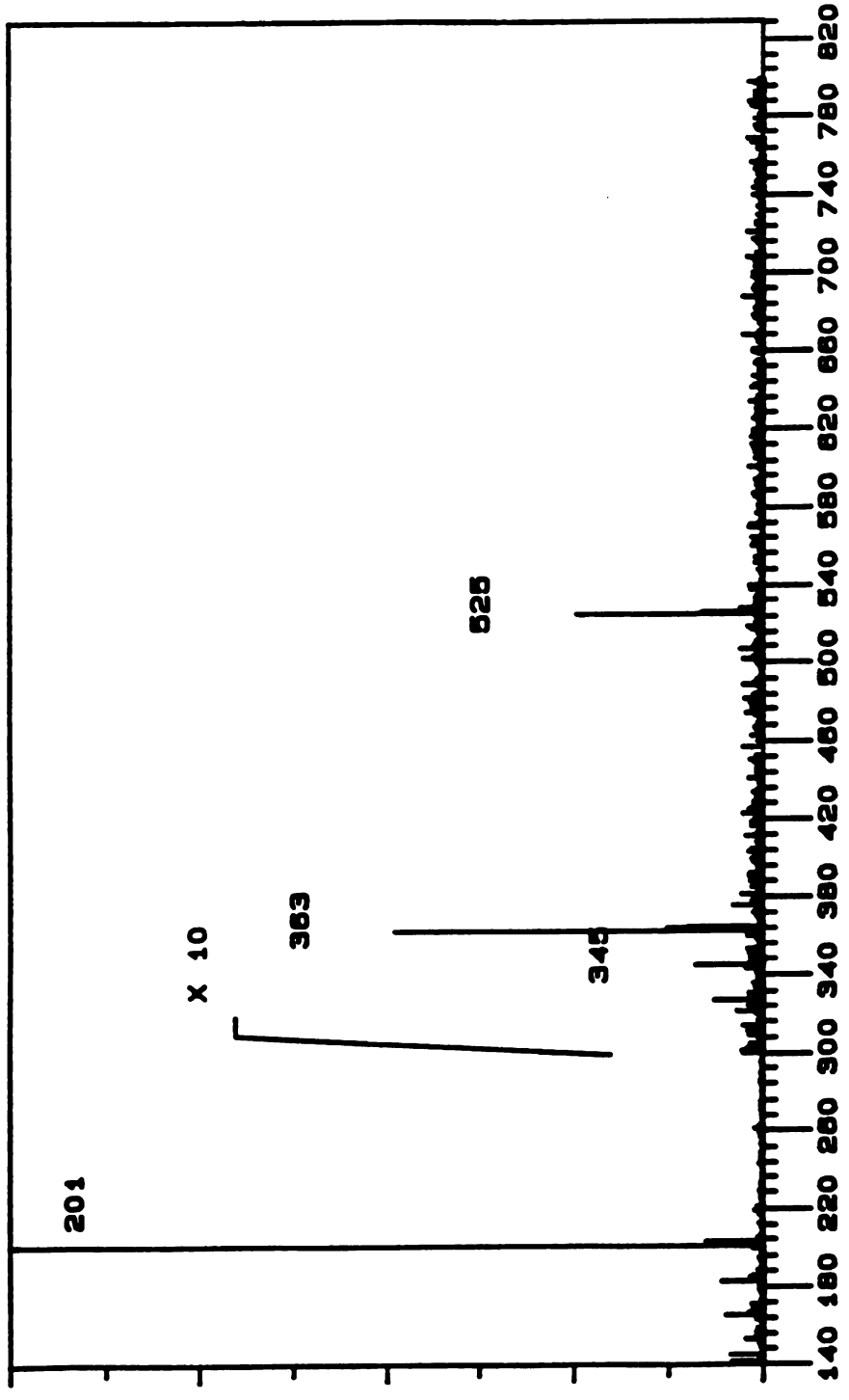


Figure 102. K^+IDS Spectrum of Glycogen.

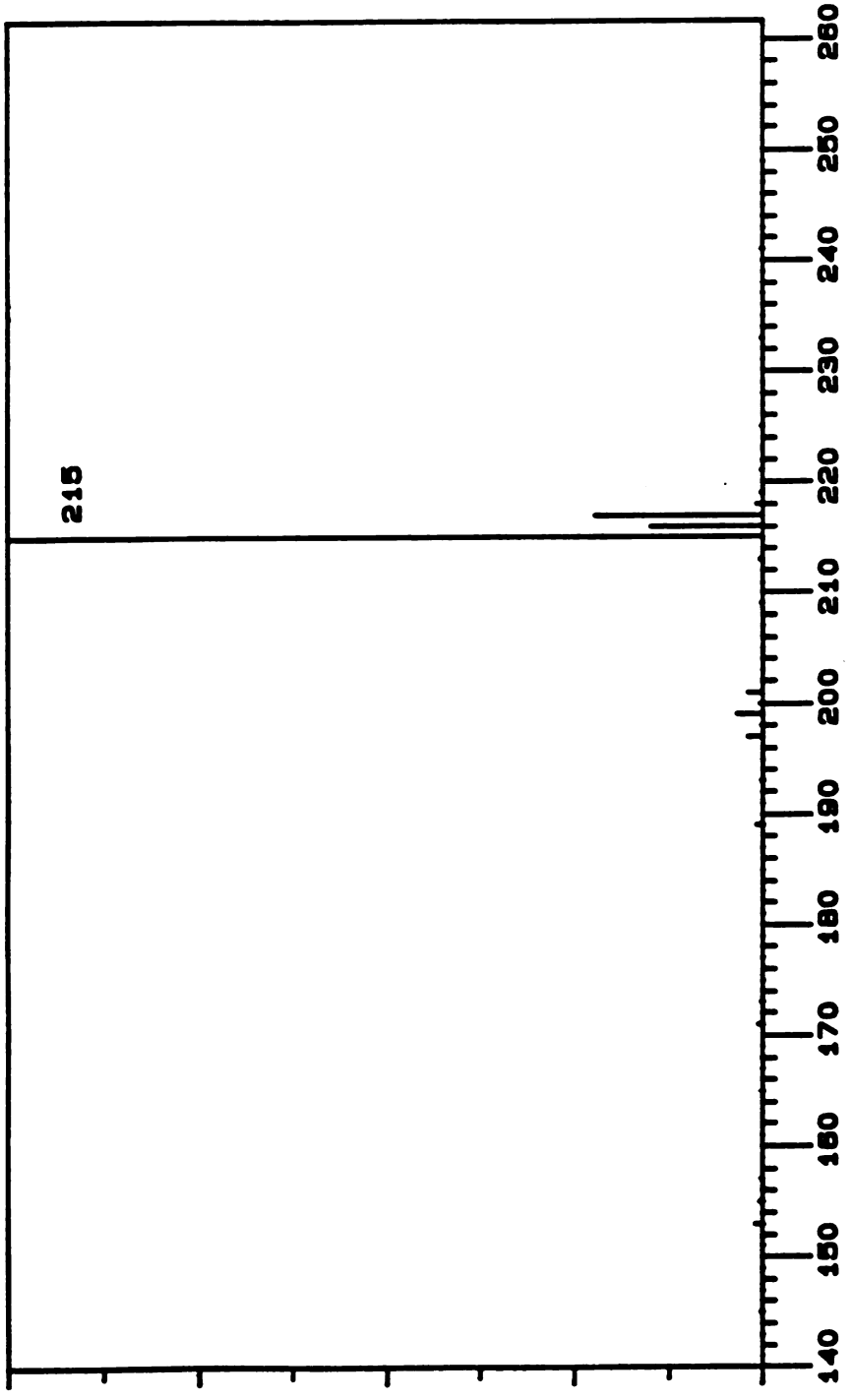


Figure 103. K^+ IDS Spectrum of Ascorbic Acid.

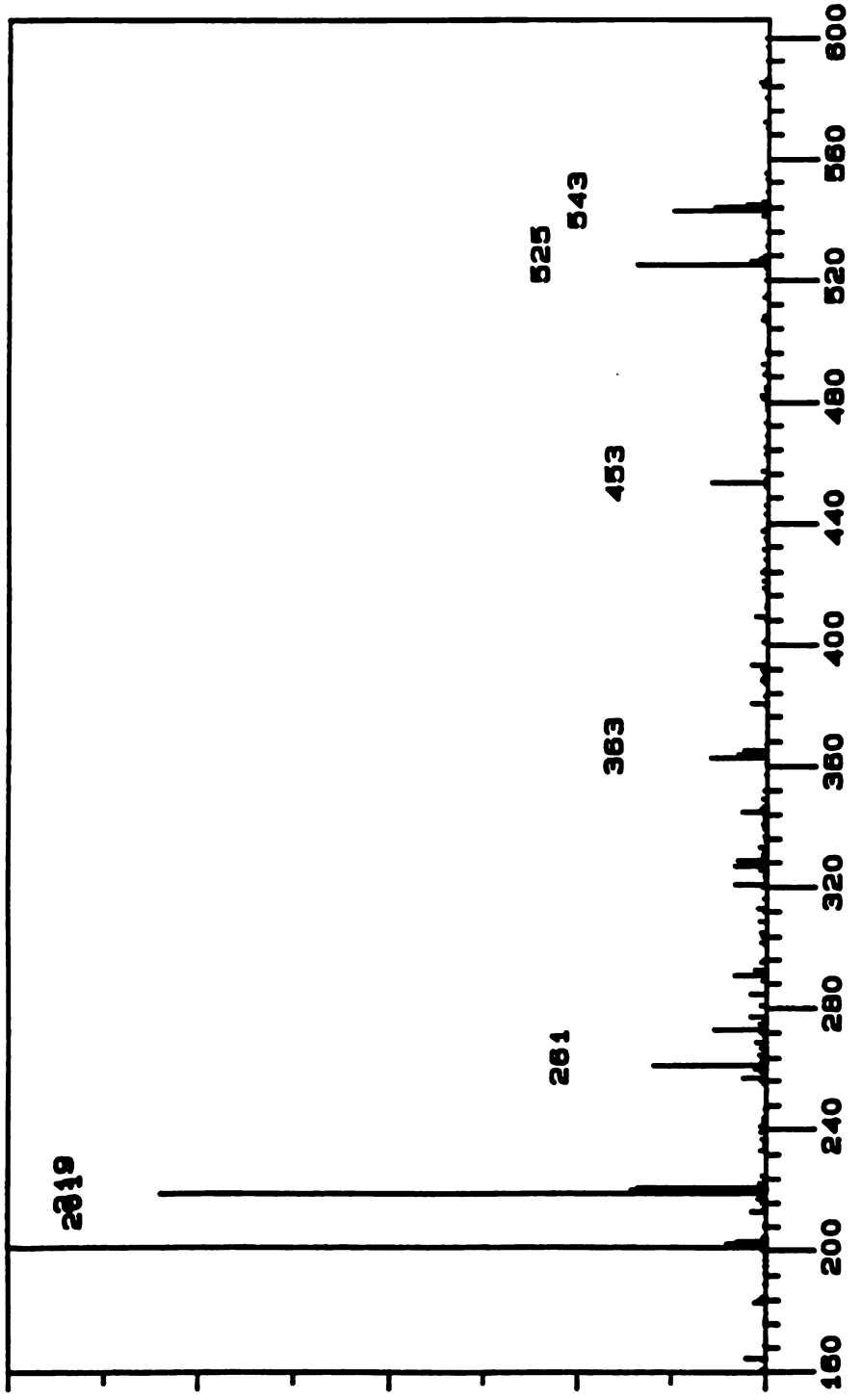


Figure 104. K^+IDS Spectrum of Melezitose.

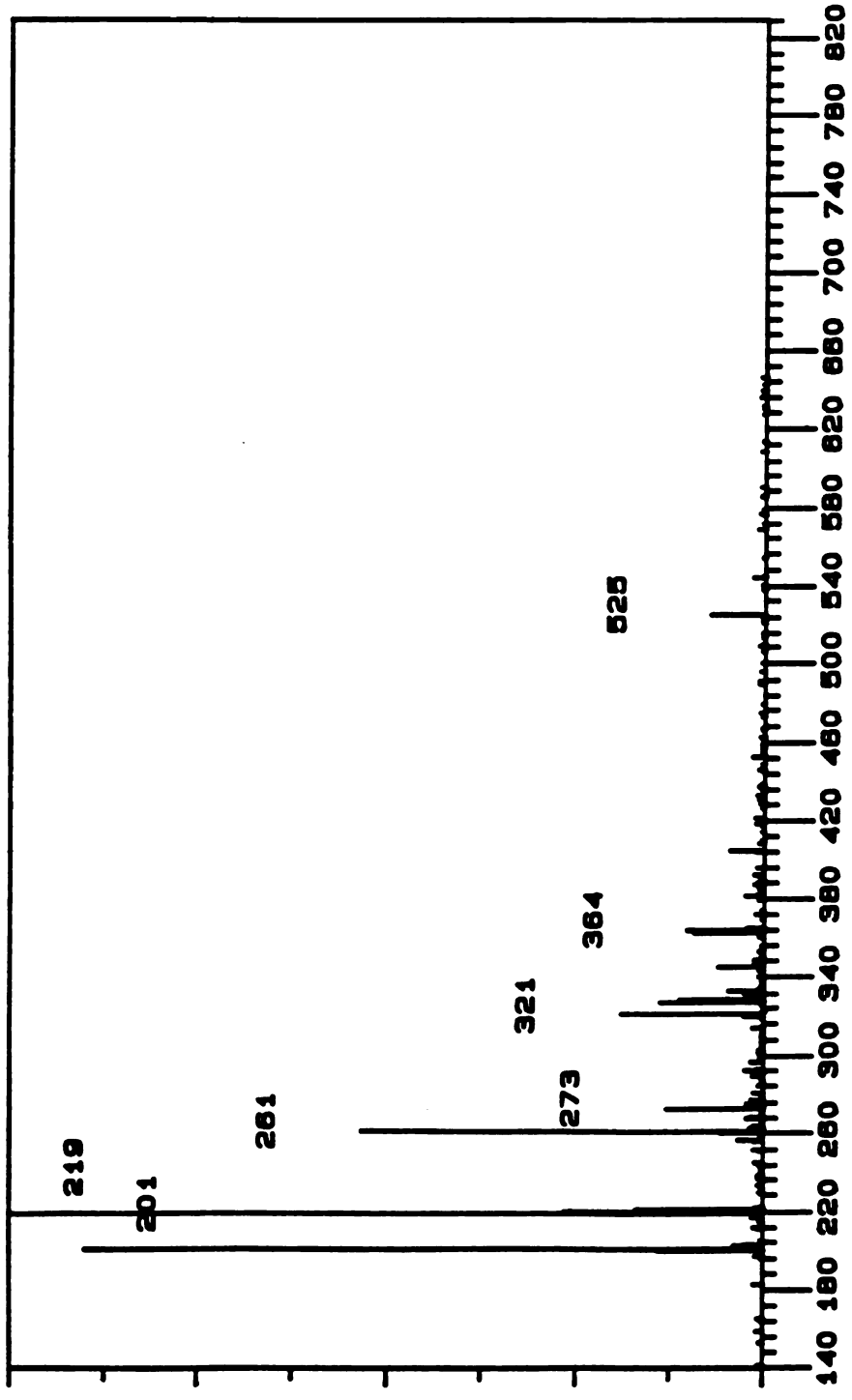


Figure 105. K^+IDS Spectrum of Raffinose.

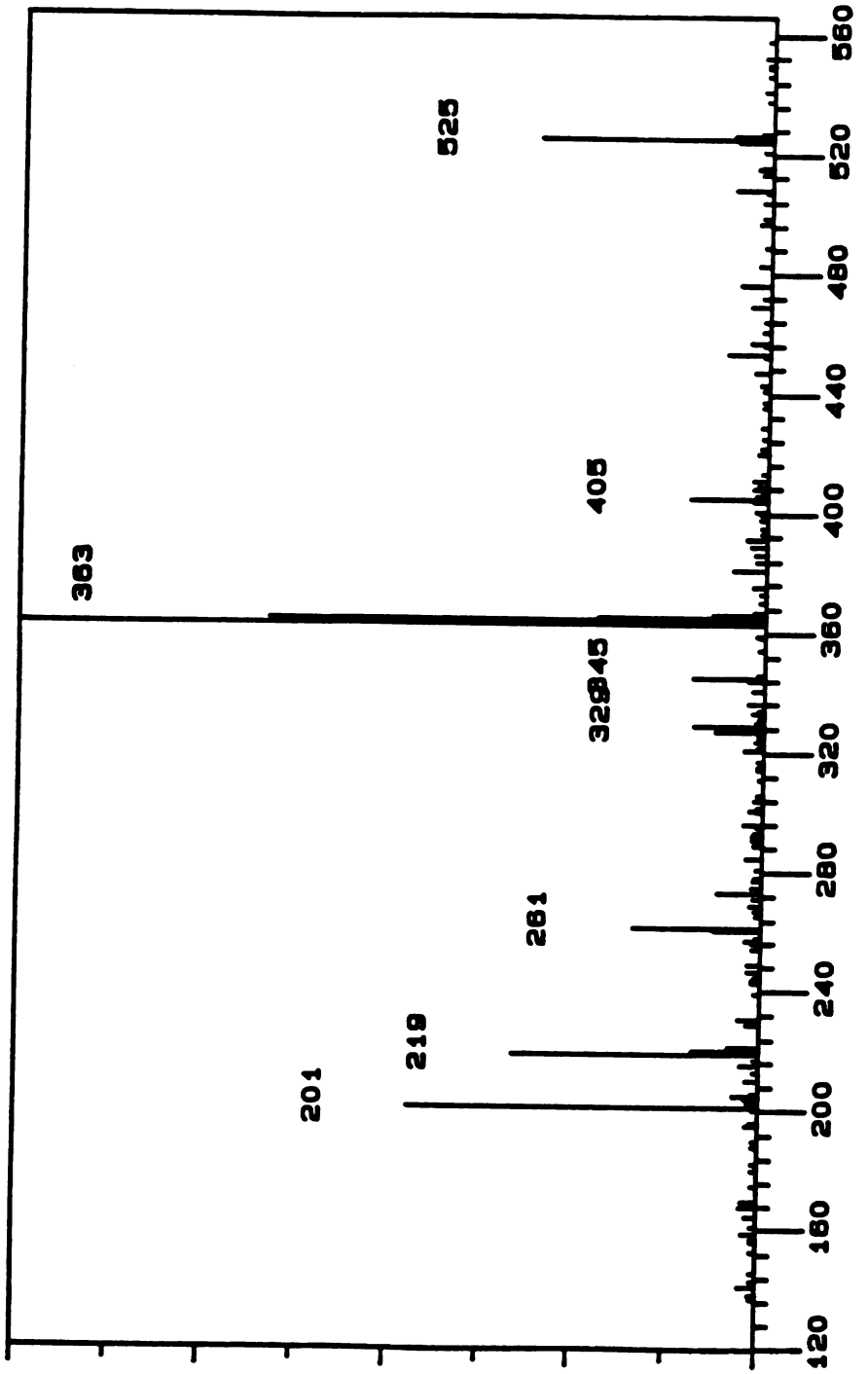


Figure 106. K^+IDS Spectrum of Inulin.

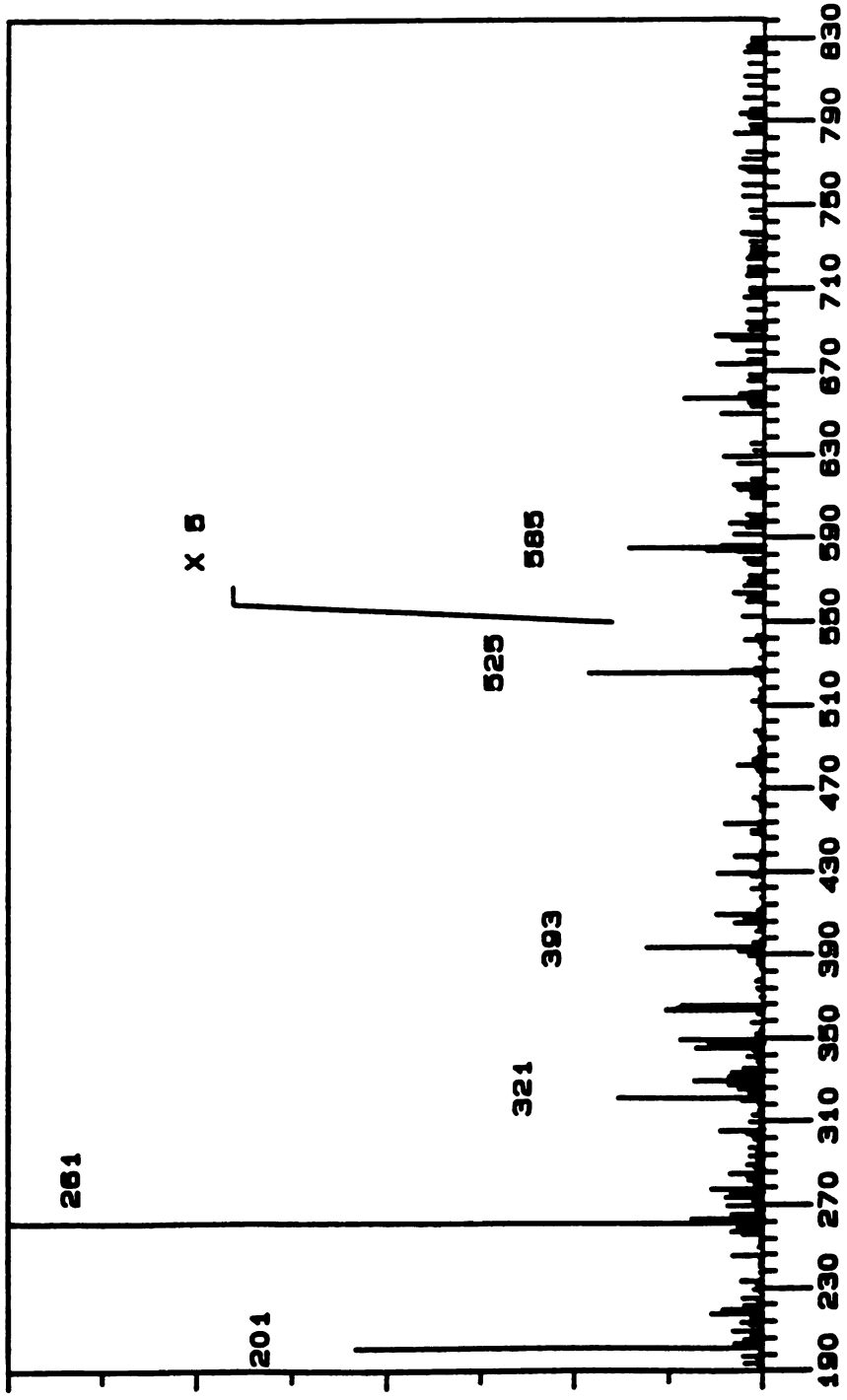


Figure 107. K^+IDS Spectrum of Amylose.

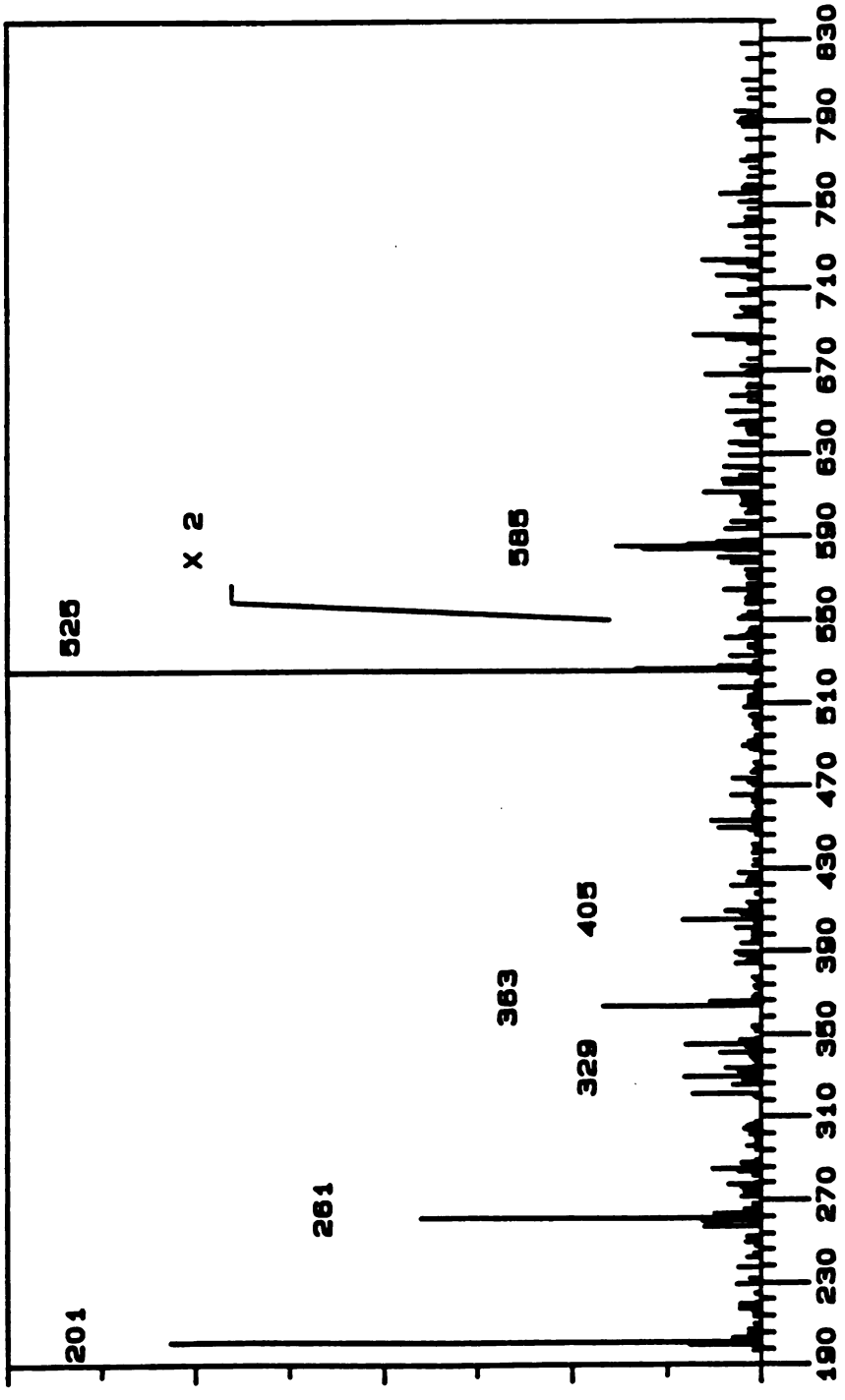


Figure 108. K^+IDS Spectrum of Amylopectin.

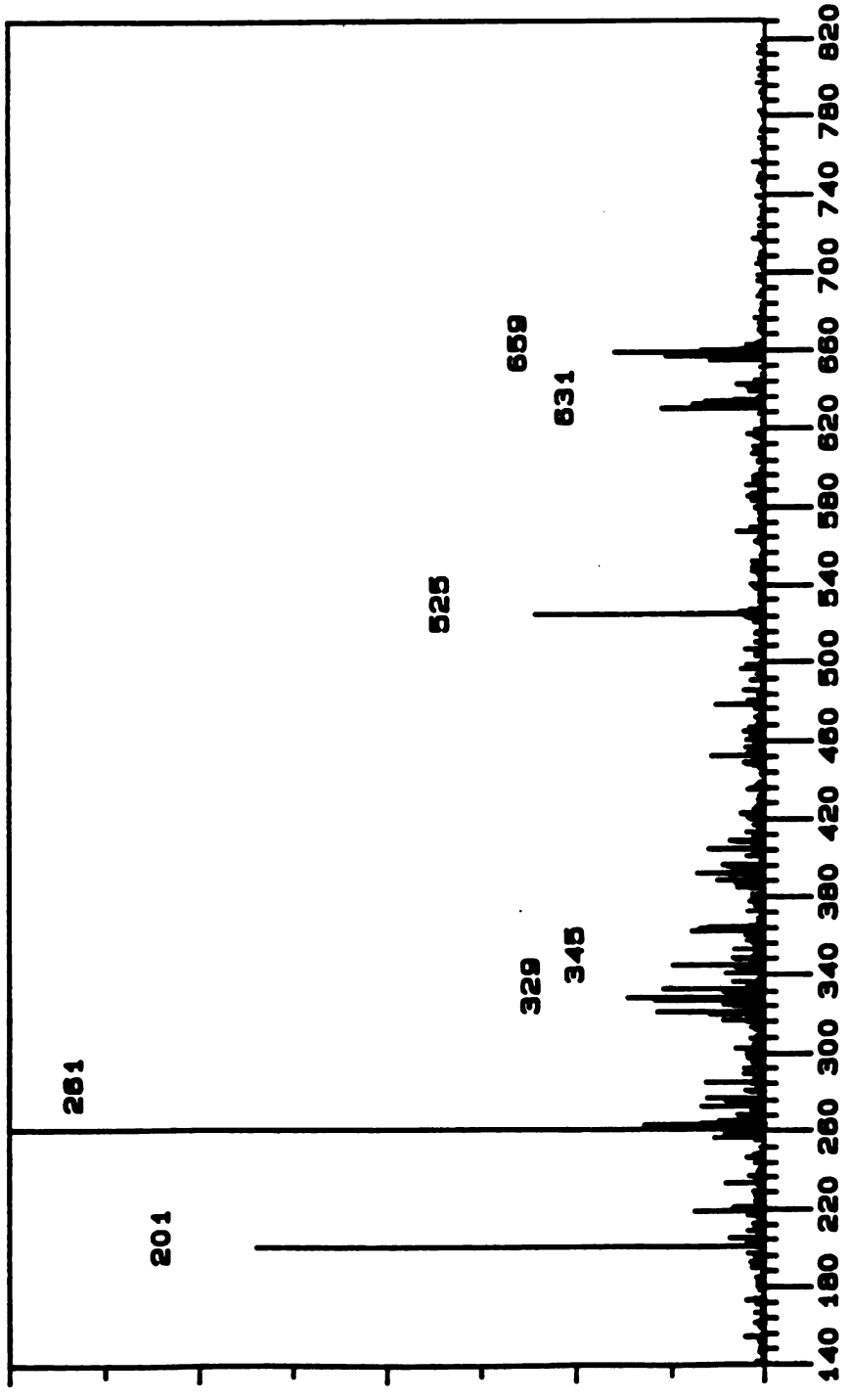


Figure 109. K^+IDS Spectrum of Locust Bean Gum.

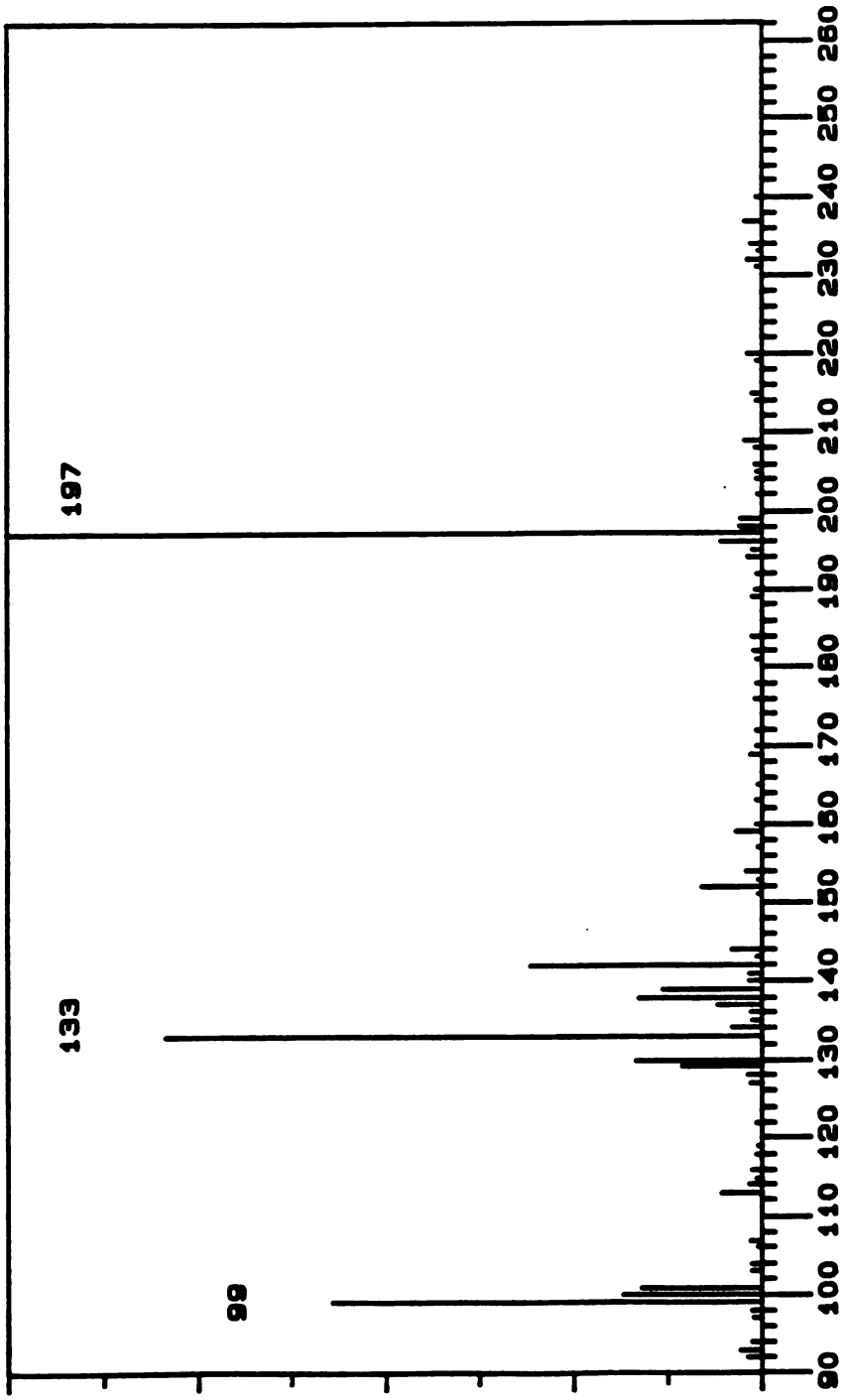


Figure 110. K^+IDS Spectrum of Allantoin.

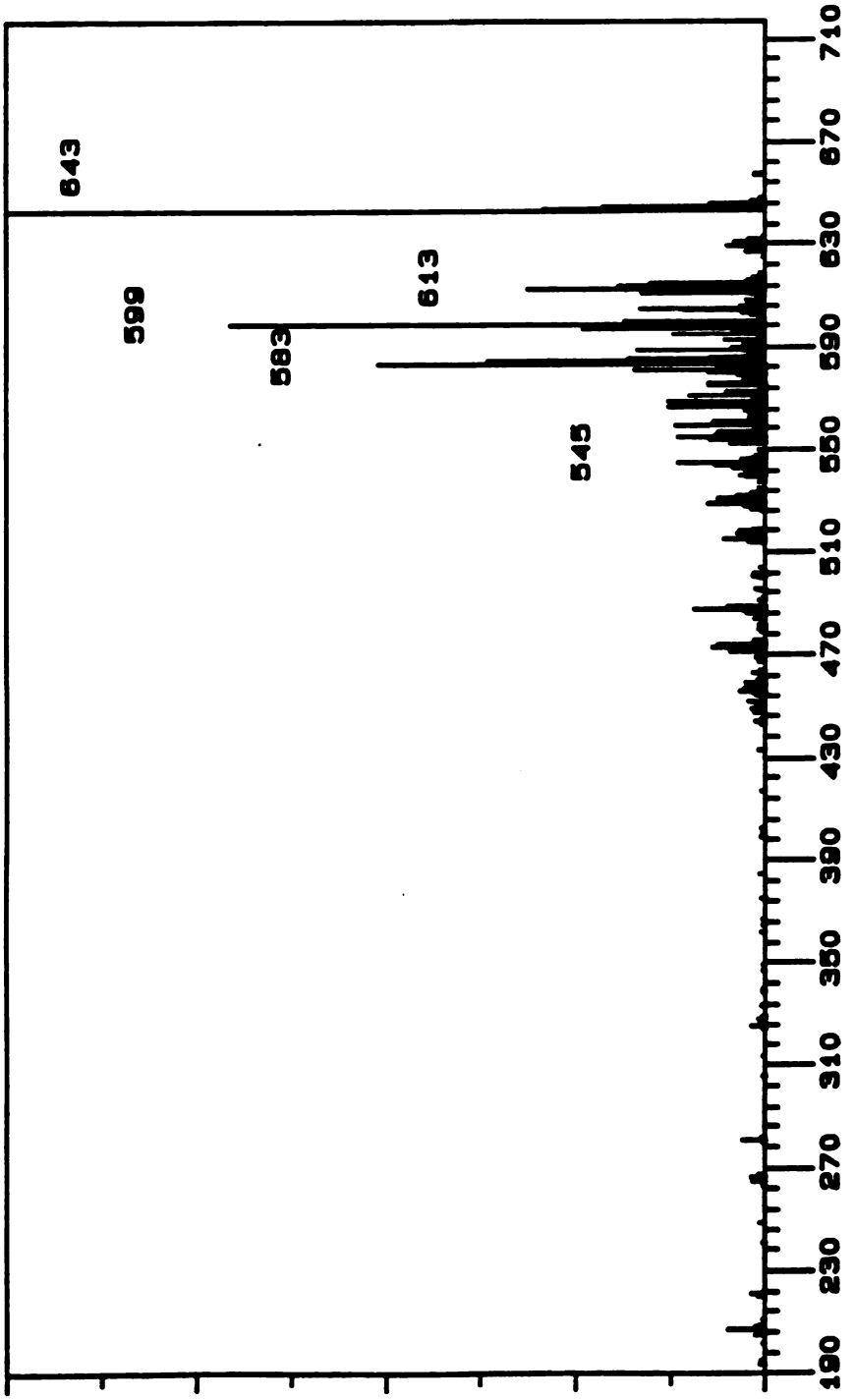


Figure 111. K^+IDS Spectrum of Porphyrin (MW=604).

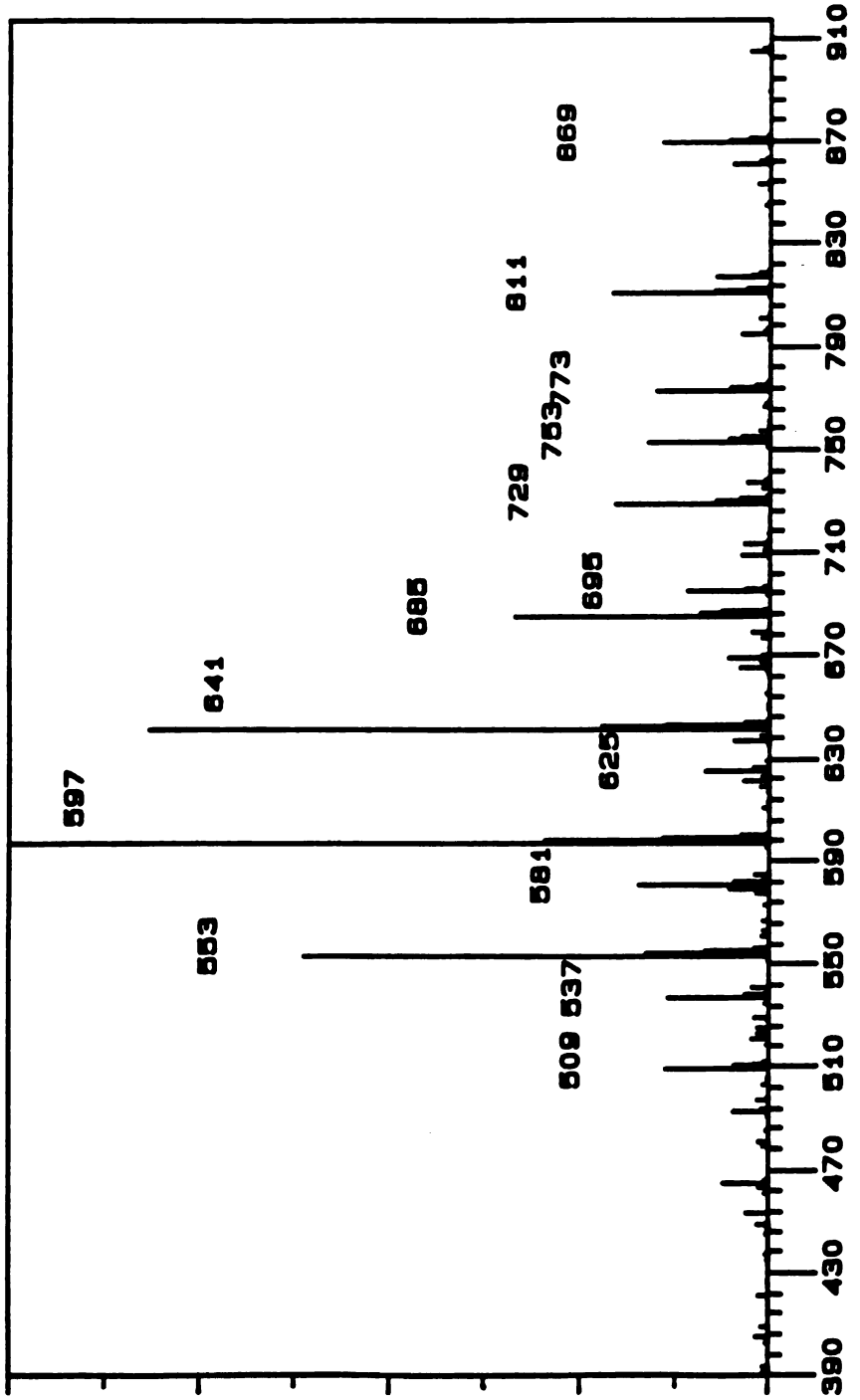


Figure 112. K^+IDS Spectrum of Triton X100.

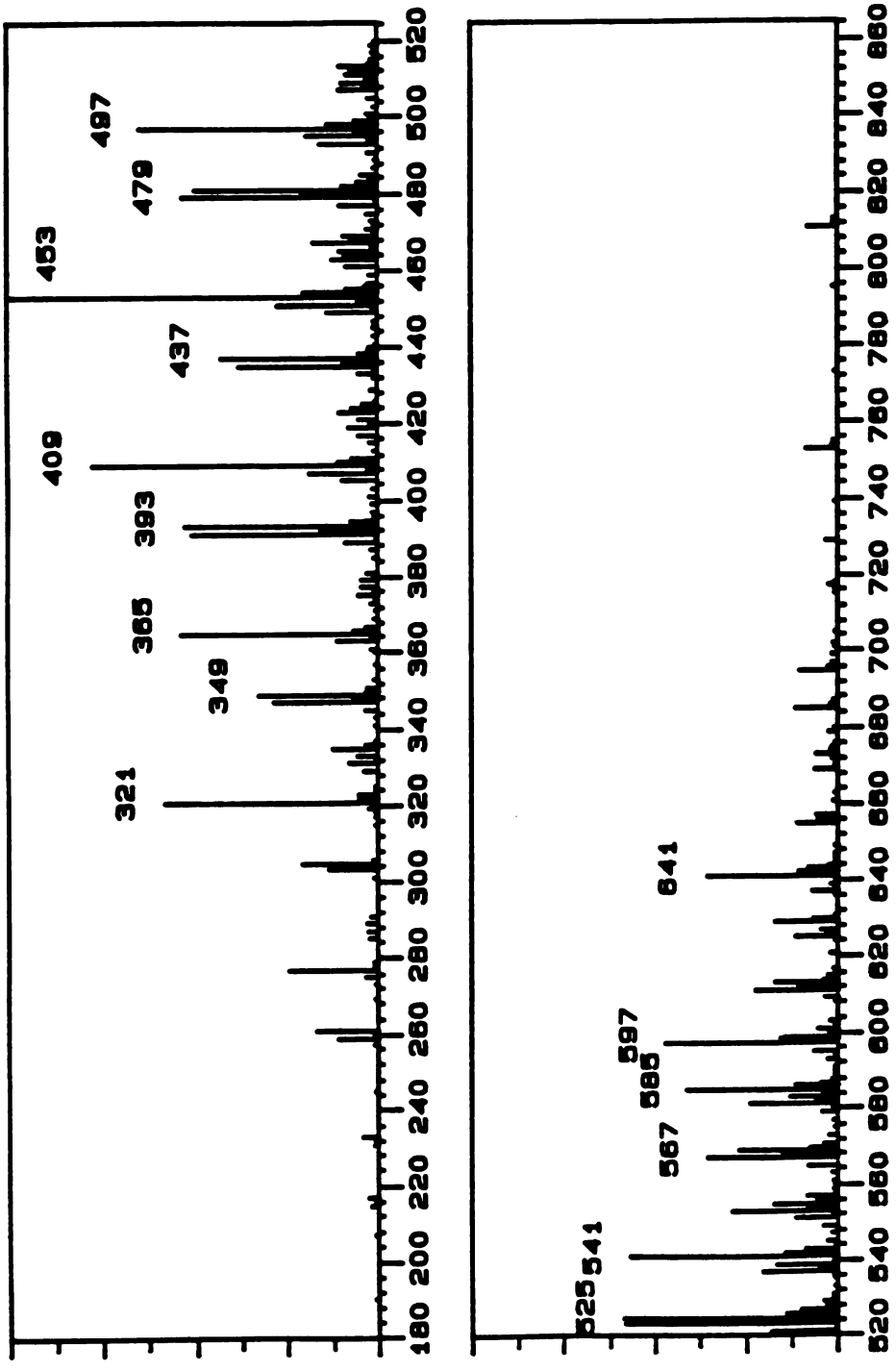


Figure 113. K^+IDS Spectrum of Tween 80.

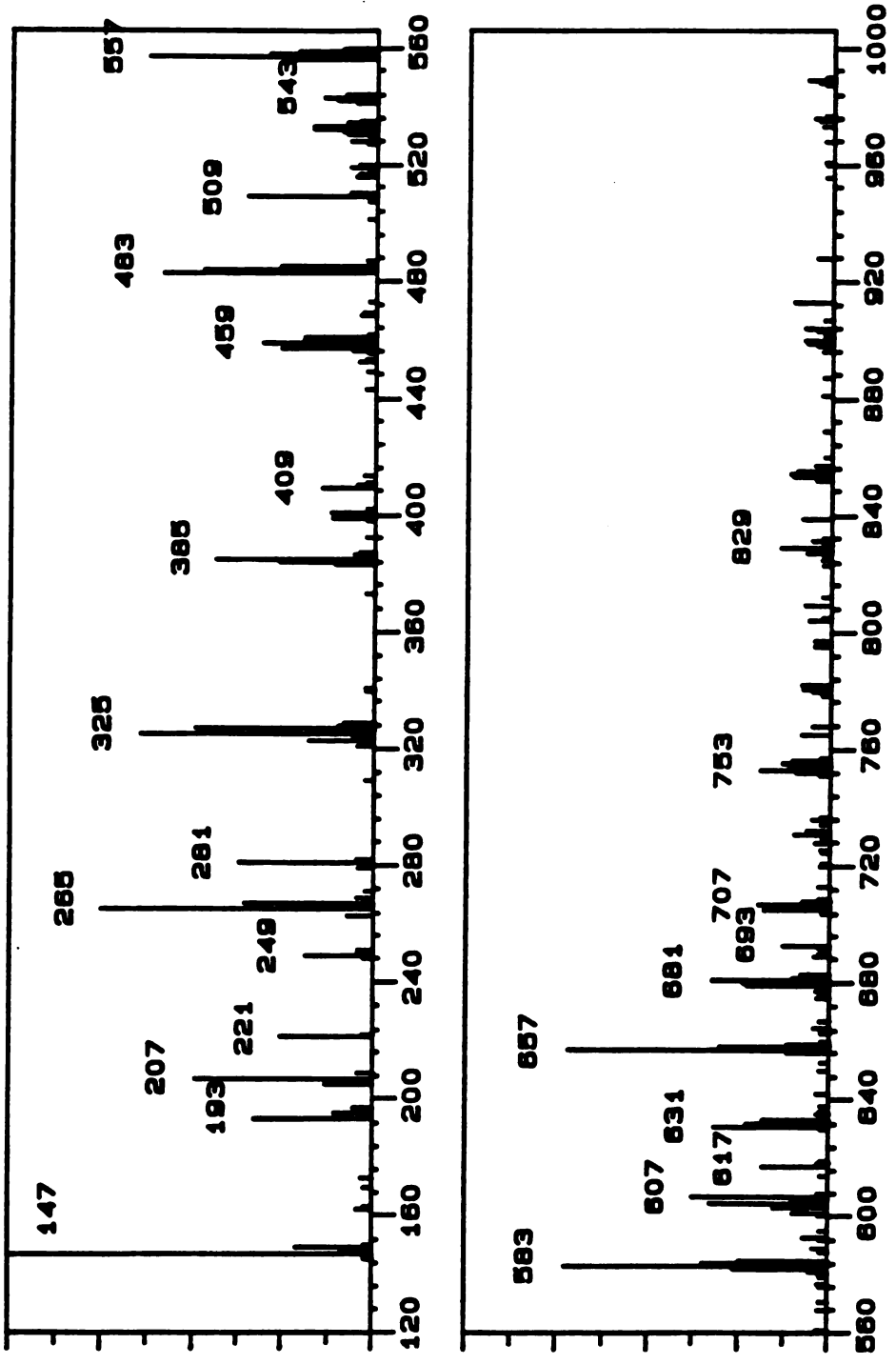


Figure 114. K^+IDS Spectrum of SE-54 (Methyl Silicone).

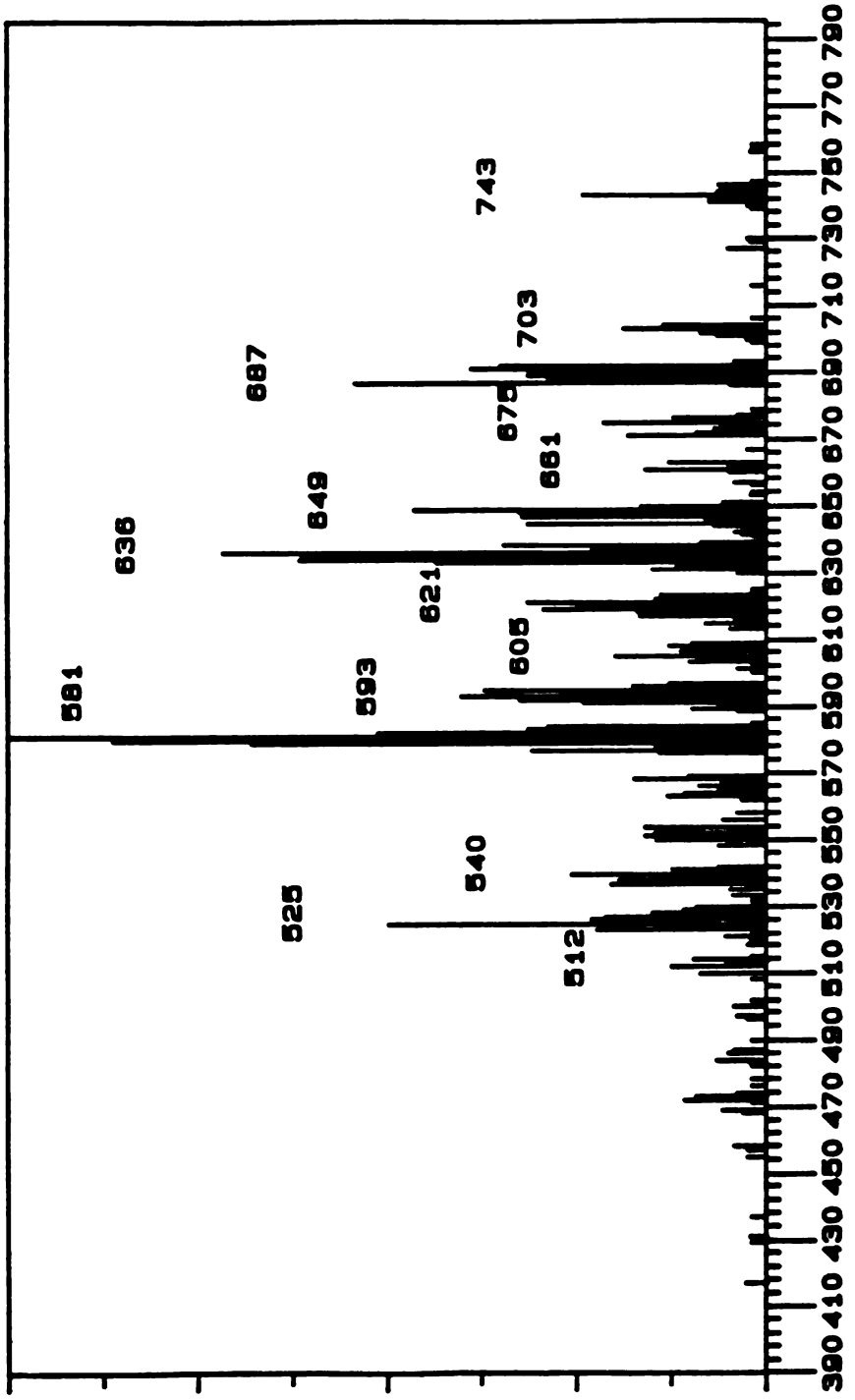


Figure 115. K^+IDS Spectrum of Polybutadiene.

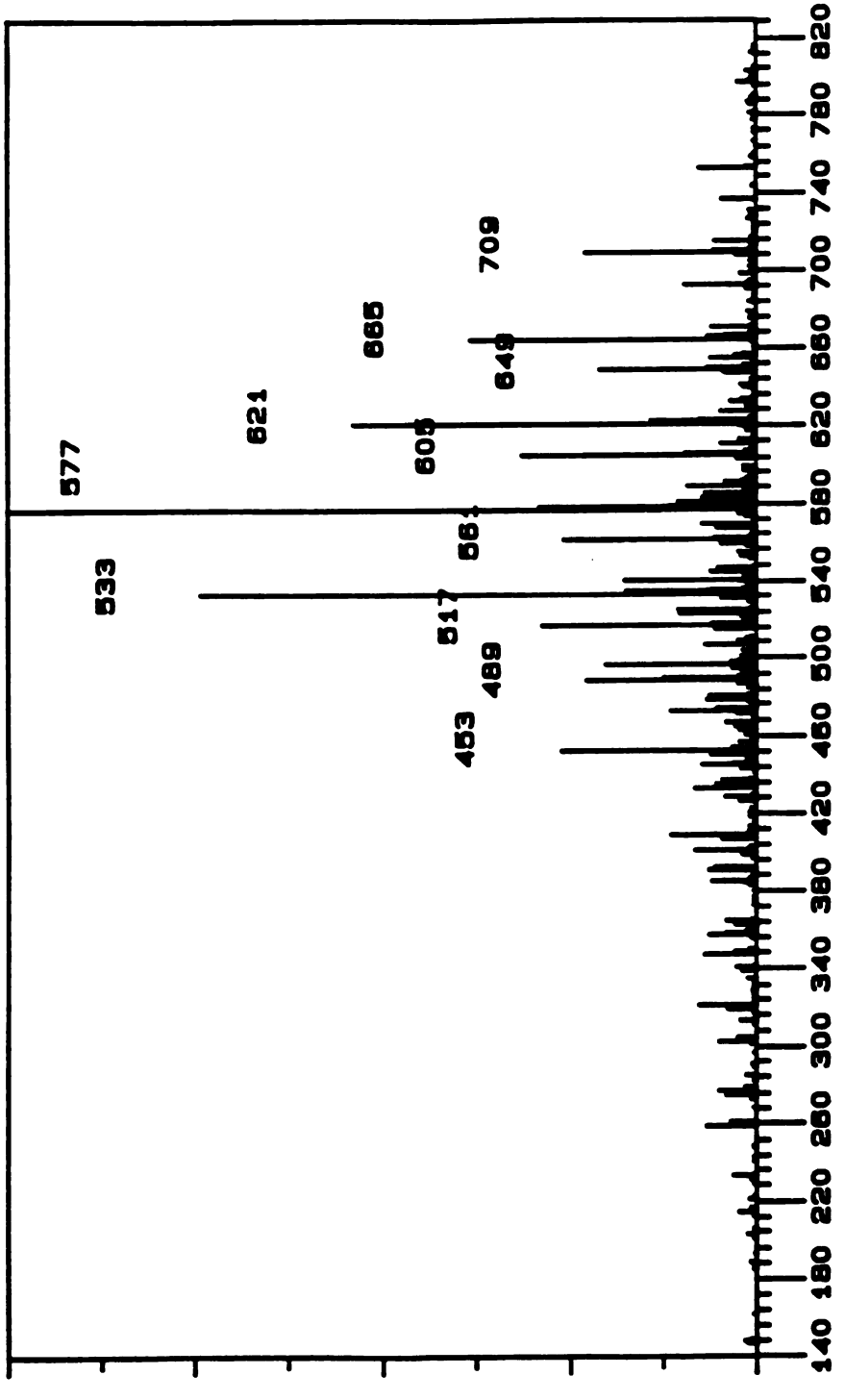


Figure 116. K^+IDS Spectrum of Polyoxyethylene Lauryl Ether.

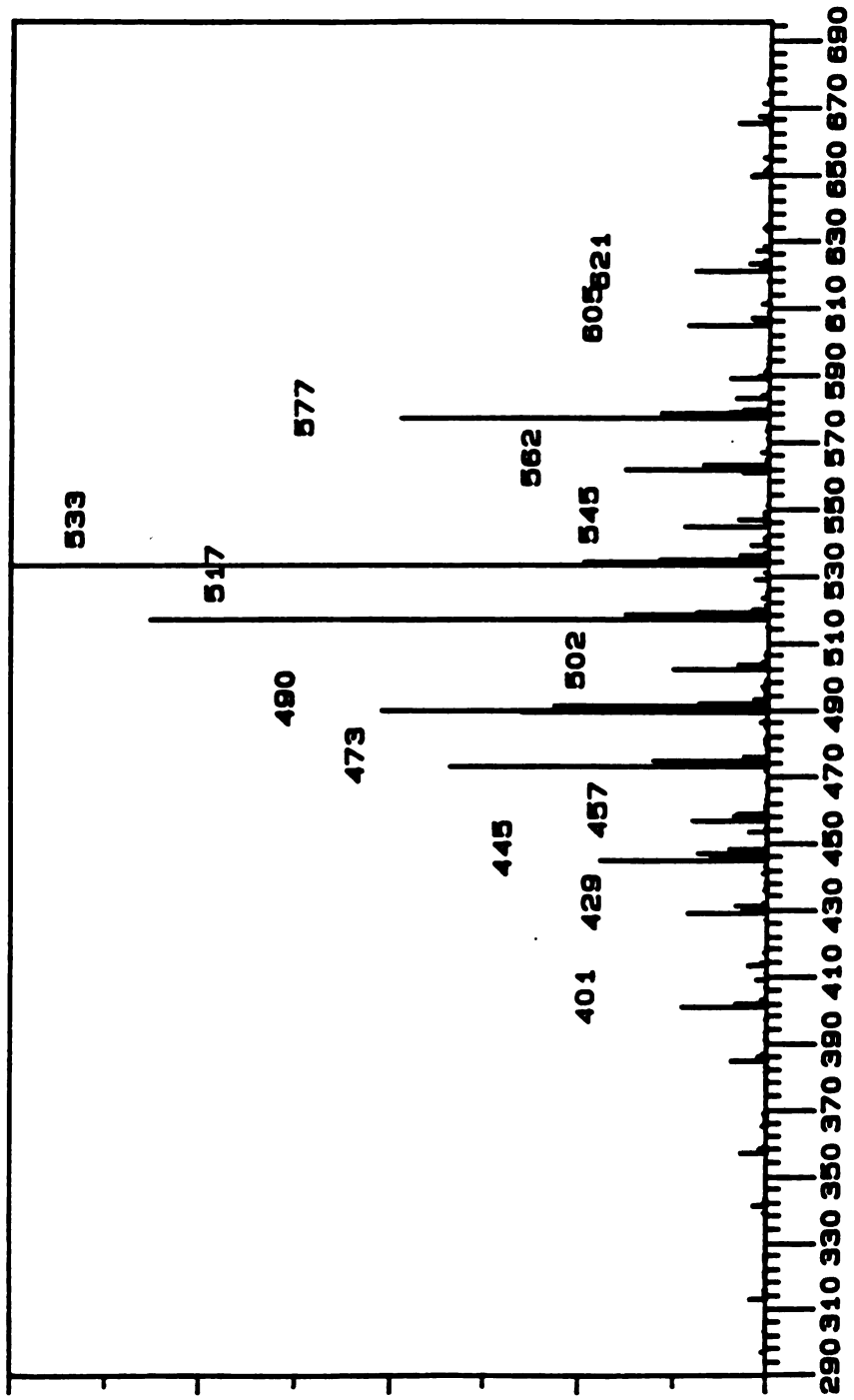


Figure 117. K^+IDS Spectrum of Brij 30.

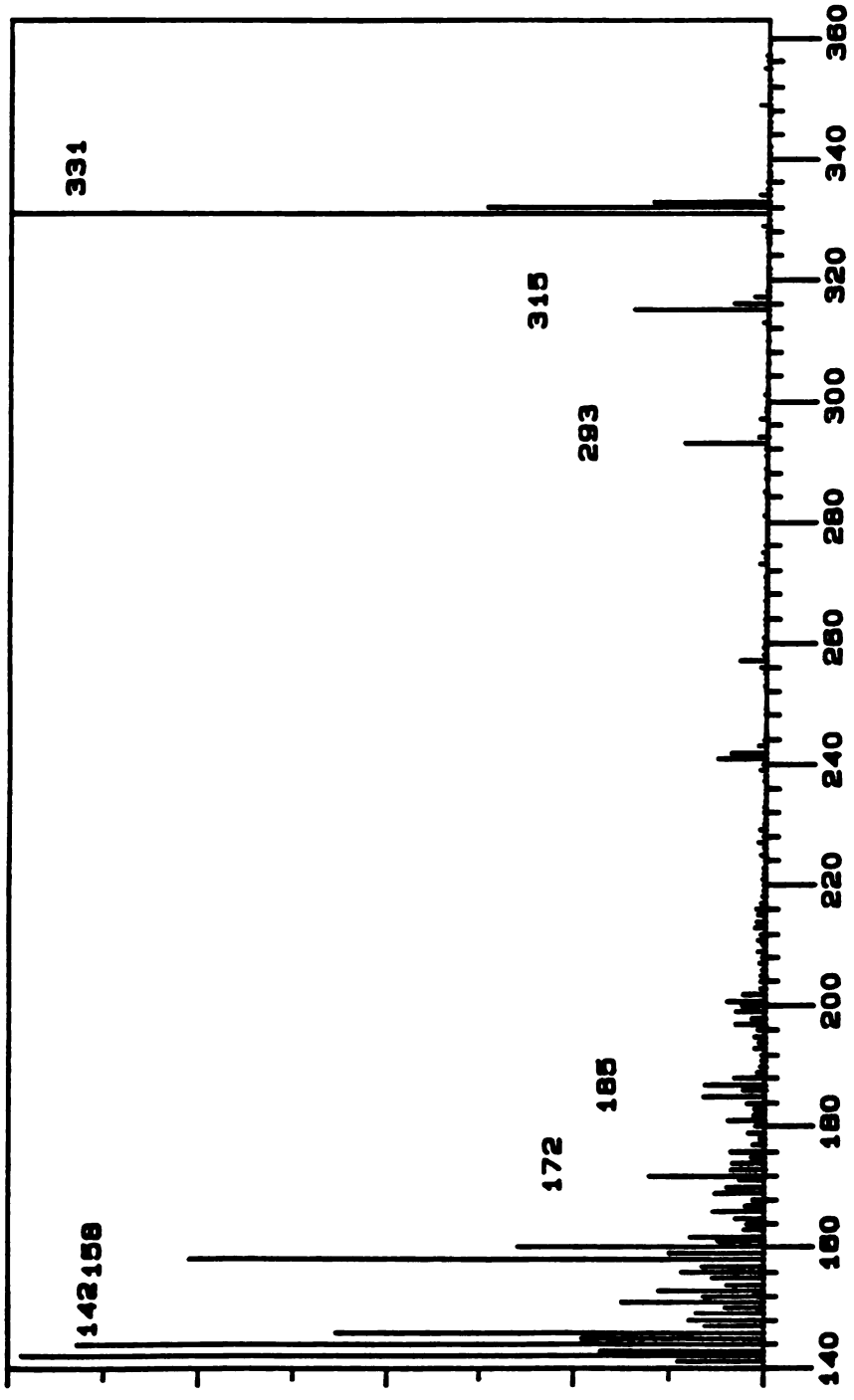


Figure 118. K^+IDS Spectrum of Quadrol.

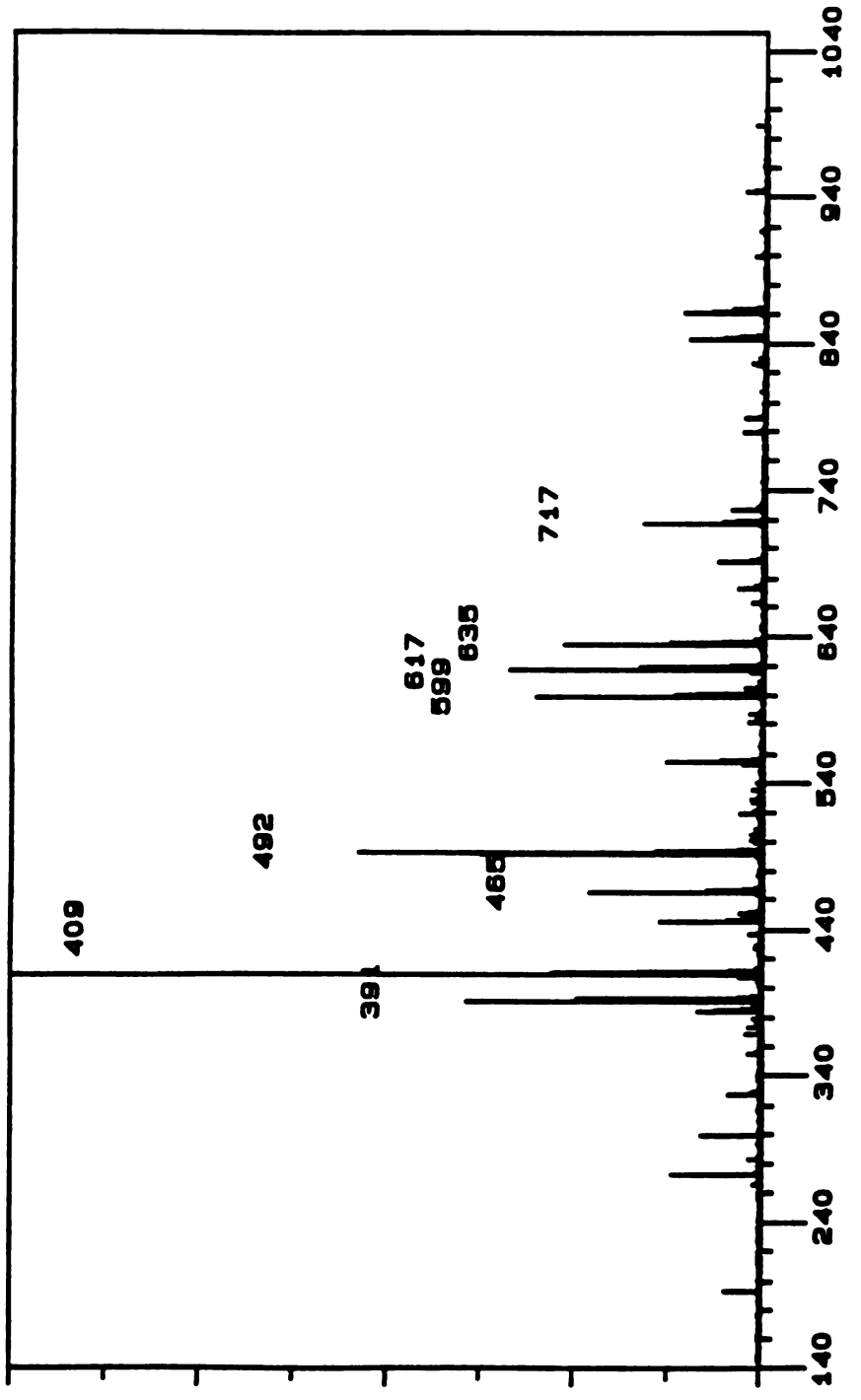


Figure 119. K^+IDS Spectrum of Poly(cyclohexanedimethanol Succinate).

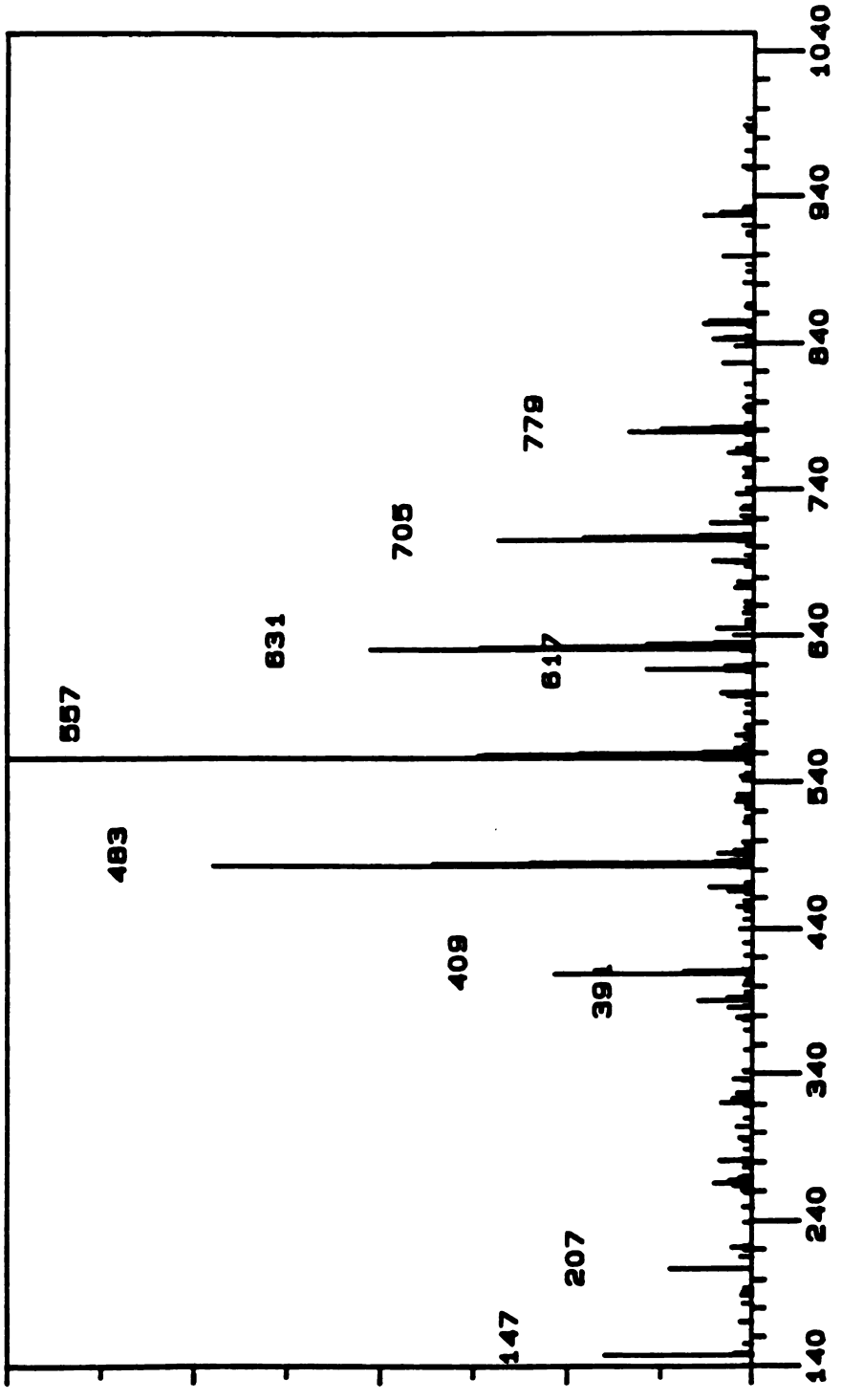


Figure 120. K^+IDS Spectrum of W-98.

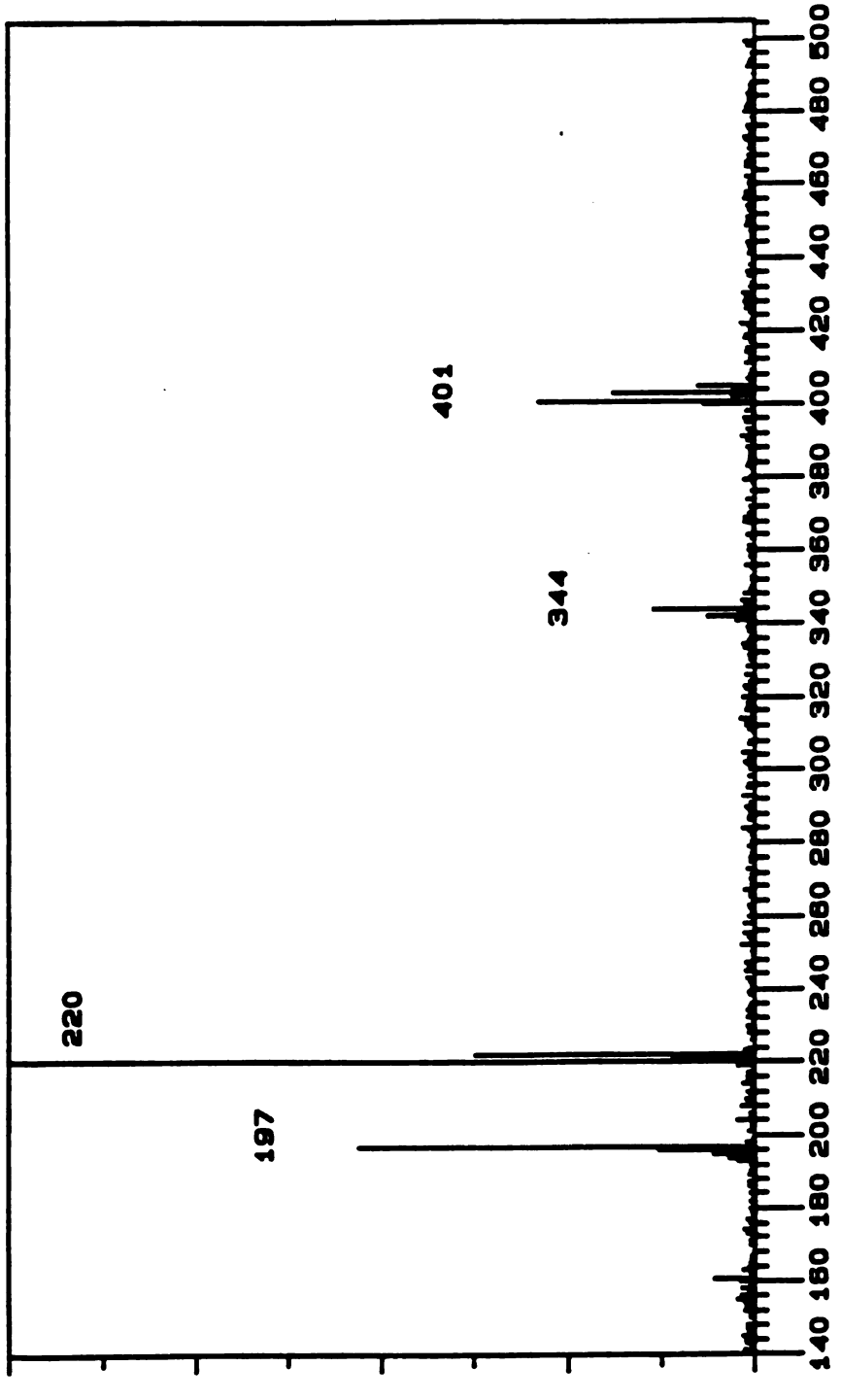


Figure 121. K^+IDS Spectrum of Cupric Acetate.

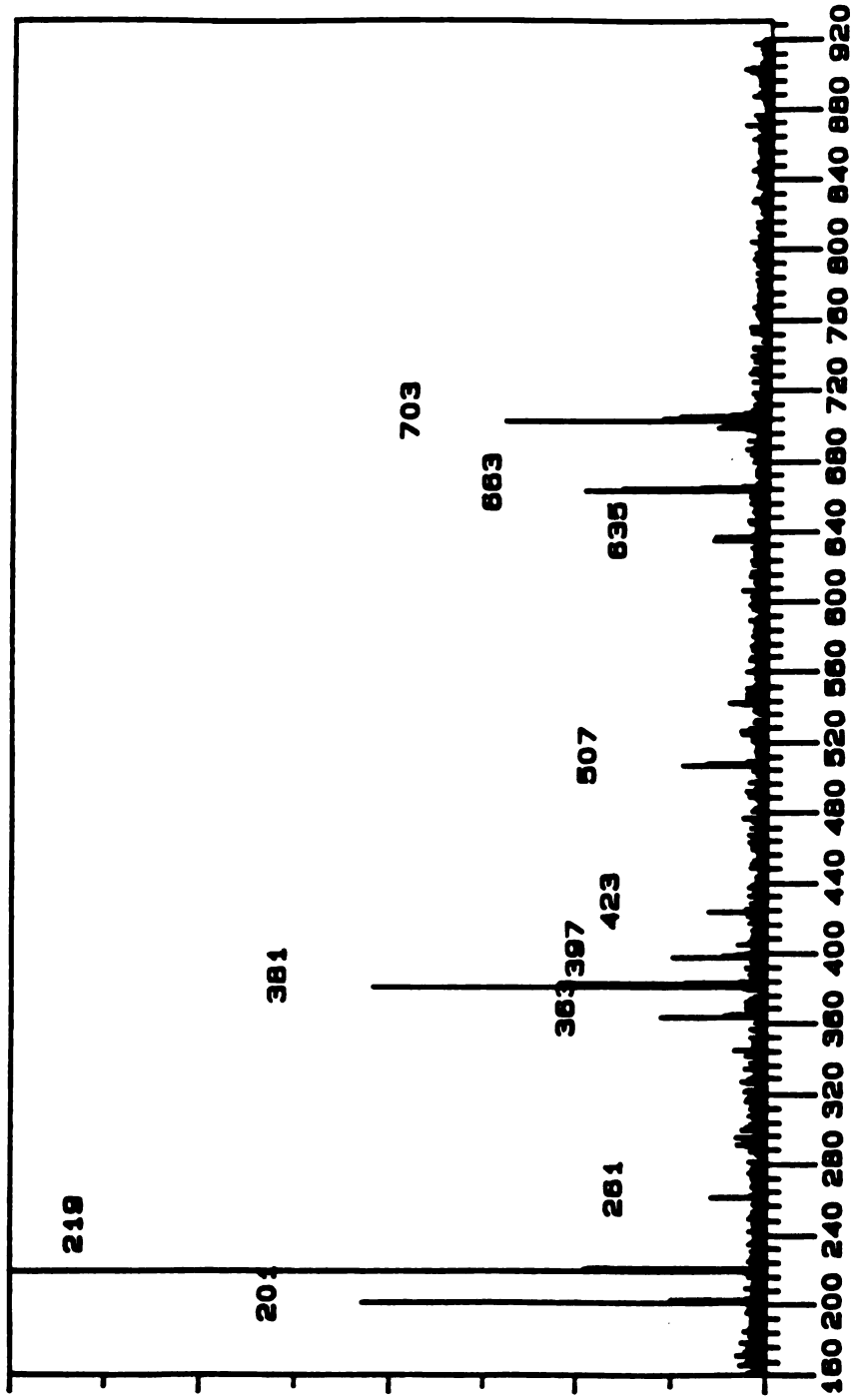


Figure 122. K^+ IDS Spectrum of Juicy Fruit Gum.

LIST OF REFERENCES

1. Richardson, O.W. Proc. Cambridge Phil. Soc. 1902, 11, 286.
2. Schottky, W. Physik Z. 1914, 15, 872.
3. von Loue, M., Jr. Radakt. Elektr. 1918, 15, 205.
4. Fowler, R.H.; Nordheim, L.W. Proc. Roy. Soc. (London) 1928, A119, 173.
5. Richardson, O.W. "The Emission of Electricity From Hot Bodies", Longmans, Green and Co., London, 2nd Ed., 1934.
6. Reimann, A.L. "Thermionic Emission", John Wiley & Sons, New York, 1934.
7. Page, F.M.; Goode, G.C. "Negative Ions and the Magnetron", Wiley Interscience, New York, 1969.
8. Madinos, A. Surf. Sci. 1982, 115, 469.
9. Fomenko, V.S.; Samsonov, G.V. "Handbook of Thermionic Properties", Plenum Press, New York, 1966.
10. Taylor, J.B.; Langmuir, I. Phys. Rev. 1933, 44, 423.
11. Copley, M.J.; Phipps, T.E. Phys. Rev. 1934, 45, 344.
12. Shelton, H. Phys. Rev. 1957, 107, 1553.
13. Child, C.D. Phys. Rev. 1911, 32, 498.
14. Langmuir, I.; Blodgett, K.B. Phys. Rev. 1924, 24, 49.
15. Chow, K.K.; Maddix, H.S.; Chorney, P. Appl. Phys. Letts. 1967, 10, 256.
16. Weber, R.E.; Cordes, L.F. Rev. Sci. Instr. 1966, 37, 112.
17. Blewett, J.P.; Jones, E.J. Phys. Rev. 1936, 50, 464.
18. Futamoto, M.; Nakazawa, M.; Kawabe, U. Surf. Sci. 1980,

100, 470.

19. Moon, P.B.; Oliphant, M.L. Proc. Roy. Soc.(A) 1932, 137, 463.
20. Smith, L.P. Phys. Rev. 1929, 34, 1496.
21. Smith, L.P. Phys. Rev. 1930, 35, 381.
22. Scheer, M.D. J. Res. 1970, 74A, 37.
23. Martenson, B.M.; Wilhelmsson, S.O.; Int. J. of Mass Spectrom. Ion Proc. 1985, 67, 179.
24. Melton, C.E. "Principles of Mass Spectrometry and Negative Ions", Marcel Dekker, New York, 1970, p.68.
25. Kelso, J.F.; Pantano, C.G.; Garofalini, S.H. Surf. Sci. 1983, 134, L543.
26. Zandberg, E.Ya.; Ionov, N.I. Sov. Phys. Uspehki 1959, 67, 255.
27. Sroubek, Z. Int. J. Mass Spectrom. Ion Phys. 1983, 53, 289.
28. Kawano, H.; Page, F.M.; Int. J. Mass Spectrom. Ion Phys. 1983, 50, 1.
29. Zandberg, E.Ya.; Rasulev, U. Kh. Russ. Chem. Rev. 1982, 51, 819.
30. Kawano, H.; Hidaka, Y.; Page, F.M. Int. J. Mass Spectrom. Ion Phys. 1983, 50, 35.
31. Kawano, H.; Hidaka, Y.; Suga, M.; Page, F.M. Int. J. Mass Spectrom. Ion Phys. 1983, 50, 77.
32. Kingdon, K.H.; Langmuir, I. Phys. Rev. 1923, 21, 380.
33. Kingdon, K.H.; Langmuir, I. Proc. Roy. Soc(A) 1925, 107, 61.
34. Reference 24, pp 64-66.
35. Fujii, T. Int. J. Mass Spectrom. Ion Proc. 1984, 57, 63.
36. Zandberg, E.Ya.; Rasulev, U.Kh. Izv. Akad. Nauk SSSR Ser.

Fiz. 1966, 40, 1561.

37. Zandberg, E.Ya.; Rasulev, U.Kh. Dokl. Akad. Nauk SSSR 1968, 178, 327.

38. Zandberg, E.Ya.; Rasulev, U.Kh.; Sharapudinov, M.R. Teoretich. i Eksper. Khim. 1970, 6, 328.

39. Zandberg, E.Ya.; Rasulev, U.Kh. Teoretich i Eksper. Khim. 1972, 8, 114.

40. Zandberg, E.Ya.; Rasulev, U.Kh. Teoretich. i Eksper. Khim. 1972, 8, 658.

41. Failes, R.L.; Joyce, J.T.; Watlon, E.C. J. Phys. B: Atom. Molec. Phys. 1979, 12, 2379.

42. Rasulev, U.Kh.; Khalikov, Sh.M. Zh. Org. Khim. 1976, 12, 479.

43. Rasulev, U.Kh. Zh. Org. Khim. 1973, 9, 1573.

44. Zandberg, E.Ya.; Rasulev, U.Kh.; Khalikov, Sh.M. Zh. Org. Khim. 1976, 12, 1143.

45. Zandberg, E.Ya.; Rasulev, U.Kh.; Takhistov, U.V.; Sharapudinov, M.R. Teoretich. i Eksper. Khim. 1970, 6, 776.

46. Zandberg, E.Ya.; Rasulev, U.Kh.; Sharapudinov, M.R. Izv. Akad. Nauk SSSR Ser. Fiz. 1971, 35, 334.

47. Zandberg, E.Ya.; Rasulev, U.Kh. Zh. Anal. Khim. 1972, 27, 2459.

48. Zandberg, E.Ya.; Rasulev, U.Kh.; Shustrov, B.N. Dokl. Akad. Nauk SSSR 1967, 172, 885.

49. Rasulev, U.Kh.; Zandberg, E.Ya.; Bogolyubov, G.M. Zh. Obshchei Khim. 1974, 44, 2198.

50. Fomin, O.K.; Tikhomirov, M.V. Russ. J. Phys. Chem. 1964,

38, 444.

51. Fomin, O.K.; Tikhomirov, M.V. Russ. J. Phys. Chem. 1964, 38, 383.
52. Persky, A.; Greene, E.F.; Kuppermann, A. J. Chem. Phys. 1968, 49, 2347.
53. Scheer, M.D.; Fine, J. Phys. Rev. Lett. 1966, 17, 283.
54. Lyons, L.E.; Palmer, L.D. Int. J. Mass Spectrom. Ion Phys. 1975, 16, 431.
55. Moran-Lopez, J.L.; Ten Bosch, A. Surf. Sci. 1977, 68, 377.
56. Somorjai, G.A. Science 1985, 227, 902.
57. Bartmess, J.E. J. Phys. Chem. Ref. (in press)
58. McLafferty, F.W. "Interpretation of Mass Spectra", 3rd Ed., University Science Books: Mill Valley, CA, 1980; Chapter 3.
59. Munson, M.S.B. Anal. Chem. 1977, 49, 772A.
60. Munson, M.S.B.; Field, F.H. J. Am. Chem. Soc. 1966, 88, 2621.
61. Allison, J.; Ridge, D.P. J. Am. Chem. Soc. 1979, 101, 4998.
62. Hodges, R.V.; Beauchamp, J.L. Anal. Chem. 1976, 48, 825.
63. Burnier, R.D.; Byrd, G.D.; Freiser, B.S. Anal. Chem. 1980, 52, 1641.
64. Weddle, G.H.; Allison, J.; Ridge, D.P. J. Am. Chem. Soc. 1977, 99, 105.
65. Cody, R.B.; Burnier, R.D.; Reents, W.D. Jr.; Carlin, T.J.; McCrery, D.A.; Lengel, R.K.; Freiser, B.S. Int. J. Mass Spectrom. Ion Phys. 1980, 33, 37.
66. Musselman, B.D.; Davenport, M.J.; Holland, J.F.; Dolnikowski, G. 30th Annual Conference on Mass Spectrometry & Allied

Topics, Honolulu, HI, 1982; p 715.

67. Freiser, B.S.; Staley, R.H.; Beauchamp, J.L. Chem. Phys. Lett. 1976, 39, 49.

68. Spears, K.G.; Ferguson, E.E. J. Chem. Phys. 1973, 59, 4174.

69. Ackermann, B.; Allison, J.; Musselman, B.; Pinkston, D.; Bombick, D.; Dolnikowski, G.; Tsarbopoulos, A.; Watson, J.T. 31st Annual Conference on Mass Spectrometry & Allied Topics, Boston, MA, 1983; p 600.

70. Oláh, K.; Szóke, A.; Vajta, Z.S. J. Chromatogr. Sci. 1979, 17, 497.

71. Patterson, P.L.; Gatten, R.A.; Ontiveros, G. J. Chromatogr. Sci. 1982, 20, 97.

72. Armentrout, P.B.; Halle, L.F.; Beauchamp, J.L. J. Chem. Phys. 1982, 76, 2449.

73. Barber, M.; Bordoli, R.S.; Elliot, G.J.; Sedgwick, R.D.; Tyler, A.N. Anal. Chem. 1982, 54, 645A.

74. Popov, A.I. Pure Appl. Chem. 1979, 51, 101.

75. Huang, S.K.; Allison, J. Organometallics 1983, 2, 883.

76. Lee, Y.C.; Popov, A.I.; Allison, J. Int. J. Mass Spectrom. Ion Phys. 1983, 51, 267.

77. Beckey, H.D. Int. J. Mass Spectrom. Ion Phys. 1969, 2, 500.

78. Barber, M.; Bordoli, R.S.; Sedgwick, R.D.; Tyler, A.N. J. Chem. Soc., Chem. Commun. 1981, 325.

79. Benninghoven, A.; Sichtermann, W. Anal. Chem. 1978, 50, 1180.

80. Posthumus, M.A.; Kistemaker, P.G.; Meuzelaar, H.L.C.; Ten Noever de Brauw, M.C. Anal. Chem. 1978, 50, 985.

81. Macfarlane, R.D. Acc. Chem. Res. 1982, 15, 268.

82. Beuhler, R.J.; Flanigan, E.; Greene, L.J.; Friedman, L. J. Am. Chem. Soc. 1974, 96, 3990.

83. Schulten, H.-R.; Lattimer, R.P. Mass Spectrom. Rev. 1984, 3, 231.

84. Grassie, N. Pure Appl. Chem. 1982, 54, 337.

85. Röllgen, F.W.; Schulten, H.-R. Z. Naturforsch. 1975, 30A, 1685.

86. Röllgen, F.W.; Schulten, H.-R. Org. Mass Spectrom. 1975, 10, 660.

87. Giessmann, U.; Röllgen, F.W. Org. Mass Spectrom. 1976, 11, 1094.

88. Borchers, F.; Giessmann, U.; Röllgen, F.W. Org. Mass Spectrom. 1977, 12, 539.

89. Röllgen, F.W.; Giessmann, U.; Borchers, F.; Levsen, K. Org. Mass Spectrom. 1978, 13, 459.

90. Van der Peyl, G.J.Q.; Isa, K.; Haverkamp, J.; Kistemaker, P.G. Org. Mass Spectrom. 1981, 16, 416.

91. Stoll, R.; Röllgen, F.W. Org. Mass Spectrom. 1981, 16, 72.

92. Cotter, R.J.; Yergey, A.L. Anal. Chem. 1981, 53, 1306.

93. Schmelzeisen-Redeker, G.; Giessmann, U.; Röllgen, F.W. Org. Mass Spectrom. 1985, 20, 305.

94. Day, R.J.; Unger, S.E.; Cooks, R.G. Anal. Chem. 1980, 52, 557A.

95. Woodin, R.L.; Beauchamp, J.L. Chem. Phys. 1979, 41, 1.

96. Röllgen, F.W.; Biessmann, U.; Stoll, R. Nucl. Instrum. Methods 1982, 198, 93.

97. Stoll, R.; Röllgen, F.W. Z. Naturforsch. 1982, 37A, 9.

98. Fagerson, I.S. J. Agric. Food Chem. 1969, 17, 747.

99. Higman, E.B.; Schmeltz, I.; Schlotzhauer, W.S. J. Agric. Food Chem. 1978, 18, 636.

100. Ohnishi, A.; Kato, K.; Takagi, E. Polym. J. 1975, 7, 431.

101. Irwin, W.J. "Analytical Pyrolysis A Comprehensive Guide; Marcel Dekker: New York, 1982; Chapter 7.3, pp 339-352.

102. Schulten, H.-R.; Gortz, W. Anal. Chem. 1978, 50, 428.

103. Shafizadeh, F. Adv. Carbohyd. Chem. 1968, 23, 419.

104. Muller, M.D.; Seibl, J.; Simon, W. Anal. Chim, Acta 1978, 100, 263.

105. Gower, J.L.; Beaugrand, C.; sallot, C. Biomed. Mass Spectrom. 1981, 8, 36.

106. Barber, M; Bordoli, R.S.; Sedgwick, R.D.; Tyler, A.N.; Greene, B.N.; Parr, V.C.; Gower, J.L. Biomed. Mass Spectrom. 1982, 9, 11.

107. Heerma, W.; Kamerling, J.P.; Slotboom, A.J.; van Scharrenburg, G.J.; Greene, B.N.; Lewis, I.R.S. Biomed. Mass Spectrom. 1983, 10, 13.

108. Westmore, J.B.; Ens, W.; Standing, K.G. Biomed. Mass Spectrom. 1982, 9, 119.

109. Ratcliff, M.A., Jr.; Medley, E.E.; Simmonds, P.G. J. Org. Chem. 1974, 39, 1481.

110. Franklin, J.L. Ind. Eng. Chem. 1949, 41, 1070.

111. Svec, H.J.; Junk, G.A. J. Am. Chem. Soc. 1964, 86, 2278.

112. Lin, Y.Y.; Low, C.-E.; Smith, L.L. J. Steroid biochem. 1981, 14, 563.

113. Smith. L.L. "Cholesterol Autoxidation", Plenum, New York, 1981.

114. Krull, U.J.; Thompson, M.; Arya, A. Talanta 1984, 31, 489.

115. Lifshitz, C.; Bergmann, E.D.; Pullman, B. Tetrahedron Lett. 1967, 46, 4587.

116. Cotter, R.J. Anal. Chem. 1980, 52, 1589A.

117. Udseth, H.R.; Friedman, L. Anal. Chem. 1981, 53, 29.

118. Chait, B.T.; Field, F.H. 31st Annual Conference on Mass Spectrometry & Allied Topics, Boston, May 8-13, 1983, p. 619.

119. Gardella, J.A., Jr.; Hercules, D.M. Anal. Chem. 1980, 52, 226.

120. Dole, M.; Cox, H.L., Jr.; Glemic, J. Adv. Chem. Ser. 1973, 125, 73.

121. Trash, C.R. J. Chromatogr. Sci. 1973, 11, 196.

122. Baiulescu, G.E.; Ilie, V.A. "Stationary Phases in Gas Chromatography:, Pergamon Press: Oxford, England, 1975; pp. 123-138.

123. Billmeyer, F.W., Jr. "Textbook of Polymer Science", 2nd ed.; Wiley: New York, 1971; p.482.

124. Fox, H.W.; Taylor, P.W.; Zisman, W.A. Ind. Eng. Chem. 1947, 39, 1401.

125. Grassie, N.; Macfarlane, I.G. Eur. Poly. J. 1978, 14, 875.

126. Grassie, N.; Macfarlane, I.G.; Francey, K.F. Eur. Poly. J. 1979, 15, 415.

127. Grassie, N. "Encyclopedia of Polymer Science and Technology", Wiley: New York, 1966; Vol. 4, p. 647.

128. Madorsky, S.L. "Thermal Degradation of Organic Polymers", Wiley: New York, 1964, Chapters 3-4.

129. Conley, R.T. "Thermal Stability of Polymers", Marcel Dekker: New York, 1970, Vol. 1, Chapter 10.

130. Luderwald, I.; Urrutia, H. Makromol. 1976, 177, 2093.

131. Doerr, M.; Luderwald, I.; Schulten, H.-R. Fresenius Z. Anal. Chem. 1984, 318, 339.

132. Luderwald, I.; Merz, F.; Rothe, M. Angew. Makromol. Chem. 1978, 67, 193.

133. Adams, R.E. Anal. Chem. 1983, 55, 414.

134. Bahr, U.; Luderwald, I.; Muller, R.; Schulten, H.-R. Angew. Makromol. Chem. 1984, 120, 163.

135. Bletsos, I.U.; Hercules, D.M.; Greifendorf, D.; Benninghoven, A. Anal. Chem. 1985, 57, 2384.

136. Ettre, L.S. J. Chromatogr. Sci. 1978, 16, 396.

137. Farwell, S.D.; Gage, D.R.; Kagel, R.A. J. Chromatogr. Sci. 1981, 19, 358.

138. Aue, W.A. J. Chromatogr. Sci. 1975, 13, 329.

139. Bonati, M.; Castelli, D.; Latini, R.; Garattini, S. J. Chromatogr. 1979, 164, 109.

140. Cochrane, W.P.; Greenhalgh, R. Chromatographia 1976, 9, 255.

141. Meola, J.M. Chromatogr. Newsletter 1977, 5, 1.

142. Vandemark, F.L.; Adams, R.F. Chromatogr. Newsletter 1977, 5, 4.

143. Ames, M.M.; Pavis, G. J. Chromatogr. 1979, 174, 245.

144. Brazhnikov, V.V.; Gur'ev, M.V.; Sakodynsky, K.I. Chromatographic Rev. 1970, 12, 1.

145. Karmen, A.; Guiffrida, L.E. Nature 1964, 201, 1204.

146. Kolb, B.; Bischoff, J. J. Chromatogr. Sci. 1974, 12, 625.

147. Burgett, C.A.; Smith, D.H.; Bente, H.B. J. Chromatogr. 1977, 134, 57.

148. Patterson, P.L. J. Chromatogr. 1978, 167, 381.

149. Bamford, C.H.; Tipper, C.F.H., Eds. "Comprehensive Chemical Kinetics"; Elsevier: New York, 1972; Vol. 5.

150. Lin, S.-T.; Klabunde, K.J. Langmuir 1985, 1, 600.

151. Leclerk, J.C.; Lorquet, J.C. J. Phys. Chem. 1967, 71, 787.

152. Walker, B.W.; Stair, P.C. Surf. Sci. 1981, 103, 315.

153. Fujii, T.; Arimoto, H. Anal. Chem. 1985, 57, 2625.

154. Folmer, O.F.; Yang, K.; Perkins, G. Anal. Chem. 1963, 35, 454.